FEDERAL UNIVERSITY OF PARÁ

INSTITUTE OF TECHNOLOGY

GRADUATE PROGRAM IN ELECTRICAL ENGINEERING

OUTPUT-ONLY METHODS FOR DAMAGE IDENTIFICATION IN STRUCTURAL HEALTH MONITORING

ADAM DREYTON FERREIRA DOS SANTOS

TD 05/2017

UFPA / ITEC / PPGEE

Guamá University Campus

Belém-Pará-Brazil

2017

FEDERAL UNIVERSITY OF PARÁ

INSTITUTE OF TECHNOLOGY

GRADUATE PROGRAM IN ELECTRICAL ENGINEERING

ADAM DREYTON FERREIRA DOS SANTOS

OUTPUT-ONLY METHODS FOR DAMAGE IDENTIFICATION IN STRUCTURAL HEALTH MONITORING

TD 05/2017

UFPA / ITEC / PPGEE

Guamá University Campus

Belém-Pará-Brazil

2017

FEDERAL UNIVERSITY OF PARÁ

INSTITUTE OF TECHNOLOGY

GRADUATE PROGRAM IN ELECTRICAL ENGINEERING

ADAM DREYTON FERREIRA DOS SANTOS

OUTPUT-ONLY METHODS FOR DAMAGE IDENTIFICATION IN STRUCTURAL HEALTH MONITORING

Ph.D. thesis submitted to the Examining Board of the Graduate Program in Electrical Engineering from the Federal University of Pará to obtain the Ph.D. Degree in Electrical Engineering, Area of Concentration in Applied Computing.

UFPA / ITEC / PPGEE

Guamá University Campus

Belém-Pará-Brazil

2017

Dados Internacionais de Catalogação-na-Publicação (CIP)
Sistema de Bibliotecas da UFPA

Santos, Adam Dreyton Ferreira dos, 1989 -
Output-only methods for damage identification in structural health monitoring / Adam Dreyton Ferreira dos Santos. - 2017.

Orientador: João Crisóstomo Weyl Albuquerque Costa;
Coorientador: Elói João Faria Figueiredo.

Tese (Doutorado) – Universidade Federal do Pará, Instituto de Tecnologia, Programa de Pós-Graduação em Engenharia Elétrica, Belém, 2017.

1. Falhas estruturais – prevenção. 2. Localização de falhas (engenharia) – processamento de dados. 3. Inteligência artificial. 4. Reconhecimento de padrões. I. Título.

CDD 23. ed. 624.171

FEDERAL UNIVERSITY OF PARÁ

INSTITUTE OF TECHNOLOGY

GRADUATE PROGRAM IN ELECTRICAL ENGINEERING

OUTPUT-ONLY METHODS FOR DAMAGE IDENTIFICATION IN STRUCTURAL HEALTH MONITORING

AUTHOR: **ADAM DREYTON FERREIRA DOS SANTOS**

PH.D. THESIS SUBMITTED TO EVALUATION OF THE EXAMINING BOARD APPROVED BY THE COMMITTEE OF THE GRADUATE PROGRAM IN ELECTRICAL ENGINEERING FROM FEDERAL UNIVERSITY OF PARÁ AND JUDGED APPROPRIATE TO OBTAIN THE PH.D. DEGREE IN ELECTRICAL ENGINEERING, AREA OF CONCENTRATION IN APPLIED COMPUTING.

APPROVED ON: 27/04/2017

EXAMINING BOARD:

Prof. Dr. João Crisóstomo Weyl Albuquerque Costa
(Advisor – PPGEE/UFPA)

Prof. Dr. Elói João Faria Figueiredo
(Co-advisor – FE/ULHT)

Prof. Dr. Ádamo Lima de Santana
(Internal Member – PPGEE/UFPA)

Prof. Dr. Diego Lisboa Cardoso
(Internal Member – PPGEE/UFPA)

Prof. Dr. Claudomiro de Souza de Sales Junior
(External Member – PPGCC/UFPA)

Prof. Dra. Regina Augusta Campos Sampaio
(External Member – PPGEC/UFPA)

SIGNATURE:

Prof. Dr. Evaldo Gonçalves Pelaes
(Coordinator of PPGEE/ITEC/UFPA)

Acknowledgements

I would like to thank my family for the kindness, encouragement, and support I have received from them during the entire Ph.D. Course in Electrical Engineering at the Federal University of Pará.

I would like to thank my girlfriend Cindy Fernandes for all the love and companionship dedicated to me during all the moments of this journey that becomes less difficult because of her presence in my life.

I would like to express my deep gratitude to Professors João C.W.A. Costa and Elói Figueiredo, my research supervisors, for their patient guidance, enthusiastic encouragement and useful critiques of this research work. I would also like to thank Professors Claudomiro Sales, Ádamo Santana, Diego Lisboa, and Regina Sampaio, for their advices and assistance in keeping my progress on schedule since the Qualifying exam.

My grateful thanks are also extended to the friends and researchers Moisés Silva and Reginaldo Santos for their support and collaboration in many publications and visionary ideas. Leaving aside the work, our friendship has great potential to last a lifetime.

I am particularly grateful for the friendship and assistance given by members of the Applied Electromagnetism Laboratory (LEA[1]): Dércio Mathe, Fabrício Lobato, Liane Barbosa, Roberto Menezes, Gilvan Borges, and Marco Sousa.

My acknowledgements for the financial support received from the CNPq[2] (under Grant 142236/2014-4 and Grant 454483/2014-7).

[1] http://www.lea.ufpa.br
[2] http://www.cnpq.br/

Table of Contents

List of Figures

List of Tables

List of Abbreviations and Acronyms

AANN Auto-associative neural network

ACH Agglomerative concentric hypersphere

AIC Akaike information criterion

BC Baseline condition

BIC Bayesian information criterion

BMS Bridge management system

DC Damaged condition

DI Damage indicator

EM Expectation-maximization

FA Factor analysis

FN False negative

FP False positive

FPR False-positive rate

GA Genetic algorithm

GADBA Genetic algorithm for decision boundary analysis

GKPCA Greedy kernel principal component analysis

GMM Gaussian mixture model

KPCA Kernel principal component analysis

MA Memetic algorithm

MCMC Markov-chain Monte Carlo

ML Maximum likelihood

MSC Mean shift clustering

MSD Mahalanobis squared-distance

PCA Principal component analysis

PDF Probability density function

PSO Particle swarm optimization

RBF Radial basis function

ROC Receiver operating characteristic

SHM Structural health monitoring

SPR Statistical pattern recognition

SSI Stochastic subspace identification

SVD Singular value decomposition

SVDD Support vector data description

SVM Support vector machine

TN True negative

TP True positive

TPR True-positive rate

Abstract

In the structural health monitoring (SHM) field, vibration-based damage identification has become a crucial research area due to its potential to be applied in real-world engineering structures. Assuming that the vibration signals can be measured by employing different types of monitoring systems, when one applies appropriate data treatment, damage-sensitive features can be extracted and used to assess early and progressive structural damage. However, real-world structures are subjected to regular changes in operational and environmental conditions (e.g., temperature, relative humidity, traffic loading and so on) which impose difficulties to identify structural damage as these changes influence different features in a distinguish manner. In this thesis by papers, to overcome this drawback, novel output-only methods are proposed for detecting and quantifying damage on structures under unmeasured operational and environmental influences. The methods are based on the machine learning and artificial intelligence fields and can be classified as kernel- and cluster-based techniques. When the novel methods are compared to the state-of-the-art ones, the results demonstrated that the former ones have better damage detection performance in terms of false-positive (ranging between 3.6–5.4%) and false-negative (ranging between 0–2.6%) indications of damage, suggesting their applicability for real-world SHM solutions. If the proposed methods are compared to each other, the cluster-based ones, namely the global expectation–maximization approaches based on memetic algorithms, proved to be the best techniques to learn the normal structural condition, without loss of information or sensitivity to the initial parameters, and to detect damage (total errors equal to 4.4%).

Keywords: Structural health monitoring, Machine learning, Damage identification, Damage detection, Environmental conditions, Operational conditions.

Resumo

No campo da monitorização de integridade estrutural (SHM), a identificação de dano baseada em vibração tem se tornado uma área de pesquisa crucial devido a sua potencial aplicação em estruturas de engenharia do mundo real. Assumindo que os sinais de vibração podem ser medidos pelo emprego de diferentes tipos de sistemas de monitorização, quando aplica-se o tratamento de dados adequado, as características sensíveis a dano podem ser extraídas e usadas para avaliar dano estrutural incipiente ou progressivo. Entretanto, as estruturas do mundo real estão sujeitas às mudanças regulares nas condições operacionais e ambientais (e.g., temperatura, umidade relativa, massa de tráfego e outros), as quais impõem dificuldades na identificação do dano estrutural uma vez que essas mudanças influenciam diferentes características de forma distinta. Nesta tese por agregação de artigos, a fim de superar essa limitação, novos métodos *output-only* são propostos para detectar e quantificar dano em estruturas sob influências operacionais e ambientais não medidas. Os métodos são baseados nos campos de aprendizagem de máquina e inteligência artificial e podem ser classificados como técnicas baseadas em kernel e clusterização. Quando os novos métodos são comparados àqueles do estado da arte, os resultados demonstraram que os primeiros possuem melhor performance de detecção de dano em termos de indicações de dano falso-positivas (variando entre 3,6–5,4%) e falso-negativas (variando entre 0–2,6%), sugerindo potencial aplicabilidade em soluções práticas de SHM. Se os métodos propostos são comparados entre si, aqueles baseados em clusterização, nomeadamente as abordagens de expectância–maximização global via algoritmos meméticos, provaram ser as melhores técnicas para aprender a condição estrutural normal, sem perda de informação ou sensibilidade aos parâmetros iniciais, e para detectar dano (erros totais iguais a 4,4%).

Palavras-chave: Monitorização de integridade estrutural, Aprendizado de máquina, Identificação de dano, Detecção de dano, Condições ambientais, Condições operacionais.

1 Introduction

1.1 Research context

Engineering structures such as aircraft, buildings, roads, railways, bridges, tunnels, dams, power generation systems, rotating machinery and offshore oil platforms are present and play a crucial role in modern societies, regardless of geographical location or economical development. The safest, economical and most durable structures are those that are well managed and maintained. Health monitoring represents an important tool in management activities as it permits one to identify early and progressive structural damage (FARRAR; WORDEN, 2007). The massive data obtained from monitoring must be transformed in meaningful information to support the planning and designing maintenance activities, increase the safety, verify hypotheses, reduce uncertainty and to widen the knowledge and insight concerning the monitored structure.

Structural health monitoring (SHM) is certainly one of the most powerful tools for infrastructure management (BROWNJOHN, 2007). The SHM process involves the observation of a structural system over time using periodically sampled response measurements from an array of sensors, the extraction of damage-sensitive features from these measurements, and the statistical analysis of these features to discriminate the actual structural condition. For long-term SHM, the output of this monitoring process is periodically updated, providing information regarding the ability of the structure to perform its intended function in light of the inevitable aging and degradation due to the operational and environmental variability (SOHN, 2007; KULLAA, 2011). After extreme events such as earthquakes or blast loadings, SHM is used for rapid condition screening and aims to provide, in nearly real time, reliable information regarding the integrity of the structure.

The process of implementing an autonomous damage identification strategy for civil, mechanical, and aerospace engineering infrastructure is traditionally referred to as SHM (FARRAR; DOEBLING; NIX, 2001). This strategy should be as detailed as possible to describe the abnormal impact on the structural system. In a broad sense, developments on this area can be broken down into damage detection, diagnosis, and prognosis. Nonetheless, damage diagnosis can be subdivided into location, type, and severity. Thus, as depicted in Figure 1, the hierarchical structure of damage identification can be decomposed in five levels, which answer the following questions (FIGUEIREDO, 2010).

1. Is the damage present in the system (detection)?
2. Where is the damage (localization)?
3. What kind of damage is present (type)?
4. What is the extent of damage (severity)?
5. How much useful lifetime remains (prognosis)?

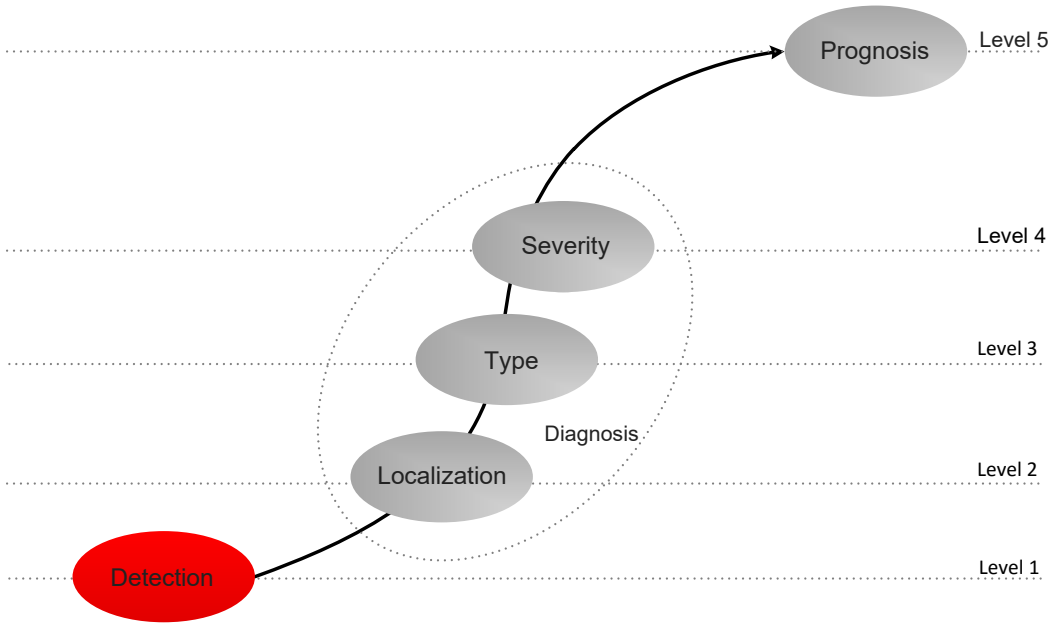

Figure 1 – Hierarchical structure of damage identification (FIGUEIREDO, 2010).

Usually, the answers to the aforementioned questions can be made in a sequential manner. For example, the answer to the severity of damage can be made with a priori knowledge of the type of damage. Note that damage prognosis at step five can not be accomplished without an understanding of the damage accumulation process. For further discussion on the concept of damage prognosis, one should see (FARRAR; J.LIEVEN, 2007). Even though the damage identification hierarchy is composed of five levels, this thesis poses the SHM process mostly in the context of the first level (damage detection) and, for some extent, the fourth level is also addressed through damage quantification.

There are arguably two main approaches to SHM: physics- and data-based. The physics-based approach uses the inverse problem technique to calibrate numerical models (e.g., finite element models) and attempts to identify damage by relating the measured data from the structures to the estimated data from the models. On the other hand, the data-based approach is rooted in the machine learning field, where algorithms are essential to learn (or to model) the structural behavior from the experience (or past monitoring data), following the same principle of the human brain, and to perform pattern recognition

for damage identification. These algorithms can be applied in supervised or unsupervised learning (WORDEN; MANSON, 2007).

In the SHM field, supervised learning refers to the case where data from undamaged and damaged conditions are available to train the algorithms. When applied in a supervised manner and coupled with physics-based models, the algorithms can be used to better determine the type of damage, the severity of damage, and the remaining useful lifetime. Unsupervised learning refers to the case where training data are only available from the undamaged condition. When applied in an unsupervised manner, machine learning algorithms are typically used to answer questions regarding the detection and localization. Nevertheless, in certain cases, it can also perform relative quantification of damage. Note that for high capital expenditure structures where the SHM systems are applied, such as most civil infrastructure, the unsupervised algorithms are often required because only data from the undamaged condition are normally available (FARRAR; WORDEN, 2013).

Several unsupervised methods have been proposed to detect structural damage by combining pattern recognition and machine learning (FIGUEIREDO et al., 2011; TORRES-ARREDONDO et al., 2014; SANTOS et al., 2016). This combination is often accomplished through a phase of a statistical pattern recognition (SPR) paradigm that establishes two steps:

1. Learn a model which comprises undamaged data from the normal structural condition, considering nearly all operational and environmental influences.

2. Test the learned model by classifying new undamaged or damaged data, i.e., assessing the actual condition of the monitored structure.

It is important to emphasize that, currently, most of the techniques used in the SPR are output-only, i.e., only the damage-sensitive features (often derived from vibration response measurements (CARDEN; FANNING, 2004)) need to be measured, not the operational and environmental parameters.

In this thesis, novel output-only methods are proposed for damage detection in the context of the SPR for SHM. These techniques are relevant in cases where damage-sensitive features extracted from the structural responses are affected by changes caused by operational and environmental variability and changes caused by damage.

1.2 Motivation

The motivations of this study are related to economic and safety considerations. The complete transition of the SHM technology from research to practice depends deeply on the economical and life safety benefits it can provide (CHANG; FLATAU; LIU, 2003). Besides the main goal to prevent catastrophic failures and the usefulness to evaluate the structure performance, as any investment, the SHM systems must prove to be a manner of reducing the overall life-cycle maintenance costs related to a structure. For example, currently for new bridges, the initial investment of an SHM system ranges between 0.5% and 3% of the total bridge construction cost. Additionally, every year the maintenance and data management typically add 5–20% of the SHM system cost. Thereby, over the first 10 years of a medium-size bridge, the SHM system may require an investment in the order of 4.5–9% of the total construction cost (INAUDI; MANETTI; GLISIC, 2009).

In the light of the above cost estimates, an SHM system must be designed as an integrated system that can be developed and maintained during the construction stage, as well as over the structure lifetime. During the construction stage, the SHM system can potentially be used to supervise the construction and thus put pressure on the contractors to deliver a high-quality product, as well as to support the construction of new lightweight structures. Monitoring during service stage provides information related to structural behavior under predicted loads (also registers the effects of unpredicted overloading). For instance, overviews of the motivations to deploy the SHM systems on bridges are well discussed by several authors (KO; NI, 2005; MAGALHAES; CUNHA; CAETANO, 2012; FIGUEIREDO; MOLDOVAN; MARQUES, 2013; YAPAR et al., 2015).

Therefore, the data obtained by monitoring are useful for damage detection, evaluation of safety and determination of the residual capacity of structures. Incipient damage detection via robust data-based methods – the main goal of this thesis – is particularly important because it leads to appropriate and timely interventions, avoiding refurbishment costs or, in some cases, the closure, dismantling and even collapse of structures.

In Brazil, for example, there have been several cases of structural collapses (as depicted in Figure 2), such as the Guararapes Battle Viaduct (Minas Gerais, 2014) (GLOBO, 2016b), the Bridge over the Aracatú River (Pará, 2014) (GLOBO, 2014), and the Bridge over the Santo Antônio River (Mato Grosso do Sul, 2016) (GLOBO, 2016a). The former collapse occurred during the construction stage of the viaduct (evaluated at that moment in R$ 905 million), killing two people and injuring other twenty-two. In the other cases, although there were no injuries, the collapses blocked the crucial connection between two cities during many days, impacting negatively on the local economy and daily activities. These scenarios demonstrate a clear demand for structural monitoring and incipient damage detection to assist timely maintenance during construction or service.

Figure 2 – Structural collapses in Brazil (from left to right): the Guararapes Battle Viaduct (Minas Gerais, 2014), the Bridge over the Aracatú River (Pará, 2014), and the Bridge over the Santo Antônio River (Mato Grosso do Sul, 2016).

To summarize, even though the main goal of the SHM systems is for incipient damage identification and, ultimately, to prevent catastrophic failures, from a more general perspective, these systems can be designed to:

1. Provide structural monitoring during the construction stage with the potential benefit of reducing manufacturing costs and to permit the construction of lightweight structures by fully exploiting the material strength;
2. Validate design assumptions by measuring the actual structural response, which can be used to improve design specifications for future structures;
3. Detect anomalies and/or damage at early stages;
4. Reduce and/or support visual inspections;
5. Provide the owners with a real-time tool to support the decision-making process, i.e., reduce unnecessary ad hoc maintenance, extend the structures' lifetime by preventive maintenance, and reduce downtime costs, traffic management and control;
6. After extreme events, such as earthquakes and blast loading, the SHM systems can be used for condition assessment regarding the integrity of the structure;
7. Finally, the main goal to deploy the SHM systems in engineering structures will always be to prevent catastrophic failures.

1.3 Problem

SHM performs the continuous monitoring of damage-sensitive features which are responsive to a certain type of structural damage. Among several feasible features (see section 2.4), the natural frequencies are usually considered, as they are intrinsically related to the global and local stiffness of a monitored structure.

Through the monitoring of damage-sensitive features over time structural damage can be detected. However, in real-world SHM applications, this approach requires some precaution to be applied because of two drawbacks. Firstly, many features are not measured directly, instead they are estimated from monitoring data using feature extraction techniques. Natural frequencies, for example, can be estimated from vibration response measurements, such as accelerations, which may introduce estimation errors. Secondly, almost all features are sensitive not only to changes caused by structural damage but also to changes in temperature, traffic loading, wind speed or relative humidity. These problems highlight that, in practical SHM solutions, the accuracy of the estimated features and the operational and environmental variability should be accounted for. In this thesis, the main focus is on the second problem.

When the environmental variability on features is considered, an important issue is that the changes in environmental conditions are much slower than the lowest structural eigenperiod for fixed conditions (REYNDERS; WURSTEN; ROECK, 2014). If a structure is monitored for a short period of time (seconds or minutes), it acts as a linear time-invariant system. This structural dynamics behavior may change when a long-term monitoring (hours, days, months or years) is performed, i.e., becomes a time-varying system. The variations in temperature can be pointed out as the main cause for this change, due to the nonlinear temperature-stiffness relationships of structural materials.

One of the main real examples presented in literature is the long-term monitoring performed in the Z-24 Bridge, subjected to environmental variability (ROECK, 2003). The damage-sensitive features extracted from vibration response measurements of the Z-24 Bridge were natural frequencies which combine one-year monitoring of the healthy condition, influenced by operational and environmental variability, with realistic damage scenarios. As demonstrated in Figure 3, the first 3470 observations correspond to the features extracted within the undamaged condition under operational and environmental variability. The last 462 observations correspond to the damage progressive testing period, which is highlighted, especially in the second frequency, by a clear decay in the magnitude of this frequency.

For the baseline condition period of the Z-24 Bridge, the observed jumps in the natural frequencies are associated to the asphalt layer in cold periods, which contributes significantly to the stiffness of the bridge, as evidenced in Figure 3. This fact indicates the need for a data normalization procedure (see subsection 2.5.1) to attenuate environmental variability, i.e., a means of removing the normal influences on features. Note that in this case, the changes caused by temperature are larger compared to those caused by damage. If not properly accounted for, changes in the structural response characteristics caused by temperature can, potentially, result in false indications of damage.

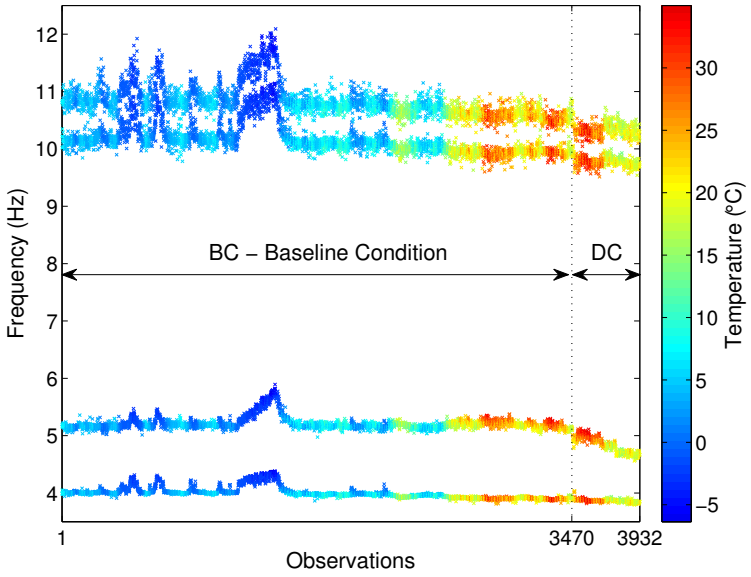

Figure 3 – Influence of temperature on the first four natural frequencies of the Z-24 Bridge: 1–3470 baseline condition (BC) and 3471–3932 damaged condition (DC).

Currently, there are two data-driven approaches to separate changes in features caused by operational and environmental influences from those caused by damage. The first approach, also known as input-output, consists of measuring the parameters related to operational and environmental variations, such as traffic loading, temperature, wind speed or relative humidity, as well as the structural response at different locations. Then, a data-driven (or black-box) model can be identified with these parameters as inputs and the corresponding features as outputs, i.e., the features corresponding to the normal condition can be parametrized as a function of the measured operational and environmental conditions (PEETERS; ROECK, 2001; NI et al., 2005). However, a major challenge with this approach is to determine which operational and environmental influences should be measured and where the corresponding sensors should be placed.

As an alternative, the second approach, also known as output-only, and the one used in this thesis, consists of applying the machine learning algorithms to develop data-driven models that assess the influence of operational and environmental variability on damage-sensitive features, i.e., only through features extracted from the structural response measurements the algorithms can eliminate the undesired normal influences (FIGUEIREDO, 2010). This approach intends to avoid the measure of operational and environmental variations and physics-based approaches (e.g., finite element models) and, therefore, pave the way for output-only data-based models applicable to structural systems of arbitrary complexity.

1.4 Related work

In this section, by considering output-only approaches and unsupervised learning, the state-of-the-art machine learning algorithms and their adaptations for data normalization and damage detection are reviewed and discussed.

1.4.1 Classical methods

Mahalanobis squared-distance (MSD) algorithm is one of the most classical methods for damage detection, having widespread use in real scenarios due to its ability to identify outliers (WORDEN et al., 2007; WORDEN; MANSON, 2007; NGUYEN; CHAN; THAMBIRATNAM, 2014; ZHOU et al., 2015). When abnormal observations appear statistically inconsistent with the rest of the data, it is conjectured that these observations have been generated by an alternative mechanism, which is not related to the normal condition established with a mean vector and a covariance matrix derived from the baseline data sets, obtained under operational and environmental conditions. However, when nonlinearities are present in the undamaged observations, the MSD fails in modeling the normal condition of a structure because it assumes the baseline data modeled by an unique cluster from a multivariate Gaussian distribution.

Kullaa (KULLAA, 1993) proposed to use the factor analysis (FA) algorithm in SHM to eliminate the effects of operational and environmental variations on the damage-sensitive features. Statistically, FA is a multivariate technique used to estimate the linear correlation among a number of observed dependent variables (features) in terms of a small number of unobserved independent variables (or operational and environmental factors). The main challenge associated with the FA-based method is the supposition, in advance, of the number of factors that influence the damage-sensitive features (DERAEMAEKER et al., 2008). Similar to the MSD, this method can not address satisfactorily nonlinearities present in the monitoring data.

In turn, Ruotolo and Surage (RUOTOLO; SURACE, 1999) proposed an output-only data normalization method based on the singular value decomposition (SVD) algorithm. This technique relies on the determination of the rank of a state matrix. If the potential outlier comes from the undamaged condition, it is expected that the rank will not change. On the other hand, if the potential outlier comes from the damaged condition, and it is independent from the others, the rank will be increased. However, when dealing with real-world monitoring data, noise is often present, which may affect the rank and introduce residual singular values (VANLANDUIT et al., 2005).

Another classical output-only technique that has been applied for eliminating operational and environmental influences is the linear principal component analysis (PCA), for which a linear static relationship between the observed features and unknown operational

and environmental factors is estimated and model residuals are then produced to support the damage detection (YAN et al., 2005a; SHAO et al., 2014). In practice, however, for long-term monitoring this relationship is in general nonlinear (PEETERS; ROECK, 2001; PEETERS; MAECK; ROECK, 2001; MOSER; MOAVENI, 2011), demanding other techniques to address this issue.

As an alternative, a piecewise linear relationship between the observed features can be determined by clustering and subsequently the linear PCA is applied for each piece (YAN et al., 2005b; KULLAA, 2006). Unfortunately, this method has narrow applicability because its parameters (e.g., number of nonlinearity tuning points) should be chosen with great care, without an effective criterion, to obtain acceptable results.

In an attempt to accommodate nonlinear environmental effects for improving the feature discrimination process, an auto-associative neural network (AANN), also known as autoencoder, has been proposed (SOHN; WORDEN; FARRAR, 2002; HSU; LOH, 2010; HAKIM; RAZAK, 2014). Leaving aside the sensitivity of neural networks to the initial weights, the AANN suffers with the definition of its architecture composed of three different layers, for which several combinations concerning the number of neurons and initial weights must be performed to select the best model via an information criterion. Similar to the FA, this technique previously assumes the number of factors (usually unknown) that influence the damage-sensitive features.

Figueiredo et al. (FIGUEIREDO et al., 2011) performed a comparison study of several output-only machine learning algorithms for data normalization and damage detection on standard data sets. This study was performed upon experimental vibration monitoring tests in the laboratory using a three-story frame structure with different structural state configurations. The operational and environmental effects were simulated by stiffness or mass changes, while damage was simulated with a bumper mechanism causing a nonlinear effect due to collisions. The four output-only methods chosen were based on the MSD, FA, SVD and AANN algorithms. A prominence of the MSD and AANN algorithms was attested when one wants to minimize false-negative indications of damage, i.e., life-safety is the primary motivation for deploying SHM systems. However, as those data sets were acquired in laboratory conditions, further analysis is required to test their applicability on real-world data sets.

1.4.2 Kernel-based methods

More recently, robust kernel-based methods have been proposed to deal with linear and nonlinear operational and environmental factors aggregated in the features. This has been accomplished by means of support vector machine (SVM) or a generalized nonlinear PCA in a high-dimensional space, which employ a kernel function and solve a simple optimization or an eigenvalue problem in a nonlinear mapped feature space, respectively.

Khoa et al. (KHOA et al., 2014) adapted the one-class SVM algorithm for learning the normal structural condition and detecting possible structural anomalies. This unsupervised method finds a small hyperplane, containing most of the undamaged observations and the anomalies elsewhere, by mapping observations into a high-dimensional feature space using a kernel and thereafter separating them from the origin with maximum margin. However, in this study, the parameters related to the bandwidth of the kernel and regularization should be provided by the user, i.e., there is no heuristic to automatically define these parameters, which naturally influence the quality of the results.

As a nonlinear version of the PCA, the kernel principal component analysis (KPCA) has been used for data normalization in changing operational and environmental conditions (OH; SOHN; BAE, 2009; CHENG et al., 2015; YUQING et al., 2015), revealing the nonlinear correlations present in the extracted features through a nonlinear mapping from an original space into a possible very high-dimensional space. After the nonlinear projection, the linear PCA is applied in the mapped feature space to retain the principal components that explain the variability in the data. In opposition to the AANN, as a kernel function is used, the type of nonlinearity is not explicitly defined and the KPCA is computationally very robust and efficient. However, again, this version of KPCA requires the specification by the user of two crucial parameters; the bandwidth of the kernel and a minimal percentage of the variance to explain the variability in the data, i.e., the number of principal components retained in the high-dimensional feature space.

An improved output-only method based on the KPCA was proposed by Reynders et al. (REYNDERS; WURSTEN; ROECK, 2014) for eliminating nonlinear environmental and operational influences on the monitored features. It was based on Gaussian KPCA, where the two parameters of the learned model are automatically determined. The first parameter, which represents the bandwidth of the Gaussian kernel, is chosen based on the maximization of Shannon's information entropy from the kernel matrix. The second parameter, which corresponds to the number of principal components in the high-dimensional feature space, is selected in such a way that the retained principal components account for nearly all normal environmental and operational variability. Although, this technique achieved satisfactory results for data normalization and can be easily adapted for damage detection, it also revealed some loss of information as the principal components are retained based on 99% of the data variability. This ensures only the fitting of a fraction of the normal condition under operational and environmental effects.

1.4.3 Cluster-based methods

Linear output-only methods to model nonlinearities in long-term monitoring of structures have been developed by means of a new concept based on a two-step strategy (FIGUEIREDO et al., 2012): (i) data normalization procedure by clustering the training observations into different data clusters and (ii) damage detection by identifying possible outliers through a distance metric between the learned clusters and a new observation.

In the study performed by Figueiredo and Cross (FIGUEIREDO; CROSS, 2013), an approach based on Gaussian mixture models (GMMs) is applied to model the main clusters that correspond to the normal or undamaged state conditions of a structural system, even when it is affected by unknown operational and environmental effects. The parameters of the GMMs are estimated from the training data, using the classical maximum likelihood (ML) estimation based on the expectation-maximization (EM) algorithm. Afterwards, the damage detection is performed on the basis of multiples MSD algorithms regarding the chosen clusters of main states. This method outperforms the MSD, AANN and PCA algorithms for damage detection when nonlinear environmental effects are presented in the measured vibration data from the Z-24 Bridge. However, the performance of the EM algorithm was shown to be strongly affected by the initial parameters.

The drawback highlighted above is also discussed by Kulla (KULLAA, 2014), where an approach, composed of GMMs, local linear models using minimum mean square error, PCA and control charts, is used to eliminate the underlying effects and detect damage from the residuals between the monitoring data and the identified model. The main disadvantages are: the EM algorithm is not guaranteed to find the global maximum; and the training phase is quite slow because it is advised to run this algorithm a couple of times with different initial parameters to find, without any guarantee, a satisfactory maximum. In consequence, this degenerated behavior of the EM algorithm may affect the stability of the results and the number of data clusters estimated for each different run.

To improve the parameter estimation of the finite mixture of Gaussian distributions, Figueiredo et al. (FIGUEIREDO et al., 2014) presented a Bayesian approach based on a Markov-chain Monte Carlo (MCMC) method to cluster structural responses into a reduced number of global state conditions, by taking into account eventual multimodality and heterogeneity of the data distribution. This approach showed some improvement over the classical ML estimation based on the EM algorithm. The Bayes approach has the advantage of providing an estimate of the marginal likelihood by an integration of the likelihood function over all possible parameters. However, in terms of damage-detection performance, both methods (GMM with EM and GMM with MCMC) achieved the same results considering the data sets used in (FIGUEIREDO et al., 2014).

1.5 Justification

In the above section, the advantages and limitations of several output-only methods (some of them are presented in more detail in subsection 2.5.1) were discussed in the context of data normalization and damage detection for SHM. In general, the methods based on nonlinear or cluster assumptions were most prominent to deal with challenging SHM scenarios under operational and environmental variability. However, these state-of-the-art techniques have some limitations related to their working principles, such as some loss of information (e.g., the PCA, FA, KPCA and AANN) or high sensitivity to the chosen initial parameters (e.g., the EM-GMM and MC-GMM). This fact highlights the need for novel methods, as the ones proposed in this study, to overcome these limitations.

Thus, novel output-only methods based on the machine learning and artificial intelligence fields are proposed to detect incipient or progressive structural damage. These techniques allow to learn the undamaged condition of a structure by considering all normal variability, without loss of information or sensitivity to the initial parameters. Since this undamaged model is determined, the proposed methods can discriminate the actual condition of the structure (i.e., undamaged or damaged) with high stability and reliability.

The improvement on the estimation of the normal condition and damage detection provided by the development of these new methods is critical for current SHM solutions, as much attention has been paid on the declining state of the aging infrastructure around the world. This concern applies not only to civil infrastructures, such as bridges, highways, and buildings, but also to other types of structures, such as aircraft. The ability to continuously assess the integrity of engineering structures in real time offers the opportunity to reduce maintenance and inspection costs, while providing increased safety to the public. Addressing these issues is the goal of this thesis.

In addition, the novel methods coupled with the SHM systems can also contribute to the aid of visual inspections. For instance, the bridge management systems (BMSs) still depend deeply on sporadic structural inspections, especially on the qualitative and not necessarily consistent or reliable visual inspections, which may impact the structural evaluation and, consequently, the maintenance decisions to avoid structural collapses (FIGUEIREDO; MOLDOVAN; MARQUES, 2013). In a cooperative sense, the SHM can aid the structural management with more reliable and quantitative information processed through data-based methods. Theses techniques are capable of reducing the global state conditions of a structure into, for example, a daily indicator that quantifies the damage level according to a predetermined threshold.

1.6 Objectives

In the hierarchical structure of damage identification, this thesis addresses the need for robust vibration-based damage detection methods. Therefore, this study is mainly concerned with detection of damage in engineering structures. Although locating and assessing the severity of damage are important in terms of estimating the residual lifetime of structures, the complete and reliable detection of damage existence must precede these more detailed damage descriptions. Damage quantification is also a final result provided by the damage detection process.

The general objective of this thesis is to adapt, develop, and apply several output-only methods for statistical modeling and feature classification, in the context of the SPR paradigm for SHM, capable of detecting and quantifying damage on structures under unmeasured operational and environmental influences. To achieve this general objective, particular objectives are addressed:

- Adapt unsupervised algorithms from the machine learning field as data normalization approaches, combining them with statistical distance metrics as a means of detecting and quantifying structural damage;
- Develop novel output-only methods based on the machine learning and artificial intelligence fields to establish the normal condition of structures and detect damage under operational and environmental conditions, such that these approaches can be applied to engineering infrastructure of arbitrary complexity;
- To test the performance of adapted and novel methods, as well as to compare them to state-of-the-art methods, the approaches are first applied on standard data sets measured from a laboratory structure and afterwards on response data from real-world structures – the Z-24 and Tamar Bridges.

Note that the novel output-only methods developed in this study can be applied in any (e.g., civil, mechanical or aerospace) engineering structure. However, the data sets available to test the damage detection performance of these methods are only from civil engineering infrastructures.

1.7 Original contributions

This thesis is a contribution to output-only data-based methods, with emphasis on the statistical modeling development for feature classification, which includes data normalization and damage detection. The following content attempts to highlight the original contributions of the papers (Appendices from A to F) which compose this study.

In Appendices A and E, several machine learning algorithms based on kernel assumptions are adapted to work as data normalization procedures to support damage detection and quantification via statistical distance metrics. The methods are based on the one-class SVM, support vector data description (SVDD), KPCA, greedy KPCA (GKPCA), and mean shift clustering (MSC) algorithms.

Particularly, in Appendix A, the main contribution is the adaptation of the proposed kernel-based algorithms for damage detection. Specifically, other contributions are: the first-known adaptation of two algorithms (the KPCA and GKPCA) for damage detection in the SHM field; and the combination between other two algorithms (the one-class SVM and SVDD) and an outlier detection method (the MSD) for data normalization purposes in the SHM field. In a different manner, in Appendix E, the MSC-based method is presented to discover the number of clusters that correspond to the normal state conditions of a structure. The main contribution is that the method is a nonparametric technique that does not require prior knowledge of the number of clusters and can identify groups of distinct shapes, sizes and density. This reliable estimation enhances the subsequent damage detection process.

Novel nonparametric methods are proposed in Appendices B and F to support the structural damage detection process, in the presence of linear and nonlinear effects caused by operational and environmental variability. A genetic algorithm for decision boundary analysis (GADBA) is described in Appendix B as a technique which searches for an optimal number of clusters in the feature space, representing the main state conditions of a structural system. This genetic-based clustering approach is supported by a novel concentric hypersphere algorithm to regularize the number of clusters and mitigate the cluster redundancy. An improved and simplified version of this method is highlighted in Appendix F as an agglomerative clustering procedure, the agglomerative concentric hypersphere (ACH), to automatically discover the optimal number of clusters as a means to assist the damage detection and quantification in engineering structures. This straightforward method does not require any input parameter, except the training data.

As an attempt to add quantitative information from the SHM systems into the visual inspections and to assess the structural integrity, in Appendices C and D, two novel methods are proposed based on the memetic algorithm (MA) theory supported by a genetic algorithm (GA) and a particle swarm optimization (PSO). They are stable and reliable versions of the classical EM-GMM, also known as the global EM-PSO (GEM-PSO) and EM-GA (GEM-GA) approaches. Thus, the main contribution of these two methods is the high reproducibility on the estimation of the normal structural condition by clustering and damage-detection results, regardless of the choice of initial parameters. The bioinspired hybridization between a local search method (the EM algorithm) and a global search method (the GA or PSO) avoids unfeasible solutions such as the ones

produced in different executions by the EM-GMM or MC-GMM approaches.

Furthermore, for the cluster-based methods proposed herein, another contribution is related to the physical interpretations about the undamaged condition under normal variability. The discovered clusters allow a better understanding of the operational and environmental sources of variability, as demonstrated in Appendices E and F.

When the novel methods are compared to the state-of-the-art ones, they clearly demonstrate their superiority in terms of data normalization and damage detection on laboratory and real-world data sets. Nevertheless, a comparison between the proposed methods is imperative to derive more conclusions related to their applicability on real-world SHM applications. This comparison is highlighted in chapter 3 with these methods applied on natural frequencies from the Z-24 Bridge, where a wide spectrum of challenges encountered in practical SHM problems were presented.

1.8 Organization of the thesis

The remainder of this thesis by papers is organized as follows. The SPR paradigm for SHM considered in this study is discussed in chapter 2, highlighting all phases of this paradigm with their advantages, limitations and challenges as well as providing the necessary background related to the state-of-the-art approaches for data normalization and structural damage detection. Taking into account the background presented in the previous chapter, the novel output-only methods proposed in this thesis are summarized and evaluated in chapter 3 (a complete version of them can be found in Appendices from A to F). Finally, chapter 4 synthesizes the main conclusions and contributions of this study, as well as points out future research topics.

2 Statistical pattern recognition paradigm for structural health monitoring

This chapter is concerned with the discussion of the SPR-SHM phases, as well as other background issues, presenting the main challenges associated to each phase. Thus, the issues related to operational evaluation and data acquisition are briefly highlighted. Feature extraction techniques used in this study are presented in terms of advantages and limitations. Finally, a major focus is given to the statistical modeling for feature classification: output-only machine learning algorithms for data normalization and damage detection based on residual errors or central Chi-square hypothesis. The methods based on the MSD, PCA, AANN, KPCA and GMMs algorithms are considered, because they are the basis for the understanding of novel methods proposed in this thesis.

2.1 Main objective of the paradigm

In this study, the output-only approaches to SHM presented in section 2.5 are posed in the context of a pattern recognition problem. Thereby, the SPR paradigm for the development of the SHM systems and solutions, SPR-SHM, can be described as a four-phase process (FARRAR; DOEBLING; NIX, 2001), as illustrated in Figure 4.

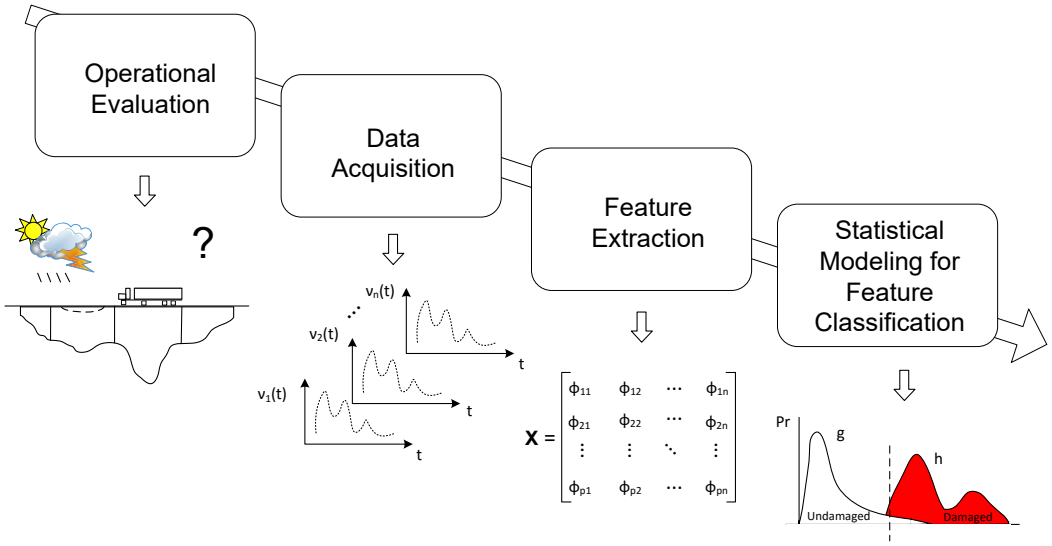

Figure 4 – The SHM process based on the SPR paradigm (FIGUEIREDO, 2010).

In the context of the SHM applications, the main objective of the SPR paradigm is to recognize and distinguish between the patterns related to an undamaged structure under operational and environmental influences and those associated to the same structure under the damaged condition. This process starts from sensor measurements of the monitored structure and ends with the assessment of the actual structural condition.

2.2 Operational evaluation

An important first phase for developing the SHM capability is to perform an operational evaluation. This part of the SHM process attempts to answer four essential questions regarding the implementation of an SHM system (FARRAR; WORDEN, 2007):

- What are the life safety and/or economic justifications for monitoring the structure?
- How is damage defined for the structural system being monitored?
- What are the operational and environmental conditions under which the structural system of interest operates?
- What are the limitations on acquiring data in the operational environment?

The operational evaluation phase defines, and to the greatest extent possible quantifies, the damage that should be identified. It also establishes the benefits to be gained from the deployment of the SHM system. This process also begins to impose limitations on what will be monitored and how to perform this task, as well as adapting the SHM system to the unique aspects of the chosen structure and unique characteristics of the damage that should be identified and analyzed.

The main challenges of the operational evaluation phase are presented in the following:

- Most high-capital-expenditure engineering structures, such as bridges, are one-of-a-kind systems, influenced by the physical environment where they are built; therefore, it is more difficult to incorporate lessons learned from other nominally similar structural systems to define anticipated damage;
- Structural designs are often driven by low-probability, but extreme-impact events, such as earthquakes, hurricanes, terrorist actions or floods;
- Generally, the structural systems degrade slowly under normal use: corrosion and fatigue cracking, freeze-thaw/thermal damage, loss of pre-stressing forces, vibration-induced connectivity degradation, and hydrogen enbrittlement;

- There is no widely accepted procedure yet to demonstrate the rate of return of the investment in an SHM system.

2.3 Data acquisition

The data acquisition phase of the SHM process, based on the SPR paradigm, involves selecting the excitation methods; the sensor types, numbers, and locations; and the data acquisition/storage/processing/transmittal hardware. The interval at which the data should be collected (e.g., daily or hourly) is another consideration that must be addressed. The actual implementation of the data acquisition systems is application-specific, where economic issues play a fundamental role in making the aforementioned choices (GLISIC; INAUDI, 2007).

A crucial premise regarding sensing and data acquisition is that these systems do not measure damage. Rather, they measure the response of a structure to its operational and environmental conditions or the response to inputs from actuators embedded with the sensing system (WORDEN; DULIEU-BARTON, 2004). Depending on the sensing technology and the type of damage to be identified, the sensor readings may be more or less directly correlated to the presence and location of damage. Data interrogation procedures (feature extraction and statistical modeling for feature classification) are necessary components of an SHM system. They convert the sensor data into information about the structural condition. Moreover, to achieve successful SHM, the data acquisition systems have to be developed in conjunction with these procedures.

The main challenges of the data acquisition phase are listed below:

- Currently, there is no sensor that measures damage. However, it is not possible to implement the SHM process without sensing;
- Definition of the data to be acquired and the data to be used in the feature extraction process: types of data to be acquired, sensor types and locations, bandwidth and sensitivity (e.g., dynamic range), data acquisition/transmittal/storage system, power requirements (e.g., energy harvesting), sampling frequencies, processor/memory requirements, excitation source (e.g., active sensing), and sensor diagnostics;
- Number of sensors. Instrumenting large structures with lots of sensors still represents a sparsely instrumented system. Large sensor systems pose many challenges for reliability and data management;

- Ruggedness of sensors. Sensing systems must last for many years with minimal maintenance. The existence of harsh environments (e.g., thermal, mechanical, moisture, radiation, and corrosion) compromises the sensor durability. Need of sensor diagnostic capability;
- The sensing system must be developed integrally with the feature selection and extraction as well as feature classification.

2.4 Feature extraction

A damage-sensitive feature is some quantity extracted from the structural response data which is correlated with the presence of damage in a structure, such as modal parameters (REYNDERS, 2012), quasi-static strains (GLISIC; INAUDI, 2012), auto-regressive model parameters and residual errors (FIGUEIREDO et al., 2011), local flexibilities (REYNDERS; ROECK, 2010), and electromechanical impedances (BAPTISTA; FILHO; INMAN, 2012). Ideally, a damage-sensitive feature will change in some consistent manner as the level of damage increases. Identifying features that can accurately distinguish a damaged structure from its undamaged condition is the focus of most SHM technical literature. Fundamentally, the feature extraction process is based on fitting some model, either physics- or data-based, to the measured response data. The parameters of the models, or the predictive errors associated with them, become the damage-sensitive features. An alternative approach is to identify features that directly compare the sensor waveforms (e.g., influence lines and acceleration time series) or spectra of these waveforms (e.g., power spectra density) measured before and after damage. Many of the features identified for impedance- and wave propagation-based SHM studies fall into this category (KESSLER; SPEARING; SOUTIS, 2002; PARK HOON SOHN; INMAN, 2003; IHN; CHANG, 2004; SOHN et al., 2004).

In the feature extraction phase, it is imperative to derive damage-sensitive features correlated with the severity of damage present in a monitored structure, minimizing false judgements in the following classification phase. Nevertheless, in real-world SHM applications, operational and environmental effects can mask damage-related changes in the features as well as alter the correlation between the magnitude of the features and the level of damage. Commonly, the more sensitive a feature is to damage, the more sensitive it is to changing in the operational and environmental conditions (e.g., temperature or wind speed). To overcome this impact, robust feature extraction procedures are usually required (MATTSON; PANDIT, 2006; FIGUEIREDO et al., 2010; FIGUEIREDO, 2010) and the primary properties of damage-sensitive features are defined as follows:

- *Sensitivity* – a feature should be sensitive to damage and completely insensitive to everything else, which rarely occurs in practical SHM applications.

- *Dimensionality* – a feature vector should have the lowest dimension without significant loss of information; high dimensionality induces undesirable complexity into the statistical models and storage mechanisms.
- *Computational requirements* – minimal assumptions and minimal processor cycles, which facilitates the embedded systems.
- *Consistency* – feature's magnitude should change monotonically with damage level.

One wants to use the simplest feature to distinguish between the undamaged and damaged conditions of a structure. However, there are a couple of challenges for feature selection and extraction, as described below:

- Feature selection is still based almost exclusively on engineering judgement;
- Quantifying the features' sensitivity to damage;
- Quantifying how the feature changes with the level of damage;
- Understanding how the feature varies with changing operational and environmental conditions.

For completeness, this section briefly reviews the theory behind of some of the widely feature extraction techniques used in different engineering fields, based on time and frequency domain analysis. It is shown that the appropriate sort of feature to use is damage-specific, and so each feature has its advantages and limitations regarding its sensitivity to a particular type of damage. Notice that this section intends to summarize some advantages and limitations of the feature extraction techniques used in this thesis, rather than showing all possible techniques presented in the SHM literature.

2.4.1 Modal parameters

Modal parameters as damage-sensitive features have been widely used in several SHM studies. The motivation behind this approach is that the modal parameters (natural frequencies, damping ratios, mode shapes, and modal scaling factors) extracted from monitoring data are strongly correlated to the physical properties of structures (mass, damping and stiffness). Therefore, any changes in the physical properties caused by structural damage will result in changes in the modal parameters. The theory behind the modal parameters has been extensively discussed in the literature related to operational modal analysis. Thus, the author recommends further reading (REYNDERS, 2012).

The most prominent dynamic system identification techniques for modal analysis are: classic and reference-based stochastic subspace identification (SSI), considering both data-driven and covariance-driven versions (PEETERS; ROECK, 1999); SSI with variance estimation (REYNDERS; PINTELON; ROECK, 2008); classic and reference-based combined deterministic-SSI (REYNDERS; ROECK, 2008); and frequency response function (GUILLAUME; PINTELON; SCHOUKENS, 1992; SAMPAIO; MAIA; SILVA, 1999; MAIA et al., 2003). Depending on the system identification method used, the modal parameter estimation can be performed, for instance, via peak picking or stabilization diagram strategy (PEETERS, 2000; REYNDERS; HOUBRECHTS; ROECK, 2012).

The applicability of the modal parameters as damage-sensitive features is subject to the operational and environmental variability, which may cause changes in the modal parameters and mask the changes resulting from damage (KIM et al., 2003; XIA et al., 2006; SOYOZ; FENG, 2009). Additionally, in many cases, modal parameters do not have the required sensitivity to small cracks in a structure (FARRAR; DOEBLING, 1997).

2.4.2 Autoregressive model

Usually, for various applications in the SHM field, the modal parameters have been used as features that characterize the global condition of structures. However, in this study, the AR model can also be used to extract damage-sensitive features, because the underlying linear stationary assumption makes it possible to detect the presence of damage state conditions as nonlinearities in the time-series. It is considered that in a structural system where different dynamics are present at different times, the estimated parameters should change between intervals (KANTZ; SCHREIBER, 2003).

Alternatively, the AR models have been also used in the SHM field to extract damage-sensitive features from time-series data, either using the model parameters or residual errors (FIGUEIREDO et al., 2011; YAO; PAKZAD, 2012). For a measured time-series $s_1, s_2, ..., s_N$ the AR(p) model of order p is given by:

$$s_i = \sum_{j=1}^{p} \phi_j s_{i-j} + e_i, \tag{2.1}$$

where s_i is the measured signal and e_i is an unobservable random error at discrete time index i. The unknown AR parameters, ϕ_j, can be estimated using the least squares or the Yule-Walker equations (BOX; JENKINS; REINSEL, 2008). The order of the model is always an unknown integer that needs to be estimated from the data. The Akaike information criterion (AIC) has been reported as one of the most efficient techniques for order optimization (KOTHAMASU et al., 2004). The AIC is a measure of the goodness-of-fit of an estimated statistical model that is based on the tradeoff between fitting accuracy

and number of estimated parameters. In the context of AR models:

$$\mathrm{AIC} = N_t \ln(\varepsilon) + 2N_p, \tag{2.2}$$

where N_p is the number of estimated parameters, N_t is the number of predicted data points, and $\varepsilon = SSR/N_t$ is the average sum-of-square residual (SSR) errors. The AR model with the lowest AIC value gives the optimal order p.

The appropriate order estimation of an AR model remains a very complex issue. A high-order model may better fit the training data, but may not generalize well to other test data sets. On the other hand, a low-order model may not necessarily capture the underlying physical system dynamics.

2.5 Statistical modeling for feature classification

The development of statistical models to enhance the damage detection process is the phase concerning the implementation of machine learning algorithms to normalize the monitoring data and to analyze the distributions of the extracted features in an effort to determine the structural condition. Even though several statistical modeling approaches have been proposed in the literature, this section only makes reference to the state-of-the-art ones used in this study. Herein, the unsupervised algorithms described in subsection 2.5.1 are used for outlier detection based on residuals errors or central Chi-square hypothesis. Additionally, the performance evaluation of feature classification for damage detection is described on the basis of Type I/Type II error tradeoffs.

2.5.1 Machine learning algorithms for data normalization

The data normalization procedure is fully connected to the data acquisition, feature extraction and statistical modeling phases of the SHM process. This procedure includes a wide range of steps for mitigating (or even removing) the effects of operational and environmental variations on the extracted features. It is also used for separating changes in features caused by damage from those caused by operational and environmental influences (SOHN; WORDEN; FARRAR, 2002). This procedure often contributes significantly to the structural damage detection process.

In the SPR-SHM, the objective of the machine learning algorithms is to enhance the damage detection in the presence of varying operational and environmental conditions under which the structural response is measured (FARRAR; WORDEN, 2013). Several output-only methods have been reported in the literature related to the data normalization procedure and damage detection (FIGUEIREDO et al., 2011; SANTOS et al., 2016). However, in this study, only the methods based on the MSD, PCA, AANN, KPCA and

GMMs algorithms are considered, because they are the basis for the understanding of novel methods proposed in Appendices from A to F. These state-of-the-art algorithms are designed and developed in such a way that their performance is improved based on the analysis of normal condition data, i.e, they learn from data acquired under operational and environmental conditions and when the structure is supposed to be undamaged.

Basically, these output-only methods develop a functional relationship that models how changing operational and environmental conditions influence the underlying distribution of the damage-sensitive features (WORDEN; MANSON, 2007). When subsequent features are analyzed with these methods and a new set of features are shown not to fit into an appropriate distribution, they might be more confidently classified as outliers or, potentially, features from a damaged structure, because the operational and environmental influences have been incorporated into the learning procedure.

Although the methods have different underlying mathematical formulations, they are implemented in a common sequence of steps. First, each algorithm is trained and its parameters are adjusted using features extracted from the normal condition. Second, in the test phase, the methods (with exception of the MSD- and GMM-based ones) transform each new input feature vector into an output residual vector of the same dimension.

For general purposes, one should consider a training data matrix composed of normal condition data, $\mathbf{X} \in \mathbb{R}^{m \times n}$, with n-dimensional feature vectors from m different operational and environmental conditions when the structure is undamaged and a test data matrix, $\mathbf{Z} \in \mathbb{R}^{l \times n}$, where l is the number of feature vectors from the undamaged and/or damaged conditions. In this context, a feature vector (or an observation) represents some property of the structural system at a given time.

2.5.1.1 Mahalanobis squared-distance

The Mahalanobis distance differs from the Euclidean distance because it takes into account the correlation between the features and does not depend on the scale of them. Considering the training matrix $\mathbf{X}$ with multivariate mean vector, $\boldsymbol{\mu}$, and covariance matrix, $\boldsymbol{\Sigma}$, the MSD (or damage indicator, DI, in the context of this study) between the feature vectors of the training matrix and any new feature vector (or observation) from the test matrix $\mathbf{Z}$ is defined as (WORDEN; MANSON; FIELLER, 2000)

$$\mathbf{d}^2 = (\mathbf{z} - \boldsymbol{\mu})^T \boldsymbol{\Sigma}^{-1} (\mathbf{z} - \boldsymbol{\mu}) . \tag{2.3}$$

The assumption is that if a new observation $\mathbf{z}$ is obtained from data collected on the damaged condition, which might include sources of operational and environmental variability, the observation is further from the mean of the normal condition. On the other hand, if an observation is obtained from a structure within its undamaged condition, even

with operational and environmental variability, this feature vector is closer to the mean of the normal condition.

2.5.1.2 Principal component analysis

PCA is a linear method for mapping multidimensional data (input space) into a lower dimension (feature space) with minimal loss of information (JOLLIFFE, 2002). Herein, PCA is used as a data normalization method as follows (YAN et al., 2005a). Assuming the training data matrix $\mathbf{X}$ decomposed in the form of

$$\mathbf{X} = \mathbf{T}\mathbf{U}^T = \sum_{i=1}^{n} \mathbf{t}_i \mathbf{u}_i^T, \tag{2.4}$$

where $\mathbf{T}$ is the scores matrix and $\mathbf{U}$ is a set of n orthogonal vectors, $\mathbf{u}_i$, also called the loadings matrix. The orthogonal vectors can be obtained by decomposing the covariance matrix of $\mathbf{X}$ in the form of $\mathbf{\Sigma} = \mathbf{U}\mathbf{\Lambda}\mathbf{U}^T$, where $\mathbf{\Lambda}$ is a diagonal matrix containing the ranked eigenvalues λ_i, and $\mathbf{U}$ is the matrix containing the corresponding eigenvectors. The eigenvectors associated with the higher eigenvalues are the principal components of the data matrix and they correspond to the dimensions that have the largest variability in the data. Basically, this method permits one to perform an orthogonal transformation by retaining only the principal components r ($\leq n$), also known as the number of factors (DERAEMAEKER et al., 2008). Precisely, choosing only the first r eigenvectors, the final matrix can be rewritten without significant loss of information as

$$\mathbf{X} = \mathbf{T}_r \mathbf{U}_r^T + \mathbf{E} = \sum_{i=1}^{r} \mathbf{t}_i \mathbf{u}_i^T + \mathbf{E}, \tag{2.5}$$

where $\mathbf{E}$ is the residual matrix resulting by the r factors. The coefficients of the linear transformation are such that if the feature transformation is applied to the data set and then reversed, there will be a negligible difference between the original and reconstructed data. The r factors can be automatically estimated by test the minimal percentage of the variance Γ (usually from 0.9 to 0.95) to explain the variability in the matrix $\mathbf{X}$

$$\Gamma \leq \frac{\sum_{i=1}^{r} \lambda_{i,i}}{\sum_{i=1}^{n} \lambda_{i,i}}. \tag{2.6}$$

In the context of data normalization, the PCA algorithm can be summarized as follows: the loadings matrix, $\mathbf{U}$, is obtained from $\mathbf{X}$, the test matrix $\mathbf{Z}$ is mapped onto the feature space $\mathbb{R}^r$ and reversed back to the original space $\mathbb{R}^n$, the residual matrix $\mathbf{E}$ is computed as the difference between the original and the reconstructed test matrix

$$\mathbf{E} = \mathbf{Z} - (\mathbf{Z}\mathbf{U}_r)\,\mathbf{U}_r^T. \tag{2.7}$$

2.5.1.3 Auto-associative neural network

The AANN, also known as nonlinear PCA, is trained to characterize the underlying dependency of the identified features on the unobserved operational and environmental factors by treating this unobserved dependency as hidden intrinsic variables in the network architecture (HSU; LOH, 2010). As illustrated in Figure 5, the AANN architecture consists of three hidden layers: mapping, bottleneck, and de-mapping. The mapping layers consist of hyperbolic tangent sigmoid transfer functions. On the other hand, the bottleneck and output layers are formed with linear transfer functions. More details on the network, including the number of nodes to use, can be found in the reference (KRAMER, 1991).

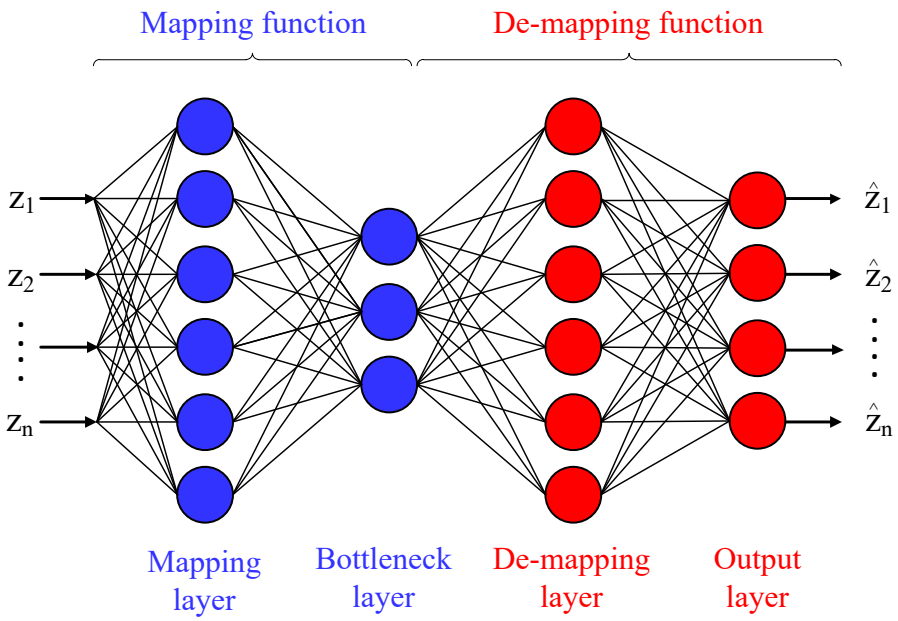

Figure 5 – Standard architecture of the AANN.

In the context of data normalization for SHM, the AANN is first trained to learn the correlations between features from the training matrix $\mathbf{X}$. Then the network should be able to quantify the unmeasured sources of variability that influence the structural response. This variability is represented at the bottleneck output, where the number of nodes (or factors) should correspond to the number of unobserved independent factors

that influence the structural response (SOHN; WORDEN; FARRAR, 2002). Second, for the test matrix $\mathbf{Z}$, the residual matrix $\mathbf{E}$ reads

$$\mathbf{E} = \mathbf{Z} - \hat{\mathbf{Z}}, \tag{2.8}$$

where $\hat{\mathbf{Z}}$ corresponds to the estimated feature vectors that are the output of the network. Assuming that the network is trained with the normal condition data, the residuals will grow when the features which are fed to the network come from the damaged condition, otherwise $\mathbf{z} \approx \hat{\mathbf{z}}$ (undamaged).

This type of network is related to a nonlinear PCA, where the target outputs are simply the inputs of the network. Thereby, the method presented herein is a mixture of two different learning approaches, i.e., supervised learning is used to quantify the operational and environmental conditions dependency although without direct measure of these conditions, while unsupervised learning is used to detect damage. A key issue is to appropriately define the number of nodes in the bottleneck layer, which depends on the independent sources of variability present in the structural response measurements and influences the damage detection performance.

2.5.1.4 Kernel principal component analysis

The KPCA method extends the standard linear PCA for dimensionality reduction in a very high-dimensional space (SCHOLKOPF; SMOLA; MULLER, 1998). This algorithm identifies a nonlinear model by fitting it to the features during a phase in which the structure is undamaged. Afterwards, the structure is monitored by comparing the model predictions with the observed features (REYNDERS; WURSTEN; ROECK, 2014).

Basically, for a feature vector f ($f = 1, 2, \ldots, l$), the part of the residual that is uncorrelated with the unknown operational and environmental variability is

$$\mathbf{e}_f = \mathbf{U}_2 \mathbf{U}_2^T \mathbf{\Phi}\left(\mathbf{z}_f\right), \tag{2.9}$$

where $\mathbf{U} = [\mathbf{U}_1\ \mathbf{U}_2]$ is the eigenvectors matrix partitioned into $\mathbf{U}_1$ that contains the r largest eigenvectors and $\mathbf{U}_2$ that comprises the $(m - r)$ shortest eigenvectors. These eigenvectors are derived from an eigenvalue decomposition of the mapped output correlation during the training phase. A nonlinear mapping of the output sequence, $\mathbf{z}_f$, onto a possibly very high-dimensional is represented by $\mathbf{\Phi}\left(\mathbf{z}_f\right)$.

However, two issues arise: the specification of the nonlinear mapping $\mathbf{\Phi}$ and an appropriate input dimension r. The number of principal components, r, to be retained in the high-dimensional can be estimated via Equation 2.6 using the ith diagonal elements of $\mathbf{\Lambda}$. A value of $\Gamma = 0.99$ can be adopted, implying that the model should account for

nearly all normal variability (REYNDERS; WURSTEN; ROECK, 2014). Note that as in KPCA the mapped feature space is very high-dimensional, Γ (or r) might be larger than the values normally used in linear PCA. The issue of specifying $\mathbf{\Phi}$ can be derived by considering that there exists an eigenvector matrix $\mathbf{A}$ for which

$$\mathbf{U} = \tilde{\mathbf{\Phi}}\mathbf{A}, \tag{2.10}$$

where

$$\tilde{\mathbf{\Phi}} := \frac{1}{\sqrt{m}} \left[\mathbf{\Phi}\left(\mathbf{x}_1\right) \ldots \mathbf{\Phi}\left(\mathbf{x}_m\right) \right]. \tag{2.11}$$

Therefore, all relevant solutions are contained in the following standard eigenvalue problem (SCHOLKOPF; SMOLA; MULLER, 1998)

$$\mathbf{K}\mathbf{A} = \mathbf{A}\mathbf{\Lambda}, \tag{2.12}$$

being $\mathbf{\Lambda}$ a diagonal matrix containing the ranked eigenvalues λ_i and $\mathbf{K}$ a kernel matrix denoted as

$$\mathbf{K} := \tilde{\mathbf{\Phi}}^T \tilde{\mathbf{\Phi}} \in \mathbb{R}^{m \times m}. \tag{2.13}$$

In Equation 2.13, the nonlinear mapping $\mathbf{\Phi}$ only appears in inner products of the form $\mathbf{\Phi}\left(\mathbf{x}_i\right)^T \mathbf{\Phi}\left(\mathbf{x}_j\right)$. Thus, a kernel function representation for the inner product reads

$$k\left(\mathbf{x}_i, \mathbf{x}_j\right) := \mathbf{\Phi}\left(\mathbf{x}_i\right)^T \mathbf{\Phi}\left(\mathbf{x}_j\right). \tag{2.14}$$

The well-known kernel trick consists of specifying the kernel $k\left(\mathbf{x}_i, \mathbf{x}_j\right)$ instead of the nonlinear mapping $\mathbf{\Phi}$, which enables to operate in a very high-dimensional feature space. A radial basis function (RBF) or Gaussian kernel is most often applied, as it implicitly defines an infinite-dimensional feature space with a single parameter

$$k\left(\mathbf{x}_i, \mathbf{x}_j\right) = \exp\left(-\frac{\| \mathbf{x}_i - \mathbf{x}_j \|^2}{2\sigma^2} \right), \tag{2.15}$$

where $\sigma > 0$ is the bandwidth of the RBF kernel and can be determined by requiring that the corresponding inner product matrix $\mathbf{K}$ is maximally informative as measured by Shannon's information entropy. A detailed step-by-step to choose the optimal value of σ is described by Reynders et al (REYNDERS; WURSTEN; ROECK, 2014).

Finally, the Euclidean norm of the residual feature vector $\mathbf{e}_f$, which is evaluated with the kernel function only (without carrying out the nonlinear mapping), can be computed as (REYNDERS; WURSTEN; ROECK, 2014)

$$\| \mathbf{e}_f \| = \sqrt{\mathbf{\Phi}\left(\mathbf{z}_f\right)^T \tilde{\mathbf{\Phi}} \mathbf{A}_2 \mathbf{A}_2^T \tilde{\mathbf{\Phi}}^T \mathbf{\Phi}\left(\mathbf{z}_f\right)}, \tag{2.16}$$

being $\mathbf{A}_2$ defined by partitioning $\mathbf{A}$ in the ranked form of

$$\mathbf{A} = \left[\mathbf{A}_1 \ \mathbf{A}_2\right], \ \mathbf{A}_2 \in \mathbb{R}^{m \times (m-r)}. \tag{2.17}$$

2.5.1.5 Gaussian mixture models

First, this method carries out a cluster-based model using GMMs that aim to capture the main clusters of features, which correspond to the normal and stable state conditions of a structure, even when it is affected by extreme operational and environmental conditions. Afterwards, an outlier detection strategy is implemented in relation to the chosen main groups of states (FIGUEIREDO; CROSS, 2013). Basically, the damage detection is performed on the basis of multiples MSD algorithms, where the mean vectors and covariance matrices are obtained from the learned clusters.

A finite mixture model, $p\left(\mathbf{x}|\mathbf{\Theta}\right)$, is the weighted sum of $Q > 1$ clusters $p\left(\mathbf{x}|\boldsymbol{\theta}_q\right)$ in $\mathbb{R}^n$ (MCLACHLAN; PEEL, 2000),

$$p\left(\mathbf{x}|\mathbf{\Theta}\right) = \sum_{q=1}^{Q} \alpha_q p\left(\mathbf{x}|\boldsymbol{\theta}_q\right), \tag{2.18}$$

where $\mathbf{x}$ is an n-dimensional feature vector and α_q corresponds to the weight of each cluster $q = 1, \ldots, Q$. These weights are constrained to be positive $\alpha_q > 0$ with $\sum_{q=1}^{Q} \alpha_q = 1$. For a GMM, each cluster $p\left(\mathbf{x}|\boldsymbol{\theta}_q\right)$ is represented as a Gaussian distribution

$$p\left(\mathbf{x}|\boldsymbol{\theta}_q\right) = \frac{\exp\left\{-\frac{1}{2}\left(\mathbf{x}-\boldsymbol{\mu}_q\right)^T \mathbf{\Sigma}_q^{-1}\left(\mathbf{x}-\boldsymbol{\mu}_q\right)\right\}}{\left(2\pi\right)^{n/2}\sqrt{\det\left(\mathbf{\Sigma}_q\right)}}, \tag{2.19}$$

being each cluster denoted by the parameters $\boldsymbol{\theta}_q = \{\boldsymbol{\mu}_q, \mathbf{\Sigma}_q\}$, composed of the mean vector $\boldsymbol{\mu}_q$ and the covariance matrix $\mathbf{\Sigma}_q$. Thus, a GMM is completely specified by the set of parameters $\mathbf{\Theta} = \{\alpha_1, \alpha_2, \ldots, \alpha_Q, \boldsymbol{\theta}_1, \boldsymbol{\theta}_2, \ldots, \boldsymbol{\theta}_Q\}$.

The EM algorithm is the most common local search method used to estimate the parameters of the GMMs (DEMPSTER; LAIRD; RUBIN, 1977; MCLACHLAN; PEEL, 2000). This method consists of an expectation and a maximization step, which are alternately applied until the log likelihood, $\log p\left(\mathbf{X}|\mathbf{\Theta}\right) = \log \prod_{i=1}^{m} p\left(\mathbf{x}_i|\mathbf{\Theta}\right)$, converges to a

local optimum. The performance of the EM algorithm depends directly on the choice of the initial parameters, $\boldsymbol{\Theta}^{t=0}$, which may imply many replications of this method during an execution without guarantees of acceptable results. To select the best GMM by means of goodness-of-fit and parsimony, the Bayesian information criterion (BIC) is used and minimized (BOX; JENKINS; REINSEL, 2008),

$$\mathrm{BIC} = -2\log p\left(\mathbf{X}|\boldsymbol{\Theta}\right) + \left\{Qn\left[\left(\frac{n+1}{2}\right)+1\right]+Q-1\right\}\log\left(m\right). \tag{2.20}$$

Similar to AIC, BIC uses the optimal log likelihood function value and penalizes for more complex models, i.e., models with additional parameters. The penalty term of BIC is a function of the training data size, and so it is often more severe than AIC.

Since the best model is selected, in the damage detection process, for each observation $\mathbf{z}$, one needs to estimate Q DIs. Particularly, for each main cluster q,

$$\mathrm{DI}_q(\mathbf{z}) = \left(\mathbf{z}-\boldsymbol{\mu}_q\right)\boldsymbol{\Sigma}_q^{-1}\left(\mathbf{z}-\boldsymbol{\mu}_q\right)^T, \tag{2.21}$$

where $\boldsymbol{\mu}_q$ and $\boldsymbol{\Sigma}_q$ represent all the observations from the cluster q, when the structure is undamaged even though under varying operational and environmental conditions. For each cluster q, if a new observation $\mathbf{z}$ is extracted from the same cluster as the undamaged data, then the test statistic MSD will be Chi-square distributed with n degrees of freedom, χ_n^2 (see subsection 2.5.3). Finally, for each new observation, the DI is given by the smallest DI estimated on each cluster,

$$\mathrm{DI}(\mathbf{z}) = \min\left[\mathrm{DI}_1(\mathbf{z}),\ldots,\mathrm{DI}_Q(\mathbf{z})\right]. \tag{2.22}$$

2.5.2 Outlier detection based on residual errors

In the test phase, the data normalization methods presented in subsection 2.5.1, namely based on the PCA, AANN, and KPCA algorithms, output a residual feature vector with dimension equal to the dimension of the input feature vector. For instance, from Equations 2.7, 2.8, and 2.16, a *quantitative measure of damage* for each feature vector can be established in the form of score. Herein, a DI is adopted in the form of the squared root of the sum-of-square errors (Euclidean norm) for each residual feature vector. Thus, a DI for each feature vector f $(f = 1, 2, ..., l)$ of a test matrix $\mathbf{Z}$ is given by

$$\mathrm{DI}(\mathbf{z}_f) = \parallel \mathbf{e}_f \parallel . \tag{2.23}$$

If the feature vector f is related to the undamaged condition, then $\mathbf{z}_f \approx \hat{\mathbf{z}}_f$ and $\mathrm{DI}(\mathbf{z}_f) \approx 0$. On the other hand, if the feature vector comes from the damaged condition, the residual errors increase, and the DI deviates from zero, indicating an abnormal condition in the monitored structure.

To take into account variability, uncertainty, and *to detect or classify* those DIs that significantly deviates from zero, it is necessary to establish confidence intervals. When considerable training data are available from the undamaged condition, one can estimate ad hoc thresholds based on values corresponding to a certain percentage of confidence (for example, 95%) over the training data. Therefore, multivariate outliers are defined as test observations having DIs beyond a specific threshold.

2.5.3 Outlier detection based on central Chi-square hypothesis

The MSD algorithm has been used as a distance measure for multivariate statistics outlier detection. Alternatively, in the outlier detection approach described herein, a hypothesis test can be established, where the null hypothesis, H_0, is the undamaged condition and the alternative hypothesis, H_1, is presumably the damaged condition. To determine whether a feature vector is from a structure within the undamaged condition, a quantitative measure of separation between a new feature vector and an existing distribution is established. In SHM, this value is often referred to as DI. In Equation 2.3 or 2.21, if a multivariate feature vector $\mathbf{z}$ is extracted from the undamaged condition that supposedly corresponds to a multivariate Gaussian random distribution, then the $\mathbf{d}^2$ or DI will be Chi-square distributed with n degrees of freedom

$$\mathrm{DI} \sim \chi^2_n. \tag{2.24}$$

When n increases the probability density function (PDF) begins to approach a normal PDF, as predicted by the central limit theorem. Therefore, multivariate outliers can simply be defined as observations having DIs above a certain level. The assumption of a Chi-square distribution is indispensable for outlier detection because it permits one to defined a cut-off value or threshold, c, for a level of significance, β, in the form of

$$c = \mathsf{inv}F_{\chi^2_n}\left(1-\beta\right), \tag{2.25}$$

where $\mathsf{inv}F_{\chi^2_n}$ is the inverse cumulative distribution function of the central Chi-square distribution. Thus, a feature vector is considered to be a multivariate outlier (the null hypothesis is rejected) when its DI is equal or greater than c. The selection of β carries a tradeoff between the false-positive and false-negative indications of damage. A level of significance equal to 5% is normally acceptable. In addition, this outlier detection

approach can be also applied on the residuals produced by the PCA, AANN and KPCA, as demonstrated in (FIGUEIREDO; CROSS, 2013).

By assuming this outlier detection approach, a schematic representation of the MSD-based method combining data normalization and statistical classification is depicted in Figure 6. First, the feature vectors extracted from time series are divided into training matrix $\mathbf{X}$ composed of undamaged data, and test matrix $\mathbf{Z}$ composed of both undamaged and damaged data. The training data sets should be representative of the operational and environmental variations present in the structure. Second, the mean vector and covariance matrix of $\mathbf{X}$ are estimated as parameters for calculating the distances. Third, the $\mathbf{d}^2$ (or DI) for each feature vector of the test data is computed. If a DI is below the chosen threshold, c, the null hypothesis is accepted, otherwise it is rejected. This approach assumes that the original features from the undamaged condition follow a multidimensional Gaussian distribution, F, and the features from the damaged condition follow an unknown distribution, H. Note that the hypothesis H is not tested since no assumptions are made regarding the form of structural damage or its effect on the feature vector.

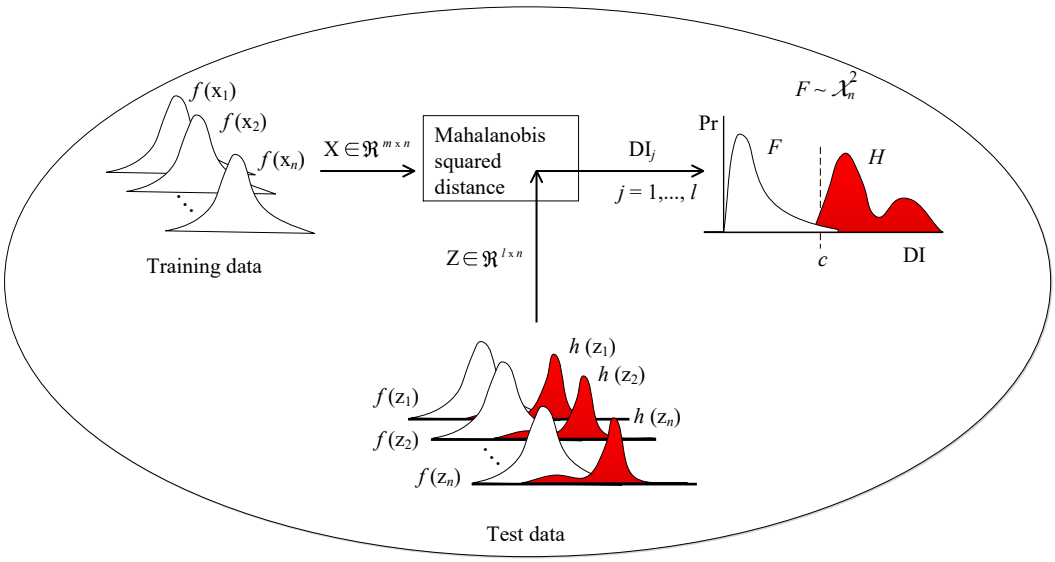

Figure 6 – The MSD-based method combining data normalization and statistical modeling for feature classification.

2.5.4 Performance evaluation of feature classification for damage detection

The performance evaluation of damage detection is a fundamental aspect for comparing models and methods. For the two-class problem (binary classification) in SHM, in which the two sets of cases are labeled as damaged (or positive, P) or undamaged (or negative, N), assuming a given threshold, there are four possible outcomes as synthesized in Table 1 and Figure 7. For a positive outcome, the case can be either true positive (TP), if the observed is positive, or false positive (FP), if the observed is negative. On the other

hand, for a negative outcome, the case can be either false negative (FN), if the observed is positive, or true negative (TN), if the observed is negative. The shaded portion of Table 1 represents the confusion matrix (also known as contingency table), where the numbers along the major diagonal represent the correct classifications, and the numbers out of the diagonal represent misclassifications, also known as Type I (FP) and Type II (FN) errors.

Table 1 – Accuracy of binary classification.

Outcome	Observed		
	Positive	Negative	Total
Positive	True Positive (TP)	False Positive (FP)	TP+FP
Negative	False Negative (FN)	True Negative (TN)	FN+TN
Total	TP+FN	FP+TN	TP+FN+FP+TN

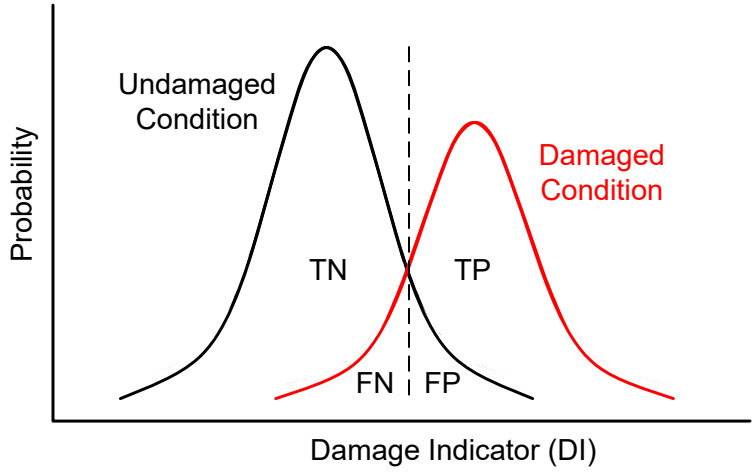

Figure 7 – Distributions from the undamaged and damaged conditions.

Therefore, false indications of damage fall into two categories: (i) false-positive (indication of damage when none is present, Type I error) and (ii) false-negative (no indication of damage when damage is present, Type II error). Errors of the first type are undesirable, as they cause unnecessary downtime and consequent loss of revenue as well as loss of confidence in the monitoring system. More importantly, there are clear safety issues if misclassifications of the second type occur (FARRAR; WORDEN, 2007). Pattern recognition algorithms allow one to weigh one type of error above the other; this weighting may be one of the questions answered at the operational evaluation phase.

Also receiver operating characteristic (ROC) curves provide a comprehensive and graphical manner to summarize the performance of different methods (BRADLEY, 1997). The ROC curves were introduced in signal detection theory by electrical and radar engineers during the World War II for detecting enemy objects in battle fields. Since that time, the ROC curves have become increasingly common in fields, such as finance, atmosphere science, engineering and medicine. In the field of machine learning, these curves have become a standard tool to evaluate the performance of binary classifiers.

The ROC curves focus on the tradeoff between sensitivity and 1-specificity. As shown in Figure 8, the sensitivity is sometimes called the true-positive rate, TPR = TP/(TP+FN), and defines the fraction of true detection. The 1-specificity is sometimes called false-positive rate, FPR = FP/(FP+TN), and defines the fraction of false alarm. Each point on the ROC curve corresponds to a specific threshold, although the values of thresholds are not evident from the square plot. The diagonal line divides the ROC space into two parts and represents a classifier that performs random classifications. Any point in the upper-left triangle means that the classifier has some understanding of the classes. Moreover, the closer the ROC plot is to the upper-left corner, the higher the overall accuracy of the classifier. On the other hand, any point in the lower-right triangle means that the classifier is performing worse than random, i.e., the classifier has some underlying information about the classes but applies it in the opposite manner.

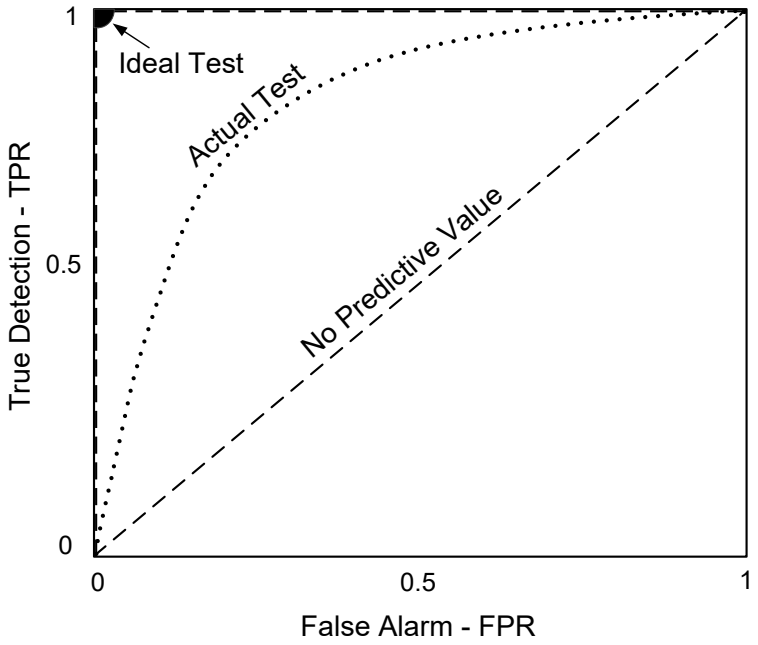

Figure 8 – Example of a ROC curve; the diagonal line divides the ROC space into two parts and represents a classifier which performs random classifications.

2.6 Challenges for statistical modeling for feature classification

In this chapter, an overview related to the SPR paradigm for SHM solutions was presented. The challenges of the first two phases of this paradigm were discussed in terms of planning for the deployment and operation of the SHM systems. In the feature extraction phase, the need for damage-sensitive features correlated to damage and completely uncorrelated to everything else was demonstrated and the techniques used in this thesis were briefly highlighted. A major focus was dedicated to the fourth phase (statistical modeling for feature classification) because the mathematical formulations of the state-

of-the-art machine learning algorithms for data normalization and the statistical models for damage detection, as well as other important issues discussed in this phase, are the basis for the understanding of novel methods proposed in Appendices from A to F.

Finally, based on the major focus of this study, some of the challenges for statistical modeling for feature classification are discussed in the following:

- The damage detection process is currently posed in the context of false-positive and false-negative indications of damage. This technique recognizes that a false-positive classification may have different consequences than false-negative ones. Thereby, analytical approaches to defining threshold levels must: balance tradeoffs between false-positive and false-negative indications of damage, minimizing false-positives when economic concerns drive the SHM applications, and minimizing false-negatives when life-safety issues are the motivations to deploy the SHM systems;
- Updating statistical models as new training data become available;
- Managing the massive volumes of data that will be produced hourly or daily by an online monitoring system;
- Learning the normal condition of a structure considering all normal variability (e.g., temperature and traffic loading) and yielding reliable results, i.e., estimating the undamaged model with a method that takes into account minimal loss of information and avoids dependence on the initial parameters;
- The choice of a method for a specific application must be done as a function of the damage-sensitive features used, as well as the distribution of these features when influenced by linear or nonlinear operational and environmental variability.

3 Summary of original work and discussion

This chapter summarizes the original methods proposed in this study for damage identification in SHM. First, the overall methodology for damage detection and quantification is presented and important rules are discussed to accomplish it. Second, the papers which composed this thesis are summarized. A brief comparison between the proposed methods is then performed on natural frequencies from the Z-24 Bridge. In addition, a list of publications in the context of this thesis is also highlighted.

3.1 Methodology for damage detection and quantification

The overall methodology for damage detection and quantification used in all papers (Appendices from A to F) is depicted in Figure 9. This flow chart shows that after several vibration signals have been acquired, the feature extraction phase estimates the damage-sensitive features, which can be natural frequencies or parameters/residuals from an AR model. Afterwards, some part of the undamaged features is used as learning data to the model and threshold estimations. Note that this selected part should cover all operational and environmental variability. The test phase is then accomplished by computing a DI (i.e., quantifying the damage) for any new feature, with support from the undamaged model estimated in the training phase. Finally, the damage detection is performed by classifying the DI as undamaged or damaged according to the threshold.

A graphic representation of the expected results from the damage detection process is shown in Figure 10. In this case, the test matrix is composed of m undamaged observations and $(l - m)$ damaged observations. After the test phase, the DIs computed from new features are classified according to a threshold with a given confidence level. The Type I errors are DIs that exceed the threshold value in the undamaged condition domain, (1 to m). On the other hand, the Type II errors are DIs that do not surpass the threshold value in the damaged condition domain, $((m + 1)$ to $l)$. Additionally, note that through the amplitude of the DIs it is possible to relatively quantify the damage. This fact can be used to discover which test case is the most severe one, and to determine whether a method can remove operational and environmental variability in the training and test phases (for example, see Appendix A).

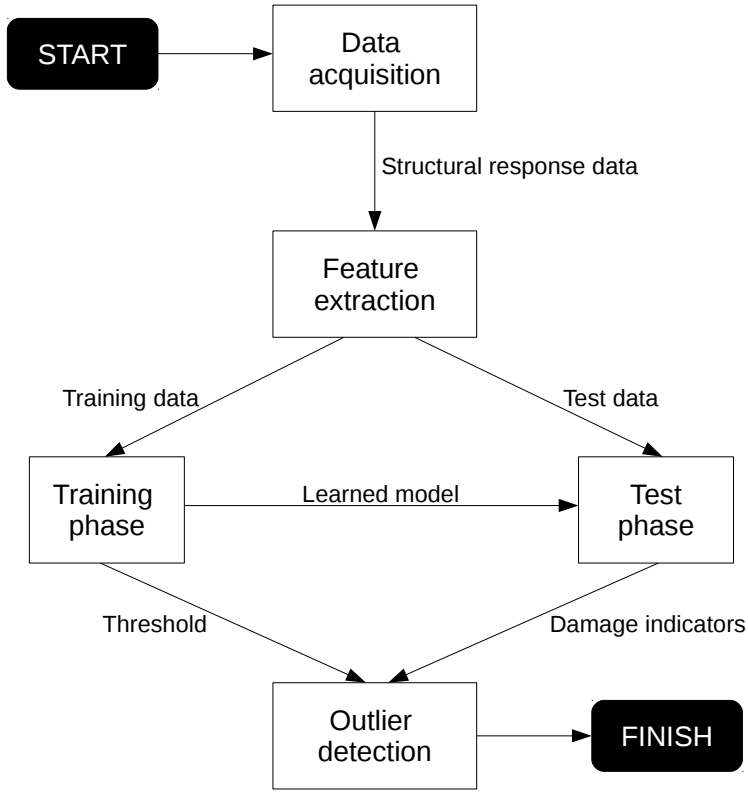

Figure 9 – Flow chart of the methodology for damage detection and quantification.

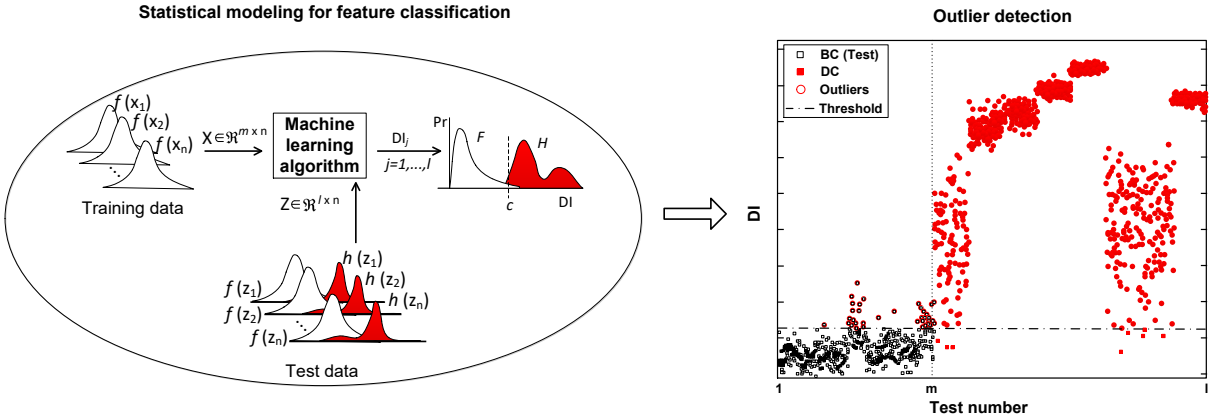

Figure 10 – Graphic representation of the statistical modeling for feature classification and results related to damage detection and quantification.

A wide range of algorithms can be employed to the training phase, test phase and threshold estimation, thus many combinations of different algorithms are available to compose a method. To avoid unfeasible combinations and to easily define the training data matrix and thresholds, some general rules applied in all papers are enumerated below.

1. The training data matrix should cover all operational and environmental variability under which the structure of interest operates. Therefore, it was assumed the need for training the machine learning algorithms with almost one-year baseline data to

cover one seasonal cycle, taking into account the temperature and humidity effects of winter and summer;

2. If the training phase is performed by the kernel- or PCA-based methods, there are three possible results from this procedure depending on the availability of the residual matrix **E** during the test phase (see subsections 2.5.2 and 2.5.3);

    a) If a method explicitly computes the matrix **E**, one can estimate an ad hoc threshold and compute the DIs with the Euclidean distance or a threshold based on central Chi-square hypothesis and compute the DIs with the MSD;

    b) If a method implicitly estimates the matrix **E**, one can estimate an ad hoc threshold and compute the DIs with the Euclidean distance;

    c) If a method does not estimate the matrix **E**, one can estimate an ad hoc threshold and compute the DIs with the Euclidean distance or MSD (depending on the undamaged model available from the training phase);

3. When the training phase or data normalization is performed by clustering, there are two possible results from this procedure: only a mean vector (also known as centroid) for each cluster, or a mean vector and a covariance matrix for each cluster;

    a) For the first case, one should estimate an ad hoc threshold and compute the DIs with the Euclidean distance;

    b) For the second case, one should estimate a threshold based on central Chi-square hypothesis and compute the DIs with the MSD. Note that the second case includes the first one when only the centroids are used.

For general purposes of correspondence, all cases from rule 2 are applicable to the proposed methods in Appendix A. The first case from rule 3 is applicable to the proposed methods in Appendices from B to F. The second case from rule 3 is applicable only to the proposed methods in Appendices C and D.

3.2 Papers which compose the thesis and enhancements

This section summarizes the six papers (Appendices from A to F) which compose this thesis. The proposed methods, data sets, and experimental results are briefly described and discussed. The general enhancements provided by these methods to the state-of-the-art damage detection process in SHM are also synthesized.

3.2.1 Paper A: Machine learning algorithms for damage detection: Kernel-based approaches

Kernel-based machine learning algorithms have been widely applied to detect damage in the SHM applications. These algorithms, mostly based on SVMs, have revealed high sensitivity and accuracy in the damage classification. This paper presents the adaptation of four kernel-based methods, based on the one-class SVM, SVDD, KPCA and GKPCA, for damage detection under operational and environmental influences. Acceleration time-series from an array of accelerometers were obtained from a laboratory structure and used for performance comparisons. The main contributions are: the first-known adaptation of two algorithms (KPCA and GKPCA) for damage detection in the SHM field; and the combination between other two algorithms (one-class SVM and SVDD) and an outlier detection method (MSD) for data normalization purposes in the SHM field. All proposed methods revealed to have better classification performance in terms of Type I (ranging between 4.7%–8.2%) and Type II (ranging between 0.8%–1.1%) errors than the state-of-the-art ones (the MSD, AANN, FA, and SVD); with special emphasis to the KPCA, which can learn the normal structural condition with minimal loss of information and detect undamaged and damaged cases on these data sets with only 2.7% of total errors.

This paper has been published in Journal of Sound and Vibration, vol. 363, 2015.

3.2.2 Paper B: A novel unsupervised approach based on a genetic algorithm for structural damage detection in bridges

This paper proposes the GADBA-based method to support the damage detection process, in the presence of linear and nonlinear effects caused by normal variability. This approach is rooted in the search of an optimal number of clusters, representing the main state conditions of a structure. The method is supported by a novel CH algorithm to mitigate the cluster redundancy. The superiority of the GADBA is compared to state-of-the-art methods based on the GMM and MSD algorithms, on data sets from the Z-24 (Switzerland) and Tamar (United Kingdom) Bridges. In terms of formulation, the proposed method assumes no particular underlying distribution and its genetically guided characteristic increases the chance to obtain a solution close to the global optimal. Besides, the CH algorithm provides special capabilities (inflation and observation density analysis) to regularize the number of clusters and define better clusters, resulting in more accurate models to accomplish data normalization. In addition, compared to the GMM, the GADBA-based method demonstrates faster convergence in both case studies. In terms of result analysis, as verified on both test cases, the GADBA demonstrates to be: as robust as the GMM to detect the existence of damage (2.6% of Type II errors); and potentially more effective to model the baseline condition and attenuate the effects of the normal

variability, as suggested by the minimization of false alarms (5.6% of Type I errors) on data sets from the Tamar Bridge.

This paper has been published in Engineering Applications of Artificial Intelligence, vol. 52, 2016.

3.2.3 Paper C: A Global Expectation-Maximization Approach Based on Memetic Algorithm for Vibration-Based Structural Damage Detection

In this paper, the GEM-GA approach is proposed, for which an MA based on GA was used to improve the stability and reliability of the EM algorithm in searching for the optimal number of data clusters and their parameters (training phase). After the main state conditions of the structure are determined, assuming multivariate Gaussian distributions, the damage detection strategy implemented through the MSD can be applied. The proposed approach is compared to the state-of-the-art ones based on the EM-GMM, MC-GMM, AANN, and KPCA, by taking into account real-world data sets from the Z-24 Bridge, where several damage scenarios were performed. The GEM-GA consists of two main parts: a global one that conducts the global search in the feature space, and a local one, which performs a more refined search around candidate solutions of the current damage detection problem. This strategy has led the GEM-GA to overcome the instability related to the alternative GMM-based approaches, providing data models with stable and reliable number of data clusters (herein 7 clusters) and approximately the same likelihood (14456.84 ± 0.04). When the GEM-GA is compared to the alternative methods, the improvements on the stability and reliability of the EM algorithm demonstrated to have a direct and positive impact on the identification of reliable data clusters (data normalization) and damage detection; reaching, in its worst case, approximately 3.6% of Type I errors and 0.6% of Type II errors, while the EM-GMM, MC-GMM, AANN, and KPCA have 2.7% and 13%, 3.2% and 1.7%, 5.3% and 0.9%, 5% and 0.9%, respectively. In conclusion,the GEM-GA not only deals with nonlinear relationships in the monitoring data, but also provides stable results in terms of data normalization and damage detection.

This paper has been published in IEEE Transactions on Instrumentation and Measurement, vol. 66, no. 4, 2017.

3.2.4 Paper D: A global expectation-maximization based on memetic swarm optimization for structural damage detection

Also considering the limitations of the EM-GMM for damage detection in SHM (see subsection 3.2.3), and as an attempt to add quantitative information from the SHM systems into the BMSs, this paper proposes an MA based on PSO, the GEM-PSO, for data normalization by clustering and damage detection process based on the Mahalanobis and

Euclidean distances. The superiority of the GEM-PSO over the state-of-the-art methods (the EM-GMM and KPCA) is attested using data sets from the Z-24 and Tamar Bridges. The damage detection on the monitoring data from the first scenario highlights that the GEM-PSO, KPCA, and EM-GMM can identify 99.35% (standard deviation of 0.2), 99.13%, and 87% (standard deviation of 30) of damaged cases and 96% (standard deviation of 5), 95%, and 98% (standard deviation of 26) of undamaged cases, respectively. For the second scenario, the GEM-PSO, KPCA, and EM-GMM can detect undamaged observations with accuracy of 94%, 80%, and 89%, respectively. Similar to the GEM-GA, the GEM-PSO has high reproducibility on the estimation of the normal structural condition and damage-detection results, regardless of the choice of initial parameters. This bioinspired hybridization between a local search method (the EM algorithm) and a global search method (the PSO) avoids unfeasible solutions eventually found in different executions of the alternative approaches. As demonstrated through the results, this hybridization proved to be a pronounced technique that can be used to add quantitative information from the SHM systems into the BMSs or visual inspections, in a controlled manner, as the main state conditions of a structure are mapped into a global DI.

This paper has been published in Structural Health Monitoring (Print), vol. 15, no. 5, 2016.

3.2.5 Paper E: Output-only structural health monitoring based on mean shift clustering for vibration-based damage detection

This paper presents a technique based on the MSC to automatically discover an unknown number of clusters that correspond to the normal state conditions of a structure. Unlike most methods in the literature, the MSC is a nonparametric technique that does not require prior knowledge of the number of clusters and can identify clusters of distinct shapes, sizes and density. This reliable estimation of clusters enhances the subsequent damage detection process, ensuring the monotonic relationship between the level of damage and the amplitude of the DI. The superiority of the MSC technique, over the alternative ones (the K-means, Fuzzy c-means, and EM-GMM), is attested by applying a damage detection strategy implemented through the Euclidean distance, using daily data sets from the Z-24 Bridge. From the results, it is possible to infer the positive impact of a data normalization procedure without sensitivity to the initialization procedure. In contrast to the alternative methods, the MSC can discriminate the normal condition of the Z-24 Bridge in a better manner, separating changes caused by regular temperatures from changes caused by extreme cold temperatures. It also can distinguish different damage levels, ignored by other approaches, when all monitoring data are clustered.

This paper has been published in 8th European Workshop On Structural Health Monitoring (EWSHM), Bilbao, Spain, 2016.

3.2.6 Paper F: Agglomerative concentric hypersphere clustering applied to structural damage detection

An improved and simplified version of the GADBA approach is highlighted in this paper as an agglomerative clustering procedure - the ACH method. It automatically discovers the structural state conditions as a means to assist the damage detection and quantification in engineering structures. This straightforward and nonparametric method does not require any input parameter (except the training data) and applies a density-based technique to identify groups of similar observations represented as inflated hyperspheres. Three initialization procedures are introduced to evaluate the impact of deterministic and stochastic initializations on the performance of this method. The ACH is compared to the EM-GMM and MSD, on daily and hourly data sets from the Z-24 Bridge. The performances of the ACH-, MSD-, and GMM-based methods are compared on the basis of Type I/II errors, as well as on their capabilities to filter nonlinear changes, when dealing with environmental effects. In terms of general results, the ACH (with the divisive initialization) demonstrated to be as effective and robust as the GMM to detect the existence of damage, and potentially more effective to model the normal condition and to attenuate the effects of normal variability as suggested by the monotonic relationship between the amplitude of the DIs and the gradual increasing of damage level. In particular, the ACH can identify 98.7% of the damaged cases, maintaining an acceptable rate of 90.8% of undamaged cases correctly assessed, while the EM-GMM and MSD can detect 97.8% and 58.7% of damaged cases, and 84.4% and 98.3% of undamaged cases, respectively.

This paper has been published in Mechanical Systems and Signal Processing, vol. 92, 2017.

3.2.7 Enhancements of the damage detection process

In the SHM literature inherent to the data-based damage detection, the state-of-the-art methods have been developed without a tradeoff between Type I/II errors. The result of this lack of proportionality has provided approaches that are very efficient at detecting damage but having a high false alarm rate, or vice versa. Usually, a poor data normalization performed by these methods is the main cause, i.e., all operational and environmental variability is not properly accounted for due to the limited nonlinear capability, some loss of information or sensitivity to the choice of the initial parameters.

In this context, one of the main enhancements of the proposed methods against the alternative ones is the estimation of the normal condition of a structure, without loss of information or sensitivity to the initialization procedure, regardless of the structural response being influenced by linear or nonlinear normal variability. This improvement on the data normalization contributes not only to minimize false alarms, but also to maximize

the damaged cases correctly identified. Thus, a high reproducibility on the estimation of the normal structural condition and damage-detection results is achieved.

For example, in Appendices C and D, it was highlighted that, via the MA-based approaches, one can estimate approximately the same undamaged model for different executions, with low standard deviation in terms of likelihood. The bioinspired clustering procedure provided by these methods covers all normal variability when the observations under the same unmeasured normal effect are grouped into a cluster. This type of learning phase improves the results of the classification phase, ensuring an acceptable tradeoff between Type I/II errors (3.7% and 0.6%, respectively).

In terms of numerical results, when the novel methods are compared to the state-of-the-art ones, the results demonstrated that the former ones have better damage detection performance in terms of false-positive (ranging between 3.6–5.4%) and false-negative (ranging between 0–2.6%) indications of damage, suggesting their applicability for real-world SHM solutions. This fact shows that the proposed techniques can detect damage with high accuracy, without diminishing their sensitivity to classify undamaged cases, i.e., they reach the desired tradeoff between economical/reliability (Type I errors) and life safety (Type II errors) issues, not accounted for by the other correlated approaches.

Furthermore, for the cluster-based methods proposed herein, another crucial enhancement is related to the physical interpretations about the undamaged structural condition under normal variability. The discovered clusters allow a better understanding of the operational and environmental sources of variability under which the structure of interest operates. For instance, from the clustering results provided by the GADBA, MSC, and ACH (see Appendices B, E, and F, respectively) on daily data sets from the Z-24 Bridge, one can distinguish between the normal condition under regular temperatures and extreme cold temperatures (which cause some changes in the structural stiffness). These methods can be also employed to identify the aforesaid normal clusters and damaged clusters when all monitoring data are used in the training phase. In Appendix E, it was evidenced that the MSC can discover distinct damaged clusters grouping observations from different levels of damage.

An undamaged model with physical interpretations is not yielded by several state-of-the-art methods, such as the PCA, SVD, MSD, AANN, and KPCA. The EM-GMM and MC-GMM, in principle, can provide this model. However, as theses approaches have sensitivity to the choice of the initial parameters, they may present different number of clusters in distinct executions. This unstable behavior limits the reliability and interpretation of the normal structural state conditions estimated by such methods.

3.3 Comparison between the proposed methods and discussion

When the novel methods are compared to the state-of-the-art ones, they clearly demonstrate their superiority in terms of data normalization and damage detection on laboratory and real-world data sets. Nevertheless, a comparison between the proposed methods is imperative to derive more conclusions related to their applicability on real-world SHM applications. This comparative study is highlighted by applying these methods on hourly natural frequencies from the Z-24 Bridge.

Some considerations should be provided before the discussion of the results. First, the hourly data sets from the Z-24 Bridge are chosen because they are more challenging regarding environmental influences and damage scenarios than the alternative data sets also used in the papers. Second, from Appendix A, only the KPCA-based method is selected for this comparison because this techniques prove to be the most promising one when applied on laboratory and real-world data sets. Finally, as the ACH is an improved version of the GADBA, only the first method is considered to simplify this comparative study. Besides, the other methods which integrate this comparison are the MSC, GEM-PSO, and GEM-GA.

For damage detection purposes, the feature vectors (or observations) are split into the training and test matrices. The training data $\mathbf{X}^{3123\times4}$ is composed of 90% of the feature vectors from the undamaged condition. The remaining 10% of these features vectors are used during the test phase to make sure that the DIs do not fire off before the damage starts. The test data $\mathbf{Z}^{3932\times4}$ is composed of all data sets (undamaged and damaged), even the ones used during the training phase. For more information about this setting, as well as about the major environmental influence and damage scenarios of the Z-24 Bridge, one can consult Appendix C.

In terms of the input parameters of the KPCA and GEM-GA, they have the same configurations defined in Appendix C, while the configurations of the GEM-PSO and ACH are obtained from Appendices D and F, respectively. In the case of the MSC, which had not yet been applied on these monitoring data, its bandwidth parameter equal to 0.25 was selected based on the best compromise between the bias and variance (COMANICIU; MEER, 2002). To ensure equality in this comparative study, for all methods, an ad hoc threshold is estimated based on the 95% cut-off value of confidence over the training data. Note that the GEM-PSO and GEM-GA can yield a centroid (similar to the ACH and MSC) and a covariance matrix for each discovered cluster. However, as a means of being consistent with the defined threshold and some rules established in section 3.1, only the centroids provided by the bioinspired methods are used in the test phase, i.e., the DIs are computed through the Euclidean distance.

The damage detection performance of all proposed methods selected for this comparison is shown in Table 2. The number of clusters discovered by each cluster-based method is also highlighted. In a first general analysis, one may conclude that the KPCA is the best method to minimize Type II errors, and the GEM-PSO and GEM-GA are the most reliable methods to minimize Type I errors. However, one should consider that the current SHM applications are typically more interested in a tradeoff between the true positive (Type II errors) and false alarm (Type I errors) rates.

Table 2 – Damage detection performance and number of clusters for each method (average ± standard deviation for 20 different executions when the method is bioinspired).

Method	Type I errors	Type II errors	#Clusters
KPCA	172 (95.04%)	4 (99.13%)	–
MSC	168 (95.16%)	12 (97.40%)	2
ACH	188 (94.58%)	6 (98.70%)	3
GEM-PSO	166.05 ± 0.22 (95.21%)	6.00 ± 0.00 (98.70%)	7.00 ± 0.00
GEM-GA	166.00 ± 0.00 (95.22%)	6.00 ± 0.00 (98.70%)	7.00 ± 0.00

Considering that all methods must misclassify 5% of the undamaged observations in the range 1–3123 (data from the training used in the test) due to the threshold of 95% of confidence, at least 156 Type I errors are expected. *This range is only considered in* Table 2, *not in the following discussion.* Although the KPCA can detect 99% of damaged cases and 95.4% of undamaged cases not used in the training (3124–3470), the GEM-PSO and GEM-GA can obtain 98.7% and 97%, respectively, which is a better tradeoff between Type I/II errors. This result is easily justified by the fact that the KPCA is only able to fit a fraction of the normal structural condition (see subsection 1.4.2). Thus, some part of the normal variability is not accounted for, yielding more Type I errors than the bioinspired methods, which can learn the normal condition with more robustness via a clustering procedure.

By analyzing the performance of all cluster-based approaches, the MSC can correctly classify 96.5% of undamaged cases and the ACH can identify 98.7% of damaged cases. However, for the first method, the Type II errors increase, and for the second one, the false alarm rate reaches 9%. The reason for such results is that, while both methods can estimate the normal condition without loss of information, their local optimizations/criteria to create new clusters play a crucial role in the characterization of all normal state conditions of the structure. In other words, the number of clusters estimated by both methods seems to be less than necessary to deal with the multimodality and heterogeneity of the present data sets. On the other hand, by using a global optimization, the GEM-PSO and GEM-GA can handle the challenges of the monitoring data and discriminate the undamaged condition with an appropriate number of clusters.

To avoid duplication of published results, only the DIs calculated from the MSC and GEM-GA methods are shown in Figure 11. Note that the DIs computed from the KPCA, GEM-PSO, and ACH, under this setting and on the same data sets, can be visualized in Appendices C, D, and F, respectively. From Figure 11, it is possible to confirm the better performance of the GEM-GA (or of the GEM-PSO) to classify undamaged and damaged observations included only in the test phase. Through the DIs from both methods, during the damaged condition, one can infer a monotonic relationship between the level of damage and the amplitude of the DIs, even with the presence of operational and environmental influences. This relationship reveals the damage progressive testing period on the Z-24 Bridge, which indicates cumulative damage on long-term monitoring.

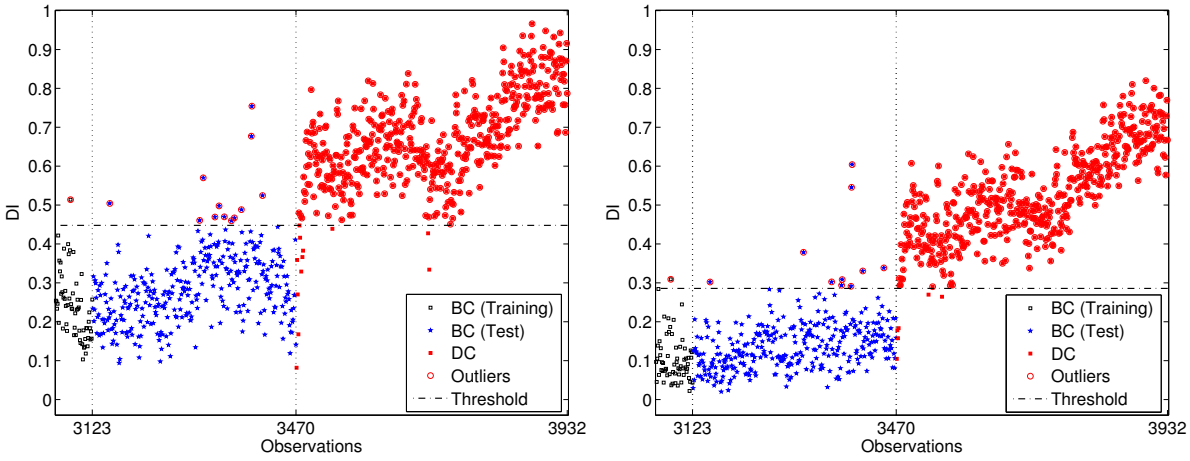

Figure 11 – DIs estimated from the application of the MSC (left) and GEM-GA (right) methods on hourly data sets from the Z-24 Bridge.

To synthesize this brief comparative study, three main conclusions related to the proposed methods are highlighted below, considering a possible extension of their applicability to other real-world SHM scenarios.

- The KPCA proved to be a method capable of detecting damage with high accuracy. However, some loss of information on the estimation of the normal structural condition is inevitable due to the working principle of this approach. Therefore, this method should be applied when life safety issues are the primary motivations of an SHM system, i.e., the minimization of Type II errors is the reason of the monitoring;

- The MSC and ACH (divisive version) methods can determine the normal condition without loss of information or sensitivity to the initialization procedure. However, their local optimizations to create the necessary number of clusters to deal with the heterogeneity of the present hourly data arise as a limitation. Nevertheless, they achieved 100% of accuracy on daily data from the Z-24 Bridge (see Appendices E and F). Thus, these approaches are appropriate to handle less complex data, possibly from an SHM system with daily frequency of data acquisition;

- When a better tradeoff between economical/reliability and life safety issues is desired for an SHM system, the bioinspired methods GEM-PSO and GEM-GA are the best indications to discriminate all normal state conditions of a structure and then to classify new observations with high confidence. The global search applied by these techniques makes them the more attractive solutions for data normalization and damage detection, regardless the different levels of practical challenges in the data.

3.4 List of publications in the context of the thesis

1. Adam Santos, Eloi Figueiredo, Moisés Silva, Claudomiro Sales and João C. W. A. Costa. "Applicability of linear and nonlinear principal component analysis for damage detection", 2015 IEEE International Instrumentation and Measurement Technology Conference (I2MTC), p. 869-874, Pisa, Italy, May 2015.

2. Adam Santos, Eloi Figueiredo, Moisés Silva, Claudomiro Sales and João C. W. A. Costa. "Machine learning algorithms for damage detection: Kernel-based approaches", Journal of Sound and Vibration, vol. 363, p. 584-599, 2015.

3. Adam Santos, Eloi Figueiredo and João C. W. A. Costa. "Clustering Strategies for Damage Detection in Bridges: A Comparison Study", 10th International Workshop on Structural Health Monitoring (IWSHM), p. 1165-1172, Stanford, CA-USA, September 2015.

4. Moisés Silva, Adam Santos, Eloi Figueiredo, Reginaldo Santos, Claudomiro Sales and João C. W. A. Costa. "A novel unsupervised approach based on a genetic algorithm for structural damage detection in bridges", Engineering Applications of Artificial Intelligence, vol. 52, p. 168-180, 2016.

5. Adam Santos, Eloi Figueiredo, Moisés Silva, Reginaldo Santos, Claudomiro Sales and João C. W. A. Costa. "Genetic-based EM algorithm to improve the robustness of Gaussian mixture models for damage detection in bridges", Structural Control & Health Monitoring (Print), vol. 24, no. 3, p. 1-9, 2017.

6. Adam Santos, Moisés Silva, Reginaldo Santos, Eloi Figueiredo, Claudomiro Sales and João C. W. A. Costa. "A global expectation-maximization based on memetic swarm optimization for structural damage detection", Structural Health Monitoring (Print), vol. 15, no. 5, p. 1-16, 2016.

7. Adam Santos, Moisés Silva, Reginaldo Santos, Eloi Figueiredo, Claudomiro Sales and João C. W. A. Costa. "Output-only structural health monitoring based on mean shift clustering for vibration-based damage detection", 8th European Workshop On Structural Health Monitoring (EWSHM), Bilbao, Spain, 2016.

8. Moisés Silva, Adam Santos, Reginaldo Santos, Eloi Figueiredo, Claudomiro Sales and João C. W. A. Costa. "A structural damage detection technique based on agglomerative clustering applied to the Z-24 Bridge", 8th European Workshop On Structural Health Monitoring (EWSHM), Bilbao, Spain, 2016.

9. Adam Santos, Arieth Silva, João Miguel, Eloi Figueiredo and João C. W. A. Costa. "Pattern recognition for experimentation of civil engineering infrastructure", 1st Conference on Testing and Experimentations in Civil Engineering (TEST&E 2016), Lisbon, Portugal, 2016.

10. Manoel Lima, Claudomiro Sales, Adam Santos, Reginaldo Santos, Moisés Silva, João C. W. A. Costa, Marissa Carvalho and Michell Cruz. "A framework for data compression and damage detection in structural health monitoring applied on a laboratory three-story structure", Revista Brasileira de Computação Aplicada, vol. 8, no. 2, p. 129-143, 2016.

11. Moisés Silva, Adam Santos, Reginaldo Santos, Eloi Figueiredo, Claudomiro Sales and João C. W. A. Costa. "Agglomerative concentric hypersphere clustering applied to structural damage detection", Mechanical Systems and Signal Processing, vol. 92, p. 196-212, 2017.

12. Adam Santos, Reginaldo Santos, Moisés Silva, Eloi Figueiredo, Claudomiro Sales and João C. W. A. Costa. "A Global Expectation-Maximization Approach Based on Memetic Algorithm for Vibration-Based Structural Damage Detection", IEEE Transactions on Instrumentation and Measurement, vol. 66, no. 4, p. 1-10, 2017.

4 Conclusions and future research

This chapter presents the main conclusions of this thesis related to the results achieved and limitations encountered. It also discusses future research topics for which the methods proposed in this study can be the fundamental basis or integrating parts.

4.1 Conclusions

In any engineering structure monitored during in-service stage, the separation of changes in features caused by damage from those caused by normal variability is one of the biggest challenges for the application of SHM technology. In some cases, changes caused by normal variability may be even larger than those caused by damage. If not properly accounted for by a data normalization procedure, changes in the structural response characteristics caused by operational or environmental influences can, potentially, result in false indications of damage during the detection process.

Output-only methods are an alternative approach to handle this drawback. They apply algorithms to develop data-driven models that can eliminate the unmeasured influences of operational and environmental variability on features, i.e., they perform data normalization. When well accomplished, this procedure contributes, significantly, to enhance damage detection and quantification. In the current SHM literature on this subject, the techniques employed to normalize the monitoring data have some limitations related to their working principles, such as limited nonlinear capability (e.g., the MSD, PCA, and FA), some loss of information (e.g., the KPCA and AANN), or high sensitivity to the initialization procedure (e.g., the EM-GMM and MC-GMM).

Therefore, to address the aforesaid problem and tackle the limitations found in the SHM literature, this thesis applied the SHM process in the context of the SPR paradigm, where novel output-only methods were proposed for damage detection and quantification based on measured vibration data from engineering structures under normal variability. These approaches are mostly based on the machine learning and artificial intelligence fields, being capable of learning from monitoring data and discovering/characterizing different patterns associated to the undamaged and damaged conditions of a structure.

As demonstrated in the published papers (Appendices from A to F) which compose this study, when the proposed methods are compared to the ones from the literature, one of the main enhancements is on the estimation of the normal condition of a structure, without loss of information or sensitivity to the initialization procedure, regardless of the structure is under linear or nonlinear variability. This improvement on the data normalization contributes not only to minimize false alarms, but also to maximize the number of damaged cases correctly identified. Thus, a high reproducibility on the estimation of the normal structural condition and damage-detection results was reached.

In terms of numerical results, the novel methods have better damage detection performance in terms of undamaged (ranging between 94.6–96.4%) and damaged (ranging between 97.4–100%) cases properly identified, suggesting their applicability for current SHM solutions. This fact shows that the proposed techniques can detect damage with high accuracy, without diminishing their sensitivity to classify undamaged cases, i.e., they reach the desired tradeoff between economical/reliability (Type I errors) and life safety (Type II errors) issues, not addressed by the state-of-the-art approaches.

In particular, it was demonstrated through the MA-based approaches that one can determine, approximately, the same baseline model for different executions, with low standard deviation in terms of likelihood. This improvement is explained by the bioinspired clustering procedure provided by these methods, where all normal variability is covered when the observations under the same unmeasured normal effect are grouped into a cluster. This type of learning improves the results of the damage classification phase, ensuring an acceptable tradeoff between TypeI/II errors (3.7% and 0.6%, respectively).

The physical interpretations about the undamaged structural condition under normal variability is another appealing improvement. The discovered clusters allow a general comprehension of the sources of variability present in the structures under normal operation. From the clustering results provided by the GADBA, MSC, and ACH on daily data sets from the Z-24 Bridge, one can distinguish between the normal condition under regular temperatures and extreme cold temperatures. These methods can be also employed to identify the normal and damaged clusters when all monitoring data are used in the training phase. It was shown that the MSC can discover distinct damaged clusters grouping observations from different levels of damage and have effective meaning.

When the proposed methods are compared to each other, on hourly natural frequencies from the Z-24 Bridge, the GEM-PSO and GEM-GA prevailed with a better tradeoff between Type I/II errors, detecting 98.7% of damaged and 97% of undamaged cases. Thus, when a better tradeoff between economical/reliability and life safety issues is desired for an SHM system, the bioinspired methods are the best indications for data normalization and damage detection. The global search applied by these techniques makes them the more reliable solutions, regardless the different levels of multimodality and het-

erogeneity in the monitoring data.

In turn, the KPCA proved to be a method capable of detecting damage with high accuracy (99% of damaged cases). However, some loss of information on the estimation of the normal structural condition is expected due to its working principle. Thereby, this method should be applied when life safety issues are the primary motivations of an SHM system, i.e., the false-negative indications of damage are more relevant.

In the case of the MSC and ACH methods, although they can determine the normal condition without loss of information or sensitivity to the initialization procedure, their intrinsic local optimizations to create the number and shape of clusters to deal with the heterogeneity of complex hourly data may limit their range of applicability. Nevertheless, they achieved 100% of accuracy in terms of damage detection on daily data from the Z-24 Bridge. Thus, these approaches are appropriate to handle less complex data, possibly from an SHM system with daily frequency of data acquisition.

In a general analysis, the proposed approaches intend to avoid the measure of operational and environmental parameters and physics-based approaches, such as finite element models. In other words, they are output-only and data-based techniques applicable to engineering structures of arbitrary complexity. It is worth noting that the novel methods developed in this thesis can be applied on vibration response measurements of any structure from civil, mechanical or aerospace engineering.

One of the main benefits delivered by the developed methods to the SHM technology is the ability to continuously assess the integrity of engineering structures, offering the opportunity to reduce maintenance and inspection costs (minimization of Type I errors, reliability/economical issues), while providing increased safety to the public (minimization of Type II errors, life safety issues). This advantage can be applied on the declining state of aging infrastructure, as well as on the construction stage of new structures.

Additionally, the novel methods can also contribute to the aid of quantitative information from the SHM systems into the BMSs or visual inspections. Theses techniques are capable of reducing the global state conditions of a structure into a global DI that quantifies the level of damage according to a predefined threshold at a given period. This information can be then registered into a BMS for further comparisons.

In terms of limitations encountered, the ones that have attracted more attention are the dependence of the proposed methods on the sensitivity of the features and the quality of the monitoring data used in the training phase.

For example, the detection of small cracks depends on the severity of these cracks. The cracks need to change the stiffness significantly, as the natural frequencies are naturally related to the stiffness of the structural system. Therefore, the success of the proposed methods depends highly on the sensitivity of the extracted features.

It is also important to consider that there are potential problems if the training data can cover only a limited range of operational and environmental variability. Hence, all sources of variability must be well characterized by the training data such that the techniques learn their influence on the structural response and perform the data normalization procedure. Thus, one should note that there is no guarantee that these approaches will work effectively when applied to new monitoring data under normal variability not included in the training phase.

4.2 Future research

Future research topics which can be derived from this thesis are pointed out below.

- The clustering procedure performed by the MSC may not be satisfactory if in the input space the clusters are not linearly separable or the distance measure is not adequate. The kernel MSC, improved for SHM purposes, can be a solution to this drawback as it maps the data to a high-dimensional space in which the clusters are often estimated in a better manner (VEDALDI; SOATTO, 2008);

- The ACH can be extended to provide a set of optimal clustering solutions, where some of them were eventually disregarded in the original agglomerative procedure. This improvement can be accomplished by means of a dendrogram along with an information criterion to decide whether a clustering solution has the required quality to the data normalization problem. Besides, to comprise the identification of clusters with distinct shapes, the distance metric of the ACH can be modified to the Mahalanobis or diagonal distances, for instance;

- To circumvent the problems related to the PCA-based approaches, data-based methods from a relatively new branch of machine learning – deep learning – can be developed. For example, the deep stacked autoencoder can be employed as a data normalization procedure in the context of SHM. This type of deep neural network allows to learn robust undamaged models in terms of generalization capabilities due to the enhancements in its two-step training phase. Thus, it is expected that the learned model can generalize the normal condition under normal variability from the training to the test with more reliability and without loss of information;

- Development of an output-only approach that combines transmissibility measurements, feature extraction, dimensionality reduction and feature classification to detect structural damage. The motivation of using the transmissibilities to detect damage relies on the assumption that they are local quantities (MAIA et al., 2011), which suggests a high sensitivity to detect changes in the structural dynamics caused

by some kind of damage. In this context, for example, a method was proposed combining transmissibilities with the KPCA. First, the dimensionality of the transmissibilities is appropriately reduced by applying the KPCA. Second, an outlier detection strategy determines the condition of the instrumented structure. The method was experimentally validated with transmissibilities acquired from a laboratory beam instrumented with accelerometers. The results demonstrated that the approach has high potential to be applied when only the structural response is available;

- An holistic pattern recognition paradigm for the SHM applications can be also considered. It takes into account physical modeling, structural monitoring and information from visual inspections, as illustrated in Figure 12. In this data fusion approach, the machine learning algorithms can learn from several physics-, data- and visual-based sources, which potentially improves their knowledge regarding the monitored structures to better identify damage at early stages. For instance, this methodology was applied on the Z-24 Bridge from physics- and data-based models. From new data yielded by the physical modeling of the structure and past monitoring data acquired on a long-term monitoring, it is possible to verify the performance of a data-based method in classifying some undamaged or damaged scenarios which were reproduced or created.

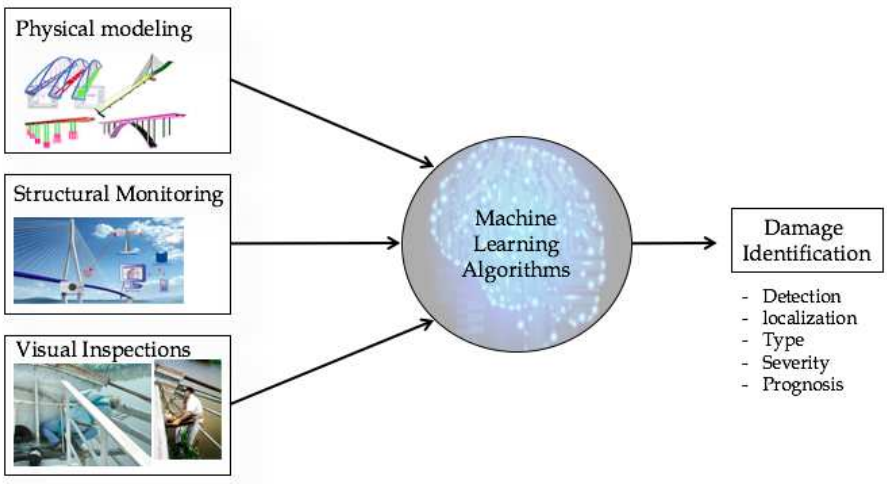

Figure 12 – A new holistic pattern recognition paradigm to comprise physical modeling, structural monitoring, and information from visual inspections.

References

BAPTISTA, F. G.; FILHO, J. V.; INMAN, D. J. Real-time multi-sensors measurement system with temperature effects compensation for impedance-based structural health monitoring. *Structural Health Monitoring*, 2012. v. 11, n. 2, p. 173–186, 2012. Cited on page 19.

BOX, G. E. P.; JENKINS, G. M.; REINSEL, G. C. *Time Series Analysis: Forecasting and Control*. 4th. ed. Hoboken NJ, United States: John Wiley & Sons, Inc., 2008. Cited 2 times on pages 21 and 29.

BRADLEY, A. P. The use of the area under the ROC curve in the evaluation of machine learning algorithms. *Pattern Recognition*, 1997. v. 30, n. 7, p. 1145–1159, 1997. Cited on page 32.

BROWNJOHN, J. M. W. Structural health monitoring of civil infrastructure. *Philosophical Transactions of the Royal Society of London A: Mathematical, Physical and Engineering Sciences*, 2007. v. 365, n. 1851, p. 589–622, 2007. Cited on page 1.

CARDEN, E. P.; FANNING, P. Vibration Based Condition Monitoring: A Review. *Structural Health Monitoring*, 2004. v. 3, n. 4, p. 355–377, 2004. Cited on page 3.

CHANG, P. C.; FLATAU, A.; LIU, S. C. Review Paper: Health Monitoring of Civil Infrastructure. *Structural Health Monitoring*, 2003. v. 2, n. 3, p. 257–267, 2003. Cited on page 4.

CHENG, L. et al. The Health Monitoring Method of Concrete Dams Based on Ambient Vibration Testing and Kernel Principle Analysis. *Shock and Vibration*, 2015. v. 2015, p. 11 pages, 2015. Cited on page 10.

COMANICIU, D.; MEER, P. Mean shift: a robust approach toward feature space analysis. *IEEE Transactions on Pattern Analysis and Machine Intelligence*, 2002. v. 24, n. 5, p. 603–619, 2002. Cited on page 43.

DEMPSTER, A. P.; LAIRD, N. M.; RUBIN, D. B. Maximum Likelihood from Incomplete Data via the EM Algorithm. *Journal of the Royal Statistical Society. Series B (Methodological)*, 1977. v. 39, n. 1, p. 1–38, 1977. Cited on page 28.

DERAEMAEKER, A. et al. Vibration-based structural health monitoring using output-only measurements under changing environment. *Mechanical Systems and Signal Processing*, 2008. v. 22, n. 1, p. 34–56, 2008. Cited 2 times on pages 8 and 24.

FARRAR, C. R.; DOEBLING, S. W. An Overview of Modal-Based Damage Identification Methods. In: *EUROMECH 365 International Workshop: DAMAS 97, Structural Damage Assessment Using Advanced Signal Processing Procedures*. Sheffield, United Kingdom: University of Sheffield, 1997. Cited on page 21.

FARRAR, C. R.; DOEBLING, S. W.; NIX, D. A. Vibration–based structural damage identification. *Philosophical Transactions of the Royal Society of London A: Mathematical, Physical and Engineering Sciences*, 2001. v. 359, n. 1778, p. 131–149, 2001. Cited 2 times on pages 1 and 16.

FARRAR, C. R.; J.LIEVEN, N. A. Damage prognosis: the future of structural health monitoring. *Philosophical Transactions of the Royal Society of London A: Mathematical, Physical and Engineering Sciences*, 2007. The Royal Society, v. 365, n. 1851, p. 623–632, 2007. Cited on page 2.

FARRAR, C. R.; WORDEN, K. An introduction to structural health monitoring. *Philosophical Transactions of the Royal Society: Mathematical, Physical & Engineering Sciences*, 2007. v. 365, n. 1851, p. 303–315, 2007. Cited 3 times on pages 1, 17, and 32.

FARRAR, C. R.; WORDEN, K. *Structural Health Monitoring: A Machine Learning Perspective*. Hoboken NJ, United States: John Wiley & Sons, Inc., 2013. Cited 2 times on pages 3 and 22.

FIGUEIREDO, E.; CROSS, E. Linear approaches to modeling nonlinearities in long-term monitoring of bridges. *Journal of Civil Structural Health Monitoring*, 2013. v. 3, n. 3, p. 187–194, 2013. Cited 3 times on pages 11, 28, and 31.

FIGUEIREDO, E. et al. Influence of the Autoregressive Model Order on Damage Detection. *Computer-Aided Civil and Infrastructure Engineering*, 2011. v. 26, n. 3, p. 225–238, 2011. Cited on page 21.

FIGUEIREDO, E.; MOLDOVAN, I.; MARQUES, M. B. *Condition Assessment of Bridges: Past, Present, and Future – A Complementary Approach*. Portugal: Universidade Católica Editora, 2013. Cited 2 times on pages 4 and 12.

FIGUEIREDO, E. et al. Machine learning algorithms for damage detection under operational and environmental variability. *Structural Health Monitoring*, 2011. v. 10, n. 6, p. 559–572, 2011. Cited 4 times on pages 3, 9, 19, and 22.

FIGUEIREDO, E. et al. Applicability of a Markov-Chain Monte Carlo Method for Damage Detection on Data from the Z-24 and Tamar Suspension Bridges. In: *Proceedings of the 6th European Workshop on Structural Health Monitoring*. Dresden, Germany: Fraunhofer Publications, 2012. p. 747–754. Cited on page 11.

FIGUEIREDO, E. et al. A Bayesian approach based on a Markov-chain Monte Carlo method for damage detection under unknown sources of variability. *Engineering Structures*, 2014. v. 80, n. 0, p. 1–10, 2014. Cited on page 11.

FIGUEIREDO, E. et al. Autoregressive modeling with state-space embedding vectors for damage detection under operational variability. *International Journal of Engineering Science*, 2010. v. 48, n. 10, p. 822–834, 2010. Cited on page 19.

FIGUEIREDO, E. J. F. *Damage Identification in Civil Engineering Infrastructure under Operational and Environmental Conditions*. Tese (Doctor of Philosophy in Civil Engineering) — Faculdade de Engenharia, Universidade do Porto, Porto, Portugal, 2010. Cited 6 times on pages VIII, 1, 2, 7, 16, and 19.

GLISIC, B.; INAUDI, D. *Fibre Optic Methods for Structural Health Monitoring*. Hoboken NJ, United States: John Wiley & Sons, Inc., 2007. Cited on page 18.

GLISIC, B.; INAUDI, D. Development of method for in-service crack detection based on distributed fiber optic sensors. *Structural Health Monitoring*, 2012. v. 11, n. 2, p. 161–171, 2012. Cited on page 19.

GLOBO. *Queda de ponte na Transamazônica deixa municípios isolados no Pará*. August 2014. Available from Internet: <http://g1.globo.com/pa/para/noticia/2014/08-/queda-de-ponte-na-transamazonica-deixa-municipios-isolados-no-para.html>. Access on: 15.02.2017. Cited on page 4.

GLOBO. *Imagem mostra queda de ponte no Mato Grosso do Sul*. January 2016. Available from Internet: <http://g1.globo.com/jornal-nacional/noticia/2016/01/imagem-mostra-queda-de-ponte-no-mato-grosso-do-sul.html>. Access on: 15.02.2017. Cited on page 4.

GLOBO. *Justiça faz em BH terceira audiência sobre queda de Viaduto Guararapes*. October 2016. Available from Internet: <http://g1.globo.com/minas-gerais/noticia/2016-/10/justica-faz-em-bh-terceira-audiencia-sobre-queda-de-viaduto-guararapes.html>. Access on: 15.02.2017. Cited on page 4.

GUILLAUME, P.; PINTELON, R.; SCHOUKENS, J. Nonparametric frequency response function estimators based on nonlinear averaging techniques. In: *9th IEEE Instrumentation and Measurement Technology Conference*. New York, United States: IEEE, 1992. p. 3–9. Cited on page 21.

HAKIM, S. J. S.; RAZAK, H. A. Modal parameters based structural damage detection using artificial neural networks - a review. *Smart Structures and Systems*, 2014. v. 14, n. 2, p. 159–189, 2014. Cited on page 9.

HSU, T.-Y.; LOH, C.-H. Damage detection accommodating nonlinear environmental effects by nonlinear principal component analysis. *Structural Control and Health Monitoring*, 2010. v. 17, n. 3, p. 338–354, 2010. Cited 2 times on pages 9 and 25.

IHN, J.-B.; CHANG, F.-K. Detection and monitoring of hidden fatigue crack growth using a built-in piezoelectric sensor/actuator network: II. Validation using riveted joints and repair patches. *Smart Materials and Structures*, 2004. v. 13, n. 3, p. 621–630, 2004. Cited on page 19.

INAUDI, D.; MANETTI, L.; GLISIC, B. Integrated Systems for Structural Health Monitoring. In: *Proceedings of the fourth International Conference on Structural Health Monitoring on Intelligent Infrastructure*. Zurich, Switzerland: Empa-Akademie, 2009. Cited on page 4.

JOLLIFFE, I. *Principal Component Analysis*. 2nd. ed. New York, United States: Springer-Verlag, 2002. Cited on page 24.

KANTZ, H.; SCHREIBER, T. *Nonlinear time series analysis*. 2nd. ed. Cambridge, United Kingdom: Cambridge University Press, 2003. Cited on page 21.

KESSLER, S. S.; SPEARING, S. M.; SOUTIS, C. Damage detection in composite materials using Lamb wave methods. *Smart Materials and Structures*, 2002. v. 11, n. 2, p. 269–278, 2002. Cited on page 19.

KHOA, N. L. et al. Robust dimensionality reduction and damage detection approaches in structural health monitoring. *Structural Health Monitoring*, 2014. v. 13, n. 4, p. 406–417, 2014. Cited on page 10.

KIM, C.-Y. et al. Effect of vehicle weight on natural frequencies of bridges measured from traffic-induced vibration. *Earthquake Engineering and Engineering Vibration*, 2003. v. 2, n. 1, p. 109–115, 2003. Cited on page 21.

KO, J. M.; NI, Y. Q. Technology developments in structural health monitoring of large-scale bridges. *Engineering Structures*, 2005. v. 27, n. 12, p. 1715–1725, 2005. SEMC 2004 Structural Health Monitoring, Damage Detection and Long-Term Performance, Second International Conference on Structural Engineering, Mechanics and Computation. Cited on page 4.

KOTHAMASU, R. et al. Comparison of Selected Model Evaluation Criteria for Maintenance Applications. *Structural Health Monitoring*, 2004. v. 3, n. 3, p. 213–224, 2004. Cited on page 21.

KRAMER, M. A. Nonlinear principal component analysis using autoassociative neural networks. *AIChE Journal*, 1991. v. 37, n. 2, p. 233–243, 1991. Cited on page 25.

KULLAA, J. Is temperature measurement essential in structural health monitoring? In: *Proceedings of the 4th International Workshop on Structural Health Monitoring: From Diagnostic & Prognostics to Structural Health Monitoring*. Stanford, United States: DEStech Publications, 1993. p. 717–724. Cited on page 8.

KULLAA, J. Removing Non-Linear Environmental Influences from Structural Features. In: *Proceedings of the third European Workshop on Structural Health Monitoring*. Granada, Spain: DEStech Publications, 2006. p. 635–642. Cited on page 9.

KULLAA, J. Distinguishing between sensor fault, structural damage, and environmental or operational effects in structural health monitoring. *Mechanical Systems and Signal Processing*, 2011. v. 25, n. 8, p. 2976–2989, 2011. Cited on page 1.

KULLAA, J. Structural Health Monitoring under Nonlinear Environmental or Operational Influences. *Shock and Vibration*, 2014. v. 2014, p. 9 pages, 2014. Cited on page 11.

MAGALHAES, F.; CUNHA, A.; CAETANO, E. Vibration based structural health monitoring of an arch bridge: From automated OMA to damage detection. *Mechanical Systems and Signal Processing*, 2012. v. 28, p. 212–228, 2012. Interdisciplinary and Integration Aspects in Structural Health Monitoring. Cited on page 4.

MAIA, N. et al. Damage detection in structures: from mode shape to frequency response function methods. *Mechanical Systems and Signal Processing*, 2003. v. 17, n. 3, p. 489–498, 2003. Cited on page 21.

MAIA, N. M. et al. Damage detection and quantification using transmissibility. *Mechanical Systems and Signal Processing*, 2011. v. 25, n. 7, p. 2475–2483, 2011. Cited on page 51.

MATTSON, S. G.; PANDIT, S. M. Statistical moments of autoregressive model residuals for damage localisation. *Mechanical Systems and Signal Processing*, 2006. v. 20, n. 3, p. 627–645, 2006. Cited on page 19.

MCLACHLAN, G. J.; PEEL, D. *Finite Mixture Models*. United States: John Wiley & Sons, Inc., Wiley Series in Probability and Statistics, 2000. Cited on page 28.

MOSER, P.; MOAVENI, B. Environmental effects on the identified natural frequencies of the Dowling Hall Footbridge. *Mechanical Systems and Signal Processing*, 2011. v. 25, n. 7, p. 2336–2357, 2011. Cited on page 9.

NGUYEN, T.; CHAN, T. H.; THAMBIRATNAM, D. P. Controlled Monte Carlo data generation for statistical damage identification employing Mahalanobis squared distance. *Structural Health Monitoring*, 2014. v. 13, n. 4, p. 461–472, 2014. Cited on page 8.

NI, Y. Q. et al. Correlating modal properties with temperature using long-term monitoring data and support vector machine technique. *Engineering Structures*, 2005. v. 27, n. 12, p. 1762–1773, 2005. SEMC 2004 Structural Health Monitoring, Damage Detection and Long-Term PerformanceSecond International Conference on Structural Engineering, Mechanics and Computation. Cited on page 7.

OH, C. K.; SOHN, H.; BAE, I.-H. Statistical novelty detection within the Yeongjong suspension bridge under environmental and operational variations. *Smart Materials and Structures*, 2009. v. 18, n. 12, p. 125022, 2009. Cited on page 10.

PARK HOON SOHN, C. R. F. G.; INMAN, D. J. Overview of Piezoelectric Impedance-Based Health Monitoring and Path Forward. *Shock and Vibration Digest*, 2003. v. 35, n. 6, p. 451–463, 2003. Cited on page 19.

PEETERS, B. *System identification and damage detection in civil engineering*. Tese (Doctor of Philosophy in Applied Sciences) — Department of Civil Engineering, Katholieke Universiteit Leuven, Leuven, Belgium, 2000. Cited on page 21.

PEETERS, B.; MAECK, J.; ROECK, G. D. Vibration-based damage detection in civil engineering: excitation sources and temperature effects. *Smart Materials and Structures*, 2001. v. 10, n. 3, p. 518–527, 2001. Cited on page 9.

PEETERS, B.; ROECK, G. D. Reference-based stochastic subspace identification for output-only modal analysis. *Mechanical Systems and Signal Processing*, 1999. v. 13, n. 6, p. 855–878, 1999. Cited on page 21.

PEETERS, B.; ROECK, G. D. One-year monitoring of the Z24-Bridge: environmental effects versus damage events. *Earthquake Engineering & Structural Dynamics*, 2001. v. 30, n. 2, p. 149–171, 2001. Cited 2 times on pages 7 and 9.

REYNDERS, E. System Identification Methods for (Operational) Modal Analysis: Review and Comparison. *Archives of Computational Methods in Engineering*, 2012. v. 19, n. 1, p. 51–124, 2012. Cited 2 times on pages 19 and 20.

REYNDERS, E.; HOUBRECHTS, J.; ROECK, G. D. Fully automated (operational) modal analysis. *Mechanical Systems and Signal Processing*, 2012. v. 29, p. 228–250, 2012. Cited on page 21.

REYNDERS, E.; PINTELON, R.; ROECK, G. D. Uncertainty bounds on modal parameters obtained from stochastic subspace identification. *Mechanical Systems and Signal Processing*, 2008. v. 22, n. 4, p. 948–969, 2008. Special Issue: Crack Effects in Rotordynamics. Cited on page 21.

REYNDERS, E.; ROECK, G. D. Reference-based combined deterministic–stochastic subspace identification for experimental and operational modal analysis. *Mechanical Systems and Signal Processing*, 2008. v. 22, n. 3, p. 617–637, 2008. Cited on page 21.

REYNDERS, E.; ROECK, G. D. A local flexibility method for vibration-based damage localization and quantification. *Journal of Sound and Vibration*, 2010. v. 329, n. 12, p. 2367–2383, 2010. Structural Health Monitoring Theory Meets Practice. Cited on page 19.

REYNDERS, E.; WURSTEN, G.; ROECK, G. D. Output-only structural health monitoring in changing environmental conditions by means of nonlinear system identification. *Structural Health Monitoring*, 2014. v. 13, n. 1, p. 82–93, 2014. Cited 5 times on pages 6, 10, 26, 27, and 28.

ROECK, G. D. The state-of-the-art of damage detection by vibration monitoring: the SIMCES experience. *Structural Control and Health Monitoring*, 2003. v. 10, n. 2, p. 127–134, 2003. Cited on page 6.

RUOTOLO, R.; SURACE, C. Using SVD to detect damage in structures with different operational conditions. *Journal of Sound and Vibration*, 1999. v. 226, n. 3, p. 425–439, 1999. Cited on page 8.

SAMPAIO, R.; MAIA, N.; SILVA, J. Damage detection using the frequency-response-function curvature method. *Journal of Sound and Vibration*, 1999. v. 226, n. 5, p. 1029–1042, 1999. Cited on page 21.

SANTOS, A. et al. Machine learning algorithms for damage detection: Kernel-based approaches. *Journal of Sound and Vibration*, 2016. v. 363, p. 584–599, 2016. Cited 2 times on pages 3 and 22.

SCHOLKOPF, B.; SMOLA, A.; MULLER, K.-R. Nonlinear Component Analysis As a Kernel Eigenvalue Problem. *Neural Computation*, 1998. v. 10, n. 5, p. 1299–1319, 1998. Cited 2 times on pages 26 and 27.

SHAO, R. et al. The fault feature extraction and classification of gear using principal component analysis and kernel principal component analysis based on the wavelet packet transform. *Measurement*, 2014. v. 54, p. 118–132, 2014. Cited on page 9.

SOHN, H. Effects of environmental and operational variability on structural health monitoring. *Philosophical Transactions of the Royal Society of London A: Mathematical, Physical and Engineering Sciences*, 2007. v. 365, n. 1851, p. 539–560, 2007. Cited on page 1.

SOHN, H. et al. Wavelet-based active sensing for delamination detection in composite structures. *Smart Materials and Structures*, 2004. v. 13, n. 1, p. 153–160, 2004. Cited on page 19.

SOHN, H.; WORDEN, K.; FARRAR, C. R. Statistical Damage Classification Under Changing Environmental and Operational Conditions. *Journal of Intelligent Material Systems and Structures*, 2002. v. 13, n. 9, p. 561–574, 2002. Cited 3 times on pages 9, 22, and 26.

SOYOZ, S.; FENG, M. Q. Long-Term Monitoring and Identification of Bridge Structural Parameters. *Computer-Aided Civil and Infrastructure Engineering*, 2009. v. 24, n. 2, p. 82–92, 2009. Cited on page 21.

TORRES-ARREDONDO, M. A. et al. Data-driven multivariate algorithms for damage detection and identification: Evaluation and comparison. *Structural Health Monitoring*, 2014. v. 13, n. 1, p. 19–32, 2014. Cited on page 3.

VANLANDUIT, S. et al. A robust singular value decomposition for damage detection under changing operating conditions and structural uncertainties. *Journal of Sound and Vibration*, 2005. v. 284, n. 3-5, p. 1033–1050, 2005. Cited on page 8.

VEDALDI, A.; SOATTO, S. Quick Shift and Kernel Methods for Mode Seeking. In: *10th European Conference on Computer Vision*. Marseille, France: Springer, Berlin, Heidelberg, 2008. p. 705–718. Cited on page 51.

WORDEN, K.; DULIEU-BARTON, J. M. An Overview of Intelligent Fault Detection in Systems and Structures. *Structural Health Monitoring*, 2004. v. 3, n. 1, p. 85–98, 2004. Cited on page 18.

WORDEN, K. et al. The fundamental axioms of structural health monitoring. *Philosophical Transactions of the Royal Society: Mathematical, Physical & Engineering Sciences*, 2007. v. 463, n. 2082, p. 1639–1664, 2007. Cited on page 8.

WORDEN, K.; MANSON, G. The application of machine learning to structural health monitoring. *Philosophical Transactions of the Royal Society: Mathematical, Physical & Engineering Sciences*, 2007. v. 365, n. 1851, p. 515–537, 2007. Cited 3 times on pages 3, 8, and 23.

WORDEN, K.; MANSON, G.; FIELLER, N. R. J. Damage detection using outlier analysis. *Journal of Sound and Vibration*, 2000. v. 229, n. 3, p. 647–667, 2000. Cited on page 23.

XIA, Y. et al. Long term vibration monitoring of an RC slab: Temperature and humidity effect. *Engineering Structures*, 2006. v. 28, n. 3, p. 441–452, 2006. Cited on page 21.

YAN, A.-M. et al. Structural damage diagnosis under varying environmental conditions–Part I: A linear analysis. *Mechanical Systems and Signal Processing*, 2005. v. 19, n. 4, p. 847–864, 2005. Cited 2 times on pages 9 and 24.

YAN, A.-M. et al. Structural damage diagnosis under varying environmental conditions–part II: local PCA for non-linear cases. *Mechanical Systems and Signal Processing*, 2005. v. 19, n. 4, p. 865–880, 2005. Cited on page 9.

YAO, R.; PAKZAD, S. N. Autoregressive statistical pattern recognition algorithms for damage detection in civil structures. *Mechanical Systems and Signal Processing*, 2012. v. 31, n. 0, p. 355–368, 2012. Cited on page 21.

YAPAR, O. et al. Structural health monitoring of bridges with piezoelectric AE sensors. *Engineering Failure Analysis*, 2015. v. 56, p. 150–169, 2015. The Sixth International Conference on Engineering Failure Analysis. Cited on page 4.

YUQING, Z. et al. NC Machine Tools Fault Diagnosis Based on Kernel PCA and k-Nearest Neighbor Using Vibration Signals. *Shock and Vibration*, 2015. v. 2015, p. 10 pages, 2015. Cited on page 10.

ZHOU, Y.-L. et al. Damage detection in structures using a transmissibility-based Mahalanobis distance. *Structural Control and Health Monitoring*, 2015. v. 22, n. 10, p. 1209–1222, 2015. Cited on page 8.

Appendices

Appendix A – Paper A: Machine learning algorithms for damage detection: Kernel-based approaches

Journal of Sound and Vibration 363 (2016) 584–599

Contents lists available at ScienceDirect

Journal of Sound and Vibration

journal homepage: www.elsevier.com/locate/jsvi

Machine learning algorithms for damage detection: Kernel-based approaches

Adam Santos [a,*], Eloi Figueiredo [b], M.F.M. Silva [a], C.S. Sales [a], J.C.W.A. Costa [a]

[a] Applied Electromagnetism Laboratory, Universidade Federal do Pará, R. Augusto Corrêa, Guamá 01, Belém, 66075-110 Pará, Brazil
[b] Faculty of Engineering, Universidade Lusófona de Humanidades e Tecnologias, Campo Grande 376, 1749-024 Lisbon, Portugal

ARTICLE INFO

Article history:
Received 9 April 2015
Received in revised form
1 October 2015
Accepted 3 November 2015
Handling Editor: K. Shin
Available online 21 November 2015

Keywords:
Structural health monitoring
Damage detection
Kernel
Operational conditions
Environmental conditions

ABSTRACT

This paper presents four kernel-based algorithms for damage detection under varying operational and environmental conditions, namely based on one-class support vector machine, support vector data description, kernel principal component analysis and greedy kernel principal component analysis. Acceleration time-series from an array of accelerometers were obtained from a laboratory structure and used for performance comparison. The main contribution of this study is the applicability of the proposed algorithms for damage detection as well as the comparison of the classification performance between these algorithms and other four ones already considered as reliable approaches in the literature. All proposed algorithms revealed to have better classification performance than the previous ones.

1. Introduction

Civil structures such as buildings, roads, railways, bridges, tunnels and dams are present in every society, regardless of culture, geographical location or economical development. The safest and most durable structures are those that are well managed and maintained. Health monitoring plays an important role in management activities [1]. The massive data obtained from monitoring must be transformed in meaningful information to support the planning and designing maintenance activities, increase the safety, verify hypotheses, reduce uncertainty and to widen the knowledge and insight concerning the monitored structure.

Structural health monitoring (SHM) is certainly one of the most powerful tools for civil infrastructure management. The SHM process consists of permanent, continuous, periodic or periodically continuous acquisition of parameters by a sensor network, feature extraction and statistical modeling for feature classification to detect possible structural damages and to support the decision making [2,3]. Damage is traditionally defined as changes in the material and/or geometric properties of the structures, including variations in the boundary conditions and system connectivity, which adversely affect the system's current or future performance. In contrast, normal condition refers to data acquired under different operational and environmental variability when the structure is known to be undamaged [4,5].

In the feature extraction phase is imperative to derive damage-sensitive features correlated with the severity of damage present in monitored structures, minimizing false judgements in the classification phase. Nevertheless, in real-world SHM applications, operational and environmental effects can camouflage damage-related changes in the features as well as alter

* Corresponding author.
E-mail address: adamdreyton@ufpa.br (A. Santos).

http://dx.doi.org/10.1016/j.jsv.2015.11.008
0022-460X/

the correlation between the magnitude of the features and the damage level. Commonly, the more sensitive a feature is to damage, the more sensitive it is to changing in the operational and environmental conditions (e.g., temperature and wind speed). To overcome this impact, robust feature extraction procedures are usually required [6–8].

Statistical modeling for feature classification phase is concerned with the implementation of machine learning algorithms that analyze the distributions of the extracted features and generate a data model in an effort to determine the structural health of the system. The algorithms used in statistical modeling usually fall into the outlier detection category, i.e., unsupervised learning is applied when training data are only available from the normal condition of the structure [9,10]. The data normalization procedure is normally present in the data acquisition, feature extraction and statistical modeling phases of the SHM process. Herein, data normalization includes a wide range of steps for removing the effect of operational and environmental variations on the extracted features [11].

Kernel-based machine learning algorithms have been widely applied to detect damage in SHM applications [12–16]. These algorithms, mostly based on support vector machines (SVMs), have revealed high sensitivity and accuracy in the damage classification. Mita and Hagiwara proposed a method using the supervised SVM to detect local damages in a building structure with limited number of sensors [17]. This method has been extended in several studies. For instance, a hybrid technique (wavelet SVM) may be considered, where damage-sensitive features are extracted through the wavelet energy spectrum and classified using the SVM [18]. In turn, a combined methodology between symbolic data analysis and classification techniques (e.g., SVM) is developed for damage assessment [19]. And, finally, an approach for detecting damage on shear structures using the SVM and the first three natural frequencies of the translational modes is assumed [20]. However, these approaches have not been implemented to remove the operational and environmental effects aggregated in extracted features; rather, they have been used to classify directly the extracted features in a supervised way, i.e., when data from the undamaged and damaged conditions are available.

However, for most civil engineering infrastructure where SHM systems are applied, the unsupervised learning algorithms are often required because only data from the undamaged condition are available [21,22]. Therefore, in this paper, an autoregressive (AR) model is used to extract damage-sensitive features upon time-series measured from an array of accelerometers, when the structure operates in different structural state conditions. Then, four unsupervised kernel-based machine learning algorithms are adapted for data normalization and damage detection. Firstly, they model the effects of the operational and environmental variability on the extracted features. Secondly, each algorithm produces a scalar output as a damage indicator (DI), which should be nearly invariant when features are extracted from the normal condition. Finally, DIs from the feature vectors of the test data are classified through a threshold defined based on the 95 percent cut-off value over the training data. The implemented algorithms are based on one-class support vector machine (one-class SVM), support vector data description (SVDD), kernel principal component analysis (KPCA) and greedy KPCA (GKPCA).

The main contribution of this study is the applicability of the proposed kernel-based algorithms for damage detection as well as the comparison of the classification performance, between these kernel-based algorithms and other reliable algorithms described in the literature [9,23–26], such as the auto-associative neural network (AANN) [11,27], factor analysis (FA) [28], Mahalanobis squared distance (MSD) [29], and singular value decomposition (SVD) [30], on standard data sets from a laboratory three-story frame aluminum structure. The performance is evaluated through receiver operating characteristic (ROC) curves, which are a means of determining performance on the basis of Type I/Type II error trade-offs. In SHM, in the context of damage detection, a Type I error is a false-positive indication of damage and a Type II error is a false-negative indication of damage. Besides, other contributions attested by the authors are the following: the first-time adaptation of the KPCA and GKPCA algorithms for damage detection in the SHM field; and the combination between one-class SVM/SVDD and MSD for data normalization purposes in the SHM field, particularly in the statistical modeling for feature classification phase.

This paper is organized as follows. Section 2 gives an explanation about the AR model for feature extraction, a brief background about the supervised SVM with the kernel trick for efficient optimization and the methodology of the four kernel-based machine learning algorithms for feature classification. A description of the test bed structure, the simulated operational and environmental variability, and a summary of the data sets is provided in Section 3. In Section 4, a comparative study between kernel-based algorithms and alternative approaches is carried out using features extracted from time-series data sets measured with accelerometers deployed on the test bed structure. Finally, Section 5 highlights a summary and discussion of the implementation and analysis carried out in this paper.

2. Feature extraction and kernel-based machine learning algorithms

The complete methodology applied in this study is depicted in Fig. 1. Basically, AR models are fitted to time series from an array of accelerometers when the structure is in different structural state conditions and their parameters are used as damage-sensitive features. Then, a training matrix, **X**, is composed of undamaged state conditions and a test matrix is composed of undamaged and damaged state conditions. Next, an unsupervised machine learning algorithm is trained and its parameters are adjusted using feature vectors from the training matrix only. In the test phase, the machine learning algorithm will transform each input feature vector from the test matrix, **Z**, into a global DI; the DIs should be nearly invariant for feature vectors extracted from the normal condition, assuming that the test data have been obtained from operational and environmental conditions represented in the training data. Finally, the classification is performed using one-sided

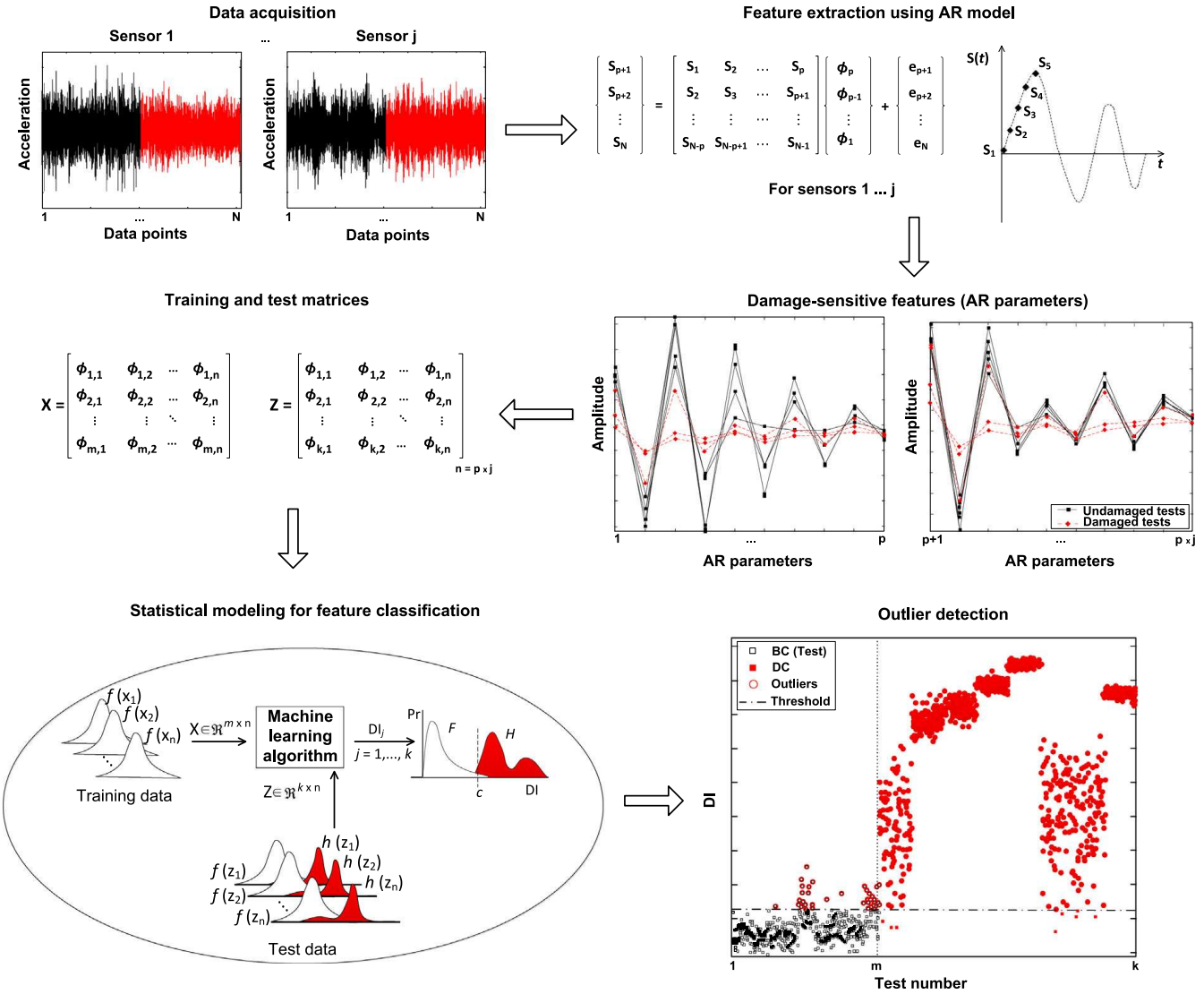

Fig. 1. Feature extraction and feature classification to determine the structural health of a system.

threshold for certain level of significance. If robust data normalization has been achieved, the DIs should be classified as outliers when feature vectors come from the damaged condition even when they include operational and environmental variability. All the methods for feature extraction and feature classification are described in detail in the next sections.

2.1. Autoregressive model for feature extraction

Usually, the modal parameters have been used in the SHM field for various applications as features that characterize the global condition of the structure. However, in this study, the AR model is used to extract damage-sensitive features, because the underlying linear stationary assumption makes it possible to detect the presence of nonlinearities in the time-series. It is considered that in a system where different dynamics are present at different times, the estimated parameters should change between intervals [31].

Alternatively, the AR models have been also used in SHM to extract damage-sensitive features from time-series data, either using the model parameters or residual errors [32,33]. For a measured time-series $s_1, s_2, \ldots, s_N$ the AR(p) model of order p is given by:

$$s_i = \sum_{j=1}^{p} \phi_j s_{i-j} + e_i, \tag{1}$$

where s_i is the measured signal and e_i is an unobservable random error at discrete time index i. The unknown AR parameters, ϕ_j, can be estimated using the least squares or the Yule–Walker equations [34]. The order of the model is always an unknown integer that needs to be estimated from the data. The Akaike information criterion (AIC) has been reported as one

of the most efficient techniques for order optimization [35]. The AIC is a measure of the goodness-of-fit of an estimated statistical model that is based on the trade-off between fitting accuracy and number of estimated parameters. In the context of AR models:

$$\mathrm{AIC} = N_t \ln(\varepsilon) + 2N_p, \tag{2}$$

where N_p is the number of estimated parameters, N_t is the number of predicted data points, and $\varepsilon = \mathrm{SSR}/N_t$ is the average sum-of-square residual (SSR) errors. The AR model with the lowest AIC value gives the optimal order p.

2.2. Support vector machine and kernel trick background

SVM is a powerful machine learning technique with strong regularization property for classification, regression, outlier detection and other learning tasks [36,37]. Given training vectors $\mathbf{x}_i \in \mathbb{R}^n$, $i = 1, \ldots, m$, in two classes, and a label vector $\mathbf{y} \in \mathbb{R}^m$ such that $\mathbf{y}_i \in \{1, -1\}$, supervised SVM solves the following primal optimization problem:

$$\begin{aligned} \min_{\mathbf{w},\boldsymbol{\xi},\mathbf{b}} \quad & \frac{1}{2}\mathbf{w}^T\mathbf{w} + \mathbf{C}\sum_{i=1}^{m}\boldsymbol{\xi}_i, \\ \text{s.t.} \quad & \mathbf{y}_i(\mathbf{w}^T\boldsymbol{\phi}(\mathbf{x}_i) + \mathbf{b}) \geq 1 - \boldsymbol{\xi}_i, \\ & \boldsymbol{\xi}_i \geq 0, \quad i = 1, \ldots, m, \end{aligned} \tag{3}$$

where $\boldsymbol{\phi}(\mathbf{x}_i)$ maps $\mathbf{x}_i$ into a high-dimensional space, $\boldsymbol{\xi}_i$ is the intermediate parameter, $\mathbf{C}$ is the regularization or penalty parameter and $\mathbf{b}$ is the adjustable parameter of the decision function; $\boldsymbol{\xi}_i$ is a slack variable for controlling how much training error is allowed and $\mathbf{C}$ is a parameter for balancing between $\boldsymbol{\xi}_i$ (the training error) and $\mathbf{w}$ (the margin). SVM finds a linear separating hyperplane with the maximal margin in the high-dimensional space. This minimization problem can be solved by Lagrangian multiplier or quadratic programming. Due to the possible high dimensionality of the vector $\mathbf{w}$, usually the problem must be transformed to the dual equivalent problem for solving:

$$\begin{aligned} \min_{\boldsymbol{\alpha}} \quad & \frac{1}{2}\boldsymbol{\alpha}^T\mathbf{Q}\boldsymbol{\alpha} - \mathbf{e}^T\boldsymbol{\alpha}, \\ \text{s.t.} \quad & \mathbf{y}^T\boldsymbol{\alpha} = 0, \\ & 0 \leq \boldsymbol{\alpha}_i \leq \mathbf{C}, \quad i = 1, \ldots, m, \end{aligned} \tag{4}$$

where $\boldsymbol{\alpha}$ is the Lagrange multipliers, $\mathbf{e} = [1, \ldots, 1]^T$ is a vector of all ones, $\mathbf{Q}$ is a positive semi-definite matrix, $\mathbf{Q}_{i,j} \equiv \mathbf{y}_i\mathbf{y}_j\mathbf{K}(\mathbf{x}_i, \mathbf{x}_j)$, and $\mathbf{K}(\mathbf{x}_i, \mathbf{x}_j) \equiv \boldsymbol{\phi}(\mathbf{x}_i)^T\boldsymbol{\phi}(\mathbf{x}_j)$ is a kernel function.

After the dual problem is solved, using the primal-dual relationship, the optimal $\mathbf{w}$ reads

$$\mathbf{w} = \sum_{i=1}^{m}\mathbf{y}_i\boldsymbol{\alpha}_i\boldsymbol{\phi}(\mathbf{x}_i) \tag{5}$$

and the decision function is

$$\mathrm{sgn}(\mathbf{w}^T\boldsymbol{\phi}(\mathbf{x}) + \mathbf{b}) = \mathrm{sgn}\left(\sum_{i=1}^{m}\mathbf{y}_i\boldsymbol{\alpha}_i\mathbf{K}(\mathbf{x}_i, \mathbf{x}) + \mathbf{b}\right). \tag{6}$$

Then, $\mathbf{y}_i\boldsymbol{\alpha}_i \forall i, \mathbf{b}$, label names, support vectors, and other information such as kernel parameters are stored in the trained model for future predictions.

The SVM algorithm mentioned early is a supervised linear classifier. In order to capture nonlinearity, nonlinear kernel function must be used. Some basic kernels are [38]:

- *linear*: $\mathbf{K}(\mathbf{x}_i, \mathbf{x}_j) = \mathbf{x}_i^T\mathbf{x}_j$;
- *polynomial*: $\mathbf{K}(\mathbf{x}_i, \mathbf{x}_j) = (\boldsymbol{\gamma}\mathbf{x}_i^T\mathbf{x}_j + r)^d$, $\boldsymbol{\gamma} > 0$;
- *radial basis function*: $\mathbf{K}(\mathbf{x}_i, \mathbf{x}_j) = \exp(-\boldsymbol{\gamma}\|\mathbf{x}_i - \mathbf{x}_j\|^2)$, $\boldsymbol{\gamma} > 0$;
- *sigmoid*: $\mathbf{K}(\mathbf{x}_i, \mathbf{x}_j) = \tanh(\boldsymbol{\gamma}\mathbf{x}_i^T\mathbf{x}_j + r)$;

where $\boldsymbol{\gamma}$, r, and d are kernel parameters. The radial basis function (RBF) kernel option is most commonly used in a large range of applications [39]. This kernel maps examples into a high-dimensional space so it, unlike the linear kernel, can handle the case when the relationship between class labels and features is nonlinear.

2.3. Feature classification

For general purposes, consider a training data matrix composed of normal condition data, $\mathbf{X} \in \mathbb{R}^{m \times n}$, with n-dimensional feature vectors from m different operational and environmental conditions when the structure is undamaged and a test data matrix, $\mathbf{Z} \in \mathbb{R}^{k \times n}$, where k is the number of feature vectors from the undamaged and/or damage conditions. Note that a feature vector represents some property of the system at a given time.

2.3.1. One-class support vector machine

The one-class SVM algorithm or distribution estimation was proposed by Schölkopf [40] for estimating the support of a high-dimensional distribution in an unsupervised way. Given training vectors $\mathbf{x}_i \in \mathbb{R}^n$, $i=1,\ldots,m$, without any class information (no labels), the primal problem of one-class SVM is

$$\begin{aligned} \min_{\mathbf{w},\boldsymbol{\xi},\rho} \quad & \frac{1}{2}\mathbf{w}^T\mathbf{w} - \rho + \frac{1}{\nu m}\sum_{i=1}^{m}\boldsymbol{\xi}_i, \\ \text{s.t.} \quad & \mathbf{w}^T\boldsymbol{\phi}(\mathbf{x}_i) \geq \rho - \boldsymbol{\xi}_i, \\ & \boldsymbol{\xi}_i \geq 0, \quad i=1,\ldots,m. \end{aligned} \tag{7}$$

The distribution estimation SVM introduces a new parameter $\nu \in (0,1]$. This parameter is an upper bound on the fraction of training errors and a lower bound of the fraction of support vectors [41]. In other words, ν has a similar effect of $\mathbf{C}$ for supervised SVM. Furthermore, the dual problem or unsupervised learning phase is

$$\begin{aligned} \min_{\boldsymbol{\alpha}} \quad & \frac{1}{2}\boldsymbol{\alpha}^T\mathbf{Q}\boldsymbol{\alpha}, \\ \text{s.t.} \quad & \mathbf{e}^T\boldsymbol{\alpha} = 1, \\ & 0 \leq \boldsymbol{\alpha}_i \leq 1/(\nu m), \quad i=1,\ldots,m, \end{aligned} \tag{8}$$

where $\mathbf{Q}_{i,j} = \mathbf{K}(\mathbf{x}_i,\mathbf{x}_j) = \boldsymbol{\phi}(\mathbf{x}_i)^T\boldsymbol{\phi}(\mathbf{x}_j)$. The decision function is defined as

$$\operatorname{sgn}\left(\sum_{i=1}^{m}\boldsymbol{\alpha}_i\mathbf{K}(\mathbf{x}_i,\mathbf{x}) - \rho\right). \tag{9}$$

When the model is obtained, a damage indicator can be generated by applying the MSD algorithm for each test vector $\mathbf{z}$ and the support vectors from the model,

$$\mathbf{DI} = (\mathbf{z}-\boldsymbol{\mu})^T\boldsymbol{\Sigma}^{-1}(\mathbf{z}-\boldsymbol{\mu}), \tag{10}$$

where $\boldsymbol{\mu}$ is the mean of the support vectors from the model and $\boldsymbol{\Sigma}$ is the covariance matrix of these support vectors. Therefore, this approach combines the robustness of the one-class SVM algorithm to derive a nonlinear model from undamaged data and the effectiveness of an outlier detection metric by means of the MSD.

2.3.2. Support vector data description

The SVDD algorithm, proposed by Tax and Duin [42], is an unsupervised method to find the boundary around a data set (a hypersphere). Given a set of training data $\mathbf{x}_i \in \mathbb{R}^n$, $i=1,\ldots,m$, the SVDD solves the following primal optimization problem:

$$\begin{aligned} \min_{\mathbf{R},\mathbf{a},\boldsymbol{\xi}} \quad & \mathbf{R}^2 + \mathbf{C}\sum_{i=1}^{m}\boldsymbol{\xi}_i, \\ \text{s.t.} \quad & \|\boldsymbol{\phi}(\mathbf{x}_i) - \mathbf{a}\|^2 \leq \mathbf{R}^2 + \boldsymbol{\xi}_i, i=1,\ldots,m, \\ & \boldsymbol{\xi}_i \geq 0, \quad i=1,\ldots,m, \end{aligned} \tag{11}$$

where the sphere is characterized by center $\mathbf{a}$ and radius $\mathbf{R}>0$, and $\boldsymbol{\phi}$ is a function mapping data to a high-dimensional space. After Eq. (11) is solved, a test instance $\mathbf{z}$ is detected as an outlier if $\|\boldsymbol{\phi}(\mathbf{z}) - \mathbf{a}\|^2 > \mathbf{R}^2$, i.e., if $\mathbf{z}$ is outside the boundary set by the SVDD model.

Because of the large number of variables in $\mathbf{a}$ after data mapping, the following Lagrange dual problem is solved in the training phase:

$$\begin{aligned} \min_{\boldsymbol{\alpha}} \quad & \sum_{i=1}^{m}\boldsymbol{\alpha}_i\mathbf{Q}_{i,i} - \boldsymbol{\alpha}^T\mathbf{Q}\boldsymbol{\alpha}, \\ \text{s.t.} \quad & \mathbf{e}^T\boldsymbol{\alpha} = 1, \\ & 0 \leq \boldsymbol{\alpha}_i \leq \mathbf{C}, \quad i=1,\ldots,m, \end{aligned} \tag{12}$$

where $\mathbf{e} = [1,\ldots,1]^T$, $\boldsymbol{\alpha} = [\boldsymbol{\alpha}_1,\ldots,\boldsymbol{\alpha}_m]^T$, and $\mathbf{Q}$ is the kernel matrix such that $\mathbf{Q}_{i,j} = \boldsymbol{\phi}(\mathbf{x}_i)^T\boldsymbol{\phi}(\mathbf{x}_j), \forall 1 \leq i,j \leq m$. The DIs are generated by the same procedure described for the one-class SVM algorithm. However, in this case, the support vectors represent a hypersphere, instead of a hyperplane.

A relationship between one-class SVM and SVDD algorithms can be established by the following expression [43]:

$$\mathbf{C} = \frac{1}{\nu m}. \tag{13}$$

2.3.3. Kernel principal component analysis

The KPCA algorithm is the nonlinear extension of the linear principal component analysis (PCA) [44]. The input training matrix $\mathbf{X}$ is mapped by $\boldsymbol{\phi}$: $\mathbf{X} \rightarrow \mathcal{F}$ to a high-dimensional feature space $\mathcal{F}$. The linear PCA is applied on the mapped data $\mathcal{T}_{\Phi} = \{\boldsymbol{\phi}(\mathbf{x}_1),\ldots,\boldsymbol{\phi}(\mathbf{x}_m)\}$. The computation of the principal components and the projection on these components can be

expressed in terms of dot products thus the kernel functions can be employed. The KPCA trains the kernel data projection:

$$\mathbf{y} = \mathbf{A}^T \mathbf{k}(\mathbf{x}) + \mathbf{o}, \tag{14}$$

where $\mathbf{A} \in \mathbb{R}^{m \times d}$ is the projection matrix, $\mathbf{k}(\mathbf{x}) = [\mathbf{k}(\mathbf{x}, \mathbf{x}_1), \ldots, \mathbf{k}(\mathbf{x}, \mathbf{x}_m)]^T$ is a vector of kernel functions centered in the training vectors and $\mathbf{o} \in \mathbb{R}^d$ is the bias vector. Additionally, $\mathbf{A}$ is the matrix containing the corresponding eigenvectors. The eigenvectors associated with the higher eigenvalues are the principal components of the data matrix and they correspond to the dimensions that have the largest variability in the data. Basically, this method permits one to perform a transformation by retaining only the principal components d, also known as the number of factors, in a high-dimensional feature space $\mathbb{R}^{m \times m}$.

The kernel mean squared reconstruction error, which must be minimized, is defined as

$$\varepsilon_{\mathrm{KMS}}(\mathbf{A}, \mathbf{o}) = \frac{1}{m} \sum_{i=1}^{m} \| \boldsymbol{\phi}(\mathbf{x}_i) - \tilde{\boldsymbol{\phi}}(\mathbf{x}_i) \|^2, \tag{15}$$

where the reconstructed vector $\tilde{\boldsymbol{\phi}}(\mathbf{x})$ is given as a linear combination of the mapped data $\mathcal{T}_{\Phi}$:

$$\tilde{\boldsymbol{\phi}}(\mathbf{x}) = \sum_{i=1}^{m} \beta_i \boldsymbol{\phi}(\mathbf{x}_i), \quad \beta = \mathbf{A}(\mathbf{y} - \mathbf{o}). \tag{16}$$

In contrast to the linear PCA, the explicit projection from the feature space $\mathcal{F}$ to the input space usually does not exist [45]. The problem is to find the vector $\mathbf{x}$ and its image $\boldsymbol{\phi}(\mathbf{x}) \in \mathcal{F}$ that well approximates the reconstructed vector $\tilde{\boldsymbol{\phi}}(\mathbf{x}) \in \mathcal{F}$. This procedure consists of the following steps:

Step 1: Project the input vector $\mathbf{x}_{\mathrm{in}} \in \mathbb{R}^n$ onto its lower-dimensional representation $\mathbf{y} \in \mathbb{R}^d$ using Eq. (14).
Step 2: Compute the output vector $\mathbf{x}_{\mathrm{out}} \in \mathbb{R}^n$ which is satisfactory pre-image of the reconstructed vector $\tilde{\boldsymbol{\phi}}(\mathbf{x}_{\mathrm{in}})$, such that

$$\mathbf{x}_{\mathrm{out}} = \underset{\mathbf{x}}{\operatorname{argmin}} \| \boldsymbol{\phi}(\mathbf{x}) - \tilde{\boldsymbol{\phi}}(\mathbf{x}_{\mathrm{in}}) \|^2. \tag{17}$$

For the test matrix $\mathbf{Z}$, the residual errors matrix $\mathbf{E}$ is given by:

$$\mathbf{E} = \mathbf{Z} - \hat{\mathbf{Z}}, \tag{18}$$

where $\hat{\mathbf{Z}}$ corresponds to the estimated feature vectors that are the output of the pre-image computation from the model obtained by KPCA in the training phase. In other words, the pre-image problem maps the feature vectors from the high-dimensional feature space back to the input space. An iterative fixed point algorithm is used for this purpose [46]. In order to establish a quantitative measure of damage, for the feature vector f ($f = 1, 2, \ldots, k$), a DI is adopted in the form of the squared root of the sum-of-square errors (Euclidean norm):

$$\mathbf{DI}(f) = \| \mathbf{e}_f \|. \tag{19}$$

If f feature vector is related to the undamaged condition, $\mathbf{z}_f \approx \hat{\mathbf{z}}_f$ and $\mathbf{DI}(f) \approx 0$. On the other hand, if the feature vector comes from the damaged condition, the residual errors increase, and the DI deviates from zero, indicating an abnormal condition in the structure.

2.3.4. Greedy kernel principal component analysis

The GKPCA algorithm is an efficient method to compute the KPCA algorithm [47]. Let $\mathcal{T}_{\mathbf{X}} = \{\mathbf{x}_1, \ldots, \mathbf{x}_m\}$, $\mathbf{x}_i \in \mathbb{R}^n$, $i = 1, \ldots, m$, be the set of input training vectors. The goal is to train the kernel data projection:

$$\mathbf{y} = \mathbf{A}^T \mathbf{k}_{\mathbf{S}}(\mathbf{x}) + \mathbf{o}, \tag{20}$$

where $\mathbf{k}_{\mathbf{S}}(\mathbf{x}) = [\mathbf{k}(\mathbf{x}, \mathbf{s}_1), \ldots, \mathbf{k}(\mathbf{x}, \mathbf{s}_m)]^T$ are the kernel functions centered in the vectors from $\mathcal{T}_{\mathbf{S}} = \{\mathbf{s}_1, \ldots, \mathbf{s}_m\}$. The vector set $\mathcal{T}_{\mathbf{S}}$ is a subset of training data $\mathcal{T}_{\mathbf{X}}$.

In opposition to the PCA, the basis vectors of the lower-dimensional space used for data representation are properly selected vectors from the training set and not as their linear combinations. The basis vectors can be selected by a simple algorithm which has low computational requirements and allows real-time processing by approximating the training set in the high-dimensional space [47]. Moreover, in contrast to the original KPCA, the subset $\mathcal{T}_{\mathbf{S}}$ does not contain all the training vectors in $\mathcal{T}_{\mathbf{X}}$ thus the complexity of the projection in Eq. (20) is reduced compared to Eq. (14). The objective of the GKPCA is to minimize the reconstruction error while the size of the subset $\mathcal{T}_{\mathbf{S}}$ is kept small. The DIs are generated by the same procedure described for KPCA, considering the residuals from $\mathbf{E}$.

3. Test bed structure and data

The standard data sets used in this study are from a three-story frame aluminum structure reported in [48], and has been intensively used for SHM validation in recent statistical damage identification approaches [13,23,25]. These data were collected by four accelerometers mounted on a test bed building model, as shown in Fig. 2, forming a essentially four-degree-of-freedom system with varied practical conditions, including variations in stiffness (e.g., to simulate temperature

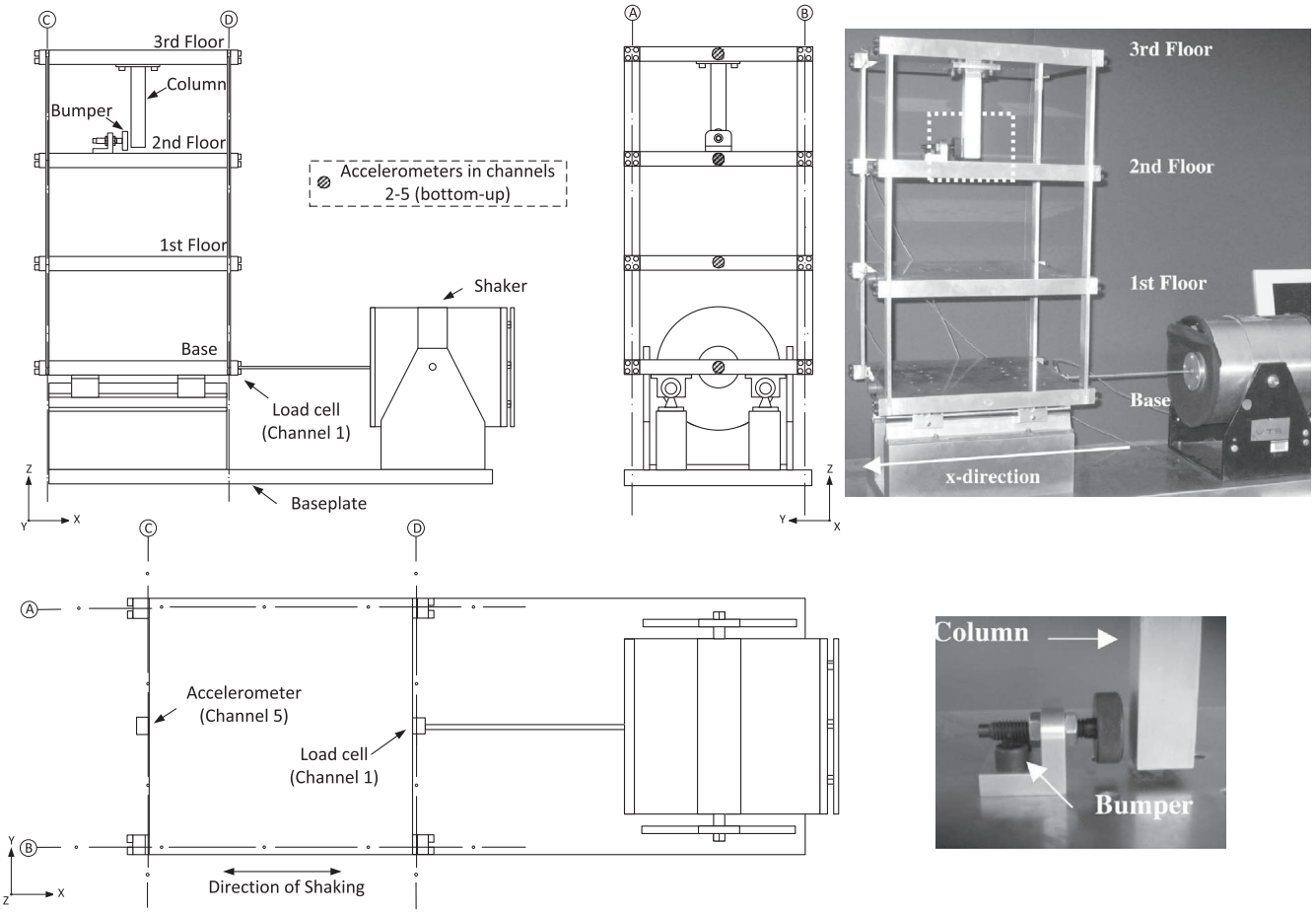

Fig. 2. Three-story frame aluminum structure and shaker.

variations) and in mass-loading (e.g., to simulate traffic). Those changes were designed to introduce variability in the fundamental natural frequency up to approximately 7 percent from the baseline condition, which is within the range normally observed in real-world structures [49,50]. Nonlinear damage was introduced by contacting a suspended column with a bumper mounted on the floor below to simulate fatigue crack that can open and close under loading conditions or loose connections in structures. Different levels of damage were created by adjusting the gap between the column and the bumper (smaller the gap, higher the level of damage). More details about the test structure can be found in [48].

Acceleration time-series (discretized into 4096 data points sampled at 3.125 ms intervals corresponding to a sampling frequency of 320 Hz) from 17 different structural state conditions were collected, as described in Table 1. For each structural state condition, data were acquired from 100 separate tests. According to the test description [51], state1 is the baseline condition (reference state) of the structure and states2–9 include those states with simulated operational and environmental variability. State14 is considered as the most severe damaged one as it corresponds to the smallest gap case, which induces the highest number of impacts. State10 is the least severe damaged scenario and states11–13 represent mid-level damage scenarios. States15–17 are the variant states of either state10 or state13 with mass added effect in order to create more realistic conditions.

4. Experimental results and analysis

In this study, the AR parameters from response time series are used as damage-sensitive features. Thus, for each test of each state condition, the parameters are estimated using the least squares technique applied upon time-series from all four accelerometers (channels 2–5) and stored into a feature vector. For each test, the number of estimated parameters is $p \times 4$ and ε is the sum of the average sum-of-square errors of channels 2–5. In this analysis is assumed an output-only damage detection approach, and so data from the channel 1 (the input force) is not used.

The linear AR models achieve enough small AIC value around $p=10$ [23]. Based on that evaluation, for each test, four individual AR(10) models are used to fit the corresponding time series from the four accelerometers and their parameters are used as damage-sensitive features in concatenated format, yielding 40-dimensional feature vectors. Note that AR parameters should be constant when estimated based on time-series data obtained from time-invariant systems. However, in the presence of operational and environmental conditions as well as damage, the parameters are expected to change

Table 1
Data labels of the structural state conditions.

Label	State condition	Description
State1	Undamaged	Baseline condition
State2	Undamaged	Added mass (1.2 kg) at the base
State3	Undamaged	Added mass (1.2 kg) on the 1st floor
State4	Undamaged	States4–9: 87.5% stiffness reduction at various positions to simulate temperature impact (more details in [48])
State5	Undamaged	
State6	Undamaged	
State7	Undamaged	
State8	Undamaged	
State9	Undamaged	
State10	Damaged	Gap (0.20 mm)
State11	Damaged	Gap (0.15 mm)
State12	Damaged	Gap (0.13 mm)
State13	Damaged	Gap (0.10 mm)
State14	Damaged	Gap (0.05 mm)
State15	Damaged	Gap (0.20 mm) and mass (1.2 kg) at the base
State16	Damaged	Gap (0.20 mm) and mass (1.2 kg) on the 1st floor
State17	Damaged	Gap (0.10 mm) and mass (1.2 kg) on the 1st floor

accordantly, as shown in Fig. 3, for instance, for one test corresponding to states1, 3, 5, 7, 9, 10, 14 and 17. The feature vectors are divided according to their structural condition into two major groups: undamaged and damaged conditions. Particular changes are noticed in the amplitude of the AR parameters at channels 4 and 5 when features are from the damaged condition (those channels are closer to the source of damage). Clearly, the AR parameters reveal high sensitivity to the presence of damage. In general, the higher the level of damage (the smaller the gap), the lower the amplitude of the AR parameters.

For generalization purposes, the feature vectors are split into the training and test matrices. The training matrix, $\mathbf{X}$, permits each algorithm to learn the underlying distribution and dependency of all undamaged states on the simulated operational and environmental variability. Thus, this matrix is composed of AR parameters from 50 out of 100 tests of each undamaged state (states1–9), and so it has a dimension of 450×40. The test matrix $\mathbf{Z}$ (1250×40) is composed of AR parameters from the remaining 50 tests of each undamaged state together with AR parameters from all the 100 tests of each damaged state (states10–17). This procedure permits one to evaluate the generalization performance of the machine learning algorithms in an exclusive manner, because time-series used in the test phase are not included in the training phase. During the test phase, the algorithms are expected to detect deviations from the normal condition when feature vectors come from damaged states, even in the presence of operational and environmental effects.

The next step is to carry out statistical modeling for feature classification. In that regard, the algorithms based on one-class SVM, SVDD, KPCA and GKPCA are implemented in an unsupervised learning mode by first taking into account features from all the undamaged state conditions (training matrix). All kernel-based algorithms use the RBF kernel with parameter $\gamma = 0.025$. The regularization parameter is defined as $\nu = 0.8$ ($\mathbf{C}$ is obtained by the equivalence between one-class SVM and SVDD). The KPCA and GKPCA algorithms are configured to retain 90 percent of the variability in the data after dimension reduction. The subset of 25 percent of the training data is used for GKPCA kernel projection. The algorithms based on AANN, FA, MSD and SVD are implemented and configured as described in [23]. Finally, for each algorithm, the DIs are stored into a 1250-length vector.

The ROC curves provide a comprehensive means of summarizing the performance of classifiers. They focus on the trade-off between true detection and false alarm rates. The point at the left-upper corner of the plot (0, 1) is called a perfect classification. Fig. 4 plots, partially, the ROC curves for the kernel-based algorithms. Qualitatively, looking at the curves, one can verify that none of the algorithms can have a perfect classification with a linear threshold because none of the curves go through the left-upper corner, neither have supremacy in terms of true detection rate for all the false alarm domain. Furthermore, one can figure out that for levels of significance around 5 percent, the KPCA and GKPCA have better true detection rate than one-class SVM and SVDD, i.e., the approaches that maximize the true detection of damaged cases with similar performances in terms of false alarm rate. Nonetheless, for low probabilities of false alarm, all the algorithms show to have acceptable true detection rate (for instance, for a false alarm rate of 0.05, the minimal true detection rate is around 0.98, given by the one-class SVM and SVDD). Note that all proposed algorithms apply data transformation in the high-dimensional feature space to achieve a data model that represents the normal structural condition. Nevertheless, the one-class SVM and SVDD algorithms discover nonlinear relationship in the data via hyperplane and hypersphere separations. On the other hand, the KPCA and GKPCA algorithms reduce the data dimensionality in high-dimensional space, storing the principal components that have the largest variability in the data.

Due to the similar classification performances of the one-class SVM and SVDD, and the superiority of the GKPCA relative to the KPCA, the authors chose the one-class SVM and GKPCA algorithms for a comparative analysis with algorithms already analyzed in the literature. In the first case, Fig. 5 shows a comparison between the FA, SVD, one-class SVM and GKPCA

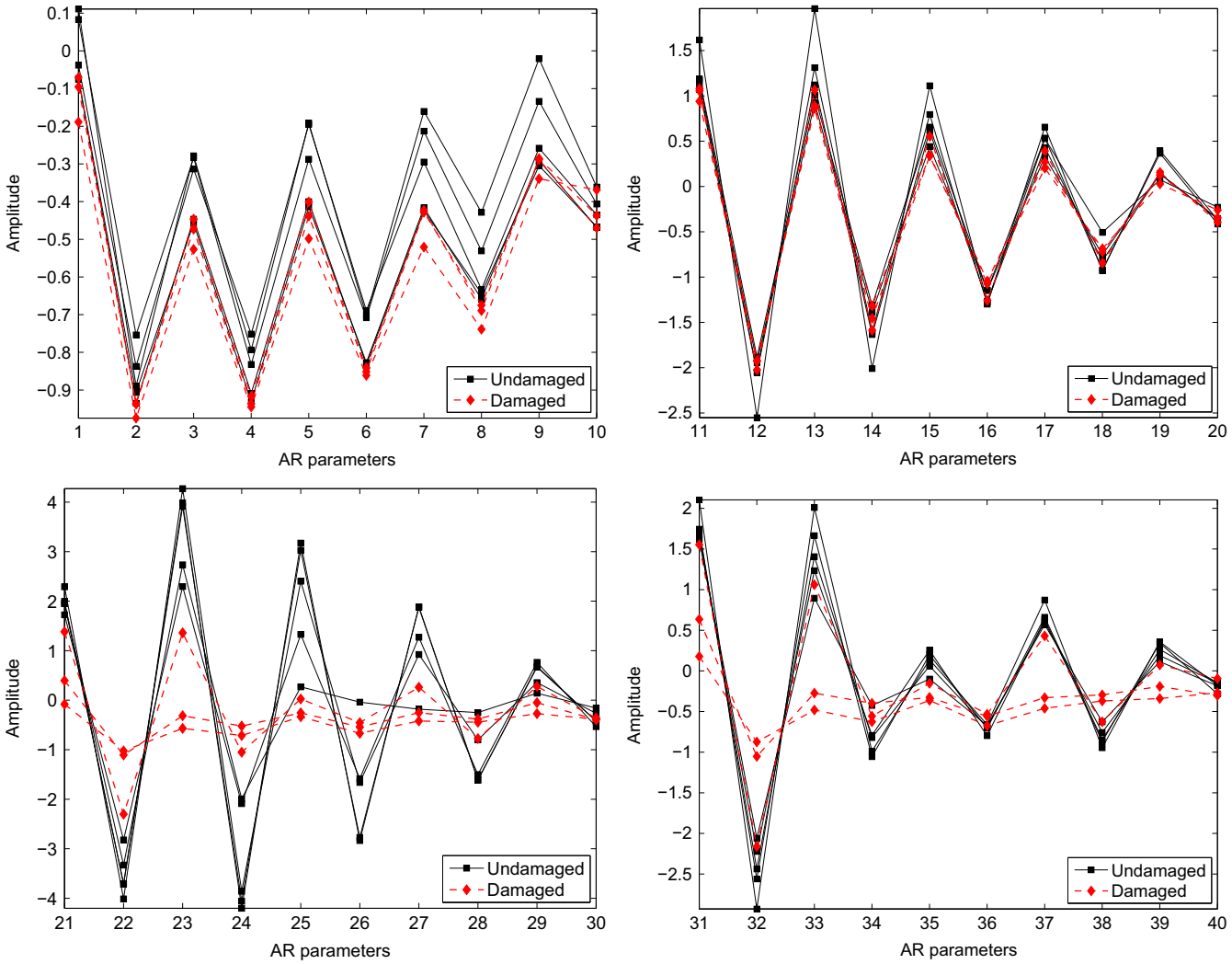

Fig. 3. Feature vectors from one test of states1, 3, 5, 7 and 9 (undamaged) and states10, 14 and 17 (damaged): AR parameters from channels 2 (upper left), 3 (upper right), 4 (lower left) and 5 (lower right).

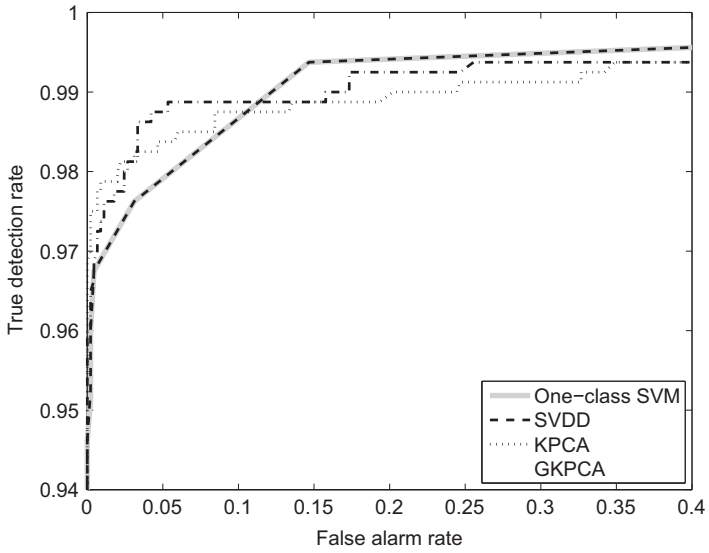

Fig. 4. Partial ROC curves for the kernel-based algorithms.

algorithms. In the whole false alarm range and for a given threshold, the kernel-based algorithms have, clearly, better performance to detect abnormal conditions in the test structure than the FA and SVD algorithms, which is expected as the FA and SVD algorithms can only capture linear patterns in the data. In the second case, Fig. 6 shows a comparison between

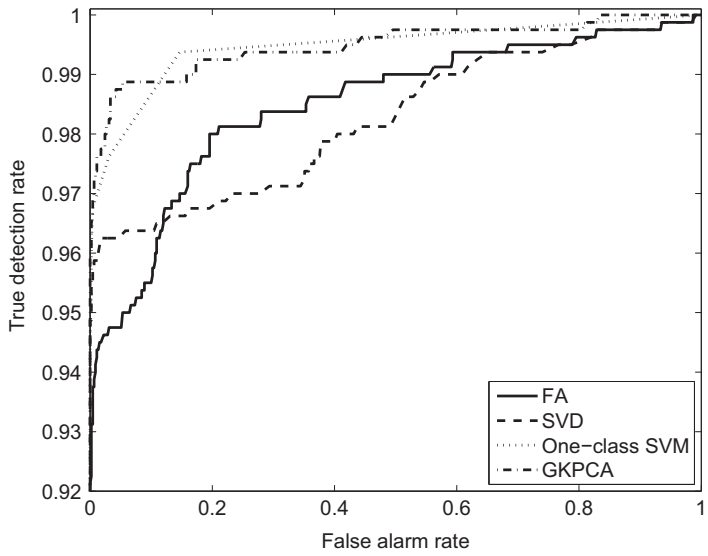

Fig. 5. ROC curves for the FA, SVD, one-class SVM and GKPCA algorithms.

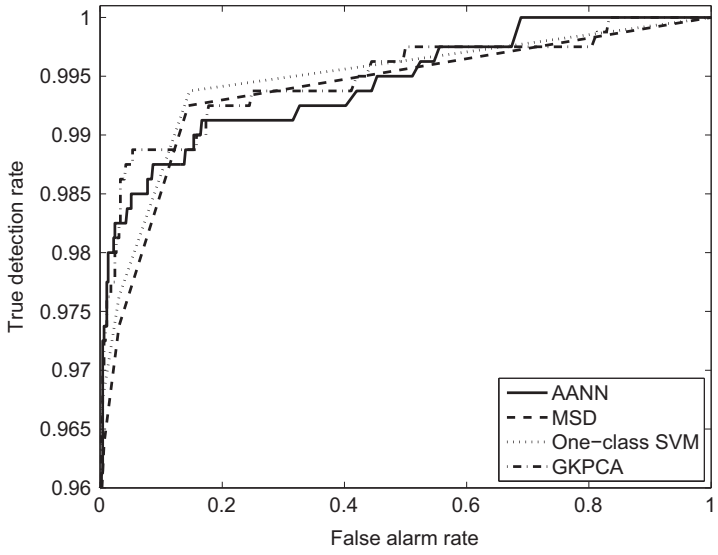

Fig. 6. ROC curves for the AANN, MSD, one-class SVM and GKPCA algorithms.

the AANN, MSD, one-class SVM and GKPCA algorithms. In general, the ROC curve of the one-class SVM follows the same behavior as the ROC curve of the MSD algorithm; the GKPCA and AANN algorithms also output similar ROC curves. In particular, the one-class SVM has superior performance in feature classification than MSD in whole false alarm rate range, by properly selecting the support vectors to represent an optimal subset of the undamaged condition; whereas the GKPCA seems to be more effective than the AANN in most points of the ROC curves by assimilating the normal structural condition embedded into the principal components, especially for false alarm rates around 5 percent (the threshold normally used in real-world scenarios).

In order to quantify the performance of the classifiers for a given threshold, Figs. 7 and 8 plot the DIs for the feature vectors of the entire test data along with a threshold defined based on the 95 percent cut-off value over the training data. All the algorithms show a monotonic relationship between the level of damage and the amplitude of the DI, even when operational and environmental variability is present, i.e., the approaches are able to remove the operational and environmental effects in such a way that DIs from states15, 16 and 10 have similar amplitude, as well as state17 is associated with state13. Recall that states15–17 are the variant states of either state10 or state13 with operational effects.

The Type I (false-positive indication of damage) and Type II (false-negative indication of damage) errors are traditionally used to report the performance of a binary classification. This technique recognizes that a false-positive classification may have different consequences than false-negative one. In Figs. 7 and 8, the Type I errors are DIs that exceed the threshold value in the undamaged condition domain (1–450). On the other hand, the Type II errors are DIs that do not surpass the threshold value in the damaged condition domain (451–1250). Table 2 summarizes the number and percentage of Type I

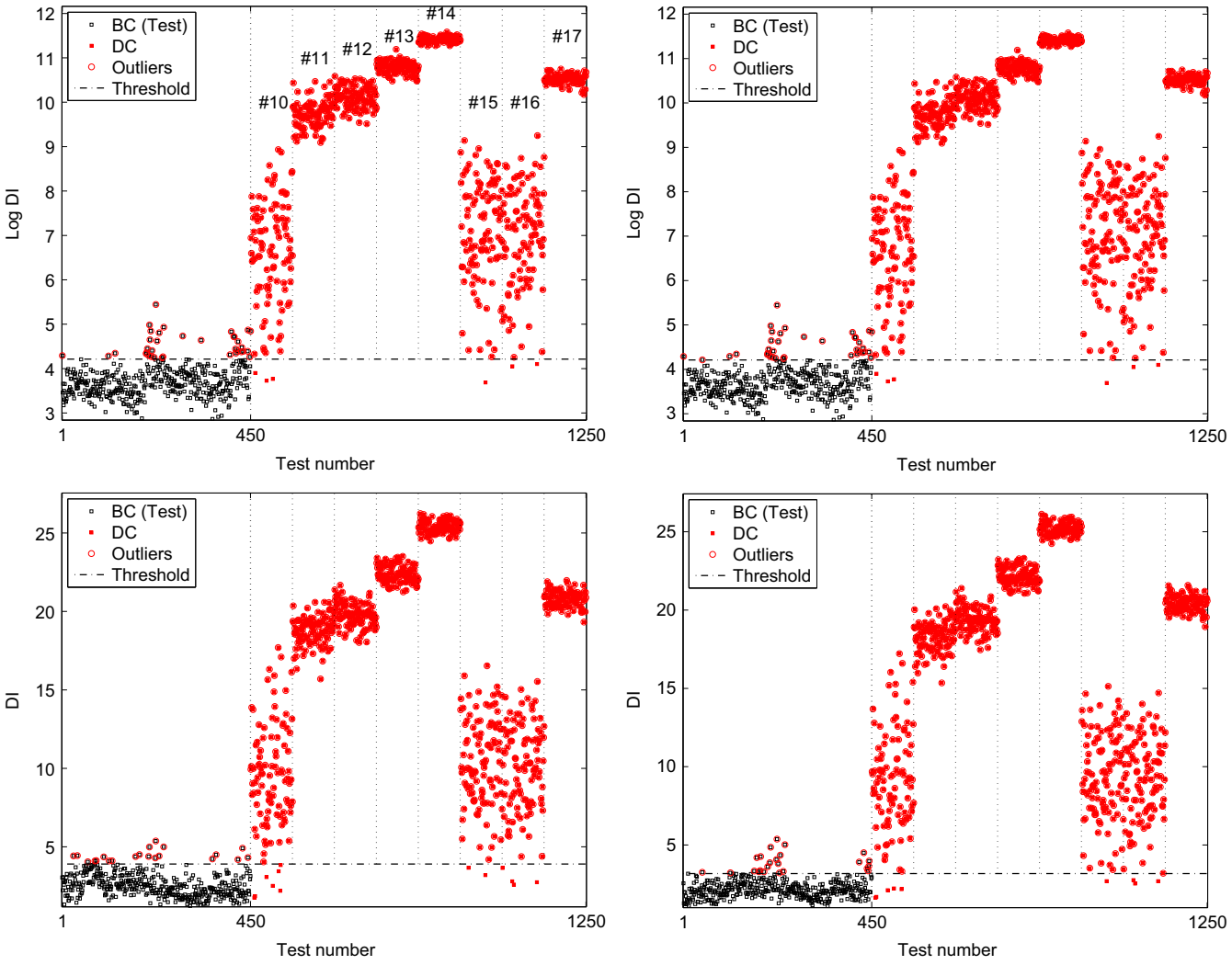

Fig. 7. DIs calculated based on feature vectors from the undamaged/baseline condition (BC) and damaged condition (DC) using the four kernel-based algorithms along with thresholds defined by the 95% cut-off value over the training data: one-class SVM (upper left), SVDD (upper right), KPCA (lower left), and GKPCA (lower right).

and Type II errors for each algorithm (based on the composition of the test matrix **Z**), demonstrating a trade-off between Type I and Type II errors for all eight algorithms.

In terms of an overall analysis, the one-class SVM and SVDD algorithms have similar performance and the best performance overall to detect damage (0.75 percent); however they output a relatively high false alarm rate (≥ 8 percent), as the selected support vectors can easily identify the damaged data, but are not properly representing the normal condition as the number of Type I errors is higher than 5 percent. The FA algorithm has the better performance to avoid false indications of damage (2.22 percent), but the worst performance to detect damage (5.38 percent) due to its sensitivity to the number of factors driving changes in features. The AANN reveals the worst performance in terms of Type I errors (9.78 percent), but a relatively good performance in terms of minimization of Type II errors (1.25 percent), which gives indications that when the sensitivity (the portion of damaged cases correctly identified) of the classifier is increased, and so it detects more damaged cases, it also increases the number to mislabels of undamaged cases. Thus, as the sensitivity goes up, specificity (the portion of undamaged cases which are correctly identified) goes down. The KPCA and GKPCA attempt a balancing between Type I and Type II errors, having the minimum errors in total, which is supported by the retention of principal components in the high-dimensional space, which eliminates variability caused by operational and environmental effects. Finally, the proposed four algorithms have a tendency to reduce the total number of misclassifications (average of 3.04 percent) when compared with the four approaches previously tested (average of 4.3 percent). This superiority might be related with the ability of the proposed algorithms to find nonlinear patterns in the data via the kernel trick, as well as the independence on the choice of the initial parameters (unlike the FA, for instance, where one needs to set the number of hidden factors driving changes in the damage-sensitive features).

In particular, and for the proposed algorithms, the one-class SVM and SVDD algorithms have similar performance in the feature classification (changing only Type I error), demonstrating the relationship between them via the regularization parameters ν and **C**. In turn, the KPCA and GKPCA algorithms have also similar performance; however, both Type I and Type

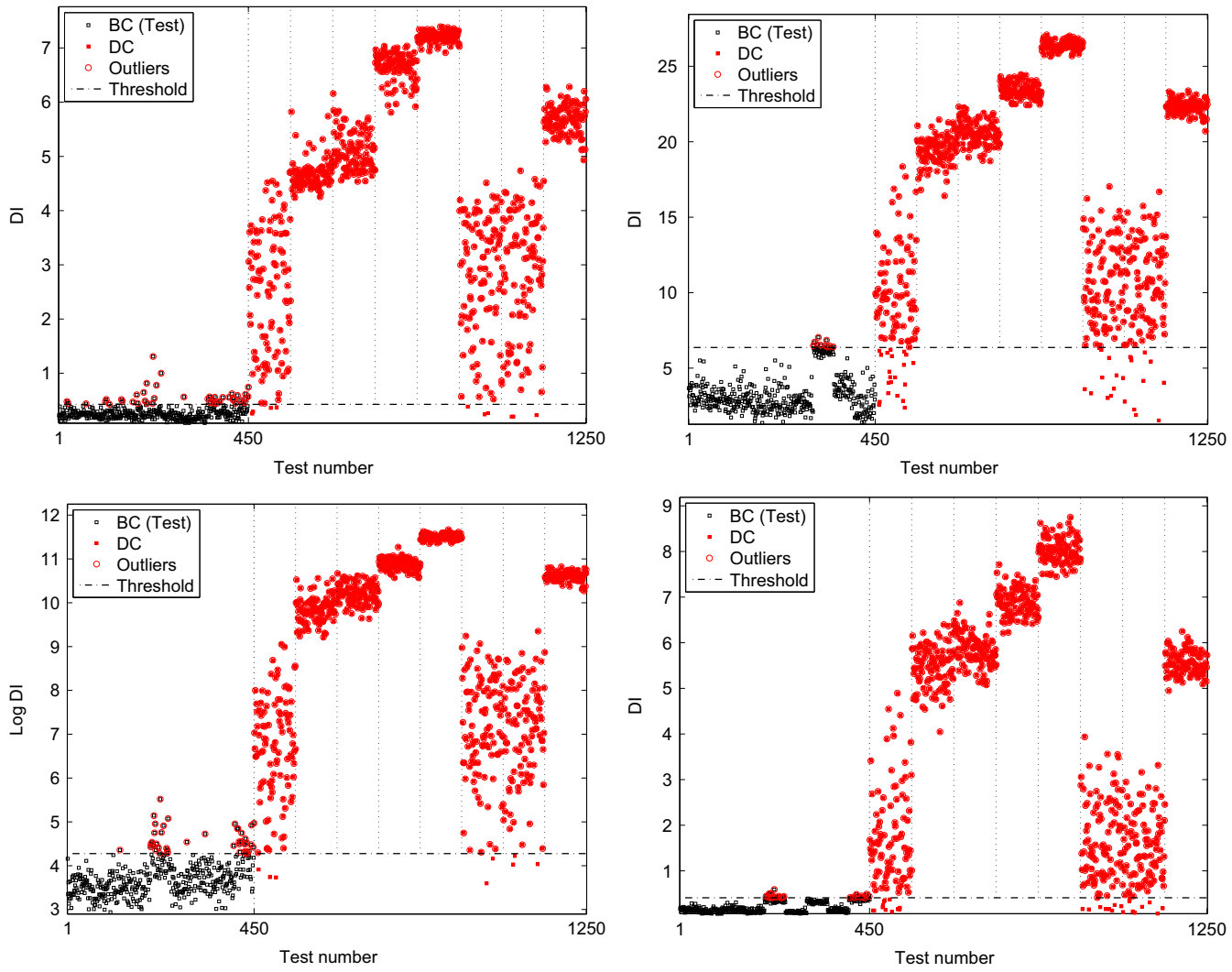

Fig. 8. DIs calculated based on feature vectors from the undamaged/baseline condition (BC) and damaged condition (DC) using the state-of-the-art algorithms along with thresholds defined by the 95% cut-off value over the training data: AANN (upper left), FA (upper right), MSD (lower left), and SVD (lower right).

Table 2
Number and percentage of Type I and Type II errors for each algorithm.

Algorithm	Error		
	Type I	Type II	Total
AANN	44 (9.78%)	10 (1.25%)	54 (4.32%)
FA	10 (2.22%)	43 (5.38%)	53 (4.24%)
MSD	42 (9.33%)	8 (1.00%)	50 (4.00%)
SVD	29 (6.44%)	29 (3.62%)	58 (4.64%)
One-class SVM	36 (8.00%)	6 (0.75%)	42 (3.36%)
SVDD	37 (8.22%)	6 (0.75%)	43 (3.44%)
KPCA	21 (4.67%)	13 (1.62%)	34 (2.72%)
GKPCA	24 (5.33%)	9 (1.12%)	33 (2.64%)

II errors change slightly and show clearly a trade-off. One should note that the indications given by the ROC curves from Fig. 4, about the true detection rate, are not consistent with the results from Table 2. Basically, from the ROC curves, one might infer that the KPCA and GKPCA have better true detection rate for a level of significance around 5 percent than the one-class SVM and SVDD. However, the table shows that the one-class SVM and SVDD minimize the number of Type II errors, i.e., maximize the true detection rate. This phenomenon is related with the threshold definition, as it was defined based only on 50 percent of the undamaged data. Additionally, for the KPCA and GKPCA, as the level of false alarm rate is very close to the 5 percent level of significance assumed to set up the threshold, it gives indications that these algorithms

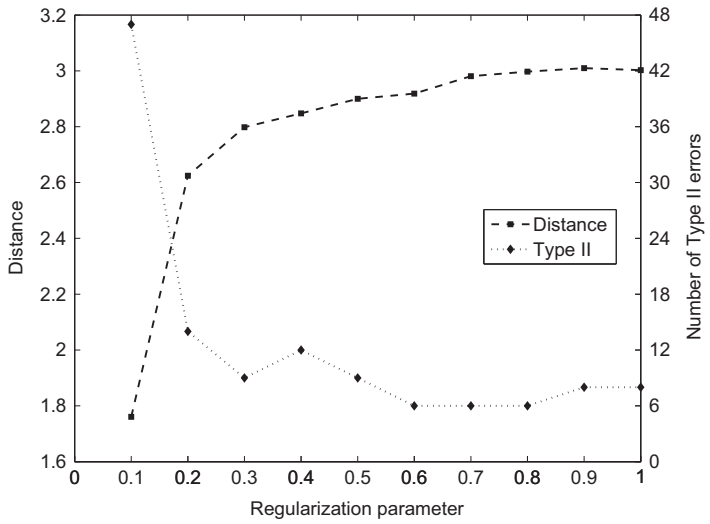

Fig. 9. Distance between the mean of the DIs from the undamaged and damaged conditions along with the number of Type II errors as a function of the regularization parameter ($\nu = 0.1, \ldots, 1$), using the one-class SVM algorithm.

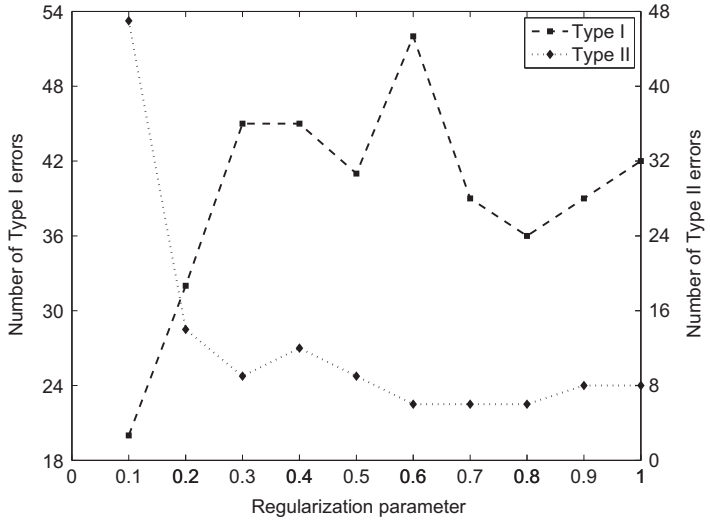

Fig. 10. Classification performance (Type I and Type II errors) as a function of the regularization parameter ($\nu = 0.1, \ldots, 1$), using the one-class SVM algorithm.

have learnt the baseline condition during the training phase and they can generalize well for new undamaged data not used in the training phase.

Nevertheless, all kernel-based algorithms perform relatively well on these standard data sets with percent of total misclassifications (Type I and Type II errors) ranging between 2.64 percent and 3.44 percent of the total number of test observations, which can be considered an acceptable result. Additionally, based on Table 2 and for these specific data sets, one can infer that the one-class SVM and SVDD algorithms are preferred when one wants to minimize false-negative indications of damage and when life safety issues are the main reason for deploying a SHM system. On the other hand, the KPCA and GKPCA algorithms are more appropriate when one wants to minimize false-positive indications of damage without increasing, significantly, the false-negative indications of damage, and reliability issues are driving a SHM system. However, the KPCA and GKPCA have shown to have better generalization performance, which is a very important advantage for real-world applications, where the thresholds are defined based on undamaged data used in the training phase.

Finally, note that the classification performance of the one-class SVM and SVDD algorithms can potentially be improved by adjusting the regularization parameters ν and $\mathbf{C}$, respectively. To highlight the influence of the regularization parameter assumed on both algorithms, Fig. 9 shows the distance between the mean of the DIs from the undamaged and damaged conditions along with the number of Type II errors as a function of the regularization parameter ν. Based on the distance between means and the minimization of number of Type II errors, the appropriate regularization parameter is 0.8 (based on the converging point) and approximately 0.0028 for the one-class SVM and SVDD algorithms, respectively. This result gives an indication that the regularization parameter assumed in the previous analysis is nearly the optimal solution.

Nonetheless, alternative solutions can be found in Fig. 10. Basically, when ν is equal to 0.2, 0.7 and 0.9, the total errors are 46 (3.68 percent), 45 (3.6 percent) and 47 (3.76 percent), respectively, which are still less than the total errors outputted by the AANN, FA, MSD and SVD. Note that when the regularization parameter increases, the number of support vectors also increases. Therefore, the choice of a regularization parameter with a small value may lead to underfitting as well as the choice of a regularization parameter with high value may lead to overfitting.

5. Summary and conclusions

In this paper, the performance of four kernel-based algorithms (one-class SVM, SVDD, KPCA and GKPCA) for structural damage detection, under varying operational and environmental conditions, was compared using benchmark data sets from a well-known base-excited three-story frame structure. The data sets are characterized by 17 different structural state conditions, including linear changes caused by varying stiffness and mass-loading conditions as well as nonlinear effects caused by damage. Different levels of damage were created by adjusting the gap between a suspended column and a bumper.

The kernel-based algorithms were shown to be reliable approaches to create a global DI that can separate damaged from undamaged conditions, even when the structure is operating under varying operational and environmental conditions. The comparison between the proposed four kernel-based algorithms and alternative algorithms studied before (AANN, FA, MSD and SVD) permitted one to conclude that the proposed ones have better classification performance as given by the lower number of misclassifications (both Type I and Type II errors). Two fundamental reasons are given to justify the general improvement of the proposed algorithms over the previous ones: (i) the previous algorithms were essentially linear in their formulation, with exception of the AANN; (ii) all the proposed algorithms (SVM, SVDD, KPCA and GKPCA) operate, essentially, in the high-dimensional space, giving them capabilities to model nonlinear patterns presented in the original observation space.

Within the four proposed algorithms, the KPCA and GKPCA outputted better results in terms of minimization of total misclassifications; two fundamental reasons are also proposed for that behavior: (i) all four algorithms map the original observations into the high-dimensional space; however, the KPCA and GKPCA map the original observations into the high-dimensional space, in order to capture the operational and environmental effects with a known percentage, and back to the original space to perform the damage detection; conversely, the SVM and SVDD performs the data normalization by means of a data subset (support vectors) selected in the high-dimensional space, which accounts for an unknown percentage of the variability; (ii) the GKPCA and KPCA perform the damage detection by retaining the principal components that take into account 90 percent of the data variability, which might be useful to discard some sort of noise and singularities from the data that can mask changes caused by damage from changes caused by operational and environmental conditions. This is actually an advantage, as shown by the trade-off between Type I and Type II errors. As the GKPCA and KPCA eliminate some noise from the data, they are not too complex and have better generalization performance.

In particular, the proposed algorithms are independent of the initial conditions, as opposed to the AANN, for instance, where the performance of the neural network is strongly dependent on the choice of the initial parameters. Therefore, if the kernel-based approaches are configured with the same parameters defined in this study, then they should provide the same results. In general, considering different application cases, the proposed algorithms are recommended to remove the influences of varying operational and environmental conditions on damage-sensitive features, especially when nonlinear temperature–stiffness relationship is present. The KPCA and GKPCA algorithms build data models where the principal components account for nearly all the operational and environmental influences, providing a better trade-off between sensitivity and specificity. On the other hand, the one-class SVM and SVDD algorithms generate data models where the normal structural condition used in the training phase is well discriminated by means of the support vectors, improving the detection of abnormal cases. However, the hyperplane and hypersphere separations are unable to generalize well, when compared with the KPCA and GKPCA algorithms, to undamaged data not provided in the training phase, i.e., the support vectors do not account for nearly all normal variability.

A parametric study carried out to establish the relationship between the classification performance and the regularization parameter, in the one-class SVM and SVDD algorithms, permitted one to verify those algorithms maximize the classification performance when the regularization parameter is chosen properly to avoid underfitting and overfitting in the data model generated for feature classification. Note that the cross-validation is the most used method to obtain the optimal regularization parameter, i.e., the best model. In order to do so, it is necessary to divide the data sets into three different subsets: training, validation and testing. In the training phase is considered only data from the undamaged condition to train the algorithms. The validation step is a sequence of iterations with different values for the regularization parameter to obtain the best model for generalization purposes, using both undamaged and damaged data. The test phase of the algorithms is done using the best model obtained in the cross-validation. However, in this study, this procedure was not taken into account, in order to be consistent with the previous study carried out by the authors.

Additionally, the proposed approaches can also perform damage localization when an AR model is applied, individually, on each sensor and the damage detection process is performed at the sensor level. In this paper, the AR model is applied on each sensor, but the AR parameters from the four sensors were concatenated into a single feature vector. Therefore, the damage detection is performed globally.

Finally, in the context of data normalization for damage detection, this study addressed the implementation and comparison of machine learning algorithms to establish the normal condition as a function of the operational and environmental variability. It is important to note that none of these algorithms require a direct measure of the sources of variability (e.g., traffic loading and temperature). Instead, the algorithms rely only on measured response time-series data acquired under varying operational and environmental effects.

Acknowledgments

The authors acknowledge the support received from CNPq (454483/2014-7), CAPES and Vale S.A. (FAPESPA-112794/2010).

References

[1] E. Figueiredo, I. Moldovan, M.B. Marques, Condition Assessment of Bridges: *Past, Present, and Future—A Complementary Approach*, in: Universidade Católica Editora, Portugal, 2013.
[2] B. Glisic, D. Inaudi, *Fibre Optic Methods for Structural Health Monitoring*, John Wiley & Sons, Inc., Hoboken, NJ, United States, 2007.
[3] C.R. Farrar, K. Worden, An introduction to structural health monitoring, *Philosophical Transactions of the Royal Society: Mathematical, Physical & Engineering Sciences* 365 (1851) (2007) 303–315, http://dx.doi.org/10.1098/rsta.2006.1928.
[4] H. Sohn, C.R. Farrar, Damage diagnosis using time series analysis of vibration signals, *Smart Materials and Structures* 10 (3) (2001) 446–451, http://dx.doi.org/10.1088/0964-1726/10/3/304.
[5] K. Worden, J.M. Dulieu-Barton, An overview of intelligent fault detection in systems and structures, *Structural Health Monitoring* 3 (1) (2004) 85–98, http://dx.doi.org/10.1177/147592170404186.
[6] S.G. Mattson, S.M. Pandit, Statistical moments of autoregressive model residuals for damage localisation, *Mechanical Systems and Signal Processing* 20 (3) (2006) 627–645, http://dx.doi.org/10.1016/j.ymssp.2004.08.005.
[7] E. Figueiredo, M. Todd, C. Farrar, E. Flynn, Autoregressive modeling with state-space embedding vectors for damage detection under operational variability, *International Journal of Engineering Science* 48 (10) (2010) 822–834, http://dx.doi.org/10.1016/j.ijengsci.2010.05.005.
[8] E.J.F. Figueiredo, Damage Identification in Civil Engineering Infrastructure under Operational and Environmental Conditions, Doctor of Philosophy in Civil Engineering, Faculdade de Engenharia, Universidade do Porto, Porto, Portugal, 2010.
[9] K. Worden, G. Manson, The application of machine learning to structural health monitoring, *Philosophical Transactions of the Royal Society: Mathematical, Physical & Engineering Sciences* 365 (1851) (2007) 515–537, http://dx.doi.org/10.1098/rsta.2006.1938.
[10] K. Worden, C.R. Farrar, G. Manson, G. Park, The fundamental axioms of structural health monitoring, *Philosophical Transactions of the Royal Society: Mathematical, Physical & Engineering Sciences* 463 (2082) (2007) 1639–1664, http://dx.doi.org/10.1098/rspa.2007.1834.
[11] H. Sohn, K. Worden, C.R. Farrar, Statistical damage classification under changing environmental and operational conditions, *Journal of Intelligent Material Systems and Structures* 13 (9) (2002) 561–574, http://dx.doi.org/10.1106/104538902030904.
[12] K. Worden, A.J. Lane, Damage identification using support vector machines, *Smart Materials and Structures* 10 (3) (2001) 540–547, http://dx.doi.org/10.1088/0964-1726/10/3/317.
[13] L. Bornn, C.R. Farrar, G. Park, K. Farinholt, Structural health monitoring with autoregressive support vector machines, *Journal of Vibration and Acoustics* 131 (2) (2009) http://dx.doi.org/10.1115/1.3025827. 021004-1–9.
[14] Y. Kim, J.W. Chong, K.H.C.J. Kim, Wavelet-based AR-SVM for health monitoring of smart structures, *Smart Materials and Structures* 22 (1) (2013) 1–12, http://dx.doi.org/10.1088/0964-1726/22/1/015003.
[15] J.W. Chong, Y. Kim, K.H. Chon, Nonlinear multiclass support vector machine-based health monitoring system for buildings employing magnetorheological dampers, *Journal of Intelligent Material Systems and Structures* 25 (12) (2014) 1456–1468, http://dx.doi.org/10.1177/1045389X13507343.
[16] N.L. Khoa, B. Zhang, Y. Wang, F. Chen, S. Mustapha, Robust dimensionality reduction and damage detection approaches in structural health monitoring, *Structural Health Monitoring* 13 (4) (2014) 406–417, http://dx.doi.org/10.1177/1475921714532989.
[17] A. Mita, H. Hagiwara, Quantitative damage diagnosis of shear structures using support vector machine, *KSCE Journal of Civil Engineering* 7 (6) (2003) 683–689, http://dx.doi.org/10.1007/BF02829138.
[18] H.-X. He, W. ming Yan, Structural damage detection with wavelet support vector machine: introduction and applications, *Structural Control and Health Monitoring* 14 (1) (2007) 162–176, http://dx.doi.org/10.1002/stc.150.
[19] A. Cury, C. Crémona, Pattern recognition of structural behaviors based on learning algorithms and symbolic data concepts, *Structural Control and Health Monitoring* 19 (2) (2012) 161–186, http://dx.doi.org/10.1002/stc.412.
[20] H. HoThu, A. Mita, Damage detection method using support vector machine and first three natural frequencies for shear structures, *Open Journal of Civil Engineering* 3 (2) (2013) 104–112, http://dx.doi.org/10.4236/ojce.2013.32012.
[21] C.M. Wen, S.L. Hung, C.S. Huang, J.C. Jan, Unsupervised fuzzy neural networks for damage detection of structures, *Structural Control and Health Monitoring* 14 (1) (2007) 144–161, http://dx.doi.org/10.1002/stc.116.
[22] C.R. Farrar, K. Worden, *Structural Health Monitoring: A Machine Learning Perspective*, John Wiley & Sons, Inc., Hoboken, NJ, United States, 2013.
[23] E. Figueiredo, G. Park, C.R. Farrar, K. Worden, J. Figueiras, Machine learning algorithms for damage detection under operational and environmental variability, *Structural Health Monitoring* 10 (6) (2011) 559–572, http://dx.doi.org/10.1177/1475921710388971.
[24] M.A. Torres-Arredondo, D.A. Tibaduiza, L.E. Mujica, J. Rodellar, C.-P. Fritzen, Data-driven multivariate algorithms for damage detection and identification: *evaluation and comparison*, *Structural Health Monitoring* 13 (1) (2014) 19–32, http://dx.doi.org/10.1177/1475921713498530.
[25] T. Nguyen, T.H. Chan, D.P. Thambiratnam, Controlled Monte Carlo data generation for statistical damage identification employing Mahalanobis squared distance, *Structural Health Monitoring* 13 (4) (2014) 461–472, http://dx.doi.org/10.1177/1475921714521270.
[26] S. Hakim, H.A. Razak, Modal parameters based structural damage detection using artificial neural networks—a review, *Smart Structures and Systems* 14 (2) (2014) 159–189, http://dx.doi.org/10.12989/sss.2014.14.2.159.
[27] T.-Y. Hsu, C.-H. Loh, Damage detection accommodating nonlinear environmental effects by nonlinear principal component analysis, *Structural Control and Health Monitoring* 17 (3) (2010) 338–354, http://dx.doi.org/10.1002/stc.320.
[28] J. Kullaa, Is temperature measurement essential in structural health monitoring?, *Proceedings of the 4th International Workshop on Structural Health Monitoring: From Diagnostic & Prognostics to Structural Health Monitoring*, DEStech Publications, Stanford, CA, USA, 1993, pp. 717–724.
[29] K. Worden, G. Manson, N.R.J. Fieller, Damage detection using outlier analysis, *Journal of Sound and Vibration* 229 (3) (2000) 647–667, http://dx.doi.org/10.1006/jsvi.1999.2514.
[30] R. Ruotolo, C. Surace, Using SVD to detect damage in structures with different operational conditions, *Journal of Sound and Vibration* 226 (3) (1999) 425–439, http://dx.doi.org/10.1006/jsvi.1999.2305.
[31] H. Kantz, T. Schreiber, *Nonlinear Time Series Analysis*, 2nd ed. Cambridge University Press, Cambridge, United Kingdom, 2003.

[32] E. Figueiredo, J. Figueiras, G. Park, C.R. Farrar, K. Worden, Influence of the autoregressive model order on damage detection, *Computer-Aided Civil and Infrastructure Engineering* 26 (3) (2011) 225–238, http://dx.doi.org/10.1111/j.1467-8667.2010.00685.x.
[33] R. Yao, S.N. Pakzad, Autoregressive statistical pattern recognition algorithms for damage detection in civil structures, *Mechanical Systems and Signal Processing* 31 (2012) 355–368, http://dx.doi.org/10.1016/j.ymssp.2012.02.014.
[34] G.E.P. Box, G.M. Jenkins, G.C. Reinsel, *Time Series Analysis: Forecasting and Control*, 4th ed. John Wiley & Sons, Inc., Hoboken, NJ, United States, 2008.
[35] R. Kothamasu, J. Shi, S.H. Huang, H.R. Leep, Comparison of selected model evaluation criteria for maintenance applications, *Structural Health Monitoring* 3 (3) (2004) 213–224, http://dx.doi.org/10.1177/1475921704042696.
[36] B.E. Boser, I.M. Guyon, V.N. Vapnik, A training algorithm for optimal margin classifiers, *Proceedings of the Fifth Annual Workshop on Computational Learning Theory*, ACM, Pittsburgh, PA, USA, 1992, pp. 144–152. http://dx.doi.org/10.1145/130385.130401.
[37] C. Cortes, V. Vapnik, Support-vector networks, *Machine Learning* 20 (3) (1995) 273–297, http://dx.doi.org/10.1023/A:1022627411411.
[38] C.-C. Chang, C.-J. Lin, LIBSVM: *a library for support vector machines*, *ACM Transactions on Intelligent Systems and Technology* 2 (3) (2011) 1–27, http://dx.doi.org/10.1145/1961189.1961199.
[39] S.S. Keerthi, C.-J. Lin, Asymptotic behaviors of support vector machines with gaussian kernel, *Neural Computation* 15 (7) (2003) 1667–1689, http://dx.doi.org/10.1162/089976603321891855.
[40] B. Schölkopf, J.C. Platt, J.C. Shawe-Taylor, A.J. Smola, R.C. Williamson, Estimating the support of a high-dimensional distribution, *Neural Computation* 13 (7) (2001) 1443–1471, http://dx.doi.org/10.1162/089976601750264965.
[41] B. Schölkopf, A.J. Smola, R.C. Williamson, P.L. Bartlett, New support vector algorithms, *Neural Computation* 12 (5) (2000) 1207–1245, http://dx.doi.org/10.1162/089976600300015565.
[42] D.M.J. Tax, R.P.W. Duin, Support vector data description, *Machine Learning* 54 (1) (2004) 45–66, http://dx.doi.org/10.1023/B:MACH.0000008084.60811.49.
[43] W.-C. Chang, C.-P. Lee, C.-J. Lin, A Revisit to Support Vector Data Description (SVDD), Technical Report, National Taiwan University, Taipei, Taiwan, 2013.
[44] B. Schölkopf, A. Smola, K.-R. Muller, Nonlinear component analysis as a kernel eigenvalue problem, *Neural Computation* 10 (5) (1998) 1299–1319, http://dx.doi.org/10.1162/089976698300017467.
[45] B. Schölkopf, A.J. Smola, *Learning with Kernels: Support Vector Machines, Regularization, Optimization, and Beyond*, The MIT Press, Cambridge, MA, United States, 2001.
[46] S. Mika, B. Schölkopf, A. Smola, K.-R. Müller, M. Scholz, G. Rätsch, Kernel PCA and de-noising in feature spaces, *Proceedings of the 1998 Conference on Advances in Neural Information Processing Systems 11*, MIT Press, Denver, CO, USA, 1999, pp. 536–542.
[47] V. Franc, V. Hlavac, *Greedy algorithm for a training set reduction in the kernel methods*, *Computer Analysis of Images and Patterns*, Springer, Groningen, Netherlands, 2003, 426–433, http://dx.doi.org/10.1007/978-3-540-45179-2_53.
[48] E. Figueiredo, G. Park, J. Figueiras, C. Farrar, K. Worden, Structural Health Monitoring Algorithm Comparisons Using Standard Data Sets, Technical Report LA-14393, Los Alamos National Laboratory, Los Alamos, NM, United States, 2009.
[49] C.R. Farrar, P.J. Cornwell, S.W. Doebling, M.B. Prime, Structural Health Monitoring Studies of the Alamosa Canyon and I-40 Bridges, Technical Report LA-13635-MS, Los Alamos National Laboratory, Los Alamos, NM, United States, 2000.
[50] B. Peeters, G.D. Roeck, One-year monitoring of the Z24-Bridge: *environmental effects versus damage events*, *Earthquake Engineering & Structural Dynamics* 30 (2) (2001) 149–171, http://dx.doi.org/10.1002/1096-9845(200102)30:2⟨149::AID-EQE1⟩3.0.CO;2-Z.
[51] E. Figueiredo, E. Flynn, Three-Story Buildings Structure to Detect Nonlinear Effects, Technical Report. SHMTools, Los Alamos National Laboratory, Los Alamos, NM, United States (2009).

Appendix B – Paper B: A novel unsupervised approach based on a genetic algorithm for structural damage detection in bridges

Engineering Applications of Artificial Intelligence 52 (2016) 168–180

Contents lists available at ScienceDirect

Engineering Applications of Artificial Intelligence

journal homepage: www.elsevier.com/locate/engappai

A novel unsupervised approach based on a genetic algorithm for structural damage detection in bridges

Moisés Silva [a,*], Adam Santos [a], Eloi Figueiredo [b], Reginaldo Santos [a], Claudomiro Sales [a], João C.W.A. Costa [a]

[a] Applied Electromagnetism Laboratory, Universidade Federal do Pará, R. Augusto Corrêa, Guamá 01, Belém, 66075-110 Pará, Brazil
[b] Faculty of Engineering, Universidade Lusófona de Humanidades e Tecnologias, Campo Grande 376, 1749-024 Lisbon, Portugal

ARTICLE INFO

Article history:
Received 18 September 2015
Received in revised form
29 February 2016
Accepted 2 March 2016

Keywords:
Structural health monitoring
Genetic algorithm
Concentric hypersphere algorithm
Damage detection
Environmental and operational variability
Clustering

ABSTRACT

This paper proposes a novel unsupervised and nonparametric genetic algorithm for decision boundary analysis (GADBA) to support the structural damage detection process, even in the presence of linear and nonlinear effects caused by operational and environmental variability. This approach is rooted in the search of an optimal number of clusters in the feature space, representing the main state conditions of a structural system, also known as the main structural components. This genetic-based clustering approach is supported by a novel concentric hypersphere algorithm to regularize the number of clusters and mitigate the cluster redundancy. The superiority of the GADBA is compared to state-of-the-art approaches based on the Gaussian mixture models and the Mahalanobis squared distance, on data sets from monitoring systems installed on two bridges: the Z-24 Bridge and the Tamar Bridge. The results demonstrate that the proposed approach is more efficient in the task of fitting the normal condition and its structural components. This technique also revealed to have better classification performance than the alternative ones in terms of false-positive and false-negative indications of damage, suggesting its applicability for real-world structural health monitoring applications.

1. Introduction

Improved and more continuous condition assessment of bridges has been demanded by modern societies to better face the challenges presented by aging civil infrastructure (Figueiredo et al., 2013). In the last two decades, bridge condition assessment approaches have been developed independently based on two concepts: bridge management systems (BMSs) and structural health monitoring (SHM). The BMS is a visual inspection-based decision-support tool developed to analyze engineering and economic factors and to assist the authorities in determining how and when to make decisions regarding maintenance, repair and rehabilitation of structures (Lee et al., 2008; Wenzel, 2009). On the other hand, the SHM traditionally refers to the process of implementing monitoring systems to measure the structural responses in real-time and to identify anomalies and/or damage at early stages (Farrar and Worden, 2007).

Even with the inherent limitation imposed by the visual inspections, the BMS has already been accepted by bridge owners around the world (Miyamoto et al., 2001; Estes and Frangopol, 2003; Gattulli and Chiaramonte, 2005). At the same time, SHM is becoming increasingly attractive due to its potential ability to detect damage, with the consequent life-safety and economical benefits (Worden et al., 2007). The authors believe that all approaches to SHM can be posed in the context of a statistical pattern recognition (SPR) paradigm. This SPR paradigm for the development of SHM solutions is described as a four-phase process (Farrar et al., 2001): (1) operational evaluation, (2) data acquisition, (3) feature extraction, and (4) statistical modeling for feature classification. Inherent in the data acquisition, feature extraction, and statistical modeling portions of this paradigm, the data normalization is the process of separating changes in damage-sensitive features caused by damage from those caused by varying operational and environmental conditions (Sohn and Farrar, 2001). Actually, these influences on the structural response have been cited as one of the major challenges for the transition of SHM technology from research to practice (Sohn, 2007; Xia et al., 2012).

The focus of this study is on the fourth phase, which is concerned with the implementation of algorithms that analyze and learn the distributions of the extracted damage-sensitive features from the raw data, in an effort to determine the structural health condition (Worden and Manson, 2007). Therefore, in the hierarchical structure of damage identification, this paper addresses the first level, i.e., the damage detection level (Figueiredo et al., 2011).

* Corresponding author.
E-mail address: moises.silva@icen.ufpa.br (M. Silva).

http://dx.doi.org/10.1016/j.engappai.2016.03.002
0952-1976/

Numerous studies have established the concept of automatically discovering and characterizing the normal condition of bridges, even when they are affected by extreme operational and environmental conditions (Figueiredo and Cross, 2013; Figueiredo et al., 2014). In those studies, the damage detection is carried out on the basis of an outlier detection strategy using distance metrics and machine learning algorithms, which permits one to track the outlier formation in time regarding the chosen groups of state conditions. In contrast with approaches that consist of measuring directly parameters related to operational and environmental variations (e.g., traffic loading and temperature) (Peeters et al., 2001; Peeters and Roeck, 2001; Ni et al., 2005; Kullaa, 2009), these algorithms pave the way for data-based models applicable to structural systems of arbitrary complexity, with the advantage to eschew the measure of operational and environmental variations and physics-based model approaches.

Therefore, coupled with the results highlighted in the previous authors' publication (Figueiredo and Cross, 2013), which suggests the potential of cluster-based algorithms for damage detection under operational and environmental variability, this paper proposes an unsupervised and nonparametric approach using a genetic algorithm (GA) to detect structural damage in bridges, namely a genetic algorithm for decision boundary analysis (GADBA). Combined with the robust search capability inherent in GAs, this study presents a new method to characterize the main clusters (components) that correspond to the normal state conditions of a bridge as well as a new algorithm to regularize the optimal number of clusters and mitigate the cluster redundancy, namely the concentric hypersphere (CH) algorithm. Additionally, an objective function is also proposed to evaluate the quality of different component configurations.

The proposed GADBA-based approach is summarized in two steps: (i) the main normal state conditions of a system are automatically discovered by clustering the training observations according to the closest centroids, which are targets of the optimization performed by the GA; this optimization defines boundary regions between the clusters and reduces the number of discovered state conditions; (ii) the damage detection strategy is based on the Euclidean distances between the test observations and the optimized centroids. For each observation, the minimum distance to the centroids represents the damage indicator (DI).

To test the superiority of the proposed approach, standard data sets from the Z-24 Bridge, in Switzerland, and the Tamar Bridge, in England, are used. The classification performance is evaluated on the basis of Type I/Type II error trade-offs. In SHM, in the context of damage detection, a Type I error is a false-positive indication of damage and a Type II error is a false-negative indication of damage.

The overall organization of this paper is as follows. In Section 2, a brief review of the most traditional cluster-based and bioinspired methods for damage detection is presented, along with a discussion that synthesizes the relevant genetic-based clustering approaches available in the literature. Section 3 describes all the new constraints and mechanisms developed to cluster the normal state conditions of bridges, by using the GADBA-based approach, and to detect damage based on the identified clusters. Section 4 highlights a structural description of both bridges as well as a summary of the data sets from the bridges that encompass a wide spectrum of challenges associated with practical damage detection problems. Section 5 presents the applicability of the proposed approach on such real-world data sets and compares its performance with other two approaches. Finally, Section 6 summarizes and discusses the implementation and analysis carried out in this study.

2. Related work

For most civil engineering infrastructure where SHM systems are applied, the unsupervised learning algorithms are often required because only data from the undamaged (or normal) condition are available (Farrar and Worden, 2013). Some of the traditional unsupervised machine learning algorithms and their adaptations for damage detection in bridges can be found in the following references Figueiredo et al. (2011); Sohn et al. (2002); Hsu and Loh (2010); Hakim and Razak (2014); Santos et al. (2016, 2015); Xu et al. (2004); Liu et al. (2011). Herein, the most traditional cluster-based and bioinspired methods for damage detection are discussed. Moreover, the most relevant genetic-based clustering methods are also introduced.

2.1. Traditional cluster-based damage detection methods

The approaches based on the Mahalanobis squared distance (MSD) and the Gaussian mixture model (GMM) are relevant, as they operate on a set of clusters representing undamaged state conditions (Figueiredo and Cross, 2013; Figueiredo et al., 2014).

The MSD-based approach is one of the most traditional methods for damage detection, having widespread use in real scenarios due to its ability to identify outliers (Worden et al., 2007; Worden and Manson, 2007; Nguyen et al., 2014), as it assumes that the normal condition is encoded by an unique cluster from a multivariate Gaussian distribution. When abnormal observations appear statistically inconsistent with the rest of the data, it is assumed that the data have been generated by an alternative source, which is not related to the normal condition established with a mean vector and a covariance matrix derived from the baseline data sets obtained under operational and environmental conditions. However, when nonlinearities are present in the observations, the MSD fails in modeling the normal condition of a bridge as it assumes that the baseline data might follow a multivariate Gaussian distribution (Figueiredo and Cross, 2013).

A new concept based on GMMs was developed in Figueiredo and Cross (2013), Figueiredo et al. (2014) as a two-step damage detection strategy. In the first step, the GMM-based approach is applied to model the main clusters that correspond to the normal and undamaged state conditions of a bridge, even when it is affected by unknown operational and environmental conditions. In the former study, the parameters of the GMMs are estimated from the training data, using the maximum likelihood estimation based on the expectation-maximization (EM) algorithm. To improve the parameter estimation of the GMMs, a Bayesian approach based on a Markov-chain Monte Carlo method is applied in the latter study. In the second step, the damage detection is performed on the basis of a MSD outlier formation regarding the chosen clusters of main states. Although these approaches have revealed better damage detection performance when compared to MSD, they also assume Gaussian distributions which may compromise the reliable estimation of structural components and their training phase is quite slow as several replications of the EM algorithm are required.

2.2. Bioinspired damage detection methods

The most traditional bioinspired methods for damage detection in SHM correlate a complex physics-based model with measured data from the monitored structure. A set of variables is updated to obtain the minimum difference between the numerical and experimental data. Then, a damage is modeled as a reduction in

structural stiffness and detected by comparing the undamaged and damaged states.

Based on this usual approach, a real-coded GA is proposed in Xia and Hao (2001) and applied to structural damage identification using vibration data and modal parameters. This approach identifies damage by directly comparing changes in the measurements before and after damage occurrence using two finite element models (FEMs) built with data from undamaged and damaged conditions. The GA minimizes an objective function that combines parameters related to mode shapes and frequency changes to update the reference FEM, and then obtain another FEM that reproduces the measured vibration data of the damaged state.

A damage detection approach based on particle swarm optimization is employed to structural elements in Gkda and Yildiz (2001). The damage location and extent are identified by minimization of an objective function based on some modal parameters. A FEM of a Timoshenko beam is used to attest the reliability of this method. Damage is simulated by adding stiffness loss in some elements.

A real-coded GA coupled with a local search method is developed in Meruane and Heylen (2011) to locate and quantify structural damage. The main goal of this approach is to select the elemental stiffness reduction factors, defined as the ratio of the stiffness reduction to the initial stiffness. The objective function is composed by five fundamental functions with an additional damage penalization term. The algorithm is compared to the inverse eigen-sensitivity and response function methods on measured data from a tridimensional frame structure with different degrees of freedom. The results indicate that this GA is more appropriate to detect damage than conventional optimization methods. However, as demonstrated by Friswell and Penny (2002), for high frequencies, this damage detection procedure has limitations to quantify the damage severity for cracks, as well as it is affected by mesh density.

In addition, a parallel genetic algorithm (PGA) to improve the time cost of the aforementioned approach is considered in Meruane and Heylen (2010). The reliability of the PGA is verified in two test case structures: an airplane subjected to three levels of damage and a multiple cracked reinforced concrete beam subjected to a nonsymmetrical static load. Despite reduction in time cost, the results indicate that the modeling improvement provided by PGA depends on each specific problem.

A new method for damage detection, localization and severity estimation on any kind of structures using a GA is proposed in Chou and Ghaboussi (2001). A physics-based model is developed from the information on the geometry of the structure using section properties treated as unknowns to be determined from undamaged condition. To determine these parameters, a GA is applied to minimize the difference between the measured displacements of the bridge under normal condition and the computed displacements from the model coded in the individuals. When compared to the FEM, the results suggest that the GA can perform damage localization and severity estimation with more reliability. However, this method was only tested in structures under normal effects of traffic loading and did not consider other common types of variability (e.g., temperature, humidity, wind speed and boundary conditions).

A two-step hybrid damage detection strategy is proposed in He and Hwang (2007). Based on grey relation analysis (GRA) and adaptive real-parameter simulated annealing genetic algorithm (ARSAGA), this method reduces the number of displacement variables by excluding the structural elements with less damage probability using a FEM that models a damaged structure. A comparison analysis between ARSAGA and a real-parameter genetic algorithm (RGA) demonstrates the superiority of the ARSAGA over to RGA, regarding the localization of damage and its extent. However, the ARSAGA may be difficult to employ in real SHM scenarios, particularly in bridge monitoring, as it depends on the availability of damaged data and the current localization of some damaged elements.

In all aforesaid methods, the use of complex physics-based models is pointed out as a drawback to full implementation of SHM, due to the high complexity imposed when modeling the operational and environmental influences, which remain not fully understood (Reynders et al.), mainly in case of bridge monitoring.

2.3. Genetic-based clustering methods

In the last years, the searching capability of GAs has been exploited to establish appropriated clusters. Basically, GAs are stochastic techniques to optimize objective functions guided by evolutionary principles, with capabilities to find solutions of multimodal complex optimization problems by taking into account several restrictions (Chambers, 2000; Goldberg, 1989).

The GA-based clustering is a well-known unsupervised algorithm to solve clustering problems in m-dimensional Euclidean space, $\mathbb{R}^m$ (Maulik and Bandyopadhyay, 2000). This approach is very similar to the K-means algorithm (Jain, 2010), where the observations are divided into a given number (K) of subsets (clusters), whose centroids are determined by applying genetic operators (selection, crossover and mutation). The main challenge of this technique is to estimate the correct number of clusters, which represents the number of normal state conditions of a system.

A GA-based clustering method – COWCLUS – is proposed in Cowgill et al. (1999). In this method, the variance ratio criteria (VRC) is used as an objective function to define the internal cluster homogeneity and the degree of isolation between different clusters. The results demonstrate that this method outperforms K-means by optimizing the VRC function. However, the number of clusters presents in the data must be defined as input of the algorithm.

A genetically guided algorithm (GGA) developed for clustering is applied to brain tissue magnetic resonance imaging in Hall et al. (1999), using objective functions from two other algorithms: fuzzy c-means (FCM) (Wen and Celebi, 2011) and hard c-means (HCM) (Runkler and Keller, 2012). This approach consists of minimizing an adapted function from the original objective ones used in FCM and HCM, rewriting the fuzzy partition matrix by another matrix that represents a distance measure from each observation to all centroids. The comparison of the GGA with FCM and HCM demonstrate that the GGA provides equivalent results in terms of a "good" clustering. Although this method has proved to be successful in modeling overlapping clusters, it may be difficult to employ in real applications, mainly when there is not prior knowledge about data structure, as well as the number of clusters.

3. Genetic algorithm for decision boundary analysis

In general, the GADBA capabilities for searching and optimizing are presented in this paper with the purpose of grouping data into logical structural components given a maximum number of clusters, $K_{\max}$, resulting in suitable geometric centers (centroids) for each cluster in the Euclidean space, $\mathbb{R}^m$. In particular, the task of the proposed CH algorithm is to support the automatic identification of the number of clusters, K, by choosing the appropriate centers $\mathbf{C} = c_1, c_2, \ldots, c_K$ of each cluster, through the maximization

F(1, 1)	F(1, ...)	F(1, m)	F(2, 1)	F(2, ...)	F(2, m)	...	F(K, 1)	F(K, ...)	F(K, m)

Fig. 1. Representation scheme of a single individual.

of the objective function proposed for the GADBA, which contributes to use the lowest number of clusters as possible. Essentially, the GADBA-based approach performs the CH algorithm in the set of solutions in each generation, aiming to estimate the correct number of components through an agglomerative clustering process.

For general purposes in SHM, the training matrix $\mathbf{X} \in \mathbb{R}^{n \times m}$ is composed of n observations under operational and environmental variability when the structure is undamaged, where m is the number of features per observation obtained during the feature extraction phase. The test matrix $\mathbf{Z} \in \mathbb{R}^{w \times m}$ is defined as a set of w observations collected during the undamaged/damaged conditions of the structure. Note that an observation represents a feature vector encoding the structural condition at a given time.

3.1. Individual representation

The individual representation assumed for a candidate solution is described herein. Each individual (also known as chromosome) is a real vector of $K \times m$ genes composed of centroid positions, as shown in Fig. 1.

In the individual representation, $F(i,j)$ is the real value of the i-th centroid in the j-th dimension. The number of genes varies between $m, \ldots, K_{\max} \times m$, in such a way that its length must be a multiple of m. The initial population $\mathbf{P}(t=0)$ is created by randomly choosing a number K in the interval $[1, \ldots, K_{\max}]$ for each individual. The K centroid positions are also randomly initialized by selecting K observations from the training matrix $\mathbf{X}$. The process is repeated for all $|\mathbf{P}|$ individuals to be generated.

3.2. Genetic operators

Aiming to perform several tasks of mutation, parent selection and survival selection, herein three well-known methods are highlighted and adopted to support the GADBA-based approach. The mutation process controls the exploration of the solution space by means of performing changes in the individuals. In this study, this process is composed of two steps:

(i) the number of centroids is changed via a stochastic variation method. An increment rate is previously determined by computing the inverse of the maximum number of clusters, $T_x = K_{\max}^{-1}$. A random real value T_r defined in the range $[0, 1]$ is used to determine the number of centroids to be enabled in the offspring individual by applying $K_{new} = \lceil \frac{T_r}{T_x} \rceil$. In the case of $K < K_{new} \leq K_{\max}$, then the miss positions are completed by selecting $K_{new} - K$ observations at random from $\mathbf{X}$, otherwise the last centroids are eliminated;

(ii) the mutation occurs in each centroid position in a stochastic manner. A mutation probability p_{mut} is associated to all positions, which are subjected to the Gaussian mutation,

$$F_{i,j} = F_{i,j} + \mathrm{N}(0,1), \tag{1}$$

where $\mathrm{N}(0,1)$ is a random number from a Gaussian distribution with zero mean and unitary standard deviation, and $F_{i,j}$ the real value of the i-th centroid in the j-th dimension.

The selection operator drives the searching towards a promising region in the feature space. The parent selection method is based on the well-known tournament with reposition. This method creates a subset $\mathbf{R}$ by randomly selecting $|\mathbf{R}|$ individuals from the population. Afterwards, only the best individual is selected from $\mathbf{R}$ and submitted to the crossover process with another individual selected in the same manner. Besides, the survival selection is based on the elitism concept (Deb et al., 2002), in which two sets of parents $\mathbf{I}_p$ and offspring $\mathbf{I}_c$ are joint, creating a set $\mathbf{I}_u = \mathbf{I}_p \bigcup \mathbf{I}_c$. Then, a new fitness value is calculated based on the Pareto Front and crowding distance. The solutions that compose the new set $\mathbf{I}_u$ are sorted to select the $|\mathbf{P}|$ better individuals as the new population set $\mathbf{P}(t+1)$.

The stopping criteria are: when the maximum number of generations is reached and/or the difference of the fitness between the two best individuals, of the last two generations, is less than a given threshold ϵ (e.g., $\epsilon = 5$).

3.3. Recombination

Recombination performs the exploration towards the known solution space aiming to refine the prior knowledges. Although a lot of different recombination operators are suggested in the literature (Hruschka et al., 2009; Mitchell, 1998), in this study is developed a strategy that combines not only useful segments of different parents, but also the centroid positions. The recombination method operates in three steps using two probability parameters defined as input, p_{rec} and p_{pos}:

(i) for each pair of parents $\mathbf{P}_i$ and $\mathbf{P}_j$, if a random number $r \leq p_{rec}$, then two cut points π_1 and π_2 are randomly generated, corresponding to a range within centroid positions of both parents, such that $1 \leq \pi_1 < \pi_2 \leq \min(K_i, K_j)$. The centroids in the range are switched to form two offspring individuals. In the case of p_{rec} is not satisfied, then both parents become the new offspring individuals;

(ii) each centroid position receives a random number $r \in [0, 1]$, in such a way if $r \leq p_{pos}$, then for each pair of parent genes, an arithmetic recombination is performed according to

$$F_{x,t}^{(i)} = F_{x,t}^{(i)} + \left(F_{y,t}^{(j)} - F_{x,t}^{(i)}\right) T, \tag{2}$$

$$F_{x,t}^{(j)} = F_{x,t}^{(j)} + \left(F_{y,t}^{(i)} - F_{x,t}^{(j)}\right) T, \tag{3}$$

where T is a random value defined in $[0, 1]$, and $F_{x,t}^{(i)}$ and $F_{x,t}^{(j)}$ are the t-th positions of the x-th centroid from the i-th and j-th parents, respectively;

(iii) finally, a length ratio, λ, defines the number of centroids enabled in each offspring individual. Note that the parents already have λ_i and λ_j length ratios associated to themselves,

$$\lambda = \frac{K}{K_{\max}}. \tag{4}$$

Hence, λ maps the number of clusters, K, to the interval $(0, 1]$. Hereafter, another arithmetic recombination is performed on the parents' length ratio to generate λ_i' and λ_j' for the offspring individuals. Thus, the number of clusters (K_i and K_j) enabled in the final offspring individuals are

$$K_i = \frac{\max(\lambda_i, \lambda_j)}{\lambda_i'}, \tag{5}$$

$$K_j = \frac{\max(\lambda_i, \lambda_j)}{\lambda_j'}. \tag{6}$$

3.4. Objective function

Based on the approaches that create clusters from circular distributions (MacQueen, 1967), a nonlinear metric to characterize

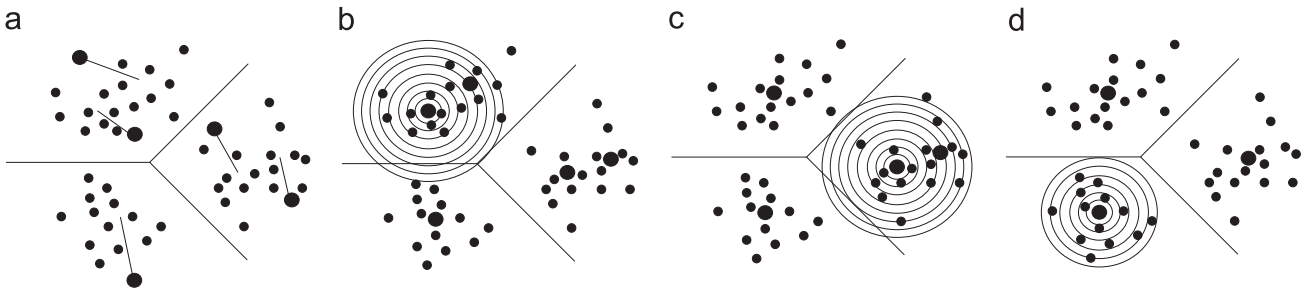

Fig. 2. CH algorithm using linear inflation.

different clusters is proposed. This metric is used as the objective function, which intends to evaluate different set of clustering solutions by taking into account the observation dispersion in relation to the centroids and the proximity between centroids. The objective function assumes that each component (representing a structural behavior) from the training matrix introduces a quasi-circular cluster of observations, allowing the damage detection in the presence of operational and environmental variability and when damage introduces new orthogonal components. In addition, to evaluate the data dispersion around each centroid, the density of the observations in the clusters is also considered.

Therefore, the first term of the objective function takes the summation of each distance among the centroids (C_i and C_j),

$$\sum_{i=1}^{K-1}\sum_{j=i+1}^{K}\mathbf{G}_1(\|C_i-C_j\|), \tag{7}$$

where $\mathbf{G}_1$ is a nonlinear penalization function defined as

$$\mathbf{G}_1(d_1)=\frac{1-e^{-d_1}}{e^{-d_1}}. \tag{8}$$

As Eq. (8) positively increases for all $d_1>0$, one easily concludes that when $\mathbf{G}_1$ increases, the distances between centroids also increase. The second term is defined as

$$\sum_{k=1}^{K}\mathbf{G}_2\left(\sum_{\forall x\in C_k}\|C_k-x\|\right), \tag{9}$$

where

$$\mathbf{G}_2(d_2)=\frac{1}{e^{2d_2}}. \tag{10}$$

In this case, Eq. (10) increases as the summation of the norms decreases for all $d_2>0$. Therefore, the objective function is defined by the combination of these two terms, regularized by the number of components and the standard deviation of all distances between centroids,

$$\mathcal{F}(x,\mathbf{C},K,\sigma)=\frac{1}{\sigma K}\left(\sum_{i=1}^{K-1}\sum_{j=i+1}^{K}\mathbf{G}_1(\|C_i-C_j\|)+\sum_{k=1}^{K}\mathbf{G}_2\left(\sum_{\forall x\in C_k}\|C_k-x\|\right)\right), \tag{11}$$

where the maximization of $\mathcal{F}(\cdot)$ provides the optimal clustering solution by maximization of distances between centroids (Eq. (7)) and minimization of data dispersion around the centroids (Eq. (9)).

3.5. Concentric hypersphere algorithm

In this study, the GAs capabilities are combined with the objective function to evaluate different clustering configurations for a given maximum number of clusters, $K_{\max}$. Thus, the novel CH algorithm is proposed to regularize the number of clusters encoded within the individuals. This algorithm works in an iterative manner on a list of centroids, by evaluating the boundary regions that limit each cluster, being divided in three steps:

Step 1: *Centroid displacement*: For each cluster, its centroid is dislocated to the position with greater observation density, i.e., the mean of its observations.

Step 2: *Linear inflation of concentric hyperspheres*: Linear inflation occurs on each centroid, of a candidate solution, by progressively increasing an initial hypersphere radius,

$$R_0=\log_{10}(\|C_i-x_{\max}\|+1), \tag{12}$$

where C_i is the centroid of the i-th cluster and $x_{\max}$ is its farthest observation, such that $\|C_i-x_{\max}\|$ is the radius of the cluster centered in C_i. However, the radius grows up in the form of an arithmetic progression with common difference equal to R_0. The creation of new hyperspheres is set by a criterion based on the positive variation of the observation density between two consecutive inflations, defined as the inverse of the variance; otherwise the process is stopped.

Step 3: *Cluster agglutination*: If there is more than one centroid inside the inflated hypersphere, these centroids are agglutinated to create an unique representative centroid as the mean of the initial centroids. On the other hand, if only the pivot centroid is within the inflated hypersphere, this centroid is assumed to be on the geometric center of a real cluster and the agglutination is not performed.

For completeness, the CH algorithm is summarized in Fig. 2, which presents an example of the method applied to a three-component scenario with a five-centroid candidate solution. Initially, in Fig. 2(a), the centroids are moved to the center of their clusters, as indicated in *Step* 1. In Fig. 2(b) and (c), two centroids are agglutinated to form one cluster, once they are under the same cluster. On the other hand, in Fig. 2(d), only one centroid is located under a real cluster, therefore the CH algorithm is stopped after the *Step* 2. In the case where the agglutination process occurs, all centroids analyzed before are evaluated again to infer whether the new one is not positioned under another cluster or closer to a boundary region.

The steps of the CH algorithm are summarized in Algorithm 1. Initially, it identifies the cluster in which each observation belongs and moves the centroids to the mean of their observations. Then, a hypersphere is built on a pivot centroid, by inflation until the density between two consecutive hyperspheres decreases. Finally, the agglutination of all centroids within the last hypersphere is performed, by replacing these centroids by their mean. The process is repeated until convergence, i.e., the solution is composed by only one centroid or there is no centroid agglutination after evaluate all centroids.

Algorithm 1. Summary of the CH algorithm.

```
1 i←1
2 createClusters (C, X, n)
3 move (C, X, n)
4 while i ≤ |C| AND |C| > 1 do
5   radius_0 ← calcRadius(C[i], X, n)
6   radius, density_0, density_1, delta_0, delta_1 ← 0
7     repeat
8     radius ← radius + radius_0
9     H ← calcHypersphere(C, i, X, n, radius)
10      density_0 ← density_1
11      density_1 ← calcDensity(H)
12      delta_0 ← delta_1
13      delta_1 ← |density_0 − density_1|
14    (until delta_0 > delta_1)
15  j ← reduce(C, H)
16   If j > 0 then
17      i ← 1
18      createClusters(C, X, n)
19   else
20      i ← i + 1
21   end if
22 end while
```

3.6. Structural damage classification

After the definition of the optimal number of components embedded in the training data, the damage detection process is carried out through a global DI estimated for each test observation. The DIs are generated through a method known as distributed DIs (Figueiredo et al., 2014). Basically, for a given test feature vector, z_i, the Euclidean distance for all centroids is calculated, where the DI (i) is considered the smallest distance,

$$\mathrm{DI}(i) = \min(\|z_i - c_1\|, \|z_i - c_2\|, \ldots, \|z_i - c_K\|), \tag{13}$$

where $c_1, c_2, \ldots, c_K$ are the centroids of K different components. In this study, the threshold is defined for 95% of confidence on the DIs taking into account only the baseline data used in the training process. Thus, if this approach has learned the baseline condition, i.e., the identified components suitably represent the undamaged and normal condition under all possible operational and environmental conditions, then this approach should output less than 5% of false alarms for the undamaged data used in test phase.

3.7. Summary of the GADBA-based approach

Many variants of genetic operators are available in literature. However, the proposed approach aims to reach satisfactory results by keeping its structure as simple as possible. A general schematic of the GADBA-based approach is summarized in Algorithm 2.

As each individual in the population represents a candidate solution, the final result is the one with best fitness provided by the objective function. In the start of the process, the CH algorithm is performed on all individuals in the population, and their associated parameters are updated at iteration $t=0$. Then, the objective function is computed for each updated individual. Genetic operators are applied until convergence, i.e., when the value given by the objective function does not change, significantly, for ten generations, providing the best set of centroids for the clustering problem. Finally, the CH algorithm is used to refine the best achieved model and the DIs are estimated by applying Eq. (13). $\mathbf{P}(t)$ denotes a population set of size $|\mathbf{P}|$ at generation t. $\mathbf{P}'(t)$ and $\mathbf{P}''(t)$ are the resulting populations after recombination and mutation, respectively. $\mathbf{P}(t+1)$ is the resulting set of selection operation in $\mathbf{P}(t) \cup \mathbf{P}''(t)$ with size $2|\mathbf{P}|$. The initial population $\mathbf{P}(t=0)$ is randomly generated.

Algorithm 2. Summary of the GADBA-based approach.

```
1  t=0
2  Initialize population P(t)
3  while convergence is not reached do
4    CH (P(t))
5    Evaluate (P(t))
6    P'(t) = Recombine (P(t))
7    P''(t) = Mutate (P'(t))
8    Evaluate (P''(t))
9    P(t+1) = Select (P(t) ∪ P''(t))
10     t = t+1
11 end while
12 P_max = max(P(t).fitness)
13 P_best = CH(P_max)
14 DI = damageIndicator(P_best, Z)
```

4. Test structures and data sets

The applicability and comparison between the proposed approach and state-of-the-art ones are evaluated using the damage-sensitive features extracted from the data sets of the Z-24 and Tamar Bridges. In the case of Z-24 Bridge, the standard data sets are unique in the sense that they combine one-year monitoring of the healthy condition, realistic damage scenarios artificially introduced and effects of operational and environmental variability. In a different manner, a monitoring system was carried out on the Tamar Bridge during almost two-years, generating data sets related only to undamaged scenarios. Its importance derives from the fact that in real monitoring systems, damage or variability effects occur naturally.

4.1. The Z-24 Bridge

The Z-24 Bridge was a standard post-tensioned concrete box girder bridge composed of a main span of 30 m and two side-spans of 14 m, as shown in Fig. 3. The bridge, before complete demolition, was extensively instrumented and tested with the purpose of providing a feasibility tool for vibration-based SHM in civil engineering. A long-term monitoring test was carried out, from 11th of November 1997 until 10th of September 1998, to quantify the operational and environmental variability present on the bridge and detect the existence of damage artificially introduced in the last month of operation. Every hour, eight accelerometers captured the vibrations of the bridge and an array of sensors measured environmental parameters, such as temperature at several locations, for 11 min. Progressive damage tests (settlement, concrete spalling, landslide at abutment, concrete hinge failure, anchor head failure, and rupture of tendons) were carried out in one-month time period shortly before the demolition of the bridge (from 4th of August to 10th of September 1998), to prove that realistic damage has a measurable influence on the bridge dynamics (Peeters et al., 2001).

To verify the applicability of the proposed approach for long-term monitoring, daily monitoring data measured at 5 a.m. (because of the lower differential temperature on the bridge) from an array of accelerometers are used to extract damage-sensitive features, which yields a feature vector (observation) per day of operation. An automatic modal analysis procedure based on the

frequency domain decomposition was developed to extract the natural frequencies (Peeters and Roeck, 1999). It was verified that the automatic procedure was only able to estimate the first three frequencies with high reliability, yielding a three-dimensional feature vector per day (Figueiredo et al., 2014). During the feature extraction process, it was observed that the first and third natural frequencies are strongly correlated (with a correlation coefficient of 0.94), which permits one to perform dimension reduction of the extracted feature vectors from three to two. The first two natural frequencies, along with circles referring the observations below 0 ° C, are depicted in Fig. 4(a).

The last 38 observations correspond to the damage progressive testing period, which is highlighted, especially in the second frequency, by a clear drop in the magnitude. Note that the damage scenarios are carried out in a sequential manner, which cause cumulative degradation of the bridge. Therefore, in this study, it is assumed that the bridge operates within its undamaged condition (baseline condition), even though under operational and environmental variability, from 11th of November 1997 to 3rd of August 1998 (1–197 observations). On the other hand, the bridge is assumed in its damaged condition from 4th of August to 10th of September 1998 (198–235 observations). The observed jumps in the natural frequencies are related to the asphalt layer in cold periods, which significantly contributes to the stiffness of the bridge. Actually, Peeters et al. (2001) showed the existence of a bilinear behavior in the natural frequencies for below and above freezing temperature.

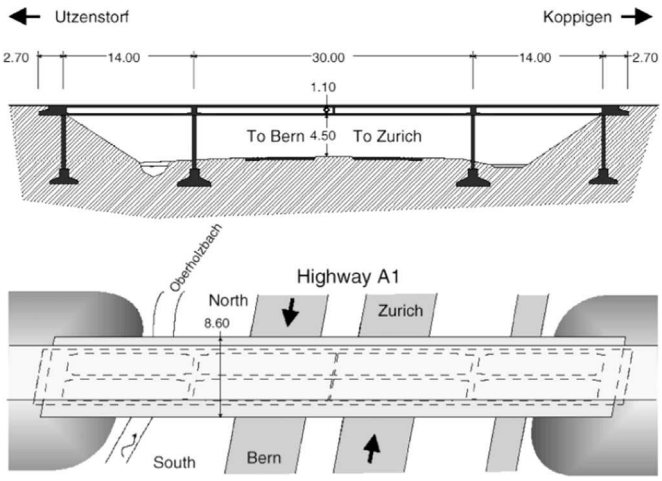

Fig. 3. Longitudinal section (upper) and top view (bottom) of the Z-24 Bridge (Peeters et al., 2001).

In conclusion, the statistical modeling is carried out taking into account only the first two frequencies and using all 235 observations, resulting in 197 observations from the undamaged condition (1–197 observations) and 38 observations from the damaged condition (198–235 observations). The corresponding training and test matrices are $\mathbf{X}^{197\times2}$ and $\mathbf{Z}^{235\times2}$, respectively. The heterogeneity among observations in a two dimensional space is evidenced in Fig. 4(b), which suggests the existence of components that may be find through latent variables and clustering methods.

4.2. The Tamar Bridge

The Tamar Bridge (Fig. 5) is situated in the south-west of the United Kingdom and connects Saltash in the county of Cornwall with the city of Plymouth in Devon. This bridge is a major road across the River Tamar and plays a significant role in the local economy. Initially, in 1961, the bridge had a main span of 335 m and side spans of 114 m. If the anchorage and approach are included, the overall length of the structure is 643 m. The bridge stands on two concrete towers with a height of 73 m with the bridge deck suspended at mid-height (Cross et al., 2013).

In the late 1990s, an upgrade was performed regarding the structure after an EU directive. Various sensor systems were installed to extract data such as tensions on stays, accelerations, wind speed, temperature, deflection and tilt. Eight accelerometers were implemented in orthogonal pairs to four stay cables and three sensors measured deck accelerations. The time series were stored with a sampling frequency of 64 Hz at 10 min intervals. The data were then passed to a computer-based system and via the covariance-driven stochastic subspace identification (Peeters and Roeck, 1999), the natural frequencies were calculated (more detail in Cross et al., 2013). The first five natural frequencies are illustrated in Fig. 6, for the period from 1st of July 2007 to 24th of February 2009 (602 observations).

Herein, there is no damaged observations known in advance, and so it is assumed that all observations are extracted from the undamaged condition. Therefore, only Type I errors can be identified. From a total amount of 602 observations, the first 363 ones are used for statistical modeling in the training process (corresponding to one-year monitoring from 1st of July 2007 to 30th of

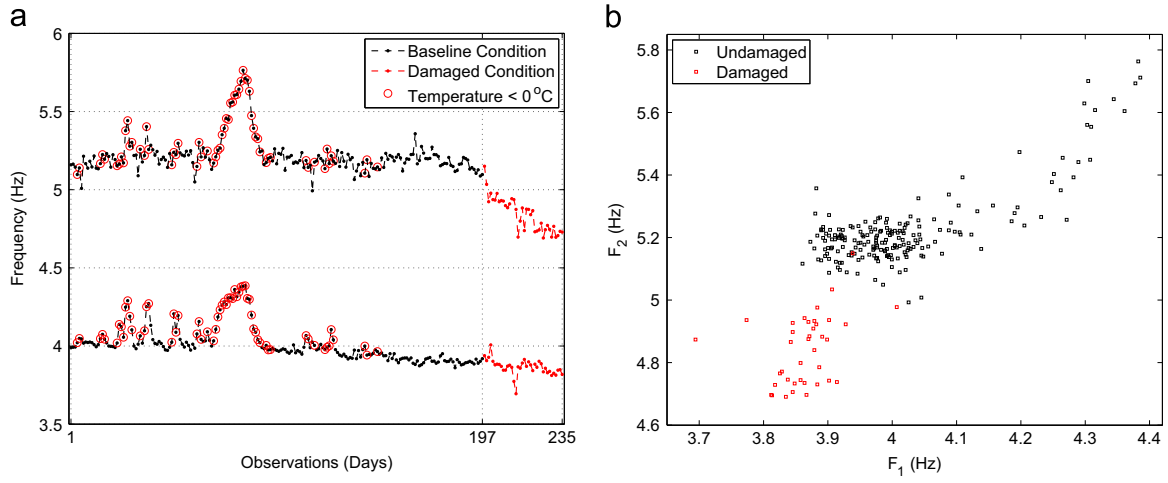

Fig. 4. The first two natural frequencies extrated daily at 5 a.m. from 11th of November 1997 to 10th of September 1998 (a); feature distribution of the two most relevant natural frequencies (b).

Fig. 5. The Tamar Suspension Bridge viewed from River Tamar margins (a) and cantilever (b) perspective.

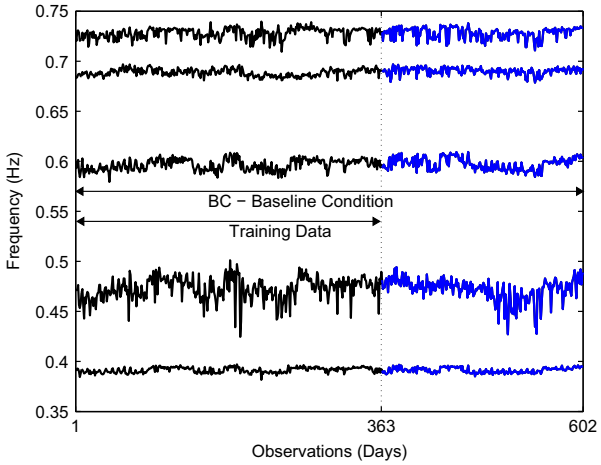

Fig. 6. The first five natural frequencies extracted from the Tamar Bridge.

June 2008) and the entire data set is used in the test process, yielding a training matrix $\mathbf{X}^{363\times5}$ (1–363 observations) and a test matrix $\mathbf{Z}^{602\times5}$ (1–602 observations).

5. Results: statistical modeling and feature classification

In this section, the performances of the GADBA-, GMM-, and MSD-based approaches are compared in terms of the Type I and Type II errors. The GADBA works through some previously defined parameters. The number of iterations required to infer the convergence of the fitness value, when the best solution is achieved, is equal to 5, considering an oscillation of the best fitness in the order of 10^{-4}. The crossover and mutation probabilities are 0.8 and 0.01, respectively. The size of the ring in the tournament method for individual selection is set to 4. Furthermore, the population size and the maximum number of components are taken to be 20 and 10, respectively. Most of the parameters were adopted based on the performance observed in recent research studies (Bandyopadhyay and Maulik, 2002). The GMM-based approach was set as described in Figueiredo et al. (2014), where the parameters are estimated from the training data using the EM algorithm. The MSD-based approach was set as described in Figueiredo and Cross (2013), where the covariance matrix and mean vector were defined based on the training data.

5.1. The Z-24 Bridge

For all 235 observations, the four centroids corresponding to the same number of clusters or structural components ($K=4$) is

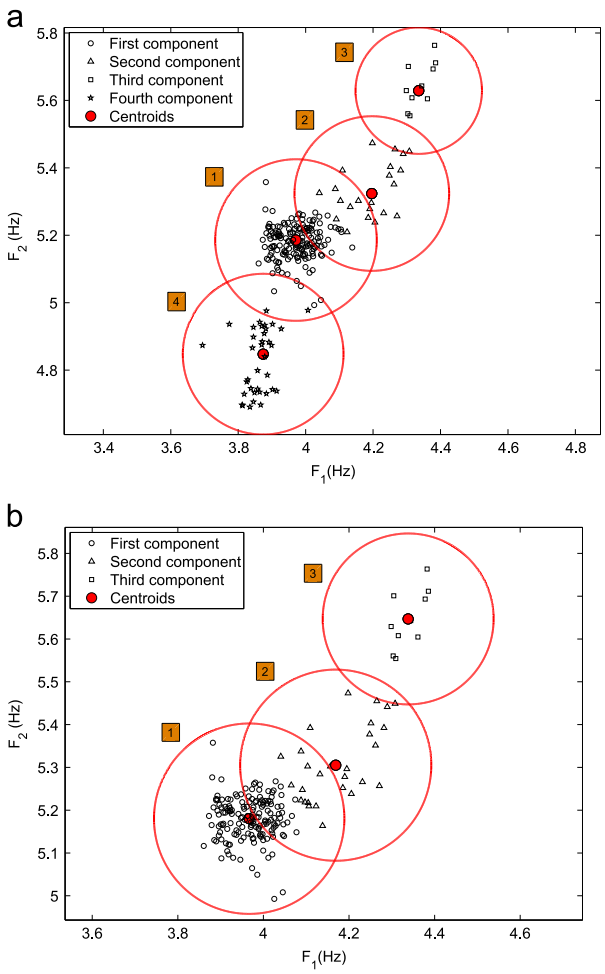

Fig. 7. Centroids along with the observations using the data sets from the Z-24 Bridge: (a) all the 235 observations; (b) 1–197 observations corresponding to the baseline condition.

Table 1
Comparison of the parameter estimation using the CH and EM algorithms on the entire data sets (1–235) from the Z-24 Bridge (standard errors smaller than $10e-003$).

Algorithm	Description	Cluster 1	Cluster 2	Cluster 3	Cluster 4
CH	Weight (%)	69	10	6	15
	Mean (Hz)	(3.97, 5.18)	(4.17, 5.28)	(4.31, 5.59)	(3.86, 4.84)
EM	Weight (%)	64	21	15	––
	Mean (Hz)	(3.97, 5.19)	(4.16, 5.32)	(3.86, 4.82)	––

plotted in Fig. 7(a), as suggested by the CH algorithm. As indicated in Table 1, the first cluster is centered at (3.97, 5.18), attracting around 69% of all assigned data. In this case, this cluster is possibly related to the baseline condition obtained under small environmental and operational influences. The second cluster is centered at (4.17, 5.28) and is assigned with 10% of the observations. The authors speculate that it might be related to gradual decrease of temperature in the asphalt layer, enough to slightly change the elastic properties of the structure. The third cluster centered at (4.31, 5.59) attracts 6% of observations and may be related to changes in the structural response derived from stiffness changes in the asphalt layer caused by freezing temperatures. The fourth cluster is positioned in the lower region of the feature space centered at (3.86, 4.84). It embeds around 15% of the entire observations and is related to the space region assigned to the damaged condition. As demonstrated in Figueiredo et al. (2014), these results suggest the possibility to correlate physical states of the structure with a finite and well defined number of main structural components. Figueiredo et al. (2014) show the existence of this phenomenon, which is assigned to the natural grouping of similar observations in certain regions of the feature space. Comparing the results from the CH and EM algorithms, one may verify the similarity of the results in Table 1. However, the EM algorithm agglutinates the second and third clusters suggested by the CH algorithm, incorporating all gradual changes in the asphalt layer to one cluster only.

The challenge to simulate damage in high capital expenditure civil engineering structures is well-known, namely due to the one-of-a-kind structural type, the cost associated with the simulation of damage in such infrastructure, and due to the unfeasibility to cover all damage scenarios (Figueiredo et al., 2014; Westgate and Brownjohn, 2011). Therefore, the unsupervised approaches are often required as long as the existence of data from the undamaged condition is known a priori. Thus, and for real applications, the centroids defined by the CH algorithm are shown in Fig. 7(b), taking into account only feature vectors from the baseline condition. In this case, three clusters are positioned in close positions as indicated in Table 2. Comparing the results obtained from the CH and EM algorithms, one can verify, once again, similarities in the cluster location. However, the CH algorithm splits the observations under gradual freezing effects into two clusters.

In relation to convergence, in average, after several runs with different initial populations, the GADBA-based approach converges to consistent results at 55 generations. In turn, the GMM executes 31 iterations when running to a three-component scenario. However, to automatically estimate the number of components, the Bayesian information criterion was adopted. Thus, it was necessary around 1000 iterations of GMM, under different initial conditions and number of parameters, before complete convergence.

The DIs obtained from the test matrix, $\mathbf{Z}^{235\times 2}$, are highlighted in Fig. 8. It shows that the GADBA-based approach outputs a monotonic relationship in the amplitude of the DIs related to the damage level accumulation; whereas the GMM fails to establish this relationship. In the case of the MSD-based approach, patterns in the DIs caused by the freezing effects can be pointed out, which indicate that this approach is not able to remove, completely, the effects of environmental variations and so demonstrates to be not effective to model the normal condition.

Therefore, to quantify the classification performance, Table 3 summarizes the Type I and Type II errors for the test matrix. Basically, the GADBA- and GMM-based approaches have the same classification performance, reaching 5.07% and 2.63% of Type I and Type II errors, respectively, and a total amount of errors equal to 4.68%. These results are quite similar due to the function adopted to evaluate the observation density within the inflated hyperspheres. However, the GADBA filters nearly all operational and environmental variability, especially in the damaged observations, instead of the GMM that provides a poor data normalization in these observations. As expected, the MSD-based approached obtained a similar result in relation to the amount of Type I errors; however, the Type II errors reached over 39%, demonstrating its inefficiency when classifying abnormal conditions.

Table 2
Comparison of the parameter estimation using the CH and EM algorithms on the baseline condition data (1–197) from the Z-24 Bridge (standard errors smaller than $10e-003$).

Algorithm	Description	Cluster 1	Cluster 2	Cluster 3
CH	Weight (%)	81	12	7
	Mean (Hz)	(3.97, 5.19)	(4.17, 5.29)	(4.30, 5.60)
EM	Weight (%)	81	19	––
	Mean (Hz)	(3.97, 5.19)	(4.22, 5.39)	––

5.2. The Tamar Bridge

The data sets from the Z-24 Bridge are unique, as it was known a priori the existence of damage. On the other hand, the data sets from the Tamar Bridge represent the most common situation observed in real-world SHM applications on bridges, as there is no indication of damage in advance.

Following the same procedure carried out in the previous subsection, the clusters and centroids defined by the GADBA-based approach, during model estimation, are shown in Fig. 9, in a two-dimensional representation. Table 4 summarizes the centroid localizations in the original five-dimensional feature space along with the distribution weights inferred by both the CH ($K=3$) and the EM ($K=3$) algorithms. Even though the number of centroids is equal for both approaches, one can assert that the CH appears to perform a better modeling of the underlying components than EM algorithm, due to the GADBA is less sensitive to the choice of the initial parameters and also guides the solutions towards the global optimal. The second frequency is observed to considerably contribute to the best distinction of these clusters, related to structural components. In addition, the GADBA-based approach converged after 86 generations and for the GMM achieve complete convergence, it was required around 1000 iterations.

Furthermore, for the CH algorithm, one can figure out that the three hyperspheres defined through the linear inflation step have the expected behavior, by stopping their inflations close to the boundary of each cluster, as shown in Fig. 9. This behavior is verified at the boundary regions, where one can find, especially between the first and third components, the lowest concentration of observations. On the other hand, one can find a high concentration of observations around the first and second centroids.

For an overall analysis purpose, the DIs for all observations in the test matrix, $\mathbf{Z}^{602\times 5}$, are plotted in Fig. 10, where the set of observations from 1 to 363 is used on the training phase. For the GMM-based approach, a concentration of outliers in the data not used in the training phase is observed, suggesting an inappropriate modeling of the normal condition. On the other hand, the GADBA-based approach seems to output a random pattern among the expected outlier observations, especially among the ones not used in training process, suggesting a properly understanding of the normal condition by the clusters defined by the CH algorithm. Note that, in this case, there is no indications about the existence of neither damage nor extreme operational and environmental variability in the data sets.

For completeness, Table 5 summarizes the Type I errors for all three approaches. The Type II errors are not summarized herein as

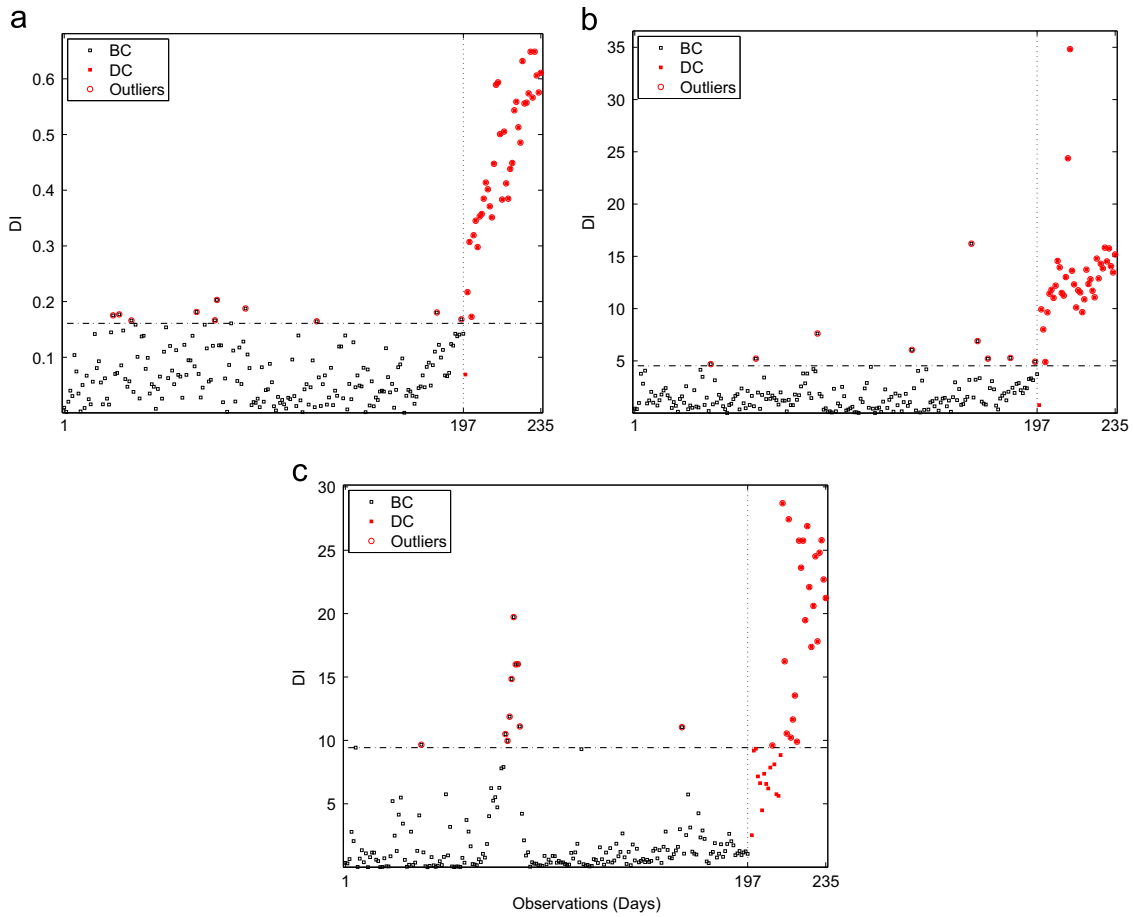

Fig. 8. Damage indicators along with a threshold based on a cut-off value of 95% over the baseline data (1–197) from the Z-24 Bridge: (a) GADBA-, (b) GMM-, and (c) MSD-based approaches.

Table 3
Number and percentage of Type I and Type II errors for each approach using the data sets from the Z-24 Bridge.

Approach	Type I	Type II	Total
GADBA	10 (5.07%)	1 (2.63%)	11 (4.68%)
GMM	10 (5.07%)	1 (2.63%)	11 (4.68%)
MSD	10 (5.07%)	15 (39.47%)	25 (10.63%)

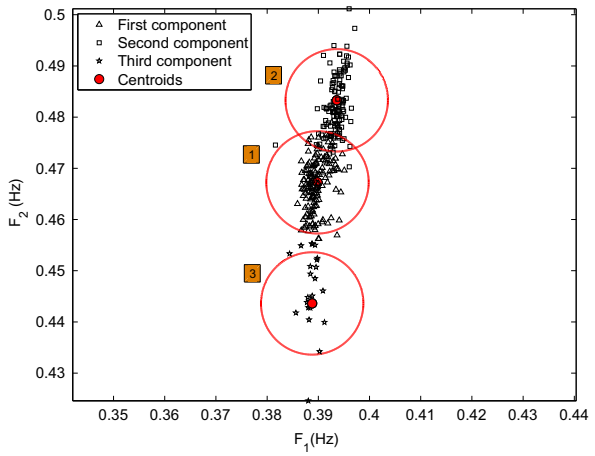

Fig. 9. The three main clusters defined by the CH algorithm, with their centroids and corresponding final hyperspheres in the two-dimensional feature space using only the first two frequencies from the Tamar Bridge.

Table 4
Parameter estimation using the CH and EM algorithms on the baseline condition data (1-363) from the Tamar Bridge (approximation errors smaller than $10e-003$).

Algorithm	Description	Feature	Cluster 1	Cluster 2	Cluster 3
CH	Weight (%)	——	36	52	12
	Mean (Hz)	F_1	0.38	0.39	0.38
		F_2	0.46	0.48	0.44
		F_3	0.59	0.60	0.59
		F_4	0.68	0.68	0.68
		F_5	0.72	0.73	0.72
EM	Weight (%)	——	40	26	34
	Mean (Hz)	F_1	0.38	0.39	0.39
		F_2	0.46	0.46	0.48
		F_3	0.59	0.59	0.60
		F_4	0.68	0.68	0.69
		F_5	0.72	0.73	0.73

there is no indications about structural damage. The total number of Type I errors is 32 (5.32%), 65 (10.8%) and 30 (4.98%) for the GADBA-, GMM- and MSD-based approaches, respectively. Therefore, as the percentage of errors given by the GADBA is close to the 5% level of significance assumed in the training process, one concludes that the GADBA-based approach offers the best model to filter the environmental and operational influences and fit the normal condition of the bridge. The importance of this result is rooted on the fact that this scenario is close to the ones found in real-world monitoring, where there is no indications of damage a

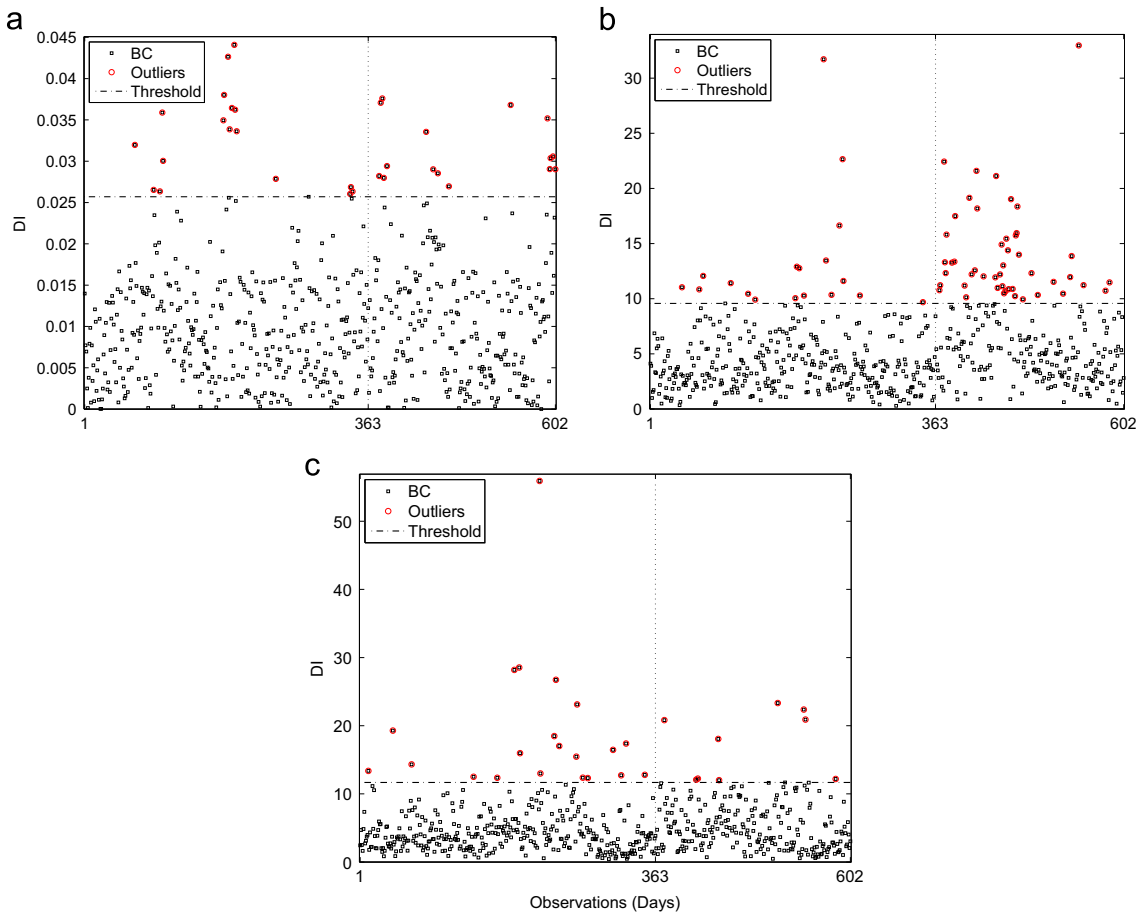

Fig. 10. Damage indicators along with a threshold based on a cut-off value of 95% over the training data: (a) GADBA-, (b) GMM- and (c) MSD-based approaches.

Table 5
Number and percentage of Type I errors for each approach using the data sets from the Tamar Bridge.

Approach	Type I
GADBA	32 (5.32%)
GMM	65 (10.8%)
MSD	30 (4.98%)

priori, which permits one to reduce the number of false alarms and increase the reliability of the SHM system.

6. Summary and conclusions

This paper presented the performance of an unsupervised and nonparametric cluster-based approach (GADBA) applied to detect damage in bridges, even in the presence of environmental and operational influences. This approach is supported by a novel method (CH) based on spacial geometry and sample density of each cluster, aiming to eliminate redundant clusters, also known as structural components.

The proposed approach was compared with two alternative parametric cluster-based approaches extensively studied in the literature (GMM and MSD), through their applications on two conceptually different but real-world data sets, from the Z-24 and Tamar Bridges, located in Switzerland and United Kingdom, respectively. The structures were subjected to environmental and operational influences, which could cause structural changes.

In terms of result analysis, as verified on both bridges, the GADBA-based approach demonstrates to be: (i) as robust as the GMM-based one to detect the existence of damage; and (ii) potentially more effective to model the baseline condition and attenuate the effects of the operational and environmental variability, as suggested by the minimization of false alarms on the data from the Tamar Bridge.

In terms of theory formulation, the proposed approach assumes no particular underlying distribution and its genetically guided characteristic increases the chance to obtain a solution close to the global optimal. On the other hand, the GMM assumes the existence of Gaussian distributions and the EM converges toward a local optimum. Therefore, the GADBA-based approach is conceptually simpler to be deployed in real-world applications and embedded in hardware (e.g., sensor nodes), in situations where it is not possible to make any assumption about the data distribution. Besides, the CH algorithm provides special capabilities (inflation and observation density analysis) to regularize the number of components and define better clusters, resulting in more accurate models to accomplish data normalization. In addition, compared to GMM, the GADBA-based approach demonstrates faster convergence in both case studies. It is also important to note that several runs of GMM are needed to automatically estimate the number of components using some off-line penalization criterion.

Finally, based on the data sets used in this study, both GADBA- and GMM-based approaches fit the well-known theorem that *there is no free lunch* in which machine learning algorithms are classified in two classes: specialized methods for some category of problems

and methods that maintain a reasonable performance in the solution of most part of problems. Thus, the GMM fits the category of specialized methods that do not generate good results for all type of applications. On the other hand, the GADBA fits the category in which results are often acceptable, i.e., it has a superiority in terms of generalization.

Acknowledgments

The authors acknowledge the financial support received from CNPq (Grant 142236/2014-4 and Grant 454483/2014-7) and CAPES. We also would like to acknowledge Prof. Guido De Roeck, from the Katholieke Universiteit Leuven, and Prof. James Brownjohn, from the University of Exeter, for giving us the entire data as well as documentation from the Z-24 and Tamar Bridges.

References

Bandyopadhyay, S., Maulik, U., 2002. An evolutionary technique based on k-means algorithm for optimal clustering in rn. Inf. Sci. 146 (1–4), 221–237. http://dx.doi.org/10.1016/S0020-0255(02)00208-6.

Chambers, L.D., 2000. The Practical Handbook of Genetic Algorithms: Applications, Second Edition, 2nd ed. Chapman and Hall CRC. Boca Raton, Florida.

Chou, J.-H., Ghaboussi, J., 2001. Genetic algorithm in structural damage detection. Comput. Struct. 79 (14), 1335–1353. http://dx.doi.org/10.1016/S0045-7949(01)00027-X.

Cowgill, M., Harvey, R., Watson, L., 1999. A genetic algorithm approach to cluster analysis. Comput. Math. Appl. 37 (7), 99–108. http://dx.doi.org/10.1016/S0898-1221(99)00090-5.

Cross, E., Koo, K., Brownjohn, J., Worden, K., 2013. Long-term monitoring and data analysis of the Tamar bridge. Mech. Syst. Signal Process. 35 (1–2), 16–34. http://dx.doi.org/10.1016/j.ymssp.2012.08.026.

Deb, K., Pratap, A., Agarwal, S., Meyarivan, T., 2002. A fast and elitist multiobjective genetic algorithm: NSGA-II. IEEE Trans. Evolut. Comput. 6 (2), 182–197. http://dx.doi.org/10.1109/4235.996017.

Estes, A., Frangopol, D., 2003. Updating bridge reliability based on bridge management systems visual inspection results. J. Bridge Eng. 8 (6), 374–382. http://dx.doi.org/10.1061/(ASCE)1084-0702(2003)8:6(374).

Farrar, C.R., Worden, K., 2007. An introduction to structural health monitoring. Philos. Trans. R. Soc.: Math. Phys. Eng. Sci. 365 (1851), 303–315. http://dx.doi.org/10.1098/rsta.2006.1928.

Farrar, C.R., Worden, K., 2013. Structural Health Monitoring: A Machine Learning Perspective. John Wiley & Sons, Inc., Hoboken NJ, United States.

Farrar, C.R., Doebling, S.W., Nix, D.A., 2001. Vibration-based structural damage identification. Philos. Trans. R. Soc.: Math. Phys. Eng. Sci. 359 (1778), 131–149. http://dx.doi.org/10.1098/rsta.2000.0717.

Figueiredo, E., Cross, E., 2013. Linear approaches to modeling nonlinearities in long-term monitoring of bridges. J. Civ. Struct. Health Monitor. 3 (3), 187–194. http://dx.doi.org/10.1007/s13349-013-0038-3.

Figueiredo, E., Park, G., Farrar, C.R., Worden, K., Figueiras, J., 2011. Machine learning algorithms for damage detection under operational and environmental variability. Struct. Health Monitor. 10 (6), 559–572. http://dx.doi.org/10.1177/1475921710388971.

Figueiredo, E., Moldovan, I., Marques, M.B., 2013. Condition Assessment of Bridges: Past, Present, and Future—A Complementary Approach, Universidade Católica Editora, Portugal.

Figueiredo, E., Radu, L., Worden, K., Farrar, C.R., 2014. A Bayesian approach based on a Markov-chain Monte Carlo method for damage detection under unknown sources of variability. Eng. Struct. 80 (0), 1–10. http://dx.doi.org/10.1016/j.engstruct.2014.08.042.

Friswell, M.I., Penny, J.E.T., 2002. Crack modeling for structural health monitoring. Struct. Health Monitor. 1 (2), 139–148. http://dx.doi.org/10.1177/147592170200100202.

Gattulli, V., Chiaramonte, L., 2005. Condition assessment by visual inspection for a bridge management system. Comput.-Aided Civ. Infrastruct. Eng. 20 (2), 95–107. http://dx.doi.org/10.1111/j.1467-8667.2005.00379.x.

Gkda, H., Yildiz, A.R., 2001. Structural damage detection using modal parameters and particle swarm optimization. Mater. Test. 54 (6), 416–420. http://dx.doi.org/10.3139/120.110346.

Goldberg, D.E., 1989. Genetic Algorithms in Search, Optimization and Machine Learning, 1st ed. Addison-Wesley Longman Publishing Co., Inc., Boston, MA, USA.

Hakim, S., Razak, H.A., 2014. Modal parameters based structural damage detection using artificial neural networks—a review. Smart Struct. Syst. 14 (2), 159–189. http://dx.doi.org/10.12989/sss.2014.14.2.159.

Hall, L., Ozyurt, I., Bezdek, J., 1999. Clustering with a genetically optimized approach. IEEE Trans. Evolut. Comput. 3 (2), 103–112. http://dx.doi.org/10.1109/4235.771164.

He, R.-S., Hwang, S.-F., 2007. Damage detection by a hybrid real-parameter genetic algorithm under the assistance of grey relation analysis. Eng. Appl. Artif. Intell. 20 (7), 980–992. http://dx.doi.org/10.1016/j.engappai.2006.11.020.

Hruschka, E., Campello, R., Freitas, A., de Carvalho, A., 2009. A survey of evolutionary algorithms for clustering. IEEE Trans. Syst. Man Cybern. Part C: Appl. Rev. 39 (2), 133–155. http://dx.doi.org/10.1109/TSMCC.2008.2007252.

Hsu, T.-Y., Loh, C.-H., 2010. Damage detection accommodating nonlinear environmental effects by nonlinear principal component analysis. Struct. Control Health Monitor. 17 (3), 338–354. http://dx.doi.org/10.1002/stc.320.

Jain, A.K., 2010. Data clustering: 50 years beyond k-means. Pattern Recognit. Lett. 31 (8), 651–666. http://dx.doi.org/10.1016/j.patrec.2009.09.011.

Kullaa, J., 2009. Eliminating environmental or operational influences in structural health monitoring using the missing data analysis. J. Intell. Mater. Syst. Struct. 20 (11), 1381–1390. http://dx.doi.org/10.1177/1045389X08096050.

Lee, J., Sanmugarasa, K., Blumenstein, M., Loo, Y.-C., 2008. Improving the reliability of a Bridge Management System (BMS) using an ANN-based Backward Prediction Model (BPM). Autom. Constr. 17 (6), 758–772. http://dx.doi.org/10.1016/j.autcon.2008.02.008.

Liu, Y.-Y., Ju, Y.-F., Duan, C.-D., Zhao, X.-F., 2011. Structure damage diagnosis using neural network and feature fusion. Eng. Appl. Artif. Intell. 24 (1), 87–92. http://dx.doi.org/10.1016/j.engappai.2010.08.011.

MacQueen, J.B., 1967. Some methods for classification and analysis of multivariate observations. In: Cam, L.M.L., Neyman, J. (Eds.), Proceedings of the fifth Berkeley Symposium on Mathematical Statistics and Probability, vol. 1. University of California Press, Berkeley, California, pp. 281–297.

Maulik, U., Bandyopadhyay, S., 2000. Genetic algorithm-based clustering technique. Pattern Recognit. 33 (9), 1455–1465. http://dx.doi.org/10.1016/S0031-3203(99)00137-5.

Meruane, V., Heylen, W., 2010. Damage detection with parallel genetic algorithms and operational modes. Struct. Health Monitor. 9 (6), 481–496. http://dx.doi.org/10.1177/1475921710365400.

Meruane, V., Heylen, W., 2011. An hybrid real genetic algorithm to detect structural damage using modal properties. Mech. Syst. Signal Process. 25 (5), 1559–1573. http://dx.doi.org/10.1016/j.ymssp.2010.11.020.

Mitchell, M., 2009. An Introduction to Genetic Algorithms. MIT Press, Cambridge, MA, USA.

Miyamoto, A., Kawamura, K., Nakamura, H., 2001. Development of a bridge management system for existing bridges. Adv. Eng. Softw. 32 (10–11), 821–833. http://dx.doi.org/10.1016/S0965-9978(01)00034-5.

Nguyen, T., Chan, T.H., Thambiratnam, D.P., 2014. Controlled Monte Carlo data generation for statistical damage identification employing Mahalanobis squared distance. Struct. Health Monitor. 13 (4), 461–472. http://dx.doi.org/10.1177/1475921714521270.

Ni, Y., Hua, X., Fan, K., Ko, J., 2005. Correlating modal properties with temperature using long-term monitoring data and support vector machine technique. Eng. Struct. 27 (12), 1762–1773. http://dx.doi.org/10.1016/j.engstruct.2005.02.020.

Peeters, B., Roeck, G.D., 1999. Reference-based stochastic subspace identification for output-only modal analysis. Mech. Syst. Signal Process. 13 (6), 855–878. http://dx.doi.org/10.1006/mssp.1999.1249.

Peeters, B., Roeck, G. De, 2001. One-year monitoring of the z24-bridge: environmental effects versus damage events. Earthq. Eng. Struct. Dyn. 30 (2), 149–171. http://dx.doi.org/10.1002/1096-9845(200102)30:2⟨149::AID-EQE1⟩3.0.CO;2-Z.

Peeters, B., Maeck, J., Roeck, G.D., 2001. Vibration-based damage detection in civil engineering: excitation sources and temperature effects. Smart Mater. Struct. 10 (3), 518. http://dx.doi.org/10.1088/0964-1726/10/3/314.

Reynders, E., Wursten, G., De Roeck, G., 2014. Output-only structural health monitoring in changing environmental conditions by means of nonlinear system identification. Struct. Health Monitor 6 (13), 82–93. http://dx.doi.org/10.1177/1475921713502836.

Runkler, T., Keller, J., 2012. Fuzzy approaches to hard c-means clustering. In: 2012 IEEE International Conference on Fuzzy Systems (FUZZ-IEEE), 2012, pp. 1–7. http://dx.doi.org/10.1109/FUZZ-IEEE.2012.6251343.

Santos, A., Silva, M., Sales, C., Costa, J., Figueiredo, E., 2015. Applicability of linear and nonlinear principal component analysis for damage detection. In: 2015 IEEE International Instrumentation and Measurement Technology Conference (I2MTC), pp. 869–874. http://dx.doi.org/10.1109/I2MTC.2015.7151383.

Santos, A., Figueiredo, E., Silva, M., Sales, C., Costa, J., 2016. Machine learning algorithms for damage detection: kernel-based approaches. J. Sound Vib. 363 (17), 584–599. http://dx.doi.org/10.1016/j.jsv.2015.11.008.

Sohn, H., 2007. Effects of environmental and operational variability on structural health monitoring. Philos. Trans. R. Soc.: Math. Phys. Eng. Sci. 365 (1851), 539–560. http://dx.doi.org/10.1098/rsta.2006.1935.

Sohn, H., Farrar, C.R., 2001. Damage diagnosis using time series analysis of vibration signals. Smart Mater. Struct. 10 (3), 446–451. http://dx.doi.org/10.1088/0964-1726/10/3/304.

Sohn, H., Worden, K., Farrar, C.R., 2002. Statistical damage classification under changing environmental and operational conditions. J. Intell. Mater. Syst. Struct. 13 (9), 561–574. http://dx.doi.org/10.1106/104538902030904.

Wen, Q., Celebi, M., 2011. Hard versus fuzzy c-means clustering for color quantization. EURASIP J. Adv. Signal Process. 2011 (1), 118. http://dx.doi.org/10.1186/1687-6180-2011-118.

Wenzel, H., 2009. Health Monitoring of Bridges. John Wiley & Sons, Inc., United States.

Westgate, K.Y.K.R.J., Brownjohn, J.M.W., 2011. Environmental effects on a suspension bridge's dynamic response, Leuven, Belgium.

Worden, K., Manson, G., 2007. The application of machine learning to structural health monitoring. Philos. Trans. R. Soc.: Math. Phys. Eng. Sci. 365 (1851), 515–537. http://dx.doi.org/10.1098/rsta.2006.1938.

Worden, K., Farrar, C.R., Manson, G., Park, G., 2007. The fundamental axioms of structural health monitoring. Philos. Trans. R. Soc.: Math. Phys. Eng. Sci. 463 (2082), 1639–1664. http://dx.doi.org/10.1098/rspa.2007.1834.

Xia, Y., Hao, H., 2001. A genetic algorithm for structural damage detection based on vibration data. In: XIX International Modal Analysis Conference, pp. 1381–1387.

Xia, Y., Chen, B., Weng, S., Ni, Y.-Q., Xu, Y.-L., 2012. Temperature effect on vibration properties of civil structures: a literature review and case studies. J. Civ. Struct. Health Monit. 2 (1), 29–46. http://dx.doi.org/10.1007/s13349-011-0015-7.

Xu, B., Wu, Z., Chen, G., Yokoyama, K., 2004. Direct identification of structural parameters from dynamic responses with neural networks. Eng. Appl. Artif. Intell. 17 (8), 931–943. http://dx.doi.org/10.1016/j.engappai.2004.08.010.

Appendix C – Paper C: A Global Expectation-Maximization Approach Based on Memetic Algorithm for Vibration-Based Structural Damage Detection

A Global Expectation–Maximization Approach Based on Memetic Algorithm for Vibration-Based Structural Damage Detection

Adam Santos, Reginaldo Santos, Moisés Silva, Eloi Figueiredo, Claudomiro Sales, and João C. W. A. Costa, *Member, IEEE*

***Abstract*— This paper proposes a novel unsupervised damage detection approach based on a memetic algorithm that establishes the normal or undamaged condition of a structural system as data clusters through a global expectation–maximization technique, using only damage-sensitive features extracted from output-only vibration measurements. The health state is then discriminated by considering the Mahalanobis squared distance between the learned clusters and a new observation. The proposed approach is compared with state-of-the-art ones by taking into account real-world data sets from the Z-24 Bridge (Switzerland), where several damage scenarios were performed. The results indicated that the proposed approach can be applied in structural health monitoring applications where life safety, economic, and reliability issues are the most important motivations to consider.**

***Index Terms*— Damage detection, data normalization, environmental conditions, memetic algorithm (MA), operational conditions, structural health monitoring (SHM), vibration measurements.**

I. Introduction

DAMAGE assessment based on the vibration response measurements from engineering structures has been an essential research area in the structural health monitoring (SHM) field [1], [2]. Vibration signals are often available and can be measured from different types of monitoring systems through a diversity of data acquisition systems and sensors. Based on suitable data treatment, valuable information from the structural dynamics can be extracted and used as damage-sensitive features for detecting early and progressive structural damage, thereby increasing safety, avoiding collapses, and supporting the decision making process regarding maintenance, repair, and rehabilitation.

Unfortunately, operational and environmental variations (e.g., temperature, operational loading, humidity, and wind speed) often arise as undesired effects in the damage-sensitive features and usually mask changes caused by damage, which might negatively influence the proper identification of damage if a data normalization procedure is not performed [3]. To handle this drawback, several machine learning algorithms with different working principles have been proposed to mitigate (or even remove) those effects on the extracted features as well as to properly separate changes in damage-sensitive features caused by damage from those caused by varying operational and environmental conditions [4]–[6]. These machine learning approaches are often characterized as unsupervised and output-only because they are trained only with damage-sensitive features related to undamaged condition without any measurement directly related to operational and environmental parameters. One of the reasons for this choice is that the supervised learning [7]–[11] work in the training phase with both conditions (undamaged and damaged) and the input–output approaches [12]–[14] should know in advance all parameters to be measured, so both have narrow applicability to real-world scenarios.

Mahalanobis squared distance (MSD) and principal component analysis (PCA) are unsupervised algorithms adapted to act as data normalization and damage detection techniques [15]–[19]. However, the linear behavior imposed for these techniques has limited their applicability in SHM. If nonlinearities are present in the monitoring data, the MSD and PCA might fail in modeling the normal condition of a structure because the former assumes the baseline data follow a multivariate Gaussian distribution (or only one data cluster) and the principal components in the latter are independent only if the baseline data is jointly normally distributed.

To extend the capabilities of traditional methods such as MSD and PCA, improved approaches based on the autoassociative neural network (AANN), kernel PCA, and Gaussian mixture models (GMMs) were proposed to deal with real-world structures and more complex SHM applications such that the nonlinear influences on the damage-sensitive features could be accounted for [20]–[25].

As presented in [20], the AANN is a nonlinear version of the PCA that seeks to accommodate the operational and environmental effects by solving a global nonlinear optimization, which is sensitive to initial parameters, after a complex definition of the number of neurons in its hidden layers. Another nonlinear version of the PCA that acts as a data normalization procedure is the kernel PCA, for which the type of nonlinearity is not explicitly defined and its two parameters can be automatically defined [22], [23]: the bandwidth of the

Manuscript received November 14, 2016; accepted November 15, 2016. Date of publication February 17, 2017; date of current version March 8, 2017. This work was supported in part by the National Council for Scientific and Technological Development, Brazil, under Grant 142236/2014-4 and Grant 454483/2014-7 and in part by the Coordination for the Improvement of Higher Education Personnel, Brazil. The Associate Editor coordinating the review process was Dr. Kurt Barbe.

A. Santos, R. Santos, M. Silva, C. Sales, and J. C. W. A. Costa are with the Applied Electromagnetism Laboratory, Federal University of Pará, Pará 66075110, Brazil (e-mail: adamdreyton@ufpa.br).

E. Figueiredo is with the Faculty of Engineering, Universidade Lusófona de Humanidades e Tecnologias, Lisbon 1749024, Portugal.

Color versions of one or more of the figures in this paper are available online at http://ieeexplore.ieee.org.

Digital Object Identifier 10.1109/TIM.2017.2663478

TABLE I
QUALITATIVE COMPARISON OF UNSUPERVISED MACHINE LEARNING APPROACHES FOR SHM

	Approach	Nonlinear capabilities	Cluster-based	Dimensionality reduction	Model interpretation	Stable results
Traditional	PCA	✗	✗	✓	✗	✓
	MSD	✗	✓	✗	✗	✓
Improved	AANN	✓	✗	✓	✗	✗
	KPCA	✓	✗	✓	✗	✓
	EM-GMM	✓	✓	✗	✓	✗
	MC-GMM	✓	✓	✗	✓	✗
	GEM-GA	✓	✓	✗	✓	✓

kernel and the number of retained principal components in the high-dimensional feature space. However, these approaches present some loss of information due to the definitions of the number of neurons and retained principal components (dimensionality reduction), which ensure only the fitting of a fraction of the normal condition under operational and environmental variability.

In a different manner, a linear output-only method was proposed to model nonlinearities in long-term monitoring of structures based on a two-step strategy [25]: data normalization procedure by clustering the training observations into different and finite data clusters and damage detection by identifying possible outliers through a distance measure between the learned clusters and a new observation. As the first step, the GMMs are applied to model the main clusters that correspond to the normal and stable state conditions of a structure. The parameters of the GMMs are estimated from the training data using the expectation–maximization (EM) algorithm. For the second step, the MSD algorithm tracks the outlier formation in relation to the chosen main group of states. Alternatively, an improved Bayesian approach based on a Markov chain Monte Carlo (MCMC) method was proposed in [26] to compute the parameters of the GMMs. Both approaches have revealed better damage detection performance compared with MSD.

Despite the EM-GMM and MC-GMM approaches can fit the normal condition of a structure without loss of information, the optimal parameters determined by the EM and MCMC algorithms are strongly dependent on the choice of the initial parameters. Thereby, these algorithms do not ensure that the global optimal solution and the training phase may be quite slow because it is often advised to run both algorithms a couple of times with different initial guesses of parameters to find a satisfactory quasi-optimal solution, which is not fully guaranteed [27]. As consequence, this degenerated behavior of the EM and MCMC algorithms may affect the stability and reliability of the damage detection or even the number of data clusters estimated for each different run.

Therefore, this paper presents a memetic algorithm (MA) based on a genetic algorithm (GA) to improve the stability and reliability of the EM algorithm in searching for the optimal number of data clusters and their parameters, a global EM-GA (GEM-GA), which improves the damage classification performance. In this case, the parameters of the GMMs are estimated via a hybrid method composed of an EM algorithm within an MA. Compared with the state-of-the-art approaches, the GEM-GA not only deals with nonlinear relationships in monitoring data but also provides stable results in terms of damage detection and data clusters as the main stable structural conditions (model interpretation), as summarized in Table I.

As long as the main stable state conditions of the structure are determined, the superiority of the GEM-GA approach over the state-of-the-art ones is attested on a damage detection strategy implemented through the MSD, using real-world data sets from the Z-24 Bridge (Switzerland). The classification performance is assessed on the basis of Type I (false positive indication of damage) and Type II (false negative indication of damage) error tradeoffs.

The remainder of this paper is organized as follows. In Section II, the GEM-GA approach is derived to determine the health state of a structure based on a reliable estimation of data clusters. Section III describes the test structure and its long-term vibration data as well as the major environmental influence. In Section IV, the experimental results on extracted damage-sensitive features that encompass a variety of challenges encountered in practical SHM applications are discussed and a comparison with state-of-the-art approaches is also emphasized. Finally, Section V synthesizes the main strengths and challenges of the GEM-GA approach.

II. MEMETIC-BASED GLOBAL EM ALGORITHM FOR DAMAGE DETECTION

This section presents the methodology of the GEM-GA approach. First, the EM algorithm for fitting GMMs is briefly discussed and an information criterion is assumed to select the best model with a given number of components. Second, the proposed GEM-GA applies this criterion as the fitness function to improve the performance of the EM algorithm via an MA, which yields a robust data model of the normal condition of a monitored structure. The section ends with a description of the damage detection strategy based on the MSD.

For theoretical purposes, one should consider a training data matrix composed of normal condition data, $\mathbf{X} \in \mathbb{R}^{m \times n}$, with n-dimensional feature vectors from m different operational and environmental conditions when the structure is assumed undamaged and a test data matrix $\mathbf{Z} \in \mathbb{R}^{l \times n}$, where l is the number of feature vectors from the undamaged condition and/or damaged condition (DC).

Although the machine learning algorithms have different mathematical formulations, they are implemented in a common sequence of steps. First, each algorithm is trained and its

parameters are adjusted using feature vectors extracted from the normal condition. In the training phase, the algorithms develop a functional relationship that models how changing operational and environmental conditions influence the underlying distribution of the damage-sensitive features. Second, in the test phase, when subsequent features are analyzed by the learned models and a new set of features are shown not to fit into an appropriate distribution, they might be more confidently classified as outliers or, potentially, features from a damaged structure, because the operational and environmental influences have been incorporated into the learning procedure.

A. Fitting Data Clusters via Global EM

A finite mixture model, $p(\mathbf{x}|\Theta)$, is the weighted sum of $K > 1$ components $p(\mathbf{x}|\boldsymbol{\theta}_k)$ in $\mathbb{R}^n$ [28]

$$p(\mathbf{x}|\Theta) = \sum_{k=1}^{K} \alpha_k \, p(\mathbf{x}|\boldsymbol{\theta}_k) \tag{1}$$

where $\mathbf{x}$ is an n-dimensional data vector and α_k corresponds to the weight of each component. These weights are positive $\alpha_k > 0$ with $\sum_{k=1}^{K} \alpha_k = 1$. For a GMM, each component $p(\mathbf{x}|\boldsymbol{\theta}_k)$ is represented as a Gaussian distribution

$$p(\mathbf{x}|\boldsymbol{\theta}_k) = \frac{\exp\left\{-\frac{1}{2}(\mathbf{x}-\boldsymbol{\mu}_k)^T \boldsymbol{\Sigma}_k^{-1}(\mathbf{x}-\boldsymbol{\mu}_k)\right\}}{(2\pi)^{n/2}\sqrt{\det(\boldsymbol{\Sigma}_k)}} \tag{2}$$

being each component denoted by its parameters, $\boldsymbol{\theta}_k = \{\boldsymbol{\mu}_k, \boldsymbol{\Sigma}_k\}$, composed of the mean vector $\boldsymbol{\mu}_k$ and the covariance matrix $\boldsymbol{\Sigma}_k$. Thus, the GMM is completely specified by the set of parameters $\Theta = \{\alpha_1, \alpha_2, \ldots, \alpha_K, \boldsymbol{\theta}_1, \boldsymbol{\theta}_2, \ldots, \boldsymbol{\theta}_K\}$.

The EM algorithm is the most common method used to estimate the parameters of the GMMs [29]. This method consists of an expectation step (E-step) and a maximization step (M-step), which are applied until the log-likelihood (LogL), $\log p(\mathbf{X}|\Theta) = \log \prod_{i=1}^{m} p(\mathbf{x}_i|\Theta)$, converges to a local optimum. The performance of the EM algorithm deeply depends on the choice of the initial parameters $\Theta^{t=0}$ (where $t = 0$ stands for the first run). The E-step and M-step are described in more detail in [28].

To select the best GMM by means of goodness of fit and parsimony, the Bayesian information criterion (BIC) is used and minimized [30] as

$$\begin{aligned}\mathrm{BIC} = &-2\log p(\mathbf{X}|\Theta) \\ &+ \left\{Kn\left[\left(\frac{n+1}{2}\right)+1\right]+K-1\right\}\log(m)\end{aligned} \tag{3}$$

where the BIC uses the optimal LogL function value and penalizes complex models (with additional parameters) through a term that is a function of the training data size.

MAs are population-based metaheuristics composed of an evolutionary framework and a set of local search algorithms [31]. A general MA can be defined as follows [32].

1) *Initialize* a population of candidate solutions P_1.
2) While a *termination criterion* is not satisfied, repeat.
   a) *Cooperate* between candidate solutions from P_1 to generate a new population P_2.
   b) *Improve* the candidate solutions from P_2 to generate a new population P_3.
   c) *Compete* within the set $P_1 \cup P_3$ to generate a new population P_1 for the next generation.
   d) If P_1 converges, *restart* some chosen solutions.
3) Return the *best solution* encountered.

The *initialize* procedure produces the initial set of random candidate solutions as high-quality solutions generated by applying a local search algorithm, and the *termination criterion* usually verifies the total number of generations and/or a maximum number of generations without improvement. The *cooperate* procedure arises on the selection and combination, determining the solutions that will be merged to create new promising solutions. The *improve* procedure applies a local search method on new solutions derived in the *cooperate* procedure. The *compete* procedure updates the current population using the old population and the new population, determining the solutions that will survive in the following generations. To overcome premature convergence to suboptimal regions of the search space, the *restart* procedure acts as a corrective measure on the population [32].

Hence, MAs comprise notions from population-based global search and local search methods. In this paper, the MA is a hybrid algorithm that combines EM algorithm (local) [29] with GA (global) [33], [34]. Hereafter, the framework of the proposed GEM-GA approach is presented, and its parameters and operators are discussed in more detail.

1) *Initialize* $P_1(t)$, $t = 0$, $r = 0$, $c = 0$.
2) $(P_2(t), \mathrm{BIC}_1) \leftarrow$ perform R EM steps on $P_1(t)$.
3) While $(t \leq 500)$ and $(r \leq 2)$ are satisfied, repeat.
   a) *Cooperate* such that $(P_3(t)) \leftarrow$ recombine on $P_2(t)$ and after $(P_4(t)) \leftarrow$ mutate on $P_3(t)$.
   b) *Improve* $P_4(t)$ such that $(P_5(t), \mathrm{BIC}_2) \leftarrow$ perform R EM steps on $P_4(t)$.
   c) *Compete* between the populations $P_2(t)$ and $P_5(t)$ such that $(P_2(t+1), \mathrm{BIC}_1, b_{\mathrm{GMM}}, \mathrm{BIC}_{\min}) \leftarrow$ select on $P_2(t)$ and $P_5(t)$ via BIC_1 and BIC_2.
   d) Increase $t = t + 1$, and $c = c + 1$ if and only if there is no improvement in $\mathrm{BIC}_{\min}$.
   e) If $c = 100$, then *restart* the worst 90% of individuals from $P_2(t)$, increase $r = r + 1$, and set $c = 0$.
4) *Improve* b_{GMM} if and only if it not converged, such that $(b_{\mathrm{GMM}}, \mathrm{BIC}_{\min}) \leftarrow$ perform EM steps on b_{GMM} until convergence of the LogL is reached.
5) Return b_{GMM} as the *best solution* encountered.

In the GEM-GA approach, each individual in the population represents a candidate solution of the GMM, i.e., a set of parameters Θ that specifies a GMM. Thus, an individual is composed of two different parts. The first part indicates whether a component is activated ($[0.5, 1]$) or not ($[0, 0.5]$) for learning the GMM and the length of this part is the maximum number of activated components $K_{\max}$. The parameters, the mean vector $\boldsymbol{\mu}_k$ and covariance matrix $\boldsymbol{\Sigma}_k$, of $K_{\max}$ components are represented in the second part. Each component includes $(n^2 + 3n)/2$ parameters. Note that the covariance matrix $\boldsymbol{\Sigma}_k$ must be symmetric, and thus only the

upper (or lower) triangular part of the matrix is encoded in the individual.

First, a random population P_1, the number of generations t, restarts r, and generations without improvement c are initialized. Afterward, by applying R EM steps on P_1, with $R = 20$, initial high-quality solutions and their fitness values are derived as P_2 and BIC_1, respectively. The evolutionary process of the GEM-GA is stopped when $t = 500$ or $r = 2$, then the convergence of the best solution b_{GMM} found so far is checked. If it converged in terms of LogL, the final solution is the current best solution; otherwise, the EM algorithm improves b_{GMM} until convergence is reached.

The *cooperate* procedure includes the parent selection, recombination, and mutation. For parent selection, the well-known binary tournament is used on the population P_2 to select parents for recombination [35]. In turn, the recombination merges the chosen parents to generate offspring individuals with the crossover probability $p_{\text{cro}} = 0.8$. The two-point crossover is applied, in which two crossover positions between $\{1, \ldots, K_{max} - 1\}$ are randomly selected within the first part of the parent individual. The values of the genes to the right of these positions are exchanged between parent individuals for the first part and this exchange is generalized to their associated parameters in the second part. A Gaussian mutation, with the mutation probability $p_{\text{mut}} = 0.05$ for each gene of each individual (excluding covariance matrices), is performed on the offspring population P_3 to yield the population P_4.

An improvement on the population P_4 is achieved by applying the EM algorithm that delivers the population P_5 and its fitness values BIC_2, which are used together with P_2 and BIC_1 to select the new population of survivors for the next generation as well as the best solution b_{GMM} and its fitness value BIC_{min}. This survival selection is based on the elitist $(\delta + \lambda)$-strategy [36]. If there is no improvement in BIC_{min} during 100 consecutive generations, the worst 90% of individuals from P_2 are restarted as high-quality solutions (generated by applying the EM algorithm) to explore other regions of the search space. In addition, the flowchart of the GEM-GA approach is illustrated in Fig. 1.

The proposed approach may be faced as a new improved and generalized version of the GA-based EM (GA-EM) algorithm proposed in [37]. The GA-EM demonstrated some limitations related to its codification (binary for the first part and real for the second part), parent selection (randomly), mutation (bit flip and uniform), and premature convergence, as discussed in [38].

B. Damage Detection Strategy

Since the best solution (model) is selected, the structural health is discriminated by generating a damage indicator (DI) and classifying it through a threshold. First, for each observation $\mathbf{z}$, one needs to estimate K DIs via MSD. Particularly, for each undamaged cluster k

$$\text{DI}_k(\mathbf{z}) = (\mathbf{z} - \boldsymbol{\mu}_k)\boldsymbol{\Sigma}_k^{-1}(\mathbf{z} - \boldsymbol{\mu}_k)^T. \tag{4}$$

For each component k, if a new observation $\mathbf{z}$ is extracted from the same component as the undamaged data, then the test statistic MSD will be Chi-square distributed with n degrees of freedom, χ_n^2. Finally, for each observation, the DI is given by the smallest DI estimated on each component

$$\text{DI}(\mathbf{z}) = \min[\text{DI}_1(\mathbf{z}), \ldots, \text{DI}_K(\mathbf{z})]. \tag{5}$$

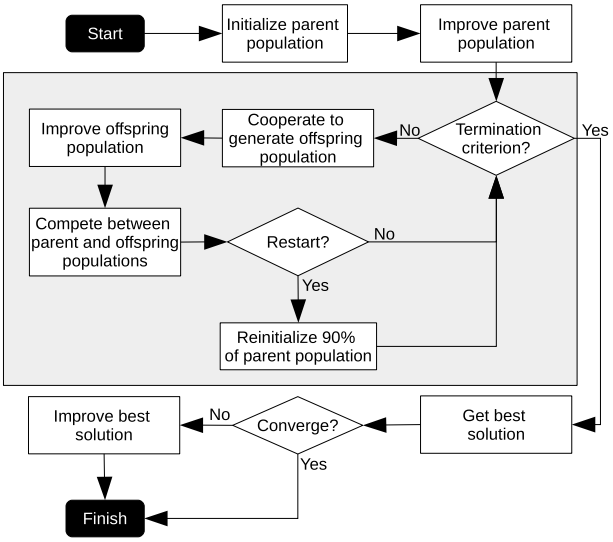

Fig. 1. Flowchart of the GEM-GA approach.

III. Test Structure and Data Sets

In this paper, the comparison between the proposed approach and state-of-the-art ones as well as their applicability is evaluated in terms of damage classification performance using damage-sensitive features (herein natural frequencies) extracted from vibration measurements of the Z-24 Bridge. These data sets are unique as they combine one-year monitoring of the healthy condition, influenced by operational and environmental variability, with realistic damage scenarios [39]. The structure and its data sets are highlighted in this section.

A. Bridge and Damage Test Scenarios

The Z-24 Bridge was a posttensioned concrete box girder bridge composed of a main span of 30 m and two side-spans of 14 m, as depicted in Fig. 2. The bridge, before complete demolition, was extensively instrumented and tested with the purpose of providing a reliable benchmark for vibration-based SHM in civil engineering [40]. A long-term monitoring test was carried out, from November 11, 1997 until September 10, 1998, to quantify the operational and environmental variability present on the bridge and to detect damage artificially introduced, in a controlled manner, in the last month of operation. Every hour, eight accelerometers captured the vibrations of the bridge as sequences of 65 536 samples (sampling frequency of 100 Hz) and other sensors measured environmental parameters, such as temperature at several locations [12]. In particular, technical specifications of the accelerometers (by Kinemetrics Inc.) applied in this monitoring are synthesized in Table II.

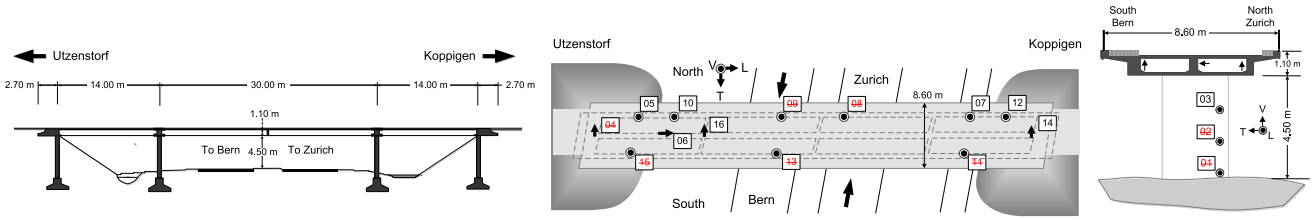

Fig. 2. Longitudinal section (left) and the location and orientation of accelerometers (right) on the Z-24 Bridge. Marked sensors failed during the monitoring campaign [12].

TABLE II

TECHNICAL SPECIFICATIONS REGARDING THE ACCELEROMETERS USED IN THE LONG-TERM MONITORING [41], [42]

Type	Mounting	Sensitivity	Range@140dB	Range@130dB
FBA11	Uniaxial	5 V/g	0–10 Hz	0–50 Hz
FBA23	Triaxial	5 V/g	0–10 Hz	0–50 Hz

TABLE III

PROGRESSIVE DAMAGE TEST SCENARIOS (THE DATES REFER TO THE ADDITIONAL VIBRATION MEASUREMENTS)

Date	Scenario Description
04-08-98	Reference measur. I (undamaged condition)
09-08-98	After installation of the settlement system
10-08-98	Pier settlement = 2 cm
12-08-98	Pier settlement = 4 cm
17-08-98	Pier settlement = 8 cm
18-08-98	Pier settlement = 9.5 cm
19-08-98	Foundation tilt
20-08-98	Reference measur. II (removal of the settlement system)
25-08-98	Spalling of concrete (12 m^2)
26-08-98	Spalling of concrete (24 m^2)
27-08-98	Landslide at abutment
31-08-98	Concrete hinge failure
02-09-98	Failure of 2 anchor heads
03-09-98	Failure of 4 anchor heads
07-09-98	Rupture of 2 out of 16 tendons
08-09-98	Rupture of 4 out of 16 tendons
09-09-98	Rupture of 6 out of 16 tendons

Fig. 3. Damage scenarios carried out in the Z-24 Bridge. Left to right: pier settlement, failure of anchor heads, and tendon rupture.

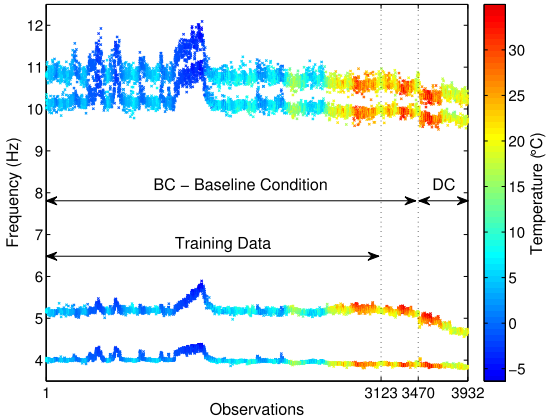

Fig. 4. First four natural frequencies of the Z-24 Bridge: 1–3470 baseline/undamaged condition (BC), 3471–3932 DC.

Progressive damage tests were carried out in one-month time period (from August 4, 1998 to September 10, 1998) before the demolition of the bridge to prove that realistic damage has a measurable influence on the bridge dynamics [39], as summarized in Table III (the dates refer to the day that additional vibration tests were performed to fully characterize the structural condition of the bridge). Three examples of damage test scenarios are illustrated in Fig. 3. Note that the monitoring system was still running during the progressive damage tests, which permits one to validate the SHM system to detect cumulative damage on long-term monitoring.

B. Extraction of Damage-Sensitive Features

In this case, the natural frequencies of the Z-24 Bridge are used as damage-sensitive features. They were estimated using a reference-based stochastic subspace identification method on vibration measurements from the accelerometers [43]. The first four natural frequencies estimated hourly from November 11, 1997 to September 10, 1998, with a total of 3932 observations, are highlighted in Fig. 4. The first 3470 observations correspond to the damage-sensitive feature vectors extracted within the undamaged structural condition under effects caused by the operational and environmental variability. The last 462 observations correspond to the damage progressive testing period, which is highlighted, especially in the second frequency, by a clear decay in the magnitude of this frequency.

The damage scenarios were performed in a sequential manner, which cause a cumulative degradation of the bridge. Therefore, in this paper, it is assumed that the bridge operates within its undamaged condition (baseline or normal condition), under operational and environmental variability, from November 11, 1997 to August 4, 1998 (1–3470 observations). On the other hand, the bridge is considered damaged from August 5, 1998 to September 10, 1998

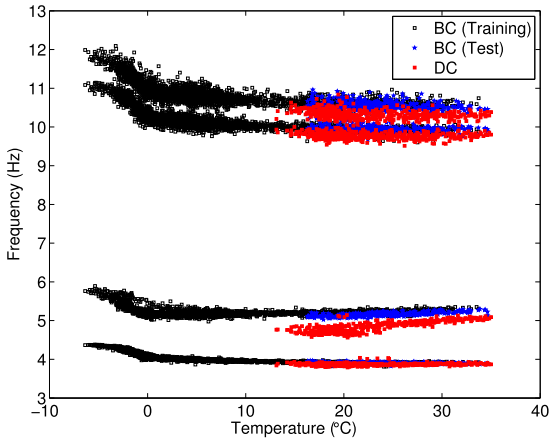

Fig. 5. Nonlinear influence of the temperature on the natural frequencies of the Z-24 Bridge.

(3471–3932 observations). For the baseline condition period, the observed jumps in the natural frequencies are associated with the asphalt layer in cold periods, which contributes significantly to the stiffness of the bridge, as evidenced in Fig. 4, indicating the need for a data normalization procedure to attenuate this variability. Besides, the existence of a high influence of the temperature on the natural frequencies as well as on the structure dynamics may be considered as nonlinear with distinguished behaviors below and above 0 °C [12], [39], as demonstrated in Fig. 5.

For generalization purposes, the feature vectors are split into the training and test matrices. Although the damaged observations are known in advance, the approaches are applied in an unsupervised manner because no information related to the presence of damage is provided during the training phase. As shown in Fig. 4, the training matrix $\mathbf{X}^{3123\times4}$ is composed of 90% of the feature vectors from the undamaged condition. The remaining 10% of the feature vectors are used during the test phase to make sure that the DIs do not fire off before the damage starts. The test matrix $\mathbf{Z}^{3932\times4}$ is composed of all the data sets, even the ones used during the training phase.

IV. Results and Discussion

In this section, the analysis is divided into two parts. First, the EM-GMM, MC-GMM, and GEM-GA approaches are executed 20 times with distinct initial parameters to verify the stability, reliability, and robustness of these techniques. Afterward, as a means of setting a damage detection strategy for the Z-24 Bridge, a model of each approach is chosen based on the BIC. Second, the GEM-GA is compared with nonlinear approaches based on AANN and kernel PCA. The damage detection strategy based on MSD is used for the EM-GMM, MC-GMM, GEM-GA, and AANN; the KPCA implicitly generated the DIs via Euclidean distance (as assumed in [23]). All thresholds are defined for a level of significance of 5%.

All approaches were implemented in MATLAB 8.3.0.532 (R2014a) combining some functions from the packages SHMTools version 0.3.0 [44] and bayesf version 2.0 [45], from the Statistics and Machine Learning Toolbox of MATLAB [46], with new functions developed by the authors.

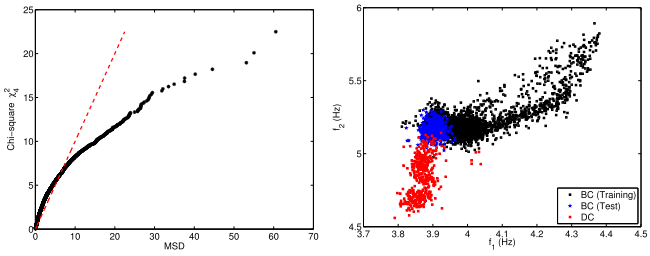

Fig. 6. Multivariate normality statistical test based on the Chi-square Q–Q plot of the MSD using the training observations (left) and the nonlinear relationship between the natural frequencies (right) from the Z-24 Bridge.

A. Reliable Estimation Of Data Clusters

In this SHM scenario, the training data reveal nonlinearities derived from changes in the structural stiffness, influenced by temperature variations, and then the relationship among the natural frequencies is nonlinear, which is evidenced through the multivariate normality statistical test and the nonlinear correlation between the first and second natural frequencies in Fig. 6. Thus, linear approaches are generally liable to relatively poor damage classification performance, which should be overcome with approaches that handle multimodality and heterogeneity of the data as nonlinear models or clusters.

As recommended in [25], to alleviate the drawbacks of the EM algorithm, for each execution of the EM-GMM approach, ten repetitions of the EM algorithm are performed (each one with $R = 1000$) and each GMM with $K_{\max} \in \{2, \ldots, 15\}$ components is fitted with the one that has the largest LogL. By following [26], for each execution of the MC-GMM approach, 5000 MCMC draws are computed after a burn-in of 1000 draws and each GMM with $K_{\max} \in \{2, \ldots, 15\}$ components is fitted with the one that has the largest marginal likelihood. For the GEM-GA approach, the initial population $P_1(t = 0)$ is composed of 20 individuals, where each one has a different number of activated components within $\{2, \ldots, 15\}$. For each execution, the best model is built with K undamaged components, as suggested by the minimization of the BIC (or fitness) for the EM-GMM and GEM-GA and maximization of the marginal likelihood for the MC-GMM.

Even with several repetitions of the EM and MCMC algorithms in each execution, the EM-GMM and MC-GMM approaches are quite unstable on the estimation of data clusters compared with the GEM-GA, as demonstrated in Table IV. This instability is due to the dependence on the choice of the initial parameters, which brings uncertainty whether the model obtained in a particular execution is acceptable or not. On the other hand, the GEM-GA ensures the same number of components for all executions and relatively low standard deviation for LogL and BIC, which indicates the stability and robustness of the MA-based approach to overcome the issues related to initial parameters.

As expected, the degenerated behavior of the EM and MCMC algorithms compromises the damage classification performance of the EM-GMM and MC-GMM approaches for several executions, as one can figure out in Fig. 7 (for visualization purposes) and Table V. Contrarily, the damage

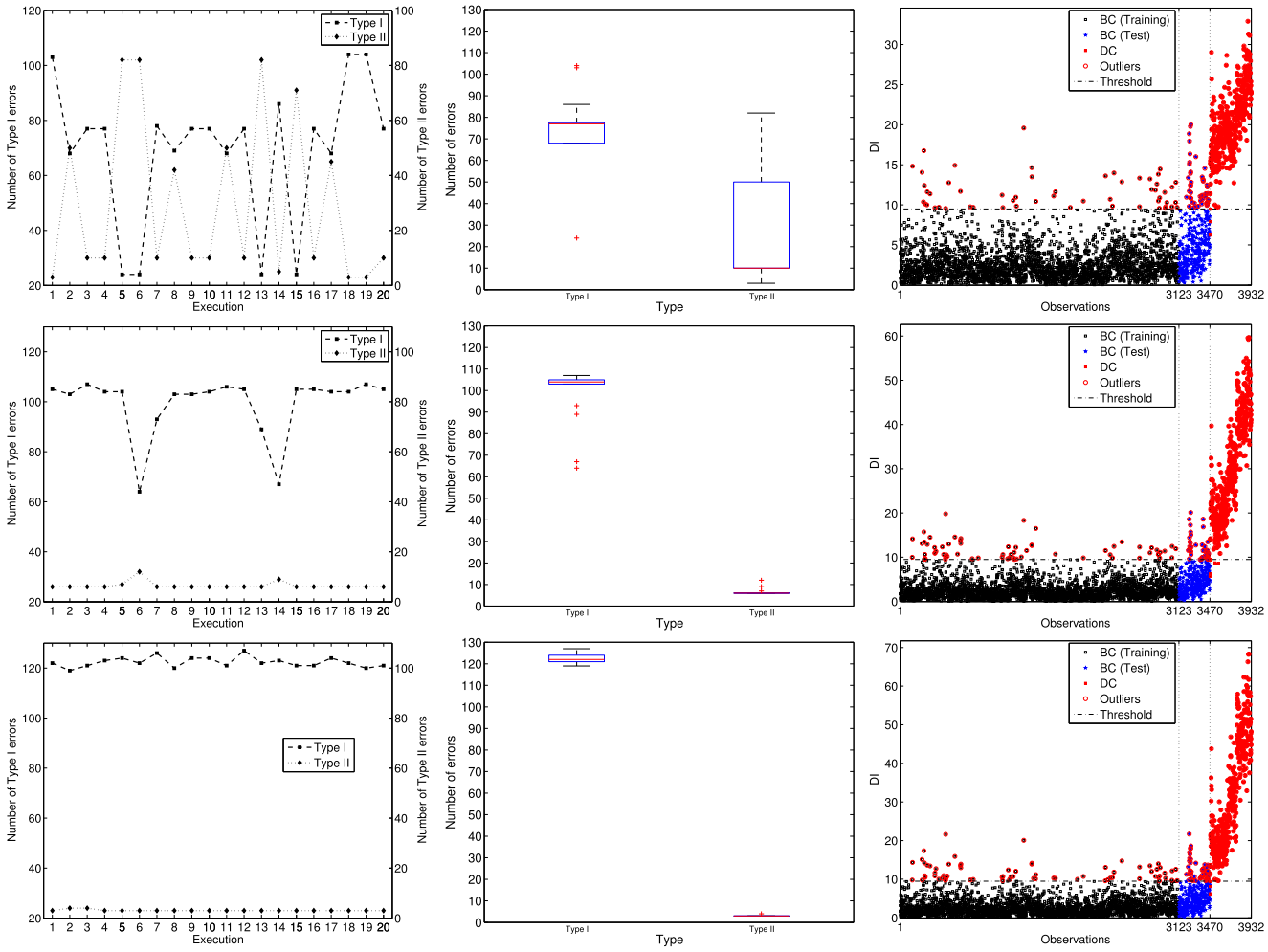

Fig. 7. Damage classification performance of the EM-GMM (top-left), MC-GMM (middle-left), and GEM-GA (bottom-left) as a function of the number of executions. Box plots for damage classification performance of the EM-GMM (top-center), MC-GMM (middle-center), and GEM-GA (bottom-center) over several executions. Outlier detection based on the EM-GMM (top-right), MC-GMM (middle-right), and GEM-GA (bottom-right) with MSD.

TABLE IV

PERFORMANCE OF THE CLUSTER-BASED APPROACHES IN TERMS OF LIKELIHOOD (LOG AND MARGINAL), BIC, AND NUMBER OF COMPONENTS. THE FORMAT OF THE RESULTS IS AVERAGE ± STANDARD DEVIATION

Approach	Likelihood	BIC	K
EM-GMM	14424.39 ± 39.34	-28054.19 ± 11.91	6.65 ± 0.6
MC-GMM	14085.48 ± 4.09	–	7.15 ± 0.4
GEM-GA	14456.84 ± 0.04	-28076.84 ± 0.08	7.00 ± 0.0

TABLE V

DAMAGE CLASSIFICATION PERFORMANCE FOR CLUSTER-BASED APPROACHES. THE FORMAT OF THE RESULTS IS AVERAGE ± STANDARD DEVIATION

Approach	Type I	Type II
EM-GMM	69.15 ± 25.68	29.90 ± 29.89
MC-GMM	99.35 ± 12.38	6.50 ± 1.47
GEM-GA	122.35 ± 2.03	3.10 ± 0.31

classification performance of the GEM-GA, which avoids any dependence of the initial parameters, demonstrates high reproducibility based on the low standard deviation of the Type I and II errors. The poor performance of the EM-GMM is attested with the relatively high standard deviation of the Type I and II errors, as highlighted in the box plots depicted in Fig. 7. Note that from Fig. 7 and for the EM-GMM in some executions, when the Type I errors are small, the Type II errors are high, and vice versa. The results from the MC-GMM are more stable compared with those from the EM-GMM, with some instability derived from the change in the number of data clusters during distinct executions. However, a better tradeoff between Type I and II errors is required for reliable SHM systems. The GEM-GA can yield this tradeoff as it maximizes the damaged cases properly identified without representative changes on the number of undamaged cases accurately detected through a reliable estimation of data clusters from damage-sensitive features of the Z-24 Bridge.

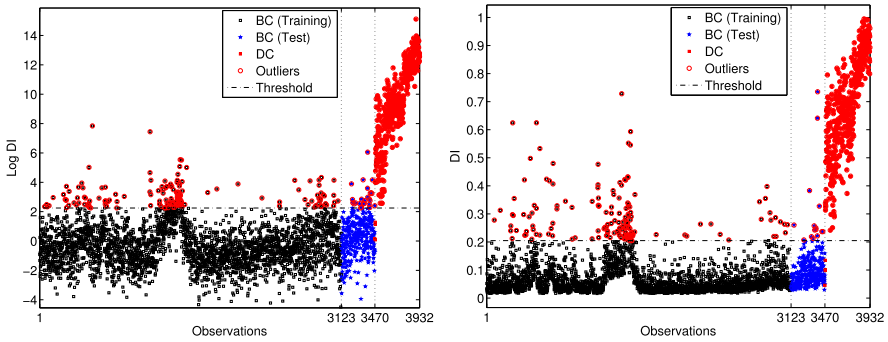

Fig. 8. Outlier detection based on two nonlinear approaches. Left: AANN. Right: kernel PCA.

To provide a damage detection strategy to unveil structural damage in the Z-24 Bridge, the best models over all executions are selected based on the BIC and marginal likelihood. In this case, the EM-GMM, MC-GMM, and GEM-GA approaches assume $K = 7$ for the number of normal components, as specified by the adopted criteria. The DIs derived from the EM-GMM, MC-GMM, and GEM-GA are shown in Fig. 7. In general, all particular models are able to remove the nonlinear patterns from the training observations as evidenced by the low concentration of outliers, in the baseline condition, during cold periods. In particular, unlike the EM-GMM, the MC-GMM and GEM-GA ably learned the baseline condition without nonlinear influences as the DIs, from the observations not used during the training phase (3124–3470), do not fire off vigorously. The best model from the MC-GMM is worse than those from the EM-GMM and GEM-GA in classifying damaged observations. Besides, all models attempt to preserve a monotonic relationship between the level of damage and the amplitude of the DIs, even with the presence of operational and environmental influences. This relationship reveals the aforesaid damage progressive testing period, which indicates cumulative damage on long-term monitoring.

B. Comparison With Nonlinear Approaches

Usually, nonlinear approaches, for which the nonlinear patterns on the damage-sensitive features are recognized in a natural manner, should provide a damage detection performance better than linear techniques as the former may eliminate the environmental influences by considering the long-term nonlinear temperature–stiffness relationship in the structures. Therefore, the AANN is configured with ten neurons in each mapping layer and four neurons (possible operational and environmental factors) in the bottleneck layer via Akaike information criterion [47]. In turn, the kernel PCA used Gaussian kernel with an estimated bandwidth of 0.384 and retained 99% of data variability by means of selected principal components (so-called factors) [23].

Thus, a comparison between the GEM-GA and state-of-the-art nonlinear approaches is carried out and their performances are highlighted in Fig. 8 (for visualization purposes) and Table VI. Similar to the GEM-GA approach, the AANN and kernel PCA have satisfactory performance in terms of minimization of Type II errors, which demonstrates that these techniques could be considered if life-safety issues were the primary motivation to deploy the SHM system in the Z-24 Bridge. However, in terms of Type I errors, the nonlinear approaches could not generalize the normal condition as the GEM-GA one, i.e., the GEM-GA could be also appropriated if one wants to minimize false positive indications of damage in the SHM system, by taking into account economic and reliability issues.

TABLE VI
DAMAGE CLASSIFICATION PERFORMANCE FOR NONLINEAR APPROACHES

Approach	Type I	Type II
AANN	183 (5.27%)	4 (0.87%)
kernel PCA	172 (4.96%)	4 (0.87%)

The limitations of the AANN and KPCA approaches to generalize and remove nearly all undesired influences are also observed in Fig. 8 via the distribution of the DIs produced by these techniques. A high concentration of outliers during the baseline condition and some unfiltered peaks are consequences of a data normalization procedure that only attenuates the operational and environmental variability rather than remove it. The similar working principles of these approaches may explain the weak normalization as the principal components (factors) are selected with some loss of information, whereas the GEM-GA groups observations influenced by the same effect (e.g., temperature, humidity, and wind) as well discriminated data clusters, which improves the data normalization and, consequently, the damage detection performance.

V. CONCLUSION

In this paper was presented the GEM-GA approach, for which an MA based on GA was used to improve the stability and reliability of the EM algorithm in searching for the optimal number of data clusters and their parameters. After the main state conditions of the structure are determined, assuming multivariate Gaussian distributions, the damage detection strategy implemented through the MSD can be applied.

In contrast to the other approaches, the GEM-GA consists of two main parts: a global one that conducts the global search in the feature space, and a local one, which performs more refined search around candidate solutions of the current damage detection problem. This strategy has led the GEM-GA to overcome the instability related to the alternative

GMM-based approaches, providing data models with stable and reliable number of data clusters (herein 7 components) and approximately the same likelihood ($14\,456.84 \pm 0.04$).

The classification performance for the real-world SHM scenario, Z-24 Bridge, attested that the GEM-GA approach is better than the alternative ones. When the GEM-GA is compared with the EM-GMM and MC-GMM, the improvements on the stability and reliability of the EM algorithm demonstrated to have a direct and positive impact on the identification of reliable data clusters (data normalization) and damage detection, reaching in its worst case approximately 3.6% of Type I errors and 0.6% of Type II errors, while the EM-GMM has 2.7% and 13% and the MC-GMM has 3.2% and 1.7%, respectively. Note that the Type I errors are undesirable, as they cause unnecessary downtime and consequent loss of revenue as well as loss of confidence in the monitoring system. More importantly, there are clear safety issues if misclassifications of Type II errors occur. The SHM applications are typically more interested in maximizing the true positive rate (minimizing Type II errors) for a given tolerable false alarm rate (Type I errors).

The AANN and kernel PCA are less affected than the EM-GMM and MC-GMM by the choice of the initial parameters; nevertheless, they are sensitive to some loss of information and generalization due to their working principles. This drawback influenced their competence to remove almost all operational and environmental variations, as evidenced by the DIs distribution, which consequently resulted in unacceptable classification performance regarding Type I errors (above 170 errors) compared with the GMM-based approaches.

As demonstrated through the experimental results, the hybridization performed by GEM-GA proved to be a pronounced technique that can be used in SHM applications where life-safety, economic, and reliability issues must be considered as primary motivations. In practice, this technique can be a module of a software system (for example, running in a server), which also receives vibration measurements acquired by sensors, extracts damage-sensitive features from these measurements, and stores the postprocessing data. When enough undamaged data have been received, processed, and stored, the GEM-GAs are offline trained with these data and the outlier detection method based on the learned clusters can classify new data promptly. In real-world monitoring solutions, when a structure is inspected in detail and accurately assessed as undamaged, all monitoring data up to that moment can be used for retraining the learned model. This updated model can cover a larger range of variability, which enhances the reliability of damage detection performed in the test phase.

REFERENCES

[1] C. R. Farrar and K. Worden, "An introduction to structural health monitoring," *Philos. Trans. Roy. Soc. London A, Math. Phys. Sci.*, vol. 365, no. 1851, pp. 303–315, 2007.

[2] E. P. Carden and P. Fanning, "Vibration based condition monitoring: A review," *Struct. Health Monitor.*, vol. 3, no. 4, pp. 355–377, Dec. 2004.

[3] H. Sohn, "Effects of environmental and operational variability on structural health monitoring," *Philos. Trans. Roy. Soc. A, Math., Phys. Eng. Sci.*, vol. 365, no. 1851, pp. 539–560, Feb. 2007.

[4] K. Worden and G. Manson, "The application of machine learning to structural health monitoring," *Philos. Trans. Roy. Soc. A, Math., Phys. Eng. Sci.*, vol. 365, no. 1851, pp. 515–537, Feb. 2007.

[5] E. Figueiredo, G. Park, C. R. Farrar, K. Worden, and J. Figueiras, "Machine learning algorithms for damage detection under operational and environmental variability," *Struct. Health Monitor.*, vol. 10, no. 6, pp. 559–572, Nov. 2011.

[6] A. Santos, E. Figueiredo, M. F. M. Silva, C. S. Sales, and J. C. W. A. Costaa, "Machine learning algorithms for damage detection: Kernel-based approaches," *J. Sound Vibrat.*, vol. 363, pp. 584–599, Feb. 2016.

[7] C. Zang, M. I. Friswell, and M. Imregun, "Structural damage detection using independent component analysis," *Struct. Health Monitor.*, vol. 3, no. 1, pp. 69–83, Mar. 2004.

[8] Y.-Y. Liu, Y.-F. Ju, C.-D. Duan, and X.-F. Zhao, "Structure damage diagnosis using neural network and feature fusion," *Eng. Appl. Artif. Intell.*, vol. 24, no. 1, pp. 87–92, Feb. 2011.

[9] H. Z. Hosseinabadi, B. Nazari, R. Amirfattahi, H. R. Mirdamadi, and A. R. Sadri, "Wavelet network approach for structural damage identification using guided ultrasonic waves," *IEEE Trans. Instrum. Meas.*, vol. 63, no. 7, pp. 1680–1692, Jul. 2014.

[10] M. Van and H.-J. Kang, "Wavelet kernel local fisher discriminant analysis with particle swarm optimization algorithm for bearing defect classification," *IEEE Trans. Instrum. Meas.*, vol. 64, no. 12, pp. 3588–3600, Dec. 2015.

[11] G. D'Angelo and S. Rampone, "Feature extraction and soft computing methods for aerospace structure defect classification," *Measurement*, vol. 85, pp. 192–209, May 2016.

[12] B. Peeters and G. D. Roeck, "One-year monitoring of the Z24-Bridge: Environmental effects versus damage events," *Earthquake Eng. Struct. Dyn.*, vol. 30, no. 2, pp. 149–171, Feb. 2001.

[13] H. Zhou, Y. Q. Ni, J. M. Ko, and K. Y. Wong, "Modeling of wind and temperature effects on modal frequencies and analysis of relative strength of effect," *Wind Struct.*, vol. 11, no. 1, pp. 35–50, Jan. 2008.

[14] J. Kullaa, "Eliminating environmental or operational influences in structural health monitoring using the missing data analysis," *J. Intell. Mater. Syst. Struct.*, vol. 20, no. 11, pp. 1381–1390, Jul. 2009.

[15] K. Worden, G. Manson, and N. R. J. Fieller, "Damage detection using outlier analysis," *J. Sound Vibrat.*, vol. 229, no. 3, pp. 647–667, Jan. 2000.

[16] A. Purarjomandlangrudi, A. H. Ghapanchi, and M. Esmalifalak, "A data mining approach for fault diagnosis: An application of anomaly detection algorithm," *Measurement*, vol. 55, pp. 343–352, Sep. 2014.

[17] A. Malhi and R. X. Gao, "PCA-based feature selection scheme for machine defect classification," *IEEE Trans. Instrum. Meas.*, vol. 53, no. 6, pp. 1517–1525, Dec. 2004.

[18] A.-M. Yan, G. Kerschen, P. D. Boe, and J.-C. Golinval, "Structural damage diagnosis under varying environmental conditions—Part I: A linear analysis," *Mech. Syst. Signal Process.*, vol. 19, no. 4, pp. 847–864, Jul. 2005.

[19] J. Xiang, Y. Zhong, and H. Gao, "Rolling element bearing fault detection using PPCA and spectral kurtosis," *Measurement*, vol. 75, pp. 180–191, Nov. 2015.

[20] T.-Y. Hsu and C.-H. Loh, "Damage detection accommodating nonlinear environmental effects by nonlinear principal component analysis," *Struct. Control Health Monitor.*, vol. 17, no. 3, pp. 338–354, Apr. 2010.

[21] A. Malhi, R. Yan, and R. X. Gao, "Prognosis of defect propagation based on recurrent neural networks," *IEEE Trans. Instrum. Meas.*, vol. 60, no. 3, pp. 703–711, Mar. 2011.

[22] R. Shao, W. Hu, Y. Wang, and X. Qi, "The fault feature extraction and classification of gear using principal component analysis and kernel principal component analysis based on the wavelet packet transform," *Measurement*, vol. 54, pp. 118–132, Aug. 2014.

[23] E. Reynders, G. Wursten, and G. D. Roeck, "Output-only structural health monitoring in changing environmental conditions by means of nonlinear system identification," *Struct. Health Monitor.*, vol. 13, no. 1, pp. 82–93, Jan. 2014.

[24] A. D. F. Santos, M. F. M. Silva, C. S. Sales, J. C. W. A. Costa, and E. Figueiredo, "Applicability of linear and nonlinear principal component analysis for damage detection," in *Proc. IEEE I2MTC*, Pisa, Italy, May 2015, pp. 869–875.

[25] E. Figueiredo and E. Cross, "Linear approaches to modeling nonlinearities in long-term monitoring of bridges," *J. Civil Struct. Health Monitor.*, vol. 3, no. 3, pp. 187–194, Aug. 2013.

[26] E. Figueiredo, L. Radu, K. Worden, and C. R. Farrar, "A Bayesian approach based on a Markov-chain Monte Carlo method for damage detection under unknown sources of variability," *Eng. Struct.*, vol. 80, pp. 1–10, Dec. 2014.
[27] J. Kullaa, "Structural health monitoring under nonlinear environmental or operational influences," *Shock Vibrat.*, vol. 2014, May 2014, Art. no. 863494.
[28] G. J. McLachlan and D. Peel, *Finite Mixture Models*. Hoboken, NJ, USA: Wiley, 2000.
[29] A. P. Dempster, N. M. Laird, and D. B. Rubin, "Maximum likelihood from incomplete data via the EM algorithm," *J. Roy. Statist. Soc., B (Methodological)*, vol. 39, no. 1, pp. 1–38, 1977.
[30] G. E. P. Box, G. M. Jenkins, and G. C. Reinsel, *Time Series Analysis: Forecasting and Control*, 4th ed. Hoboken, NJ, USA: Wiley, 2008.
[31] P. Moscato and C. Cotta, "A gentle introduction to memetic algorithms," *Handbook Metaheuristics*. Boston, MA, USA: Springer, 2003, pp. 105–144.
[32] F. Neri and C. Cotta, "Memetic algorithms and memetic computing optimization: A literature review," *Swarm Evol. Comput.*, vol. 2, pp. 1–14, Feb. 2012.
[33] D. E. Goldberg, *Genetic Algorithms in Search, Optimization and Machine Learning*, 1st ed. Boston, MA, USA: Addison-Wesley, 1989.
[34] F. Herrera, M. Lozano, and J. L. Verdegay, "Tackling real-coded genetic algorithms: Operators and tools for behavioural analysis," *Artif. Intell. Rev.*, vol. 12, no. 4, pp. 265–319, Aug. 1998.
[35] B. L. Miller and D. E. Goldberg, "Genetic algorithms, tournament selection, and the effects of noise," *Complex Syst.*, vol. 9, no. 3, pp. 193–212, 1995.
[36] T. Back and H.-P. Schwefel, "Evolutionary computation: An overview," in *Proc. IEEE Int. Conf. Evol. Comput.*, May 1996, pp. 20–29.
[37] F. Pernkopf and D. Bouchaffra, "Genetic-based EM algorithm for learning Gaussian mixture models," *IEEE Trans. Pattern Anal. Mach. Intell.*, vol. 27, no. 8, pp. 1344–1348, Aug. 2005.
[38] J. Tohka *et al.*, "Genetic algorithms for finite mixture model based voxel classification in neuroimaging," *IEEE Trans. Med. Imag.*, vol. 26, no. 5, pp. 696–711, May 2007.
[39] B. Peeters, J. Maeck, and G. De Roeck, "Vibration-based damage detection in civil engineering: Excitation sources and temperature effects," *Smart Mater. Struct.*, vol. 10, no. 3, pp. 518–527, 2001.
[40] G. De Roeck, "The state-of-the-art of damage detection by vibration monitoring: The SIMCES experience," *Struct. Control Health Monitor.*, vol. 10, no. 2, pp. 127–134, Apr. 2003.
[41] *Operation Instructions for FBA 11 Force Balance Accelerometer, Part Number 105610*, Kinemetrics/Systems Inc., Pasadena, CA, USA, 1991.
[42] *Operation Instructions for FBA 23 Force Balance Accelerometer, Part Number 105610*, Kinemetrics/Systems Inc., Pasadena, CA, USA, 1991.
[43] B. Peeters and G. De Roeck, "Reference-based stochastic subspace identification for output-only modal analysis," *Mech. Syst. Signal Process.*, vol. 13, no. 6, pp. 855–878, Nov. 1999.
[44] LANL/UCSD, *Structural Health Monitoring Tools (SHMTools)—Getting Started*, document LA-CC-10-032, LA-UR 10-01259, Los Alamos National Security, The Engineering Institute, Los Alamos National Laboratory (LANL), Los Alamos, NM, USA, 2010.
[45] S. Frühwirth-Schnatter, *Finite Mixture and Markov Switching Models—Implementation in MATLAB Using the Package Bayesf Version 2.0*. New York, NY, USA: Springer, 2008.
[46] *Statistics and Machine Learning Toolbox—User's Guide, R2014a*, The MathWorks Inc., Apple Hill, MA, USA, 2014.
[47] M. A. Kramer, "Nonlinear principal component analysis using autoassociative neural networks," *AIChE J.*, vol. 37, no. 2, pp. 233–243, Feb. 1991.

Adam Santos received the M.Sc. degree in electrical engineering (telecommunications) from the Federal Univesity of Pará, Belém, Brazil, in 2014, where he is currently pursuing the Ph.D. degree in electrical engineering (applied computing).

His current research interests include machine learning, artificial intelligence, and structural health monitoring.

Reginaldo Santos received the M.Sc. degree in computer science from the Federal University of Pará, Belém, Brazil, in 2016, where he is currently pursuing the Ph.D. degree in computer science.

His current research interests include intelligent systems, parallel evolutionary algorithms, and structural health monitoring.

Moisés Silva received the B.Sc. degree in computer science from the Federal University of Pará, Belém, Brazil, in 2015, where he is currently pursuing the M.Sc. degree in electrical engineering (applied computing).

His current research interests include machine learning, structural health monitoring, intelligent systems, evolutionary computing, and computer theory.

Eloi Figueiredo received the Ph.D. degree in civil engineering from the University of Porto, Porto, Portugal, in 2010.

In 2010, he started teaching at the Catholic University of Portugal, Lisbon, Portugal. He is currently a Professor with the Faculty of Engineering of the Universidade Lusófona, Lisbon, an Invited Professor with the Universidade Fernando Pessoa, Porto, and an Integrated Member of Construct-the Institute of Research and Development in Structures and Construction, Porto, Portugal. His current research interests include structural health monitoring, maintenance of bridges, vibration-based damage detection, machine learning, and physics-based models.

Claudomiro Sales received the Ph.D. degree in electrical engineering from the Federal University of Pará (UFPA), Belém, Brazil, in 2009.

Since 2010, he has been with UFPA, where he is currently with the Computer Science Graduate Program. He is involved in research on binder identification, phantom-mode transmission, and copper-based system in a research project developed jointly by Ericsson, Stockholm, Sweden, and UFPA. His current research interests include machine learning for system identification, with applications to copper-based broadband network and structural health monitoring.

João C. W. A. Costa (S'94–M'95) received the B.Sc. degree in electrical engineering from the Federal University of Pará (UFPA), Belém, Brazil, in 1981, the M.Sc. degree in electrical engineering from the Pontifical Catholic University of Rio de Janeiro, Rio de Janeiro, Brazil, in 1989, and the Ph.D. degree in electrical engineering from the State University of Campinas, Campinas, Brazil, in 1994.

He is currently a Professor with the Institute of Technology, UFPA, and a Researcher with the Brazilian Research Funding Agency National Council for Scientific and Technological Development, Brasília, Brazil. His current research interests include broadband systems and optical sensors.

Appendix D – Paper D: A global expectation-maximization based on memetic swarm optimization for structural damage detection

Original Article

SHM Structural Health Monitoring

Structural Health Monitoring
2016, Vol. 15(5) 610–625

DOI: 10.1177/1475921716654433
shm.sagepub.com
SAGE

A global expectation-maximization based on memetic swarm optimization for structural damage detection

Adam Santos[1], Moisés Silva[1], Reginaldo Santos[1], Eloi Figueiredo[2], Claudomiro Sales[1] and João C. W. A. Costa[1]

Abstract

During the service life of engineering structures, structural management systems attempt to manage all the information derived from regular inspections, evaluations and maintenance activities. However, the structural management systems still rely deeply on qualitative and visual inspections, which may impact the structural evaluation and, consequently, the maintenance decisions as well as the avoidance of collapses. Meanwhile, structural health monitoring arises as an effective discipline to aid the structural management, providing more reliable and quantitative information; herein, the machine learning algorithms have been implemented to expose structural anomalies from monitoring data. In particular, the Gaussian mixture models, supported by the expectation-maximization (EM) algorithm for parameter estimation, have been proposed to model the main clusters that correspond to the normal and stable state conditions of a structure when influenced by several sources of operational and environmental variations. Unfortunately, the optimal parameters determined by the EM algorithm are heavily dependent on the choice of the initial parameters. Therefore, this paper proposes a memetic algorithm based on particle swarm optimization (PSO) to improve the stability and reliability of the EM algorithm, a global EM (GEM-PSO), in searching for the optimal number of components (or data clusters) and their parameters, which enhances the damage classification performance. The superiority of the GEM-PSO approach over the state-of-the-art ones is attested on damage detection strategies implemented through the Mahalanobis and Euclidean distances, which permit one to track the outlier formation in relation to the main clusters, using real-world data sets from the Z-24 Bridge (Switzerland) and Tamar Bridge (United Kingdom).

Keywords

Structural health monitoring, data normalization, damage detection, memetic algorithm, particle swarm optimization, expectation-maximization

Introduction

Structural management systems (SMSs) plan to cover all activities performed during the service life of engineering structures, considering public safety, authorities' budgetary constraints and transport network functionality. They possess mechanisms to ensure the structures are regularly inspected, evaluated and maintained in a proper manner. Hence, an SMS, specified as a visual inspection-based decision-support tool, is developed to analyze engineering and economic factors and to attend the authorities in determining how and when to make decisions regarding maintenance, repair and rehabilitation of structures.[1]

However, the SMSs still depend deeply on structural inspections, especially on the qualitative and not necessarily consistent visual inspections, which may impact the structural evaluation and, consequently, the maintenance decisions as well as the avoidance of structural collapses.[2] In a cooperative sense, in the last few years, the structural health monitoring (SHM) discipline has emerged to aid the structural management

[1]Applied Electromagnetism Laboratory, Universidade Federal do Pará, Brazil
[2]Faculty of Engineering, Universidade Lusófona de Humanidades e Tecnologias, Portugal

Corresponding author:
Adam Santos, Applied Electromagnetism Laboratory, Universidade Federal do Pará, R. Augusto Corrêa, Guamá 01, Belém, 66075-110 Pará, Brazil.
Email: adamdreyton@ufpa.br

with more reliable and quantitative information. The SHM process involves the observation of a system over time using periodically sampled response measurements from an array of sensors, the extraction of damage-sensitive features from these measurements, and the statistical analysis of these features to discriminate the current state of system health.[3]

In this study, all approaches to SHM are posed in the context of a pattern recognition paradigm. Therefore, this paradigm for the development of SHM solutions is described as a four-phase process:[4] operational evaluation; data acquisition; feature extraction; and statistical modeling for feature classification. Particularly, in the feature extraction phase, damage-sensitive features (e.g. natural frequencies) are derived from the raw data, being correlated with the severity of damage present in the monitored structure. Nevertheless, in real-world SHM applications, operational and environmental effects may mask damage-related changes in the features as well as alter the correlation between the magnitude of the features and the damage level.[5] Thus, statistical modeling for the feature classification phase is concerned with the implementation of machine learning algorithms that analyze and learn the distributions of the extracted features and generate a data model in an attempt to determine the structural health of the system.[6]

The data normalization procedure is fully connected to the data acquisition, feature extraction and statistical modeling phases of the SHM process. This procedure includes a wide range of steps for mitigating (or even removing) the effects of operational (e.g. traffic loading) and environmental (e.g. temperature) variations on the extracted features as well as for separating changes in damage-sensitive features caused by damage from those caused by varying operational and environmental conditions.[7,8] This procedure usually contributes significantly to detecting structural damage.

To attenuate undesired effects and detect structural anomalies, a variety of output-only machine learning algorithms with different working principles has been explored.[9–13] A comparison study of several machine learning algorithms was performed on standard data sets upon experimental vibration monitoring tests using a three-story frame structure with different structural state configurations.[14] The operational and environmental effects were simulated by mass or stiffness changes, while damage was simulated with a bumper mechanism causing a nonlinear effect due to collisions. The prominence of the Mahalanobis squared distance (MSD) and auto-associative neural network algorithms is attested when life-safety is the primary motivation for deploying the SHM systems.

More recently, an improved output-only method based on kernel principal component analysis (KPCA) was proposed for eliminating nonlinear environmental and operational influences on the extracted features.[15] The method is based on Gaussian KPCA, where the parameters of the output-only global model are automatically determined. Although this improved version of KPCA achieved satisfactory results for data normalization and can be easily adapted for damage detection,[16] it also revealed some loss of information as the principal components are retained based on 99% of variance.

In a different manner, remarkable linear output-only methods for modeling nonlinearities in long-term monitoring of structures have been developed by means of a new concept based on a two-step strategy.[17–19]

1. Data normalization procedure by clustering the training observations into different components (or data clusters).
2. Damage detection by identifying possible outliers through a distance metric between the fitted clusters and a new observation.

In that regard, the first step may consist of Gaussian mixture models (GMMs) applied to fit the main clusters that correspond to the normal and stable state conditions of a structure, even when it is affected by different operational and environmental conditions. The parameters of the GMMs are estimated from the training data using the expectation-maximization (EM) algorithm. The second step runs a MSD-based algorithm to track the outlier formation in relation to the chosen main clusters.[17–19] This cluster-based EM-GMM approach has outperformed the traditional output-only damage detection methods (for instance, based on MSD, principal component analysis and neural network) when they are compared on data sets from the Z-24 Bridge.[17]

In general, GMMs have been widely applied in the SHM field to recognize different normal or undamaged patterns in the structural response under varying operational and environmental conditions. As long as the normal condition is characterized, deviations from this condition, which may reveal a damaged condition, can be identified through a distance metric or another clustering phase.

In aerospace engineering applications of SHM technology, a combination of guided wave, GMMs and Kullback–Leibler divergence as a damage propagation monitoring method is proposed to reduce the maintenance cost and meanwhile ensure the operational safety of aircraft structures under realistic load conditions.[20,21] However, this method requires a priori knowledge of damage and time-varying conditions.

In the long-term SHM of bridges, the EM-GMM as a data normalization approach, along with MSD as a

distance metric, has been applied to handle the effects of the operational and environmental variability on the structural responses for early damage detection.[17,18,22] Despite this approach taking into account the eventual multimodality and heterogeneity of the data sets (natural frequencies) from the Z-24 and Tamar Bridges,[23] when several different executions are demanded, the monitoring results may change drastically due to the unstable behavior of the EM algorithm.

As an alternative, the vibration signals may be fitted as time series-based autoregressive processes, where autoregressive coefficients are damage-sensitive features learned or modeled through the EM-GMM supported by the EM algorithm. The MSD between a new test GMM and the baseline (undamaged) GMM is an indicator of damage severity.[24,25] Unfortunately, in this case, the aforementioned limitations of the EM algorithm also arise on the baseline and new test data-based models.

GMMs are also applied, along with acoustic emission methods, to classify crack modes in reinforced concrete structures, which are subjected to deterioration due to aging, increased load and natural hazards.[26] However, to minimize the maintenance costs and to increase the operation lifetime of reinforced concrete structures, the GMMs must know in advance all types of crack modes, which may be not fully available in real scenarios.

Despite the fact that the EM-GMM approach can fit the normal condition of a structure, the optimal parameters determined by the EM algorithm are strongly dependent on the choice of the initial parameters.[27] Thereby, the cluster configuration provided by the EM-GMM may change during many executions with different initial parameters and, consequently, it may affect the damage detection process. This drawback is also discussed by Kullaa,[22] indicating that the EM algorithm does not guarantee the global optimal solution and the training phase of the GMMs may be very computationally expensive (because it is often advised to run the EM algorithm several times with different initial parameters to find a satisfactory local optimal solution, which is not fully guaranteed). As consequence, this degenerated behavior of the EM algorithm may affect the stability and reliability of the results or even the number of components estimated for each different run.

Therefore, this paper presents a memetic algorithm (MA) based on particle swarm optimization (PSO) to improve the stability and reliability of the EM algorithm, a global EM (GEM-PSO), in searching for the optimal number of components and their parameters, which ameliorates the damage classification performance. In this case, the parameters of the GMMs are estimated via a hybrid method composed of an EM algorithm within an MA. As long as the main stable state conditions of the structure are determined, the superiority of the GEM-PSO approach, over the state-of-the-art ones, is attested on damage detection strategies implemented through the Mahalanobis and Euclidean distances, using real-world data sets from the Z-24 Bridge (Switzerland) and Tamar Bridge (United Kingdom). The classification performance is assessed on the basis of Type I/II error trade-offs, where a Type I error is a false-positive indication of damage and a Type II error is a false-negative one.

The remainder of this study is structured as follows. In the section "Memetic-based global EM algorithm for damage detection", the GEM-PSO approach is derived as a novel methodology to unveil hidden clusters representing the normal condition of a structure and discriminate its health state based on the components. Two real-world structures and their long-term vibration data are described in the section "Test structures and data sets". Experimental results on real data sets that encompass a wide spectrum of challenges encountered in practical SHM problems are discussed in the "Results and discussion" section; a comparison with state-of-the-art approaches is also presented. In the "Conclusions" section, a discussion related to the principal strengths and challenges of the GEM-PSO approach is emphasized.

Memetic-based global EM algorithm for damage detection

This section deals with the methodology of the GEM-PSO approach, which explores the search space more thoroughly than the EM algorithm. First, the classical EM algorithm for fitting GMMs is discussed and an information criterion is presented to select the number of components. Second, the proposed GEM-PSO approach applies this criterion as a fitness function to improve the performance of the EM algorithm via an MA, which consequently provides a robust generalization of the normal condition of a structure. The section ends with a description of the damage detection strategies based on the Mahalanobis and Euclidean distances.

For general purposes, one should assume a training data matrix, $\mathbf{X} \in \mathbb{R}^{m \times n}$, with n-dimensional feature vectors from m different operational and environmental conditions when the structure is undamaged and a test data matrix, $\mathbf{Z} \in \mathbb{R}^{l \times n}$, where l is the number of feature vectors from the undamaged and/or damaged conditions.

Classical EM algorithm for fitting GMMs

A finite mixture model,[28] $p(\mathbf{x}|\Theta)$, is the weighted sum of $K>1$ components $p(\mathbf{x}|\theta_k)$ in $\mathbb{R}^n$

$$p(\mathbf{x}|\Theta) = \sum_{k=1}^{K} \alpha_k p(\mathbf{x}|\theta_k) \quad (1)$$

where $\mathbf{x}$ is an n-dimensional data vector and α_k corresponds to the weight of each component. These weights are positive $\alpha_k > 0$ with $\sum_{k=1}^{K} \alpha_k = 1$. For a GMM, each component $p(\mathbf{x}|\theta_k)$ is represented as a Gaussian distribution

$$p(\mathbf{x}|\theta_k) = \frac{\exp\left\{-\frac{1}{2}(\mathbf{x}-\mu_k)^{\mathrm{T}} \sum_k^{-1} (\mathbf{x}-\mu_k)\right\}}{(2\pi)^{n/2}\sqrt{\det\left(\sum_k\right)}} \quad (2)$$

with each component denoted by the parameters, $\theta_k = \{\mu_k, \sum_k\}$, composed of the mean vector, μ_k and the covariance matrix, $\sum_k$. Thus, a GMM is completely specified by the set of parameters $\Theta = \{\alpha_1, \alpha_2, \ldots, \alpha_K, \theta_1, \theta_2, \ldots, \theta_K\}$.

The EM algorithm is the most widespread local search method used to estimate the parameters of the GMMs.[28,29] This method consists of an expectation and a maximization step, which are alternately applied until the log-likelihood (LogL), $\log p(\mathbf{X}|\Theta) = \log \prod_{i=1}^{m} p(\mathbf{x}_i|\Theta)$, converges to a local optimum.[29] The performance of the EM algorithm depends directly on the choice of the initial parameters $\Theta^{t=0}$, which may imply many replications of this method during an execution.[27] To select the best GMM by means of goodness-of-fit and parsimony, the Bayesian information criterion (BIC) is used and minimized[30]

$$\begin{aligned} \mathrm{BIC} = & -2\log p(\mathbf{X}|\Theta) \\ & + \left\{ Kn\left[\left(\frac{n+1}{2}\right)+1\right] + K - 1 \right\} \log(m) \end{aligned} \quad (3)$$

Similar to the Akaike information criterion (AIC), BIC uses the optimal LogL function value and penalizes for more complex models, i.e. models with additional parameters. The penalty term of BIC is a function of the training data size, and so it is often more severe than AIC.

Global EM for fitting GMMs

MAs are population-based metaheuristics composed of an evolutionary framework and a set of local search algorithms.[31,32] A general framework of MAs reads as follows.

1. *Initialize* a population of candidate solutions P_1.
2. While a *termination criterion* is not satisfied, repeat.
   (i) *Cooperate* between candidate solutions from P_1 to generate a new population P_2.
   (ii) *Improve* the candidate solutions from P_2 to generate a new population P_3.
   (iii) *Compete* within the set of populations $P_1 \cup P_3$ to generate a new population P_1 for the next iteration.
3. Return the *best solution* encountered.

The *Initialize* procedure produces the initial set of random candidate solutions as high-quality solutions generated by applying a local search algorithm and the *termination criterion* usually verifies the total number of iterations and/or a maximum number of iterations without improvement. The *Cooperate* procedure arises from the selection that determines the solutions that will be used to create new solutions, and the combination that creates new promising solutions by merging existing solutions. The *Improve* procedure applies a local search method on new solutions derived in the *Cooperate* procedure, improving the quality of these solutions as far as possible. The *Compete* procedure updates the current population using the old population P_1 and the new population P_3, determining the solutions that will survive in the following iterations.[32]

Therefore, MAs comprise concepts from population-based search and local search methods.[31] In this study, the MA is a hybrid algorithm that combines PSO (global) with EM algorithm (local). In turn, PSO is a stochastic optimization metaheuristic based on swarm learning that iteratively exploits the search space through a population (swarm) of candidate solutions (particles).[33]

Each particle moves with its own velocity within the search space and stores the best position it has encountered so far. Usually, the information exchange among the particles is local, i.e. each particle is assigned to a neighborhood consisting of Υ particles.[34] In this case, Υ neighboring particles are determined based on their actual distance in the search space and the particle that attained the best previous position among all the particles in the neighborhood is selected based on its fitness.

When a d-dimensional search space $\mathcal{D}$ and a swarm composed of η particles are assumed, the i-th particle is a d-dimensional vector

$$q_i = [q_{i,1}, q_{i,2}, \ldots, q_{i,d}] \in \mathcal{D} \quad (4)$$

the velocity of this particle is denoted by

$$v_i = [v_{i,1}, v_{i,2}, \ldots, v_{i,d}] \quad (5)$$

and the best previous position encountered by this particle in $\mathcal{D}$ reads

$$p_i = [p_{i,1}, p_{i,2}, \ldots, p_{i,d}] \in \mathcal{D} \quad (6)$$

If g_i is admitted as the index of the particle that achieved the best previous position among all the particles in the neighborhood of q_i, then the swarm is manipulated by the following equations[34]

$$v_i^{t+1} = \xi\left[v_i^t + c_1 r_1\left(p_i^t - q_i^t\right) + c_2 r_2\left(p_{g_i}^t - q_i^t\right)\right] \quad (7)$$

$$q_i^{t+1} = q_i^t + v_i^{t+1} \quad (8)$$

where ξ is a constriction parameter; c_1 and c_2 are the cognitive and social parameters, respectively; and r_1 and r_2 are random vectors uniformly distributed within $[0, 1]$.

The constriction coefficient controls the convergence of the particle and is derived as

$$\xi = \frac{2}{\Psi - 2 + \sqrt{\Psi^2 - 4\Psi}} \quad (9)$$

where $\Psi = c_1 + c_2 > 4$ and commonly $\Psi = 4.1$,[35] which implies in $\xi = 0.729$.

In the following, the framework of the proposed GEM-PSO approach is presented, and its parameters and operators are discussed in more detail.

1. *Initialize* q_i^t, v_i^t, $i = \{1, \ldots, \eta\}$, $t = 0$.
2. $(q^t, pFit) \leftarrow$ perform R EM steps on q^t.
3. *Initialize* the best previous position encountered as $p_i^t \leftarrow q_i^t$, $i = \{1, \ldots, \eta\}$, $b = 0$.
4. While $(t < \tau)$ and $(b < \beta)$ is satisfied, repeat.
   (i) *Cooperate* between particles from q_i^t and p_i^t to update v_i^{t+1} and q_i^{t+1}, according to equations (7) and (8), restricting each particle $q_i^{t+1} \in [q_{\min}, q_{\max}]$, $i = \{1, \ldots, \eta\}$.
   (ii) *Improve* q^{t+1} such as $(q^{t+1}, qFit) \leftarrow$ perform R EM steps on q^{t+1}.
   (iii) *Compete* between the swarms q^{t+1} and p^t such as if $qFit_i < pFit_i$ then $p_i^{t+1} \leftarrow q_i^{t+1}$ and $pFit_i \leftarrow qFit_i$, otherwise $p_i^{t+1} \leftarrow p_i^t$, $i = \{1, \ldots, \eta\}$. Store $\mathrm{BIC}_{\min} \leftarrow \min(pFit)$ and $\mathrm{bestGMM} \leftarrow \arg\min_{p^{t+1}}(pFit)$. Increase $t = t + 1$, and $b = b + 1$ if and only if there is no improvement in $\mathrm{BIC}_{\min}$.
5. *Improve* bestGMM if and only if it not converged, such as $(\mathrm{bestGMM}, \mathrm{BIC}_{\min}) \leftarrow$ perform EM steps on bestGMM until convergence of the LogL is reached.
6. Return the *best solution*, bestGMM encountered.

In the GEM-PSO approach, each particle in the swarm represents a candidate solution of the GMM, i.e. a set of parameters Θ that models a GMM with K in the range $[2, K_{\max}]$, where $K_{\max}$ is the maximum number of allowed components. Thus, a particle is composed of two different parts. The first part indicates whether a component is activated ($[0.5, 1]$) or not ($[0, 0.5[$) for fitting the GMM, and the length of this part is $K_{\max}$. The mean vector μ_k and covariance matrix $\sum_k$ parameters of $K_{\max}$ components are represented in the second part. Each component includes $(n^2 + 3n)/2$ parameters. Note that the covariance matrix Σ_k must be symmetric, thus only the upper (or lower) triangular part of the matrix is in the particle.

The BIC metric (see equation (3)) is applied as a fitness function to select the best GMM, thereby the best solution is the one that has the lowest BIC value. The evaluation of the particles in the swarm is conducted in two-steps. First, R iterations of the EM method are performed on each particle, which results in an update of the set of parameters at iteration t, Θ^t, and consequently of the particle that represents these parameters. Second, the BIC value is computed for each updated particle to evaluate the model. Therefore, the evaluation process of the i-th particle provides an update of the parameters included within the particle (e.g. q_i^t and q_i^{t+1}) and a fitness value (e.g. $pFit_i$ and $qFit_i$).

The evolutionary process of the GEM-PSO is stopped when the maximum number of iterations τ or the maximum number of iterations without improvement β is achieved. As long as the MA is terminated, the convergence of the best solution bestGMM found so far is checked. If it converged in terms of LogL, the final solution is the current best solution, otherwise the EM algorithm improves bestGMM until convergence is reached.

Choice of parameters

As aforementioned, a set of parameters should be chosen for the GEM-PSO approach, such as η, τ, β, R, Y, c_1 and c_2. Hence, few recommendations are provided to determine these parameters.

The parameters η and β can be chosen based on a previous multivariate normality statistical test (MNST) using the training observations. If the test highlights few deviations from a global normal and stable condition, these parameters can be $\eta = [15, 30]$ and $\beta = [15, 30]$ to deal with a simple scenario, otherwise $\eta = [40, 60]$ and $\beta = [40, 60]$ to handle a heterogeneous scenario. Note that the parameter η is often set empirically on the basis of the dimensionality and perceived complexity of a problem. Nevertheless, values in the range $\eta = [20, 50]$ are quite usual.[34]

In the case of the parameters τ and R, the ranges $\tau = [100, 200]$ and $R = [20, 40]$ seem to be an acceptable alternative as fewer iterations of the local method are required due to the global exploration performed by the PSO that converges fast when it is hybridized with a local search.[36]

Finally, the parameters c_1 and c_2 are determined by assuming that $\Psi = 4.1$, $\xi = 0.729$ and $c_1 = c_2 = 2.05$, i.e. the magnitudes of the random forces toward the cognitive best p_i and social best p_{g_i} are identical.[35] In addition, the parameter Υ should be selected by taking into account that a small neighborhood may impact the search for a better solution and a large neighborhood may negatively influence the computational performance of the GEM-PSO approach. Thus, the range $\Upsilon = [5, 10]$ can be defined as an admissible trade-off between the aforesaid situations.[34]

Damage detection strategies

Since the best GMM is selected, for the damage detection strategy, in this study, two possibilities are considered to discriminate the structural health by generating a damage indicator (DI) and classifying it through a threshold.

First, for each observation $\mathbf{z}$, one needs to estimate K DIs via MSD. Particularly, for each main component k

$$\mathrm{DI}_k(\mathbf{z}) = (\mathbf{z} - \boldsymbol{\mu}_k) \sum\nolimits_k^{-1} (\mathbf{z} - \boldsymbol{\mu}_k)^{\mathrm{T}} \tag{10}$$

where μ_k and $\sum_k$ represent all the observations from the component k, when the structure is undamaged even though under varying operational and environmental conditions. For each component k, if a new observation $\mathbf{z}$ is extracted from the same component as the undamaged data, then the test statistic MSD will be Chi-square distributed with n degrees of freedom, χ_n^2. Finally, for each observation, the DI is given by the smallest DI estimated on each component

$$\mathrm{DI}(\mathbf{z}) = \min[\mathrm{DI}_1(\mathbf{z}), \ldots, \mathrm{DI}_K(\mathbf{z})] \tag{11}$$

Second, for each observation $\mathbf{z}$, the Euclidean distance (ED) for each μ_k is computed and the DI is the smallest one

$$\mathrm{DI}(\mathbf{z}) = \min(\|\mathbf{z} - \boldsymbol{\mu}_1\|, \ldots, \|\mathbf{z} - \boldsymbol{\mu}_K\|) \tag{12}$$

where $\boldsymbol{\mu}_1, \ldots, \boldsymbol{\mu}_K$ can be also considered as centroids of K different components. In this case, the threshold is defined based on values that correspond to a certain percentage of confidence over the training data. Hence, multivariate outliers can be defined as DIs above a specific threshold.

Test structures and data sets

In this study, the applicability and comparison between the proposed and state-of-the-art approaches are evaluated using the damage-sensitive features extracted from the Z-24 and Tamar Bridges. In the case of the Z-24 Bridge, the standard data sets are unique in the sense that they combine one-year monitoring of the healthy condition, under operational and environmental variability, with realistic damage scenarios. In a different manner, a monitoring system was carried out on the Tamar Bridge over almost two years, generating only data sets related to undamaged scenarios. These test structures and their data sets are highlighted in this section.

Z-24 Bridge

The Z-24 Bridge was a post-tensioned concrete box girder bridge composed of a main span of 30 m and two side-spans of 14 m, as shown in Figure 1. The bridge, before complete demolition, was extensively instrumented and tested for the purpose of providing a feasibility tool for vibration-based SHM in civil engineering.[37] A long-term monitoring test was carried out, from 11 November 1997 until 10 September 1998, to quantify the operational and environmental variability present on the bridge and to detect damage artificially introduced, in a controlled manner, in the last month of operation. Every hour, for 11 minutes, eight accelerometers captured the vibrations of the bridge and an array of sensors measured environmental parameters, such as temperature, at several locations.

Progressive damage tests were performed over a one month time period (from 4 August to 10 September 1998) before the demolition of the bridge to prove that realistic damage has a measurable influence on the bridge dynamics,[37] as summarized in Table 1. Note that the continuous monitoring system was still running during the progressive damage tests, which permits one to validate the SHM system to detect cumulative damage on long-term monitoring.

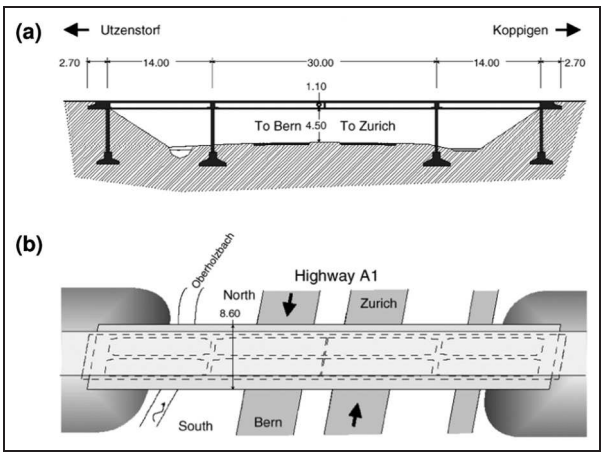

Figure 1. Longitudinal section (a) and top view (b) of the Z-24 Bridge.[37]

Table 1. Progressive damage test scenarios (the dates refer to the additional vibration measurements).

Date	Scenario description
4 Aug 1998	Undamaged condition
9 Aug 1998	Installation of the settlement system
10 Aug 1998	Pier settlement, 2 cm
12 Aug 1998	Pier settlement, 4 cm
17 Aug 1998	Pier settlement, 8 cm
18 Aug 1998	Pier settlement, 9.5 cm
19 Aug 1998	Foundation tilt
20 Aug 1998	New reference condition
25 Aug 1998	Spalling of concrete, 12 m^2
26 Aug 1998	Spalling of concrete, 24 m^2
27 Aug 1998	Landslide at abutment
31 Aug 1998	Concrete hinge failure
2 Sept 1998	Anchor head failure I
3 Sept 1998	Anchor head failure II
7 Sept 1998	Tendon rupture I
8 Sept 1998	Tendon rupture II
9 Sept 1998	Tendon rupture III

In this case, the natural frequencies of the Z-24 Bridge are used as damage-sensitive features. They were estimated using a reference-based stochastic subspace identification method on the time series from the accelerometers.[38] The first four natural frequencies estimated hourly from 11 November 1997 to 10 September 1998, with a total of 3932 observations, are highlighted in Figure 2. The first 3470 observations correspond to the damage-sensitive feature vectors extracted within the undamaged structural condition under operational and environmental influences. The last 462 observations correspond to the damage progressive testing period, which is highlighted, especially in the second frequency, by a clear drop in the magnitude of the frequency.

Note that the damage scenarios are carried out in a sequential manner, which cause a cumulative degradation of the bridge. Therefore, in this study, it is assumed that the bridge operates within its undamaged condition (baseline or normal condition), under operational and environmental variability, from 11 November 1997 to 4 August 1998 (1-3470 observations). On the other hand, the bridge is considered damaged from 5 August to 10 September 1998 (3471-3932 observations). For the baseline condition period, the observed jumps in the natural frequencies are associated to the asphalt layer in cold periods, which contributes significantly to the stiffness of the bridge. This large influence of the temperature on the natural frequencies, as well as on the structure dynamics, may be considered as nonlinear with different behaviors below and above 0 °C.[39]

For generalization purposes, the feature vectors were split into the training and test matrices. As shown in Figure 2, the training matrix, $\mathbf{X}^{3123\times4}$, is composed

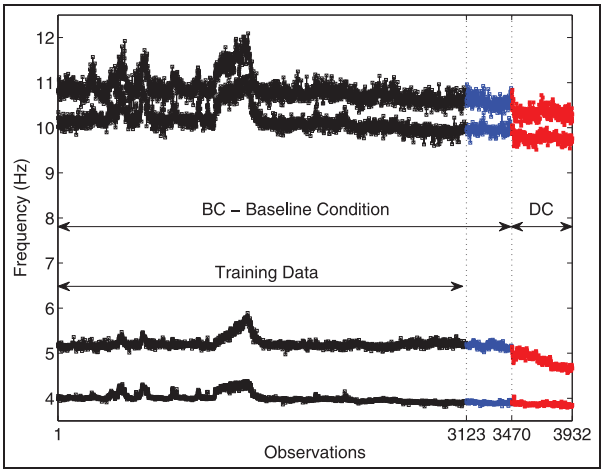

Figure 2. First four natural frequencies of the Z-24 Bridge: 1-3470 baseline/undamaged condition (BC), 3471-3932 damaged condition (DC).

of 90% of the feature vectors from the undamaged condition. The remaining 10% of the feature vectors are used during the test phase to make sure that the DIs do not fire off before the damage starts. The test matrix, $\mathbf{Z}^{3932\times4}$, is composed of all the data sets, even the ones used during the training phase.

Tamar Bridge

The Tamar Bridge (depicted in Figure 3) is situated in the south west of the United Kingdom and connects Saltash (Cornwall) with the city of Plymouth (Devon). This bridge is a major road across the River Tamar and plays a significant role in the local economy. Initially, in 1961, the bridge had a main span of 335 m and side spans of 114 m. If the anchorage and approach are included, the overall length of the structure is 643 m. The bridge stands on two concrete towers with a height of 73 m and a deck suspended at mid-height.[40]

From 1961 the bridge structure was a steel truss supported vertically by a pair of suspension cables. To meet a European Union directive, in which bridges should be capable of carrying lorries of up to 40 tonnes, the bridge underwent a strengthening and widening upgrade scheme, which was completed in 2001.[41] The upgrade consisted of adding cantilevered lanes either side of the truss to provide a total of four lanes for traffic and a footpath for pedestrians. The heavy composite deck was replaced by an orthotropic steel deck and eight pairs of stay cables connected to the towers were added to support the increased weight of the deck.

To track the effects of the upgrade, various sensor systems were installed to extract monitoring data such as tensions on stays, acceleration, wind velocity, temperature, deflection and tilt. Eight accelerometers were

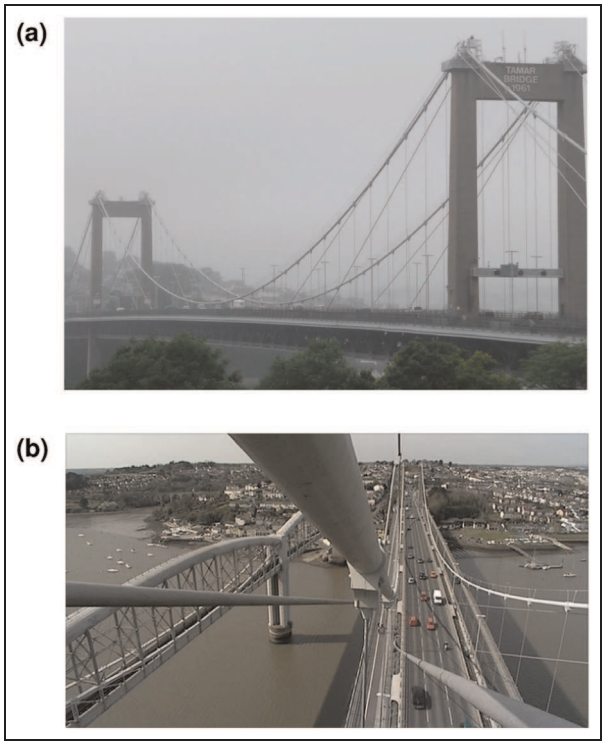

Figure 3. The Tamar Suspension Bridge viewed from River Tamar margins (a) and cantilever perspective (b).

implemented in orthogonal pairs for four stay cables and three sensors measured deck accelerations. The time series was stored with a sampling frequency of 64 Hz at 10 minute intervals.[40] The data collected in the period from 1 July 2007 to 24 February 2009 (602 observations) were then passed directly to a computer-based system and via a reference-based stochastic subspace identification technique,[38] the natural frequencies were estimated. The first five natural frequencies obtained daily during the feature extraction phase are illustrated in Figure 4.

Herein, there are no damaged observations known in advance,[41] and so it is assumed that all observations are extracted from the undamaged condition. Therefore, only Type I errors can be identified. From a total of 602 observations, the first 363 are used for statistical modeling in the training process (corresponding to one-year monitoring from 1 July 2007 to 30 June 2008) and the entire data sets are used in the test process, yielding a training matrix $\mathbf{X}^{363\times5}$ (1-363 observations) and a test matrix $\mathbf{Z}^{602\times5}$ (1-602 observations).

Results and discussion

In this section, the analysis is divided in two parts. Firstly, the EM-GMM and GEM-PSO approaches are executed 20 times with different initial parameters to test their stability, reliability and robustness. Secondly,

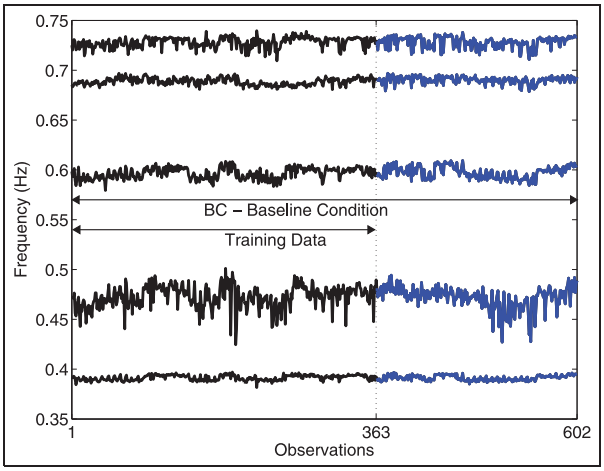

Figure 4. First five natural frequencies of the Tamar Bridge: 1-602 baseline/undamaged condition (BC).

the best model of each approach is chosen, based on the BIC, as a means of laying out a damage detection strategy for the bridges. The strategy based on MSD is used for comparison between EM-GMM and GEM-PSO; additionally, the one based on ED is employed for comparison between KPCA and GEM-PSO. Note that the ED is applied in the second comparison because the KPCA only generates the DIs in an implicit manner via this distance.[15]

To alleviate the particular limitations posed by the EM algorithm, for each execution of the EM-GMM approach, 10 repetitions of the EM algorithm are performed (each one with $R = 1000$) and each GMM with $2, \ldots, K_{max}$ components is fitted with the one that has the largest LogL. Afterwards, for each execution, the best model is built with K normal components, as suggested by the minimization of the BIC. This approach is implemented following all recommendations provided by Figueiredo and Cross.[17]

For the GEM-PSO approach, the initial swarm $q^{t=0}$ is composed of η particles, where each one has a different number of activated components. Thus, $q^{t=0}$ consists of particles with $2, \ldots, K_{max}$ components. The general parameter setting is $K_{max} = 15$, $\tau = 100$, $R = 20$, $\Upsilon = 5$ and $c_1 = c_2 = 2.05$. This setting provides a satisfactory trade-off between performance and execution time of the GEM-PSO on the data sets from the two bridges.

Furthermore, the adaptation of the Gaussian KPCA for damage detection is strictly based on the data normalization technique proposed by Reynders et al.[15]

Damage detection on data sets from the Z-24 Bridge

In this scenario, the data sets present nonlinearities derived from changes in the structural stiffness, influenced by temperature variations, which can be

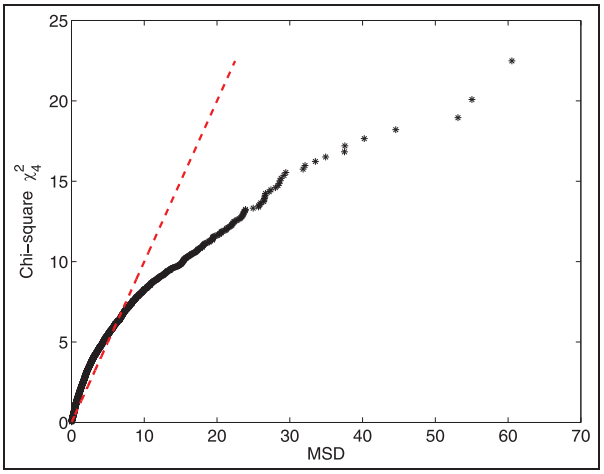

Figure 5. MNST based on the Chi-square Q-Q plot of the MSD using the training observations from the Z-24 Bridge.

Table 2. Z-24 Bridge: damage classification performance (average ± standard deviation) of the GEM-PSO and EM-GMM approaches with MSD for 20 executions.

Approach	Number of errors	
	Type I	Type II
GEM-PSO	123.65 ± 5.05	3.05 ± 0.22
EM-GMM	69.15 ± 25.68	29.90 ± 29.89

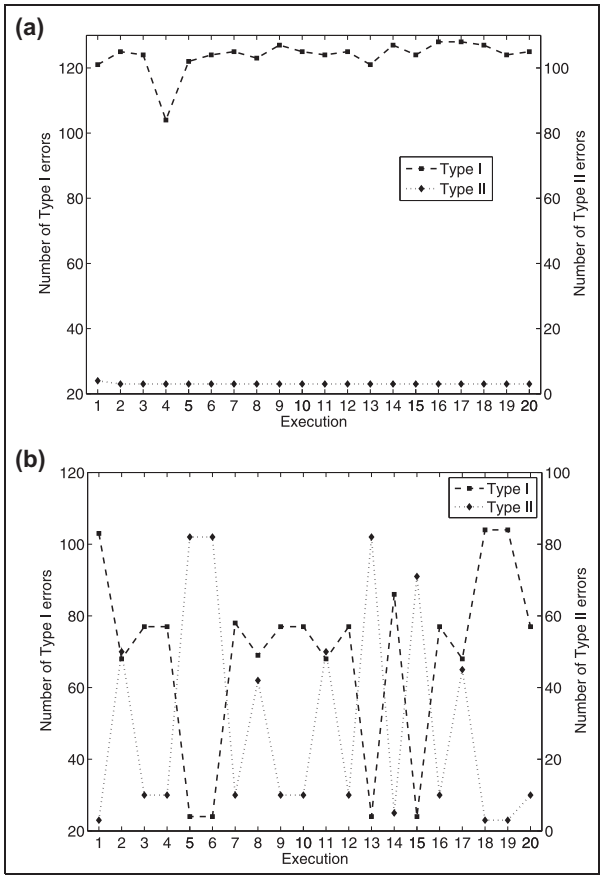

Figure 6. Z-24 Bridge: damage classification performance of the GEM-PSO (a) and EM-GMM (b) approaches with MSD as a function of the number of executions.

evidenced through the MNST in Figure 5. Therefore, classical linear approaches based on Gaussian assumptions are susceptible to relatively poor damage classification performance. On the other hand, approaches to hand multimodality and heterogeneity in the data as components often improve the damage detection. A particular parameter setting for the GEM-PSO approach to deal with this scenario is $\eta = \beta = 40$.

The damage classification performance of the GEM-PSO and EM-GMM approaches for a level of significance of 5% is summarized in Table 2; for visualization purposes, the performance of these approaches over all executions is shown in Figure 6. Although there were several repetitions of the EM algorithm, in each execution, the EM-GMM is very unstable when compared to the performance of the GEM-PSO. Clearly, the unpredictability of the EM-GMM derives from its dependency on the choice of the initial parameters. On the other hand, the damage classification performance of the GEM-PSO, which avoids dependency of the initial parameters, demonstrates high stability and reliability, in terms of reproducibility, based on the low standard deviation of the Type I and II errors. The degenerate behavior of the EM-GMM is confirmed with the high standard deviation of the Type I and II errors, which is highlighted in the box plots depicted in Figure 7. In addition, one should note that in some executions of the EM-GMM when the number of Type I errors decreases, the number of Type II errors increases drastically, and vice versa. However, a more reliable trade-off between these errors is desired for safety SHM applications, such as the one yielded by the GEM-PSO.

Besides, the instability depicted in Figure 6(b) for the EM-GMM approach is also related to the interchangeable number of components ($K = 6.65 \pm 0.59$) present in each execution. Contrarily, the GEM-PSO maintains the same number of components ($K = 7$) in all executions, which increases the robustness of the MA to overcome the sensitivity issue caused by the initial parameters. Recall that the number of components is selected via BIC, which depends on the LogL. The LogL and BIC for both approaches are summarized in Table 3.

To provide specific results with respect to a damage detection strategy to unveil structural damage in a real scenario, the best models over all executions

Table 3. Z-24 Bridge: the performance of the GEM-PSO and EM-GMM approaches in terms of log-likelihood and BIC (average ± standard deviation) for 20 executions.

Approach	Metric	
	LogL	BIC
GEM-PSO	1,4456.68 ± 0.43	−2,8076.52 ± 0.85
EM-GMM	1,4424.39 ± 39.34	−2,8054.19 ± 11.91

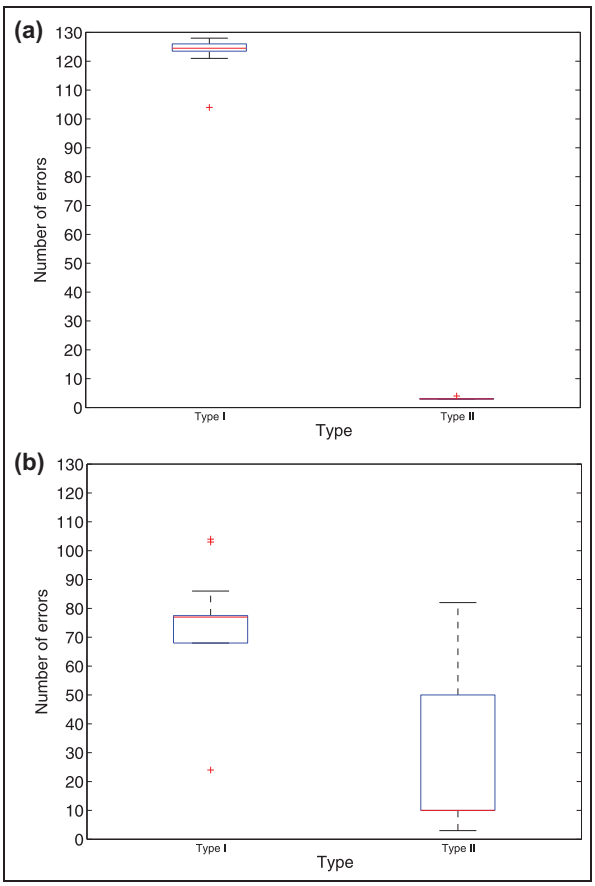

Figure 7. Z-24 Bridge: box plots for damage classification performance of the GEM-PSO (a) and EM-GMM (b) approaches with MSD. The horizontal red mark is the median, the edges of the box are the 25th and 75th percentiles, the whiskers extend to the most extreme data points not considered outliers, and outliers are plotted individually.

are selected based on the BIC. In this case, the GEM-PSO and EM-GMM approaches assume $K = 7$ for main normal components, as suggested by the minimization of the fitness function and the minimization of the BIC, respectively. The DIs derived from the GEM-PSO and EM-GMM approaches are shown in Figure 8, along with a threshold defined for a level of significance of 5%. From a general perspective, both models

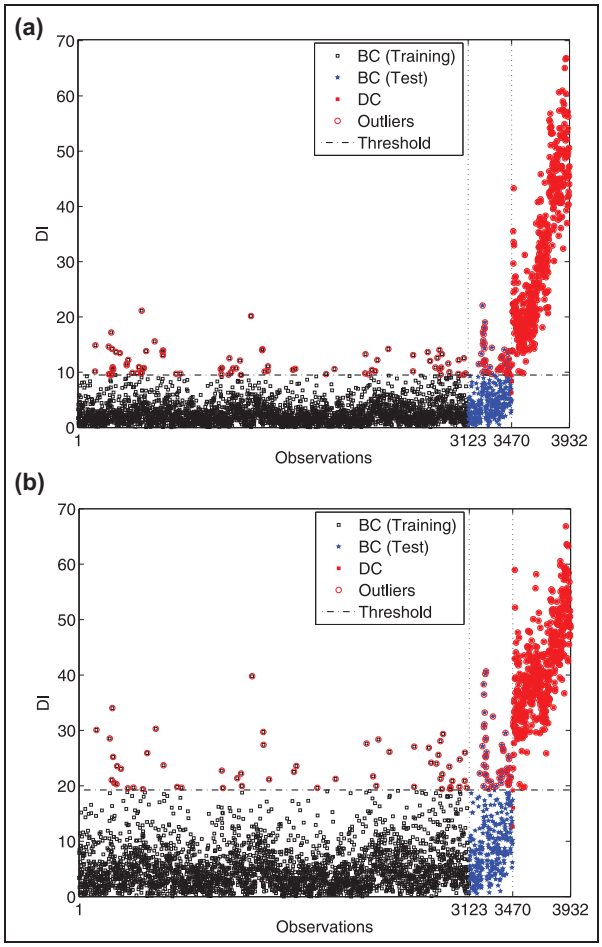

Figure 8. Z-24 Bridge: outlier detection based on the GEM-PSO (a) and EM-GMM (b) approaches with MSD.

are able to remove the nonlinear patterns from the undamaged observations caused by a period of extremely cold temperatures (changes in the structural stiffness) as evidenced by the low concentration of outliers in the baseline condition during this period.

In particular, from Figure 8(a), unlike the EM-GMM approach, GEM-PSO satisfactorily fitted the baseline condition without extreme cold temperatures as the DIs, from the observations not used during the training process (3124-3470), do not fire off vigorously before the damage starts. Moreover, both models attempt to maintain a monotonic relationship between the level of damage and the amplitude of the DIs, even when operational and environmental variability is present. This monotonic relationship reveals the damage progressive testing period, which indicates cumulative damage on long-term monitoring. However, the GEM-PSO seems to emphasize the monotonic relationship with more accuracy.

By using the ED as a metric technique in the damage detection strategy, the damage classification performance that the GEM-PSO and KPCA

Table 4. Z-24 Bridge: damage classification performance (average ± standard deviation) of the GEM-PSO and KPCA approaches with ED for 20 executions.

Approach	Number of errors	
	Type I	Type II
GEM-PSO	166.05 ± 0.22	6.00 ± 0.00
KPCA	172	4

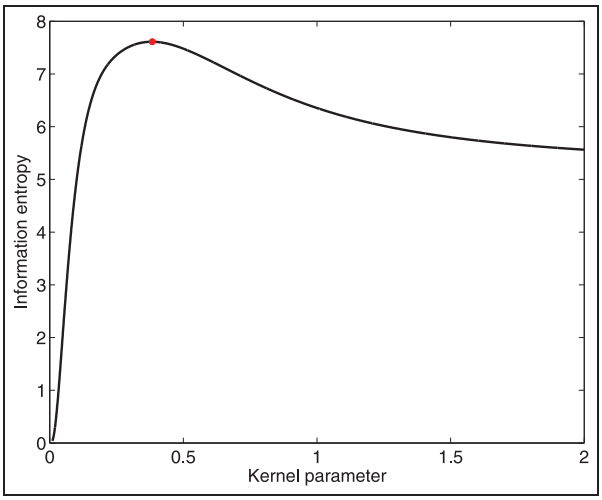

Figure 9. Z-24 Bridge: maximization of the information entropy as a function of the kernel parameter (the optimal is 0.384).

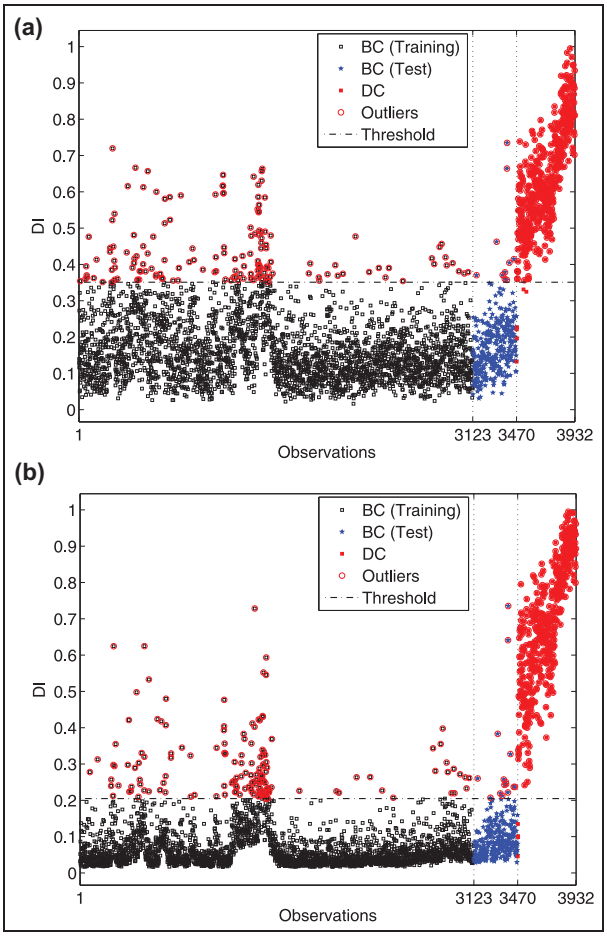

Figure 10. Z-24 Bridge: outlier detection based on the GEM-PSO (a) and KPCA (b) approaches with ED.

approaches for a level of significance of 5% over the training data is summarized in Table 4. The optimal kernel parameter required for the KPCA approach can be computed by the maximization of the information entropy,[15] as demonstrated in Figure 9. Although the KPCA approach seems to be more attractive for minimizing the Type II errors, the GEM-PSO one can fit the normal and stable state conditions of the Z-24 Bridge in a more balanced manner, which can be proved by the maximization of specificity (the portion of undamaged cases correctly identified) without significant minimization of the sensitivity (the portion of damaged cases correctly identified).

The DIs derived from the GEM-PSO and KPCA approaches are highlighted in Figure 10, along with a threshold defined for a level of significance of 5% over the training data. Both approaches present quite similar behavior during the training undamaged conditions (1-3123) and damage progressive testing period (3471-3932). In this case, the bilinear behavior in the natural frequencies for below and above 0 °C is more obvious in the form of peaks during the baseline condition (training).[39] Nevertheless, the GEM-PSO approach generalizes almost all the normal structural states more efficiently than the KPCA one, which impacts in fewer Type I errors for undamaged observations not used during the training process (3124-3470).

Damage detection on data sets from the Tamar Bridge

In contrast to the Z-24 Bridge, the data sets from the Tamar Bridge do not have any reported damaged condition, and are characterized by few deviations from a global normal and stable condition, as demonstrated from the MNST in Figure 11. However, these data sets from an extensive monitoring campaign present the dynamic response of the structure to the most common operational and environmental variations observed in real applications of SHM, e.g. temperature, traffic loading and wind velocity.[40] Clustering such normal conditions as components is a crucial data normalization step that impacts positively on the damage detection

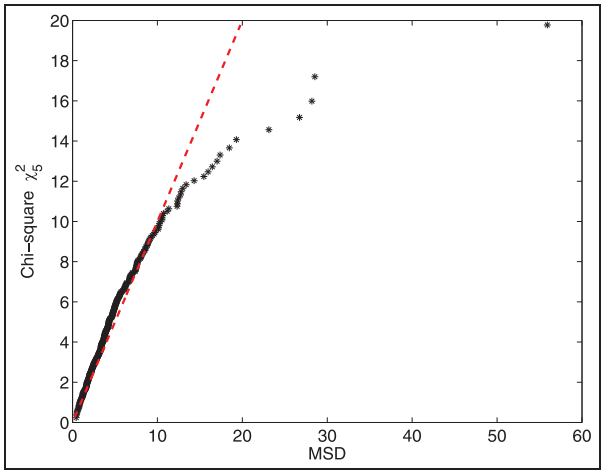

Figure 11. MNST based on the Chi-square Q-Q plot of the MSD using the training observations from the Tamar Bridge.

Table 5. Tamar Bridge: damage classification performance (average ± standard deviation) of the GEM-PSO and EM-GMM approaches with MSD for 20 executions.

Approach	Number of Type I errors
GEM-PSO	42.40 ± 0.91
EM-GMM	43.75 ± 0.92

process. A particular parameter setting for the GEM-PSO approach to deal with this scenario is $\eta = \beta = 20$.

Assuming a level of significance of 5%, the damage classification performance (only Type I errors) of the GEM-PSO and EM-GMM approaches is presented in Table 5. Both approaches have achieved nearly the same performance with negligible advantage to the GEM-PSO, for which the components derived to accommodate the operational and environmental effects are fitted with more reliable LogL and BIC in terms of standard deviation, as attested in Table 6.

When the best models of the GEM-PSO and EM-GMM approaches over all executions are chosen based on the BIC, the number of components for both approaches is $K = 3$ and the DIs derived from these approaches are highlighted in Figure 12, along with a threshold defined for a level of significance of 5%. Basically, the approaches can deal very well with the data from the undamaged condition present in the training phase (1-363), by clustering the undesired effects into different normal and stable components. Unfortunately, this conclusion cannot be extended to observations not used in training (364-602), where a major concentration of outliers took place; it may be attributed to the fact that some source of variability is

Table 6. Tamar Bridge: the performance of the GEM-PSO and EM-GMM approaches in terms of log-likelihood and BIC (average ± standard deviation) for 20 executions.

Approach	Metric	
	LogL	BIC
GEM-PSO	7,705.72 ± 0.0018	−1,5045.98 ± 0.0036
EM-GMM	7,705.72 ± 0.0028	−1,5045.98 ± 0.0056

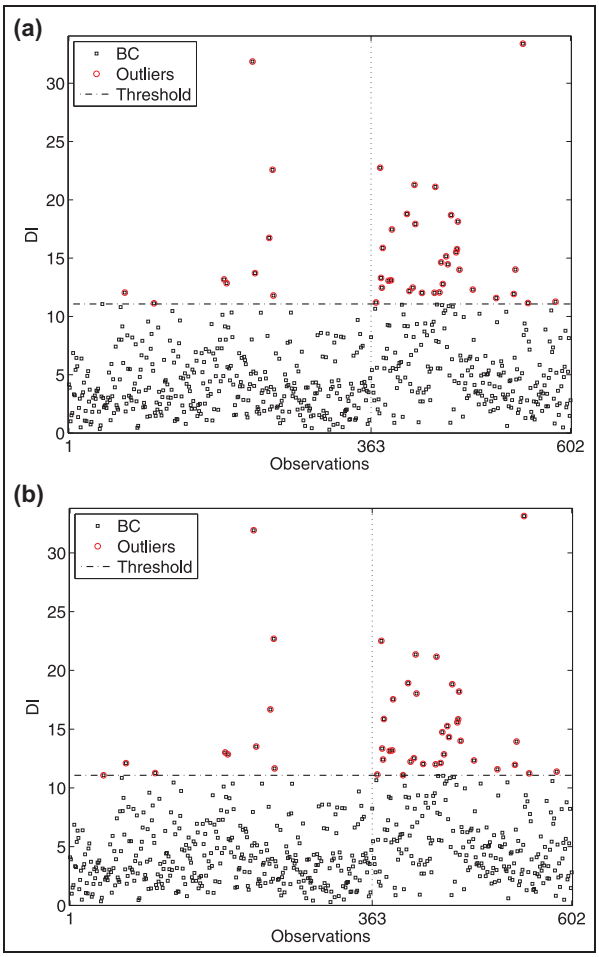

Figure 12. Tamar Bridge: outlier detection based on GEM-PSO (a) and EM-GMM (b) approaches with MSD.

not characterized in the training data. Additionally, the best model of the GEM-PSO has slightly fewer Type I errors than the best one of the EM-GMM, as expected due to the slightly lower standard deviations in the models summarized in Table 6.

A more acceptable damage classification performance for this scenario can be reached when the ED is applied as a damage detection strategy. In this case, the damage classification performance of the GEM-PSO

Table 7. Tamar Bridge: damage classification performance (average ± standard deviation) of the GEM-PSO and KPCA approaches with ED for 20 executions.

Approach	Number of Type I errors
GEM-PSO	32.00 ± 0.00
KPCA	67

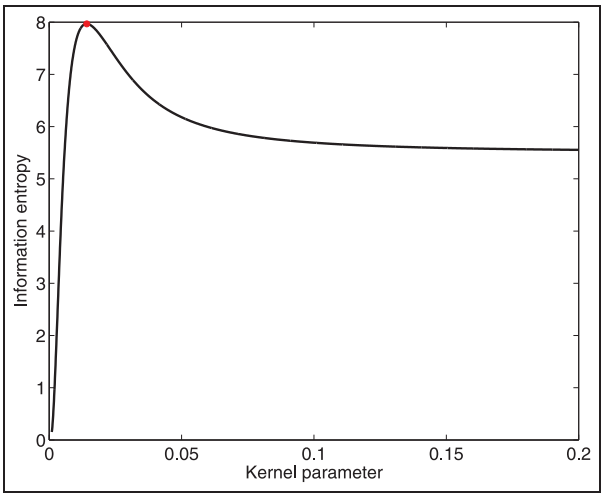

Figure 13. Tamar Bridge: maximization of the information entropy as a function of the kernel parameter (the optimal is 0.0142).

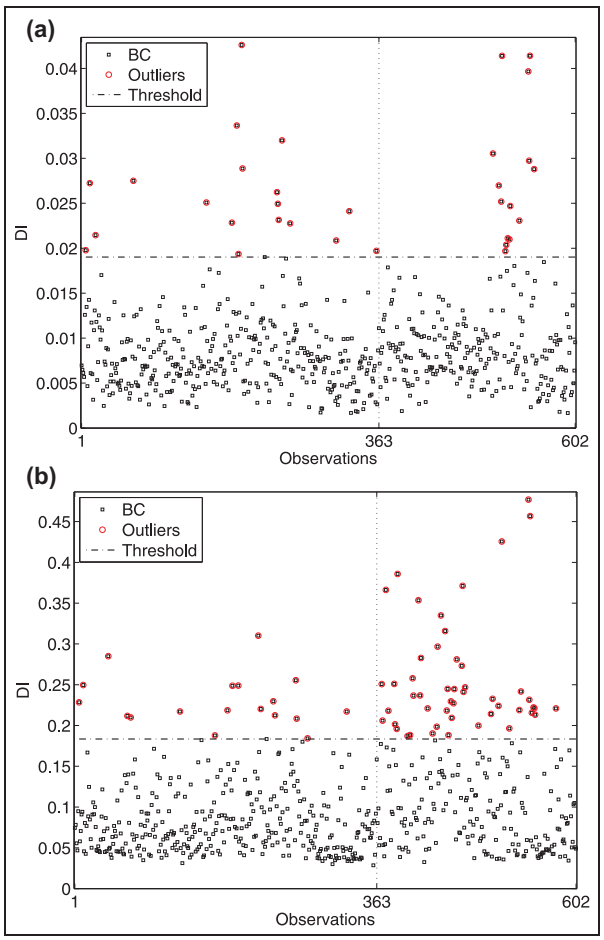

Figure 14. Tamar Bridge: outlier detection based on the GEM-PSO (a) and KPCA (b) approaches with ED.

and KPCA approaches, for a level of significance of 5% over the training data, is synthesized in Table 7. The KPCA, with optimal kernel parameter, as shown in Figure 13, has a limited performance assigned to some loss of information, as the retained principal components in the high-dimensional feature space are chosen based on a certain fraction of the normal variability; in this case, 99% of variance. In contrast, the GEM-PSO reveals suitable performance to generalize the undamaged conditions not handled in the training phase, since the level of significance admitted implies a tolerance of Type I errors equal to 18 within 1-363 observations, then only 2.33% of all test cases are misclassified (as false-positive indications of damage) within 364-602 observations.

The comparison of the GEM-PSO approach against KPCA can also be visualized through the DIs produced by both approaches as established in Figure 14, along with a threshold defined for a level of significance of 5% over the training data. Undoubtedly, a high concentration of outliers is noticed in the classification performed by the KPCA, suggesting that if the dynamic response of the Tamar Bridge is available for structural condition assessment, all variations due to operational and environmental factors are not taken into account. On the other hand, if such changes can be accounted for and filtered out to normalize monitoring data, then any changes in dynamic characteristics are correlated to some structural change. In this case, the GEM-PSO seems to attenuate, or even remove, the predominant environmental and operational variations that affect the natural frequencies: temperature and traffic loading.

Influence of parameters on the damage monitoring results of the GEM-PSO approach

The influence of different parameters on the damage monitoring results of the GEM-PSO approach, along with MSD, for both SHM scenarios is demonstrated in Tables 8 and 9. The parameters η, R, Υ, c_1 and c_2 are not considered in this study as they are easily defined based on the recommendations provided in "Choice of parameters", presenting minor influences in the results when they are modified within their predefined ranges.

Table 8. Z-24 Bridge: influence of parameters on damage classification performance (average ± standard deviation) of the GEM-PSO approach with MSD for 20 executions.

τ	β	Type I errors	Type II errors
100	40	123.65 ± 5.05	3.05 ± 0.22
150	40	123.61 ± 5.03	3.04 ± 0.23
200	40	123.64 ± 4.99	3.04 ± 0.24
100	50	123.60 ± 4.95	3.05 ± 0.22
150	50	123.64 ± 4.93	3.05 ± 0.21
200	50	123.63 ± 5.01	3.05 ± 0.21
100	60	123.60 ± 4.95	3.05 ± 0.22
150	60	123.61 ± 4.96	3.05 ± 0.20
200	60	123.62 ± 5.02	3.05 ± 0.22

Table 9. Tamar Bridge: influence of parameters on damage classification performance (average ± standard deviation) of the GEM-PSO approach with MSD for 20 executions.

τ	β	Type I errors
100	15	42.40 ± 0.90
150	15	42.39 ± 0.89
200	15	42.41 ± 0.93
100	20	42.40 ± 0.91
150	20	42.41 ± 0.92
200	20	42.40 ± 0.90
100	30	42.40 ± 0.92
150	30	42.40 ± 0.93
200	30	42.39 ± 0.90

Thus, only τ and β are modified to some values within their predefined ranges.

When the parameters τ and β are set to different values, in both scenarios, the damage monitoring results provided by the GEM-PSO remain very stable and reliable, indicating, once again, that the proposed approach is not dependent on the choice of the initial parameters from GMM or PSO.

Execution time on data sets from the Z-24 and Tamar Bridges

The average execution time for each approach on data sets from the SHM scenarios used in this study is presented in Table 10. All the experiments ran on an Intel Core i7-4500U processor 1.8 GHz (2.4 GHz) system with 4 GB of main memory. In an overall analysis, the EM-GMM approach has the best time performance for both data sets, followed by the GEM-PSO one. The KPCA has a very fast time performance, 74.79 and 0.13 seconds, when the time to determine the kernel parameter, 1155.37 and 19.42 seconds, is not taken into account. However, the determination of this parameter was assumed to be a step of the KPCA approach,[15] thereby in this paper the time for this initial step should be considered for the total execution time of the KPCA.

Table 10. Z-24 and Tamar Bridges: execution time for each approach considering training and test phases (20 executions).

Approach	Average time (seconds)	
	Z-24 Bridge	Tamar Bridge
GEM-PSO	117.92	12.32
EM-GMM	100.63	11.50
KPCA	1155.37 + 74.79	19.42 + 0.13

Despite several repetitions of the EM algorithm performed by the EM-GMM and some iterations of the GEM-PSO, these approaches have acceptable execution times for the data sets extracted hourly, in the case of the Z-24 Bridge, and daily for the Tamar Bridge. The training phase of the approaches comprises almost all the execution time and the test phase, where the DIs are computed based on distance metrics, runs very fast. In the case of the KPCA, the chosen range of kernel parameter directly influences the execution time of the training phase and the test phase has a negligible execution time.

Conclusions

This paper introduced the GEM-PSO approach, for which an MA based on PSO was used to improve the stability and reliability of the EM algorithm in searching for the optimal number of components and their parameters. As long as the main stable state conditions of the structure are determined, assuming multivariate Gaussian distributions, the damage detection strategy implemented through the Mahalanobis and Euclidean distances can be applied. The damage classification performance of the GEM-PSO on challenging vibration-based data sets was evaluated and compared to state-of-the-art methods.

The classification performance for both real-world SHM scenarios attested that the GEM-PSO approach is better than the alternative ones. When the GEM-PSO is compared to the EM-GMM, the improvement of the stability and reliability of the EM algorithm was demonstrated to have a direct and positive impact on the identification of global components (data normalization) and damage detection. This explains the relatively poor performance of the EM-GMM on data sets from the Z-24 Bridge. The KPCA is less affected than the EM-GMM by the choice of the initial parameters, nevertheless it is sensitive to some loss of information in the high-dimensional feature space as only a certain

fraction of the normal variability is retained. This drawback influenced its competence to attenuate undesired operational and environmental variations, and consequently resulted in unacceptable classification performance on data sets from the Tamar Bridge.

The average execution time of each approach was presented. The EM-GMM approach revealed the best execution time for both data sets, followed by GEM-PSO. The estimation of the kernel parameter took longer for KPCA, which negatively impacted its total execution time.

Unlike the other approaches, the GEM-PSO consists of two main parts: a global one that conducts the global search in the feature space; and a local one, which performs a more refined search around candidate solutions of the current problem. As demonstrated through the experimental results, this hybridization proved to be a pronounced technique that can be used to add quantitative information from the SHM systems into the SMSs, in a controlled manner, as the main state conditions of a structure are mapped into a DI.

In general, the choice of parameters, as well as the tuning of them, for population-based metaheuristics becomes very challenging when different scenarios are considered. To deal with this issue, few recommendations were suggested for the GEM-PSO approach, taking into account the heterogeneity of monitoring data and parameter settings widely tested and established in the specialized literature.

Acknowledgements

The authors would like to acknowledge Professor Guido De Roeck, from the Katholieke Universiteit Leuven, and Professor James Brownjohn, from the University of Exeter, for giving us the data as well as documentation from the Z-24 and Tamar Bridges.

Funding

The author(s) disclosed receipt of the following financial support for the research, authorship, and/or publication of this article: This work was supported in part by the National Council for Scientific and Technological Development (in Portuguese: Conselho Nacional de Desenvolvimento Científico e Tecnológico), Brazil (grant numbers 142236/2014-4 and 454483/2014-7); and in part by the Coordination for the Improvement of Higher Education Personnel (in Portuguese: Coordenação de Aperfeiçoamento de Pessoal de Nível Superior), Brazil.

References

1. Figueiredo E, Moldovan I and Marques MB. *Condition assessment of bridges: Past, present, and future - a complementary approach*. Lisbon, Portugal: Universidade Católica Editora, 2013. Publisher's city: Lisbon
2. Wenzel H. *Health monitoring of bridges*. West Sussex, UK: John Wiley and Sons, Inc., 2009.
3. Farrar CR and Worden K. *Structural health monitoring: A machine learning perspective*. West Sussex, UK: John Wiley and Sons, Inc., 2013.
4. Farrar CR, Doebling SW and Nix DA. Vibration-based structural damage identification. *Philos T R Soc A* 2001; 359(1778): 131–149.
5. Sohn H. Effects of environmental and operational variability on structural health monitoring. *Philos T R Soc A* 2007; 365(1851): 539–560.
6. Worden K and Manson G. The application of machine learning to structural health monitoring. *Philos T R Soc A* 2007; 365(1851): 515–537.
7. Sohn H, Worden K and Farrar CR. Statistical damage classification under changing environmental and operational conditions. *J Intel Mat Syst Str* 2002; 13(9): 561–574.
8. Kullaa J. Distinguishing between sensor fault, structural damage, and environmental or operational effects in structural health monitoring. *Mech Syst Signal Pr* 2011; 25(8): 2976–2989.
9. Ruotolo R and Surace C. Using SVD to detect damage in structures with different operational conditions. *J Sound Vib* 1999; 226(3): 425–439.
10. Worden K, Manson G and Fieller NRJ. Damage detection using outlier analysis. *J Sound Vib* 2000; 229(3): 647–667.
11. Kullaa J. Is temperature measurement essential in structural health monitoring? In: *Proceedings of the 4th international workshop on structural health monitoring: From diagnostic and prognostics to structural health monitoring*, 15–17 September 2003, pp.717–724. Stanford, CA: DES-tech Publications.
12. Yan AM, Kerschen G, Boe PD, et al. Structural damage diagnosis under varying environmental conditions - Part I: A linear analysis. *Mech Syst Signal Pr* 2005; 19(4): 847–864.
13. Hsu TY and Loh CH. Damage detection accommodating nonlinear environmental effects by nonlinear principal component analysis. *Struct Control Hlth* 2010; 17(3): 338–354.
14. Figueiredo E, Park G, Farrar CR, et al. Machine learning algorithms for damage detection under operational and environmental variability. *Struct Health Monit* 2011; 10(6): 559–572.
15. Reynders E, Wursten G and Roeck GD. Output-only structural health monitoring in changing environmental conditions by means of nonlinear system identification. *Struct Health Monit* 2014; 13(1): 82–93.
16. Santos A, Figueiredo E, Silva M, et al. Machine learning algorithms for damage detection: Kernel-based approaches. *J Sound Vib* 2016; 363: 584–599.
17. Figueiredo E and Cross E. Linear approaches to modeling nonlinearities in long-term monitoring of bridges. *J Civil Struct Health Monit* 2013; 3(3): 187–194.
18. Figueiredo E, Radu L, Worden K, et al. A Bayesian approach based on a Markov-chain Monte Carlo method for damage detection under unknown sources of variability. *Eng Struct* 2014; 80: 1–10.

19. Santos A, Figueiredo E and Costa J. Clustering strategies for damage detection in bridges: A comparison study. In: *Proceedings of the 10th international workshop on structural health monitoring: System reliability for verification and implementation*, 1–3 September 2015, pp.1165–1172. Stanford, CA: DEStech Publications.
20. Qiu L, Yuan S, Mei H, et al. An improved Gaussian mixture model for damage propagation monitoring of an aircraft wing spar under changing structural boundary conditions. *Sensors* 2016; 16(3): 291–308.
21. Qiu L, Yuan S, Bao Q, et al. Crack propagation monitoring in a full-scale aircraft fatigue test based on guided wave-Gaussian mixture model. *Smart Mater Struct* 2016; 25(5): 1–13.
22. Kullaa J. Structural health monitoring under nonlinear environmental or operational influences. *Shock Vib* 2014; 2014: 1–9.
23. Figueiredo E, Radu L, Westgate R, et al. Applicability of a Markov-chain Monte Carlo method for damage detection on data from the Z-24 and Tamar suspension bridges. In: *Proceedings of the 6th European workshop on structural health monitoring*, 3–6 July 2012, pp.747–754. Dresden, Germany: NDT.net Publications.
24. Nair KK and Kiremidjian AS. Time series based structural damage detection algorithm using Gaussian mixtures modeling. *J Dyn Syst-T ASME* 2006; 129(3): 285–293.
25. Slonski M. Gaussian mixture model for time series-based structural damage detection. *Comp Assist Mech Eng Sci* 2012; 19(4): 331–338.
26. Farhidzadeh A, Salamone S and Singla P. A probabilistic approach for damage identification and crack mode classification in reinforced concrete structures. *J Intel Mat Syst Str* 2013; 24(14): 1722–1735.
27. Figueiredo MAT and Jain AK. Unsupervised learning of finite mixture models. *IEEE T Pattern Anal* 2002; 24(3): 381–396.
28. McLachlan GJ and Peel D. *Finite mixture models*. New York, NY: John Wiley and Sons, Inc., 2000.
29. Dempster AP, Laird NM and Rubin DB. Maximum likelihood from incomplete data via the EM algorithm. *J Roy Stat Soc B Met* 1977; 39(1): 1–38.
30. Box GEP, Jenkins GM and Reinsel GC. *Time series analysis: Forecasting and control*. 4th ed. Hoboken, NJ: John Wiley and Sons, Inc., 2008.
31. Moscato P and Cotta C. A modern introduction to memetic algorithms In: *Handbook of metaheuristics*. Boston, MA: Springer US, 2010, pp.141–183.
32. Neri F and Cotta C. Memetic algorithms and memetic computing optimization: A literature review. *Swarm Evol Comput* 2012; 2: 1–14.
33. Kennedy J and Eberhart R. Particle swarm optimization. In: *Proceedings of the IEEE international conference on neural networks*, 27 November–01 December 1995, pp.1942–1948. Perth, WA: IEEE.
34. Poli R, Kennedy J and Blackwell T. Particle swarm optimization: An overview. *Swarm Intell* 2007; 1(1): 33–57.
35. Clerc M and Kennedy J. The particle swarm - Explosion, stability, and convergence in a multidimensional complex space. *IEEE T Evolut Comput* 2002; 6(1): 58–73.
36. Hart WE. *Adaptive global optimization with local search*. PhD Thesis, University of California, USA, 1994.
37. Peeters B and Roeck GD. One-year monitoring of the Z24-Bridge: Environmental effects versus damage events. *Earthq Eng Struct D* 2001; 30(2): 149–171.
38. Peeters B and Roeck GD. Reference-based stochastic subspace identification for output-only modal analysis. *Mech Syst Signal Pr* 1999; 13(6): 855–878.
39. Peeters B, Maeck J and Roeck GD. Vibration-based damage detection in civil engineering: Excitation sources and temperature effects. *Smart Mater Struct* 2001; 10(3): 518–527.
40. Cross E, Koo K, Brownjohn J, et al. Long-term monitoring and data analysis of the Tamar Bridge. *Mech Syst Signal Pr* 2013; 35(1–2): 16–34.
41. Koo KY, Brownjohn JMW, List DI, et al. Structural health monitoring of the Tamar Suspension Bridge. *Struct Control Hlth* 2013; 20(4): 609–625.

Appendix E – Paper E: Output-only structural health monitoring based on mean shift clustering for vibration-based damage detection

Output-only structural health monitoring based on mean shift clustering for vibration-based damage detection

Adam Santos[1], **Moisés Silva**[1], **Reginaldo Santos**[1], **Eloi Figueiredo**[2,3], **Claudomiro Sales**[1], **João C. W. A. Costa**[1]

[1] Applied Electromagnetism Laboratory, Universidade Federal do Pará, R. Augusto Corrêa, Guamá 1, Belém, 66075-110 Pará, Brazil, adamdreyton@ufpa.br

[2] Faculty of Engineering, Universidade Lusófona de Humanidades e Tecnologias, Campo Grande 376, 1749-024 Lisbon, Portugal, eloi.figueiredo@ulusofona.pt

[3] CONSTRUCT, Institute of R&D in Structures and Construction, R. Dr. Roberto Frias s/n, 4200-465 Porto, Portugal

Keywords: Structural health monitoring, Data normalization, Damage detection, Mean shift clustering, Kernel density estimation.

Abstract

Damage assessment based on vibration response measurements from engineering structures has been an essential research area in the structural health monitoring field. Vibration signals are often available and can be measured from different types of monitoring systems through a diversity of data acquisition systems and sensors. Based on suitable data treatment, valuable information from the structural dynamics can be extracted and used as damage-sensitive features for detecting early and progressive structural damage, thereby increasing safety and avoiding collapses. However, the operational and environmental variations often arise as undesired effects in the damage-sensitive features, which might negatively influence the proper identification of damage. To deal with this drawback, this paper presents an output-only technique based on mean shift clustering (MSC) to automatically discover an unknown number of clusters that correspond to the normal and stable state conditions of a structure. Unlike most methods in the literature, MSC is a nonparametric technique that does not require prior knowledge of the number of clusters and can identify clusters of distinct shapes, sizes and density. The superiority of the MSC technique, over the state-of-the-art ones, is tested by applying a damage detection strategy implemented through the Euclidean distance, which permits one to locate the outlier formation in relation to the chosen data clusters, using data sets from the Z-24 Bridge in Switzerland.

1. INTRODUCTION

Damage detection based on vibration response measurements from engineering structures has been a crucial research area in the structural health monitoring (SHM) field [1, 2]. Vibration signals are often available and can be measured from different types of monitoring systems through a diversity of data acquisition systems and sensors. Based on suitable data treatment, valuable information from the structural dynamics can be extracted and used as damage-sensitive features for detecting early and progressive structural damage, thereby increasing safety, avoiding collapses and supporting the decision making process regarding maintenance, repair, and rehabilitation.

Unfortunately, operational and environmental variations (e.g., temperature, operational loading, humidity and wind speed) often arise as unwanted effects in the damage-sensitive features and usually mask changes caused by damage, which might negatively influence the proper identification of damage [3]. To deal with this drawback, several machine learning algorithms with different working principles have been proposed to mitigate (or even remove) these effects on the extracted features as well as to separate changes in damage-sensitive features caused by damage from those caused by varying operational and environmental conditions [4–9]. These approaches are often characterized as unsupervised

and output-only because they are trained only with damage-sensitive features related to undamaged condition without any measurement directly related to operational and environmental parameters.

In [7] and [10], an approach based on the Gaussian mixture model (GMM) is applied to model the main clusters that correspond to the normal state conditions of a bridge. The damage detection is performed on the basis of an outlier formation regarding the chosen clusters of main states. Although this approach has revealed better damage detection performance when compared to other traditional methods, it assumes Gaussian distributions which may compromise the reliable estimation of clusters. As an alternative, the Fuzzy c-means (FCM) approach is used in [11] and [12] to distinguish between undamaged and damaged state conditions. However, this approach can not assess the damage severity in a clear manner and often produces a significant number of false-negative indication of damage, as demonstrated in [11]. K-means clustering is also a possible approach to identify the normal condition of a structure in terms of a finite number of clusters and then classify new unknown state conditions. Despite this approach was used in [9] and [13, 14] with relative success, its applicability is limited due to the stochastic behavior and invariant shapes of clusters.

Therefore, this paper presents an output-only technique based on mean shift clustering (MSC) [15] to automatically discover an unknown number of data clusters that correspond to the normal and stable state conditions of a structure. Unlike most methods in the literature, MSC is a nonparametric technique that does not require prior knowledge of the number of clusters and can identify clusters of distinct shapes, sizes and density [16]. As long as the main stable state conditions of the structure are determined, the superiority of the MSC approach, over the state-of-the-art ones based on K-means, FCM and GMM, is tested by applying a damage detection strategy implemented through the Euclidean distance (ED), which permits one to locate the outlier formation in relation to the chosen data clusters, using data sets from the Z-24 Bridge in Switzerland. The classification performance is assessed on the basis of Type I (false-positive indication of damage) and Type II (false-negative indication of damage) error trade offs.

The remainder of this study is organized as follows. In Section 2, the MSC approach is derived to determine the health state of a structure based on a reliable estimation of data clusters. Section 3 describes the Z-24 structure, the long-term vibration data, and the major environmental influence. In Section 4, the experimental results on extracted damage-sensitive features from the test structure are discussed and a comparison with state-of-the-art approaches is also emphasized. Finally, Section 5 synthesizes the main strengths and limitations of the MSC approach.

2. DAMAGE DETECTION BASED ON MEAN SHIFT CLUSTERING

This section presents the methodology of the MSC approach, which is divided into two steps. First, the estimation of data clusters through MSC is presented. Second, the damage detection strategy based on the ED is described taking into account the main data clusters estimated in the first step.

For general purposes, one may assume a training data matrix, $\mathbf{X} \in \mathbb{R}^{m \times n}$, with n-dimensional feature vectors from m different operational and environmental conditions when the structure is undamaged and a test data matrix, $\mathbf{Z} \in \mathbb{R}^{l \times n}$, where l is the number of feature vectors from the undamaged and/or damaged conditions.

2.1 Estimation of data clusters

MSC seeks to discover modes or clusters in a smooth density of observations [15, 16]. This algorithm is a centroid-based method, which works by updating candidates for centroids to be the mean of the observations within a given region. Afterwards, these candidates are filtered in a post-processing phase to eliminate redundancies to form the final set of centroid.

Given a candidate centroid $\mathbf{x}_i$ for iteration t, the centroid is updated according to

$$\mathbf{x}_i^{t+1} = \mathbf{x}_i^t + \lambda\left(\mathbf{x}_i^t\right), \tag{1}$$

where $\lambda(\mathbf{x}_i^t)$ is the mean shift vector that is computed for each centroid located in a region of the maximum increase in the density of observations.

Assuming m observations $\mathbf{x_i}$ on a n-dimensional space $\mathbb{R}^n$ and the associated diagonal bandwidth matrices $h_i\mathbf{I}_{m\times m}$, $i=1,\ldots,m$, the observation density estimator obtained with the kernel profile $k(\mathbf{x})$ is denoted by

$$f(\mathbf{x}) = \frac{1}{m}\sum_{i=1}^{m}\frac{1}{h_i^n}k\left(\left\|\frac{\mathbf{x}-\mathbf{x}_i}{h_i}\right\|^2\right). \tag{2}$$

Herein, the multivariate normal profile is considered such as

$$k(x) = e^{-\frac{1}{2}x} \qquad x \geq 0. \tag{3}$$

By computing the gradient of Equation (2), the stationary observations of the density function satisfy

$$\frac{2}{m}\sum_{i=1}^{m}\frac{1}{h_i^{n+2}}(\mathbf{x}_i-\mathbf{x})\,g\left(\left\|\frac{\mathbf{x}-\mathbf{x}_i}{h_i}\right\|^2\right) = 0, \tag{4}$$

where $g(x) = -k'(x)$. The solution of Equation (4) is a local maximum of the density function which can be iteratively reached applying mean shift procedure, i.e., effectively updating a centroid to be the mean of the observations within its neighborhood

$$\lambda(\mathbf{x}) = \frac{\sum_{i=1}^{m}\frac{\mathbf{x}_i}{h_i^{n+2}}g\left(\left\|\frac{\mathbf{x}-\mathbf{x}_i}{h_i}\right\|^2\right)}{\sum_{i=1}^{m}\frac{1}{h_i^{n+2}}g\left(\left\|\frac{\mathbf{x}-\mathbf{x}_i}{h_i}\right\|^2\right)} - \mathbf{x}, \tag{5}$$

where $\mathbf{x}$ is the current mean, $\lambda(\mathbf{x})$ is the mean shift vector and $g(.)$ is the kernel function that uses a bandwidth parameter h for multivariate kernel density estimation. The Gaussian and Epanechnikov kernels are the options most commonly used in a large range of applications [17, 18]. In this study, the Gaussian kernel is considered, thereby only the bandwidth parameter h should be defined.

The MSC algorithm automatically determines the number of data clusters relying on the bandwidth, which dictates the size of the region to search through. These clusters are automatically correlated to the number of discovered modes. The nonparametric characteristic of MSC makes it a powerful tool to discover arbitrarily shaped clusters present in the monitoring data from SHM applications, aiming to establish the baseline or normal condition of the monitored structure.

2.2 Damage detection using discovered clusters

After the definition of the optimal number of data clusters embedded in the training data, the damage detection process is performed through a global damage indicator (DI) estimated for each test observation. Basically, for a given test feature vector, $\mathbf{z}_i$ ($i=1,\ldots,l$), the ED for all centroids is calculated, where the DI(i) is considered the smallest distance,

$$\mathrm{DI}(i) = \min\left(\|\,\mathbf{z}_i-\mathbf{c}_1\,\|,\|\,\mathbf{z}_i-\mathbf{c}_2\,\|,\ldots,\|\,\mathbf{z}_i-\mathbf{c}_Q\,\|\right), \tag{6}$$

where $\mathbf{c}_1,\mathbf{c}_2,\ldots,\mathbf{c}_Q$ are the centroids of Q different data clusters. In this study, the threshold for damage classification is defined for 95% of confidence on the DIs taking into account only the baseline data used in the training process. Thus, if the MSC approach has learned the baseline condition, i.e., the identified data clusters suitably represent the undamaged and normal condition under all possible operational and environmental conditions, then this approach should output approximately 5% of false alarms for the undamaged data used in test phase.

3. TEST STRUCTURE AND DATA SETS

The Z-24 Bridge was a post-tensioned concrete box girder bridge composed of a main span of 30 m and two side-spans of 14 m, as depicted in Figure 1. The bridge, before complete demolition, was extensively instrumented and tested with the purpose of providing a feasibility benchmark for vibration-based SHM in civil engineering [19]. A long-term monitoring test was carried out, from 11 November 1997 until 10 September 1998, to quantify the operational and environmental variability present on the bridge and detect damage artificially introduced, in a controlled manner, in the last month of operation. Every hour, eight accelerometers captured the vibrations of the bridge as sequences of 65536 samples (sampling frequency of 100 Hz) and other sensors measured environmental parameters, such as temperature at several locations [20].

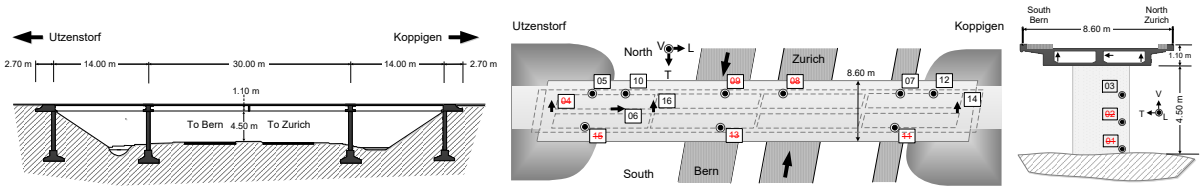

Figure 1 : Longitudinal section (left), and the location and orientation of accelerometers (right) on the Z-24 Bridge. Marked sensors failed during the monitoring campaign.

In this case, the natural frequencies of the Z-24 Bridge are used as damage-sensitive features. They were estimated using a reference-based stochastic subspace identification method on vibration measurements from the accelerometers [21]. The first two natural frequencies estimated daily from 11 November 1997 to 10 September 1998, with a total of 235 observations, are highlighted in Figure 2. The first 198 observations correspond to the damage-sensitive feature vectors extracted within the undamaged structural condition under effects caused by the operational and environmental variability. The last 37 observations correspond to the damage progressive testing period, which is highlighted, especially in the second frequency, by a clear decay in the magnitude of such frequency. The damage scenarios were carried out in a sequential manner, which cause cumulative degradation of the bridge. Moreover, the observed jumps in the natural frequencies are related to the asphalt layer in cold periods, which significantly contributes to the stiffness of the bridge.

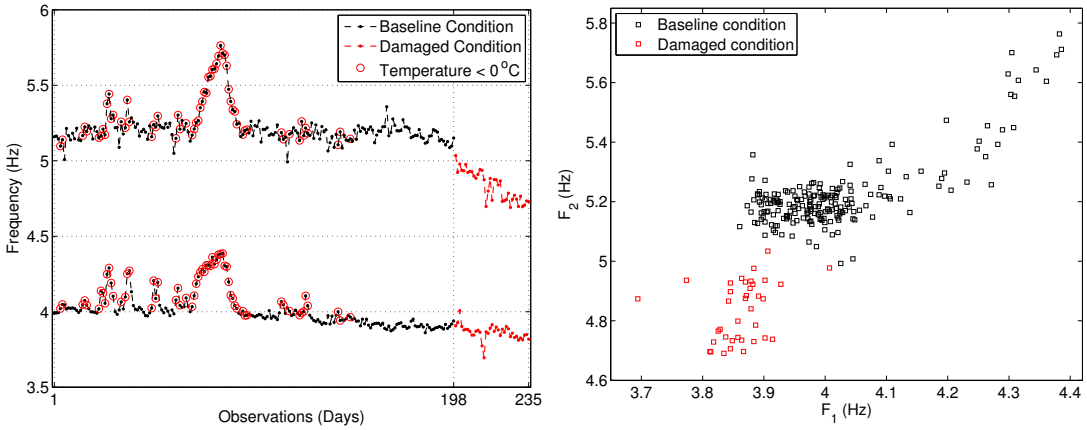

Figure 2 : The first two natural frequencies extracted daily from 11 November 1997 to 10 September 1998 (left); feature distribution of the two natural frequencies (right).

Progressive damage tests were performed in one-month time period (from 4 August to 10 September 1998) before the demolition of the bridge to prove that realistic damage has a measurable influence on the bridge dynamics, as summarized in Table 1. The continuous monitoring system was still running

during the progressive damage tests, which permits one to validate the SHM system to detect accumulative damage on long-term monitoring.

Table 1 : Progressive damage test scenarios. Consider pier settlement system as PSS.

Date	Scenario description	Date	Scenario description
04-08-98	Undamaged condition	25-08-98	Spalling of concrete at soffit (12 m^2)
09-08-98	Installation of the PSS	26-08-98	Spalling of concrete at soffit (24 m^2)
10-08-98	Lowering of pier, 2 cm	27-08-98	Landslide of 1 m at abutment
12-08-98	Lowering of pier, 4 cm	31-08-98	Failure of concrete hinge
17-08-98	Lowering of pier, 8 cm	02-09-98	Failure of 2 anchor heads
18-08-98	Lowering of pier, 9.5 cm	03-09-98	Failure of 4 anchor heads
19-08-98	Lifting of pier, tilt of foundation	07-09-98	Rupture of 2 out of 16 tendons
20-08-98	New reference condition (after removal of the PSS)	08-09-98	Rupture of 4 out of 16 tendons
		09-09-98	Rupture of 6 out of 16 tendons

In conclusion, the damage detection process will be carried out by taking into account the first two natural frequencies and using all 235 observations, resulting in 198 observations from the undamaged condition (1–198 observations) and 37 observations from the damaged condition (199–235 observations). The corresponding training and test matrices are $\mathbf{X}^{198\times 2}$ and $\mathbf{Z}^{235\times 2}$, respectively. The multimodality and heterogeneity among observations in a two dimensional space suggests the existence of data groups that may be find through cluster-based methods.

4. RESULTS AND DISCUSSION

In this section the performances of the K-means-, FCM-, GMM-, and MSC-based approaches are compared in terms of a reliable estimation of data clusters for the undamaged condition and all conditions (undamaged and damaged conditions), and Type I/Type II errors to evaluate the damage classification performance. For K-means and FCM, the Calinski-Harabasz criterion [22] was used to off-line infer the number of clusters. The bandwidth parameter h for the MSC was selected based on the best compromise between the bias and variance [17]. The GMM was set as described in [7], where the model parameters are estimated from the data using the expectation-maximization (EM) algorithm.

4.1 Estimation of data clusters for the undamaged condition

The clustering performance of all approaches for baseline condition is shown in Figure 3. K-means, FCM, and GMM have approximately the same cluster configuration, with two data clusters, where the black one is possibly related to the baseline condition obtained under relatively small environmental and operational influences; and the blue one may be assigned to the baseline condition under severe temperature variations, which corresponds to changes in the structural stiffness [20]. On the other hand, the MSC with $h = 0.147$ presents three data clusters, where the black one is, again, possibly related to the undamaged condition obtained under minor environmental and operational factors; the blue and cyan ones are related to gradual decrease of temperature in the asphalt layer (enough to slightly change the elastic properties of the structure) and changes in the structural response derived from stiffness variations in the asphalt layer caused by freezing temperatures, respectively.

Comparing the results from the MSC and state-of-the-art algorithms, one may verify the similarity of the clustering results for the first data cluster. However, the state-of-the-art algorithms agglutinate the second and third clusters suggested by the MSC algorithm, incorporating all gradual changes in the asphalt layer to one cluster only. Therefore, the proposed approach can discriminate the normal and stable state conditions of the Z-24 Bridge in a better manner, separating changes caused by regular temperatures from changes caused by extreme cold temperatures.

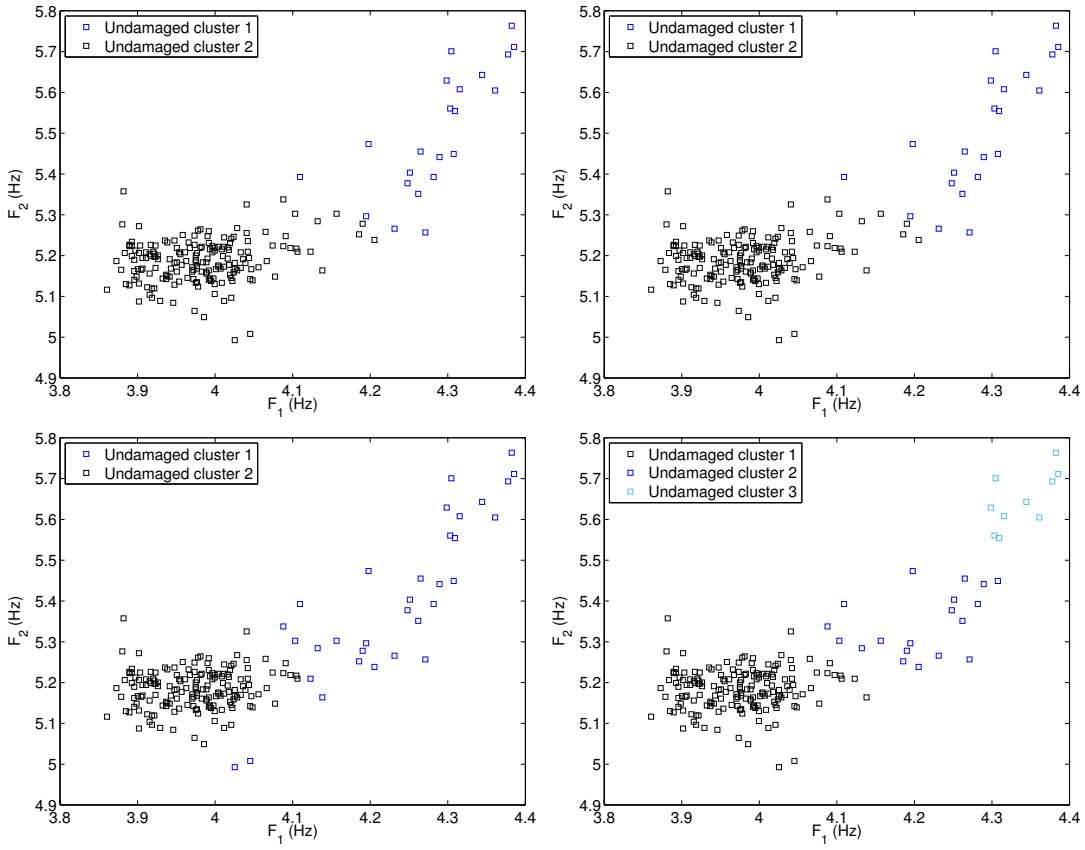

Figure 3 : Clustering performance of the approaches on the training data: K-means (upper left), FCM (upper right), GMM (lower left), and MSC (lower right).

4.2 Estimation of data clusters for all conditions

The clustering performance of all approaches for undamaged and damaged conditions is highlighted in Figure 4. In this case, K-means and FCM have approximately the same cluster configuration, with three data clusters, where the red one is related to the damage progressive test period, integrating all damaged scenarios into one cluster only and presenting 1 or 2 mislabels for all conditions. As the worst case, GMM seems to define data clusters without a logic distinction between undamaged and damaged conditions, outputting several mislabels for all conditions. On the other hand, the MSC with $h = 0.126$ presents five data clusters, where the damage progressive test period is better specified in a logic manner. The second damaged cluster (in magenta) is related to the first few damaged scenarios that consist of installing a settlement system in one pier and then simulating pier settlements of increasing magnitude, followed by a simulated foundation tilt. After these scenarios, on the 20 August 1998, the pier was brought back to its initial position, causing cracks in the bridge deck. The first damaged cluster (in red) is related to the additional damage introduced incrementally, from 25 August 1998, resulting in a pronounced increase in the accumulated damage level in long-term monitoring.

When the results from the MSC and state-of-the-art algorithms are compared, one may infer the advantage of the cluster configuration provided by MSC as it can capture and distinguish different damage levels, ignored by other approaches, which illustrates that the output-only monitoring strategy proposed in this study is a powerful method for SHM.

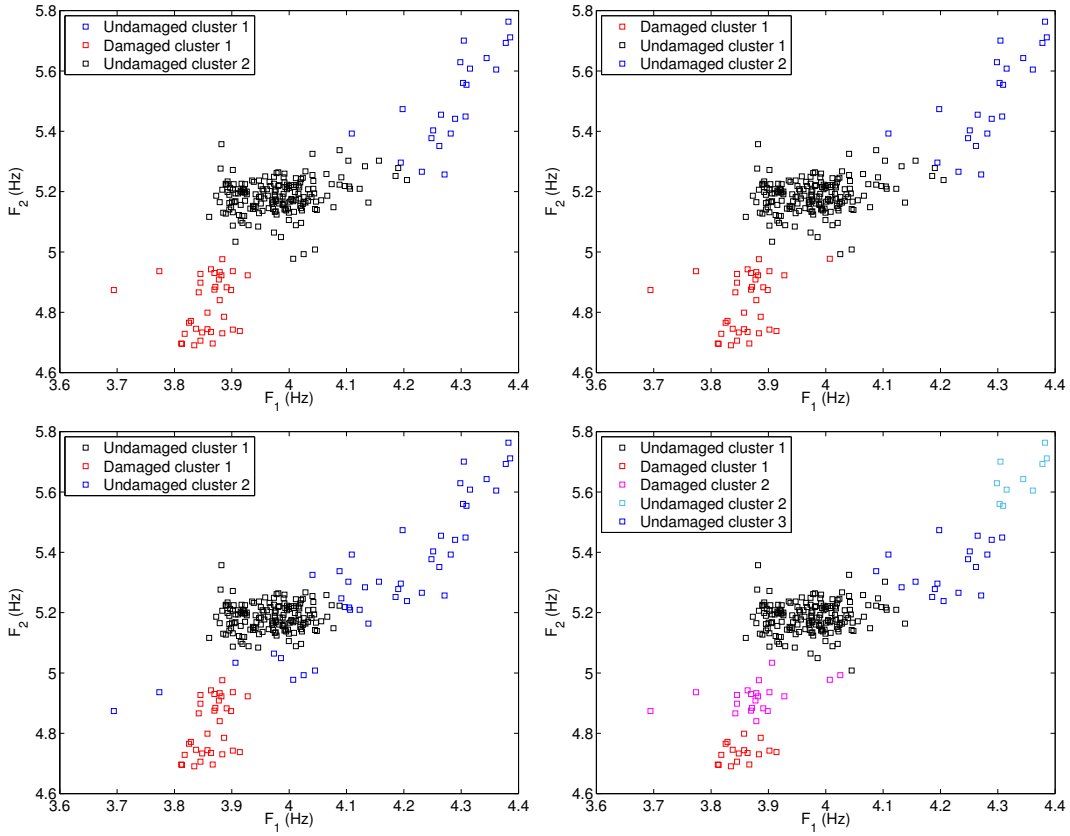

Figure 4 : Clustering performance of the approaches on the test data: K-means (upper left), FCM (upper right), GMM (lower left), and MSC (lower right).

4.3 Damage detection performance

The DIs obtained from the test matrix, $\mathbf{Z}^{235\times 2}$, along with a threshold defined based on the 95% cut-off value over the training data, are depicted in Figure 5. It shows that the K-means-, FCM- and MSC-based approaches outputs a monotonic relationship between the level of damage and the amplitude of the DIs, which may be attributed to the reliable estimation of data clusters provided by these methods during the training phase; whereas the GMM fails to establish this relationship, which may be assigned to an inappropriate definition of data clusters during training phase due to the stochastic behavior of the EM algorithm that compromises the estimation of posterior probability that the observation came from the corresponding cluster. Besides, when one look at the range of baseline condition, the patterns in the DIs caused by the freezing effects can not be pointed out for the MSC, which indicates that this approach is able to remove almost all effects of environmental variations and so demonstrates to be effective to model the normal condition.

Therefore, to quantify the damage classification performance for the test matrix, Table 2 synthesizes the Type I and Type II errors for all approaches. Basically, the GMM- and MSC-based approaches have the same classification performance, reaching 5.05% of Type I errors (as expected) and no misclassification of Type II errors, respectively, and a total amount of errors equal to 4.26%. These results are quite similar due to the damage detection based on ED adopted to identify outliers. However, the MSC filters nearly all operational and environmental variability, especially in the damaged observations, instead of the GMM that provides a poor data normalization in these observations. As expected, the K-means an FCM-based approaches obtained similar results in relation to the amount of Type I errors; however, the Type II errors reached over 2.7%, demonstrating some inefficiency when classifying abnormal conditions.

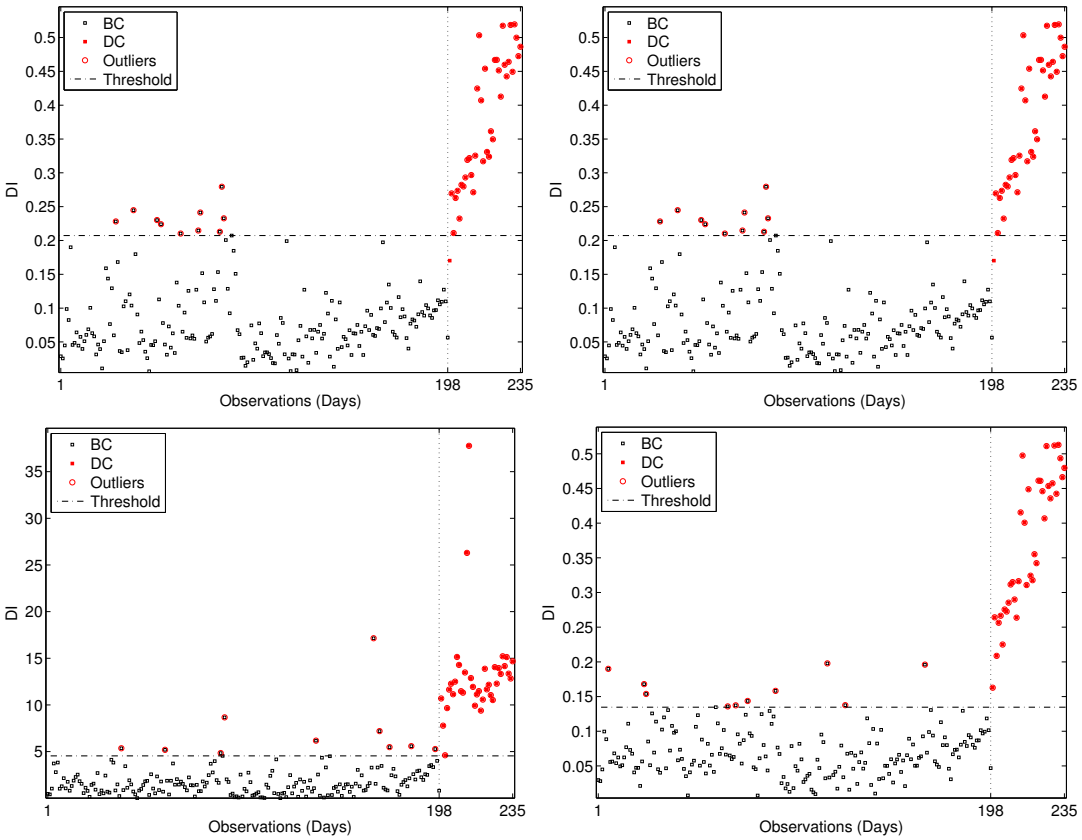

Figure 5 : Outlier detection for each approach: K-means (upper left), FCM (upper right), GMM (lower left), and MSC (lower right).

Table 2 : Damage detection performance for each approach.

Approach	Type I errors	Type II errors	Total errors
K-means	10 (5,05%)	1 (2.70%)	11 (4.68%)
FCM	10 (5,05%)	1 (2.70%)	11 (4.68%)
GMM	10 (5,05%)	0 (0.00%)	10 (4.26%)
MSC	10 (5,05%)	0 (0.00%)	10 (4.26%)

5. CONCLUSIONS

In this paper was presented the MSC approach that automatically discovers data clusters in a smooth density of observations by updating candidate centroids to be the mean of the observations (highest density region) within a given region defined by the bandwidth of a Gaussian kernel. After the main state conditions of the structure are determined, assuming no underlying distributions, the damage detection strategy based on ED is applied. The damage classification performance of the MSC on challenging vibration-based data sets was evaluated and compared to state-of-the-art methods.

The classification performance for the real-world SHM scenario, Z-24 Bridge, attested that the MSC approach is better than the alternative ones presented in this study. When the MSC is compared to the GMM, the instability and unreliability of the EM algorithm demonstrated to have a direct and negative impact on the identification of reliable data clusters (data normalization), which affected the

relationship between the level of damage and the amplitude of the DIs in the damage detection phase; whereas the MSC discovers well-defined clusters, improving the data normalization and damage detection processes. The K-means and FCM appear to be less affected than the GMM by the choice of the initial parameters, nevertheless they are dependent on the choice of the number of clusters in advance. Such drawback may influenced their competence to remove almost all undesired operational and environmental variations and, consequently, resulted in worst classification performance regarding Type II errors.

In contrast to the other approaches, the MSC is a nonparametric technique that does not require prior knowledge of the number of data clusters and can identify clusters of distinct shapes, sizes and density. Unfortunately, the MSC is not highly scalable, as it requires multiple nearest neighbor searches during the execution of the algorithm. This disadvantage is circumvented through parallel implementation of the MSC. As demonstrated through the experimental results, this cluster-based approach proved to be a pronounced technique that can be used in SHM applications where life-safety, economic and reliability issues must be considered as primary motivations.

REFERENCES

[1] Charles R. Farrar, Scott W. Doebling, and David A. Nix. Vibration-based structural damage identification. *Philosophical Transactions of the Royal Society A*, 359(1778):131–149, Jan 2001.

[2] E. Peter Carden and Paul Fanning. Vibration Based Condition Monitoring: A Review. *Structural Health Monitoring*, 3(4):355–377, Dec 2004.

[3] Hoon Sohn. Effects of environmental and operational variability on structural health monitoring. *Philosophical Transactions of the Royal Society A*, 365(1851):539–560, Feb 2007.

[4] Eloi Figueiredo, Gyuhae Park, Charles R Farrar, Keith Worden, and Joaquim Figueiras. Machine learning algorithms for damage detection under operational and environmental variability. *Structural Health Monitoring*, 10(6):559–572, Nov 2011.

[5] Adam Santos, Eloi Figueiredo, M.F.M. Silva, C.S. Sales, and J.C.W.A. Costa. Machine learning algorithms for damage detection: Kernel-based approaches. *Journal of Sound and Vibration*, 363:584–599, Feb 2016.

[6] Moisés Silva, Adam Santos, Eloi Figueiredo, Reginaldo Santos, Claudomiro Sales, and João C.W.A. Costa. A novel unsupervised approach based on a genetic algorithm for structural damage detection in bridges. *Engineering Applications of Artificial Intelligence*, 52:168–180, 2016.

[7] Eloi Figueiredo and Elizabeth Cross. Linear approaches to modeling nonlinearities in long-term monitoring of bridges. *Journal of Civil Structural Health Monitoring*, 3(3):187–194, Aug 2013.

[8] Edwin Reynders, Gersom Wursten, and Guido De Roeck. Output-only structural health monitoring in changing environmental conditions by means of nonlinear system identification. *Structural Health Monitoring*, 13(1):82–93, Jan 2014.

[9] Adam Santos, Eloi Figueiredo, and João Costa. Clustering studies for damage detection in bridges: A comparison study. In *Proceeding of 10th International Workshop on Structural Health Monitoring*, pages 1165–1172, Stanford University, Stanford, CA-USA, Sep 2015.

[10] Eloi Figueiredo, Lucian Radu, Keith Worden, and Charles R. Farrar. A Bayesian approach based on a Markov-chain Monte Carlo method for damage detection under unknown sources of variability. *Engineering Structures*, 80:1–10, Dec 2014.

[11] Samuel da Silva, Milton Dias Júnior, Vicente Lopes Junior, and Michael J. Brennan. Structural damage detection by fuzzy clustering. *Mechanical Systems and Signal Processing*, 22(7):1636–1649, Oct 2008.

[12] Samuel da Silva, Milton Dias Júnior, and Vicente Lopes Junior. Damage detection in a benchmark structure using AR-ARX models and statistical pattern recognition. *Journal of the Brazilian Society of Mechanical Sciences and Engineering*, 29(2):174–184, Apr 2007.

[13] Seunghee Park, Jong-Jae Lee, Chung-Bang Yun, and Daniel J. Inman. Electro-Mechanical Impedance-Based Wireless Structural Health Monitoring Using PCA-Data Compression and k-means Clustering Algorithms. *Journal of Intelligent Material Systems and Structures*, 19(4):509–520, Apr 2008.

[14] Alberto Diez, Nguyen Lu Dang Khoa, Mehrisadat Makki Alamdari, Yang Wang, Fang Chen, and Peter Runcie. A clustering approach for structural health monitoring on bridges. *Journal of Civil Structural Health Monitoring*, pages 1–17, Feb 2016.

[15] K. Fukunaga and L. Hostetler. The estimation of the gradient of a density function, with applications in

pattern recognition. *IEEE Transactions on Information Theory*, 21(1):32–40, Jan 1975.

[16] Yizong Cheng. Mean shift, mode seeking, and clustering. *IEEE Transactions on Pattern Analysis and Machine Intelligence*, 17(8):790–799, Aug 1995.

[17] D. Comaniciu and P. Meer. Mean shift: a robust approach toward feature space analysis. *IEEE Transactions on Pattern Analysis and Machine Intelligence*, 24(5):603–619, May 2002.

[18] Kuo-Lung Wu and Miin-Shen Yang. Mean shift-based clustering. *Pattern Recognition*, 40(11):3035–3052, Nov 2007.

[19] Guido De Roeck. The state-of-the-art of damage detection by vibration monitoring: the SIMCES experience. *Structural Control and Health Monitoring*, 10(2):127–134, Apr 2003.

[20] Bart Peeters and Guido De Roeck. One-year monitoring of the Z24-Bridge: environmental effects versus damage events. *Earthquake Engineering & Structural Dynamics*, 30(2):149–171, Feb 2001.

[21] Bart Peeters and Guido De Roeck. Reference-based stochastic subspace identification for output-only modal analysis. *Mechanical Systems and Signal Processing*, 13(6):855–878, Nov 1999.

[22] T. Calinski and J. Harabasz. A dendrite method for cluster analysis. *Communications in Statistics*, 3(1):1–27, Jun 1974.

Appendix F – Paper F: Agglomerative concentric hypersphere clustering applied to structural damage detection

Mechanical Systems and Signal Processing 92 (2017) 196–212

Contents lists available at ScienceDirect

Mechanical Systems and Signal Processing

journal homepage: www.elsevier.com/locate/ymssp

Agglomerative concentric hypersphere clustering applied to structural damage detection

Moisés Silva [a,*], Adam Santos [a], Reginaldo Santos [a], Eloi Figueiredo [b,c], Claudomiro Sales [a], João C.W.A. Costa [a]

[a] Applied Electromagnetism Laboratory, Universidade Federal do Pará, R. Augusto Corrêa, Guamá 01, Belém, 66075-110 Pará, Brazil
[b] Faculty of Engineering, Universidade Lusófona de Humanidades e Tecnologias, Campo Grande 376, 1749-024 Lisbon, Portugal
[c] CONSTRUCT, Institute of R&D in Structures and Construction, R. Dr. Roberto Frias s/n, 4200-465 Porto, Portugal

ARTICLE INFO

Article history:
Received 31 August 2016
Received in revised form 15 January 2017
Accepted 18 January 2017

Keywords:
Agglomerative concentric hypersphere
Clustering
Damage detection
Structural health monitoring
Environmental conditions
Operational conditions

ABSTRACT

The present paper proposes a novel cluster-based method, named as agglomerative concentric hypersphere (ACH), to detect structural damage in engineering structures. Continuous structural monitoring systems often require unsupervised approaches to automatically infer the health condition of a structure. However, when a structure is under linear and nonlinear effects caused by environmental and operational variability, data normalization procedures are also required to overcome these effects. The proposed approach aims, through a straightforward clustering procedure, to discover automatically the optimal number of clusters, representing the main state conditions of a structural system. Three initialization procedures are introduced to evaluate the impact of deterministic and stochastic initializations on the performance of this approach. The ACH is compared to state-of-the-art approaches, based on Gaussian mixture models and Mahalanobis squared distance, on standard data sets from a post-tensioned bridge located in Switzerland: the Z-24 Bridge. The proposed approach demonstrates more efficiency in modeling the normal condition of the structure and its corresponding main clusters. Furthermore, it reveals a better classification performance than the alternative ones in terms of false-positive and false-negative indications of damage, demonstrating a promising applicability in real-world structural health monitoring scenarios.

1. Introduction

In the last few decades, the continuous structural condition assessment has demanded strong research efforts to support the management of structures during their lifetime. In particular, for the civil engineering infrastructure [1], the bridge management systems (BMSs) and structural health monitoring (SHM) have been used to cover the most relevant activities concerning the bridge management process. The BMS is a visual inspection-based decision-support tool developed to analyze engineering and economic factors and to assist the authorities in determining how and when to make decisions regarding maintenance, repair and rehabilitation of structures [2,3]. On the other hand, the SHM traditionally refers to the process of implementing monitoring systems to measure structural responses in real-time and to identify anomalies and/or damage at early stages [4].

* Corresponding author.
E-mail address: moises.silva@icen.ufpa.br (M. Silva).

http://dx.doi.org/10.1016/j.ymssp.2017.01.024
0888-3270/

Even with the inherent limitation imposed by the visual inspections, the BMS has already been accepted by structural managers around the world [5–7]. At the same time, SHM is becoming increasingly attractive due to its potential ability to detect damage, contributing positively to life-safety and economical issues [8]. It can be also integrated into the BMS in a systematic way [9]. Posed in the context of a statistical pattern recognition (SPR) paradigm, the SHM is described as a four-phase process [10]: (1) operational evaluation, (2) data acquisition, (3) feature extraction, and (4) statistical modeling for feature classification.

The feature extraction phase estimates damage-sensitive features, from the raw data, which are potentially correlated to the level of damage present in the monitored structure. Nevertheless, when one deals with real-world monitoring scenarios, the influence of operational and environmental effects may cause changes in the magnitude of features as well as alter their correlation with the level of damage. Generally, the more sensitive a feature is to damage, the more sensitive it is to changes in the operational and environmental conditions (e.g. temperature, wind speed and traffic loading) [11]. Therefore, robust feature extraction methods and data normalization procedures are required to overcome this problem. The data normalization is the process of separating changes in damage-sensitive features caused by damage from those caused by varying operational and environmental conditions [12,13]. These influences on the structural response have been cited as one of the major challenges for the transition of SHM technology from research to practice [14–17]. Although the data normalization occurs in almost all phases (except the first one) of the SPR paradigm, the focus of this study is on the fourth phase, which is concerned with implementation of algorithms to analyze and learn the distributions of the extracted features, aiming to distinguish between the undamaged and damaged structural state conditions [18].

Some studies in literature have established the concept of automatically discovering and characterizing the normal condition of structures as clusters [9,19]. In those studies, the damage detection strategy is carried out as an outlier detection approach based on machine learning algorithms and distance metrics, allowing one to track the outlier formation in relation to time. One important note is related to the output-only nature of those approaches, implying the accomplishment of data normalization without any information about the operational or environmental parameters.

Highlighting the fact that in most engineering infrastructure only data from undamaged (or normal) condition is available on the training phase, the unsupervised learning algorithms are often required for data normalization purposes [20], i.e. training is carried out using only data from the normal structural condition. In this context, cluster-based algorithms are attractive due to their ability to discover groups of similar observations related to the same structural state at a given period of time. This unsupervised implementation permits one to detect damage formation regarding the chosen main groups of states [21–23]. Although numerous traditional unsupervised machine learning algorithms have been reported [24–27], herein the approaches based on Mahalanobis Squared Distance (MSD) and Gaussian Mixture Model (GMM) are relevant, due to their cluster-based performance, operating in a set of stable and undamaged state conditions [9,19].

In this paper, a straightforward and nonparametric method based on agglomerative clustering and inflated hyperspheres is proposed to learn the normal condition of structures. The proposed method does not require any input parameter, except the training data matrix. Two deterministic initialization procedures rooted on eigenvectors/eigenvalues decomposition and uniform data sampling are presented. Furthermore, a random initialization is also introduced. These mechanisms pave the way for a novel Agglomerative Concentric Hypersphere (ACH) algorithm that discovers an appropriate number of clusters using a density-based approach.

The classification performance is investigated on the basis of Type I/Type II errors (false-positive and false-negative indications of damage, respectively) trade-off through application on two data sets from the Z-24 Bridge, located in Switzerland. The remainder of this paper is organized as follows. In Section 2, a review of the most traditional machine learning and cluster-based approaches for structural damage detection is introduced. The clustering constraints and initialization procedures related to the ACH algorithm are presented in Section 3. Section 4 is devoted to describe the data sets used as damage-sensitive features from the Z-24 Bridge. Section 5 describes the experimental results and carries out comparisons and discussions. This study concludes in Section 6 with a summary and the main conclusions.

2. Related work

Traditionally, in most civil applications, the damage detection process is carried out using physics-based methods and parametric approaches. However, in complex engineering structures, those methods may not be practical due to the level of expertise and time required to their development [28,29]. On the other hand, nonparametric approaches rooted in the machine learning field, especially cluster-based ones, have become an alternative, as they are very useful to find hidden patterns from monitoring data and are computationally efficient [30,31]. Herein, machine learning-based approaches addressing damage assessment are discussed; moreover, the most relevant cluster-based methods and their adaptation to damage detection in SHM are also considered.

2.1. Machine learning approaches for damage detection

Principal component analysis (PCA) is a common method to perform data normalization and feature classification without measurements of the sources of variability. Yan et al. [32] presented a PCA-based approach to model linear environmental and operational influences using only undamaged features. The number of principal components from extracted features

is implicitly assumed to correspond to the number of independent factors related to the normal variations. A further extension of this method was presented in [33]. In this case, a local extension of PCA is used to learn nonlinear relationships by applying a local piecewise PCA in some regions of the feature space. Although both approaches demonstrated adequate damage detection performance, the use of PCA imposes several limitations in practical SHM solutions, such as: only linear transformations can be performed through the orthogonal components; the larger the variance of a principal component, the greater its importance (in some cases this assumption is incorrect); and scale variant [34].

To overcome the limitations of PCA and detect damage in structures under changing environmental and operational conditions, an output-only vibration-based damage detection approach was proposed by Deraemaeker et al. [35]. Two types of feature extraction methods based on an automated stochastic subspace identification and the Fourier transform were used as damage sensitive-features. In this case, the data normalization and damage detection were carried out by factor analysis (FA) and statistical process control, respectively. The results demonstrated that when the FA is applied to deal with normal variations, both type of features provided reliable damage classification performances. However, this approach has been tested only using numerical models, which does not ensure its performance in real monitoring scenarios. Besides, the FA is only capable to learn linear influences as linear PCA.

Auto-associative neural network (AANN) is a nonlinear version of PCA intended to perform feature extraction, dimensionality reduction, and damage detection from multivariate data. As demonstrated by Kramer [36], the AANN is capable to perform, intrinsically, a nonlinear PCA (NLPCA), as it characterizes the underlying dependency of the identified features on the unobserved operational and environmental factors. Worden [28] developed a novelty detection technique by applying an AANN to learn the normal condition of structures. Once the model is trained, the residual error tends to increase when damaged cases are presented. A later study [27] applied the AANN to model nonlinearities in a laboratory structure under simulated effects of variability. In this study, the AANN was not able to model, properly, the normal condition, which was verified in terms of Type I/II errors. Zhou et al. [37] proposed a new damage index to avoid the occurrence of several errors. However, the results of this approach strongly depend on the type of damage-sensitive features.

The aforementioned drawbacks lead the research efforts to kernel-based machine learning algorithms, which have been widely used in the SHM field. Approaches based on support vector machines (SVM) have demonstrated high reliability and sensitivity to damage. A supervised SVM method to detect damage in structures with a limited number of sensors was proposed in [38]. Khoa et al. [39] proposed an unsupervised adaptation to dimensionality reduction and damage detection in bridges. Santos et al. [40] carried out a comparison study on kernel-based methods. The results demonstrated that those SVM-based approaches have been outperformed by kernel PCA (KPCA), in terms of removing environmental and operational effects and damage classification performance.

KPCA is an alternative approach to perform NLPCA. The kernel-trick allows the mapping of feature vectors to high dimensional spaces, which provides nonlinear strengths to linear PCA. Cheng et al. [41] applied the KPCA to detect damage on concrete dams subjected to normal variations. Similarly, novelty detection methods were proposed in [42,43] by applying the KPCA as a data normalization procedure. In these approaches, the problems related to the choice of suitable damage index and estimation of some parameters were addressed. However, the issues related to the choice of an optimal kernel bandwidth and the number of retained components were not fully addressed. Reynders et al. [44] developed an alternative approach to eliminate the environmental and operational influences in terms of retained components, and presented a complete scheme to solve the previous issues. However, this approach is not able to completely remove the normal effects, as it deals only with a fraction of the environmental and operational effects.

2.2. Cluster-based approaches for damage detection

Over the years, the approaches based on MSD have been widely used in real-world monitoring campaigns due to its ability to identify outliers [18,45,46]. The MSD-based approach assumes that the normal condition can be modeled by a unique cluster from a multivariate Gaussian distribution. In this context, an abnormal condition is considered as a statistical deviation from the normal pattern learned during the training phase as a mean vector and a covariance matrix, allowing one to infer whether the data were generated by a source not related to the normal condition. However, as noticed in [9], when nonlinearities are present in the monitoring data, the MSD fails in modeling the normal condition of a structure because it assumes the baseline data as a unique multivariate Gaussian distribution.

A two-step damage detection strategy based on GMMs was developed in [9,19,47] and applied to long-term monitoring of bridges. In the first step, the GMM-based approach models the main clusters that correspond to the normal and stable set of undamaged state conditions, even when normal variations affect the structural response. To learn the parameters of the GMMs, the classical maximum likelihood estimation based on the expectation-maximization (EM) algorithm is adopted in [9]. This approach applies an expectation step and a maximization step until the log-likelihood converges to a local optimum. However, the convergence to the global optimum is not guaranteed [48].

To overcome the limitations imposed by EM, in [19] the parameter estimation was carried out using a Bayesian approach based on Markov-chain Monte Carlo method. In [47], a genetic-based approach was employed to drive the EM searching towards the global optimum. In these approaches, as long as the parameters have been learned, a second step was performed to detect damage on the basis of a MSD outlier formation considering the chosen main clusters.

Silva et al. [22] proposed a fuzzy clustering approach to detect damage in an unsupervised manner. PCA and autoregressive moving average methods were used for data reduction and feature extraction purposes. The normal condition

was modeled by two different fuzzy clustering algorithms: fuzzy c-means clustering and Gustafson-Kessel (GK) algorithms. The results demonstrated that the GK algorithm outperformed the alternative one with a better generalization performance. However, the damage quantification was not properly assessed and both approaches produced a significant number of false-negative indications of damage.

3. Agglomerative clustering

Agglomerative clustering is part of a hierarchical clustering strategy which treats each object as a single cluster, and iteratively merges (or agglomerates) subsets of disjoint groups, until some stop criterion is reached (e.g. number of clusters equal to one) [49–51]. These bottom-up algorithms create suboptimal clustering solutions, which are typically visualized in the form of a dendrogram representing the level of similarity between two adjacent clusters, allowing to rebuild step-by-step the resulting merging process. Any desired number of clusters can be obtained by cutting the dendrogram properly.

The common flow chart of an agglomerative clustering procedure is summarized in Fig. 1. Initially, each observation is defined as a centroid. Then, a similarity matrix composed of the distances between each cluster is computed to determine which clusters can be merged. Usually, this agglomerative process is repeated until only one cluster remains. As described in [52], when the cluster diameter is small, the corresponding data group is defined more precisely as this group is composed by few members strongly correlated. The fundamental assumption is that small clusters are more coherent than large ones [52,53].

The ACH algorithm is an agglomerative cluster-based algorithm, working in the feature space, composed of two main steps: (1) off-line initialization and (2) bottom-up clustering procedure. Depending on the type of initialization mechanism, the algorithm becomes completely deterministic or random. The initialization has a direct influence on the algorithm performance. Hereafter, all clusters are merged through an agglomerative clustering procedure. These two steps allow, automatically, the discover of the number of clusters, without the estimation of any parameter.

In SHM, for general purposes, the training matrix $\mathbf{X} \in \mathbb{R}^{n \times m}$ is composed of n observations from the undamaged structure under operational and environmental variability, where m is the number of features per observation obtained during the feature extraction phase. The test matrix $\mathbf{Z} \in \mathbb{R}^{t \times m}$ is defined as a set of t observations collected during the undamaged/damaged conditions of the structure. Note that an observation represents a feature vector encoding the structural condition at a given time, and a data cluster represents a set of feature vectors corresponding to a normal and stable state condition of the structural system. In the following, all constraints related to initialization and clustering procedures are described.

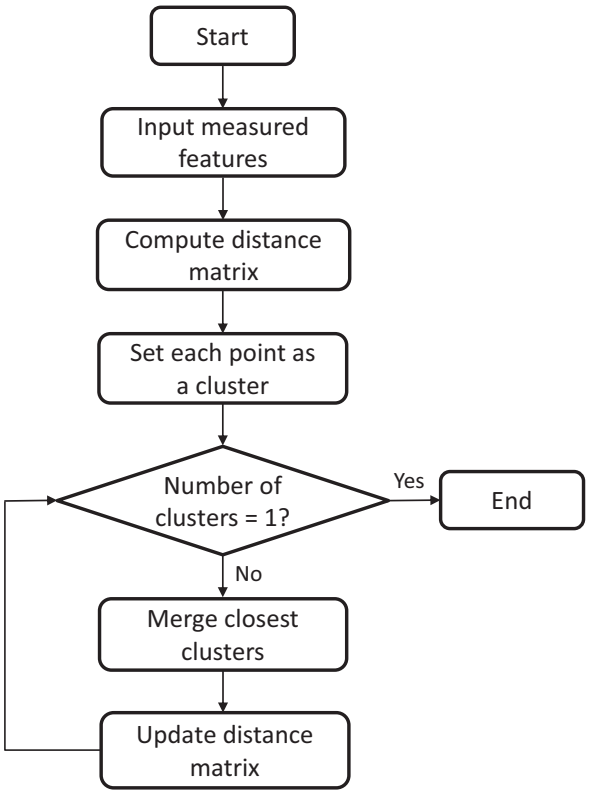

Fig. 1. Flow chart of agglomerative hierarchical clustering.

3.1. Agglomerative concentric hypersphere clustering

In this section, an unsupervised cluster-based algorithm which does not assume any underlying distribution and has no input parameter is fully described. This algorithm works in an iterative manner on a set of centroids, by evaluating the boundary regions that limit each cluster through inflation of a concentric hypersphere. This process is divided into three main phases:

(i) *Centroid displacement.* For each cluster, its centroid is dislocated to the position with higher observation density, i.e., the mean of its observations.

(ii) *Linear inflation of concentric hyperspheres.* Linear inflation occurs on each centroid by progressively increasing an initial hypersphere radius,

$$R_0 = \log_{10}\left(\|C_i - x_{max}\|^2 + 1\right), \tag{1}$$

where C_i is the centroid of the i-th cluster, used as a pivot, and x_{max} is its farthest observation, such that $\|C_i - x_{max}\|^2$ is the radius of the cluster centered in C_i. The radius of the cluster grows up in the form of an arithmetic progression (AP) with common difference equal to R_0. The increasing of the hypersphere is set by a criterion based on positive variation of the observation density between two consecutive inflations, defined as the inverse of variance; otherwise the process is stopped.

(iii) *Cluster merging.* If there is more than one centroid inside the inflated hypersphere, they are merged to create a unique representative centroid positioned at the mean of the chosen centroids. On the other hand, if only the pivot centroid is within the inflated hypersphere, this centroid is assumed to be on the geometric center of a cluster, thus the merging is not performed.

For completeness, Fig. 2 presents an example of the ACH algorithm applied to a three-cluster scenario with a five-centroid initial solution. First, in Fig. 2a, the centroids are moved to the center of their clusters, as indicated in the first phase. In Fig. 2b and c, two centroids are merged to form one cluster, as they are within the same inflated hypersphere. On the other hand, in Fig. 2d only the pivot centroid is located in the center of a cluster, therefore the ACH algorithm does not perform the merging process. In the case where the merging occurs, all centroids analyzed before are evaluated again to infer if the new one is not poorly positioned in another cluster or closer to a boundary region.

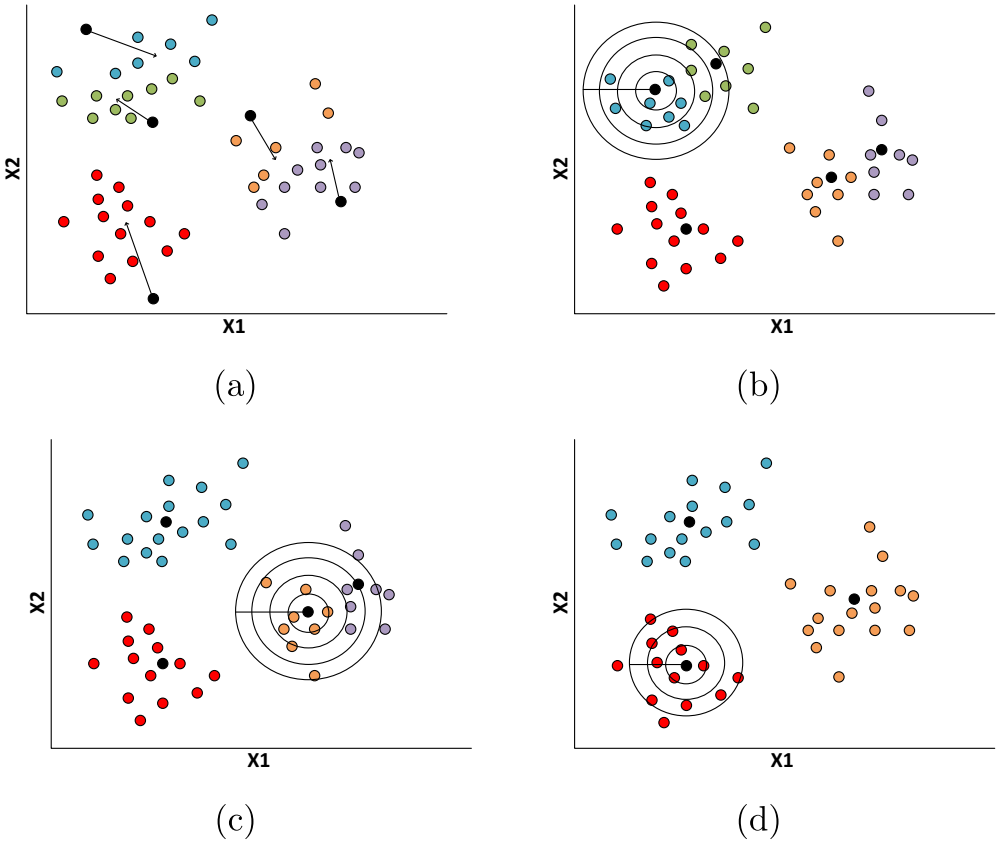

Fig. 2. ACH algorithm using linear inflation running in a three-cluster scenario.

The Algorithm 1 summarizes the proposed algorithm. Initially, it identifies the observations belonging to each cluster and moves the centroids to the mean of their observations. Then, a hypersphere is built on the pivot centroid and it is inflated until the observation density decreases. Finally, the centroids within a hypersphere are merged, by replacing these centroids by only one centroid positioned at the mean of them. The process is repeated until one convergence criterion be satisfied, i.e. there is no centroid merging after the evaluation of all centroids or the final solution is composed by only one centroid.

Note that, the main goal of the clustering step is to maximize the observation density related to each cluster. In other words, locating the positions with maximum observation concentration, also known as mass center, in such manner that when a hypersphere starts to inflate its radius, it reaches the decision boundaries of the cluster. This process is described by maximizing the cost function

$$\begin{aligned} \max \quad & \sum_{k=1}^{K}\left(\sum_{x_i \in C_k} \frac{\|x_i - C_k\|^2}{N_k}\right)^{-1}, \\ \text{s.t.} \quad & n = \sum_{k=1}^{K} N_k, \\ & 1 \leqslant N_k \leqslant n, \end{aligned} \tag{2}$$

where C_k is the k-th centroid, x_i is the i-th observation assigned to the k-th cluster, and N_k is the number of observations in the cluster k. The clustering procedure naturally carries out the optimization of the cost function by means of density evaluation, thus its direct computation is not necessary. The convergence is guaranteed by gradual decreasing of the observation density as the hypersphere keeps inflating. More theoretical details and complexity analysis are provided in Appendixes A and B, respectively.

Algorithm 1. Summary of the ACH algorithm.

```
1  calcIndexes(C, X)
2  while not cover all elements of C do
3    move(C, X)
4    c_pivo = nextCenter(C)
5    radius_init = calcRadius(c_pivo, X)
6    radius, density_0, density_1, delta_0, delta_1 = 0
7    repeat
8      radius = radius + radius_init
9      H = calcHypersphere(C, c_pivo, X, radius)
10     density_0 = density_1
11     density_1 = calcDensity(H)
12     delta_0 = delta_1
13     delta_1 = |density_0 − density_1|
14   until (delta_0 > delta_1);
15   reduce(C, H)
16   if merging occurred then
17     calcIndexes(C, X)
18   end if
19 end while
```

3.2. Initialization procedures

Three procedures can be employed to choose the initial centroids, depending on the application. The *random* initialization is performed by choosing $p < n$ distinct observations from the training matrix as initial centroids. This is quite similar to the initialization procedure often used in the K-means algorithm [54].

To accomplish a deterministic clustering, two nonstochastic initializations are presented as well. The first one performs an eigenvector decomposition to create as many centroids as the number of observations in the training set, through a *divisive* procedure, quite similar to the one described in [55]. Primarily, the mean value of all data points is divided in other two points generated by

$$y_{new} = y \pm U_i \sqrt{2\frac{T_{i,i}}{\pi}}, \tag{3}$$

where U_i and $T_{i,i}$ are the most significant eigenvector and eigenvalue, respectively, and y is the point being divided. Each new point is divided in other two points in opposite directions placed around dense regions of the feature space. The process is repeated until the number of points is equal to p; then they are used as initial centroids. At the end of this divisive procedure, each point has moved towards the regions of higher concentration of observations, benefiting posterior clustering approaches. The second nonstochastic initialization divides the training matrix *uniformly* and chooses equally spaced observations as the initial centroids. The gap between each chosen observation is a factor of the number of training observations, usually equal to $\lceil n/p \rceil$. The selected observations are used as initial centroids. The parameter p, in all cases, can be equal to $\lceil n/2 \rceil$.

3.3. Structural damage classification

After the definition of the optimal number of clusters embedded in the training data, the damage detection process is carried out through a global damage indicator (DI) estimated for each test observation. The DIs are generated through a method known as distributed DIs [19]. Basically, for a given test feature vector, z_i, the Euclidean distance for all centroids is calculated, where the DI(i) is considered the smallest distance,

$$\mathrm{DI}(i) = \min\left(\|z_i - C_1\|, \|z_i - C_2\|, \ldots, \|z_i - C_K\|\right), \tag{4}$$

where $C_1, C_2, \ldots, C_K$ are the centroids of K different clusters. Then, a linear threshold corresponding to a certain percentage of confidence over the training data must be determined. In this study, the threshold is defined for 95% confidence on the DIs taking into account only the baseline data used in the training process. Thus, if the ACH has learned the baseline condition, i.e., the identified clusters suitably represent the undamaged condition under all possible operational and environmental influences, then it is statistically guaranteed, approximately, 5% of misclassifications in the DIs derived from undamaged observations not used for training.

4. Test structure description

The Z-24 Bridge was a standard post-tensioned concrete box girder bridge composed of a main span of 30 m and two side-spans of 14 m, as shown in Fig. 3a. The bridge, before complete demolition, was extensively instrumented and tested with the aim of providing a feasibility tool for vibration-based SHM in civil engineering. A long-term monitoring test was carried out, from 11th of November 1997 to 10th of September 1998, resulting in four natural frequencies and 3932 observations, where the first 3470 observations are correlated to undamaged condition and the last 462 correspond to damaged condition progressively introduced in this structural system. One should note that the bridge was intensively influenced by thermal variations caused by freezing temperatures [56].

To verify the applicability of the proposed approach for long-term monitoring, hourly monitoring data from an array of accelerometers are used to extract damage-sensitive features, which yields a feature vector (observation) per hour. A reference-based stochastic subspace identification method was developed to extract the natural frequencies [57].

The use of observations related to the baseline condition in the statistical modeling phase (training), implies the application of the proposed approach in an unsupervised mode. The training matrix permits the algorithm to learn the underlying distribution of the observations affected by environmental and operational variability. As shown in Fig. 3b, the training matrix **X** (1–3123 observations) is defined with almost 90% of the feature vectors from the undamaged condition, corresponding to approximately one-year monitoring period. On the other hand, the remaining 10% of the undamaged feature vectors are used, along with the damaged ones and the training data, to build a test matrix **Z** (1–3932 observations) for the test phase to make sure that the DIs do not fire off before damage starts to appear.

In addition, to evaluate the performance of the ACH algorithm in handling a limited amount of training data, and for visual purposes, a daily data set from the same structure is used. This data set corresponds to daily monitoring data measured at 5 a.m. (because of the lower differential temperature on the bridge), yielding a unique feature vector per day of operation. Then, the same modal analysis procedure used in hourly data set was applied to extract the natural frequencies. The automatic procedure was only able to estimate the first three frequencies with high reliability, which outputs a three-dimensional feature vector per day [19]. During the feature extraction process, it was observed that the first and the third natural frequencies are strongly correlated (with a correlation coefficient of 0.94), which permits one to perform dimension reduction of the extracted feature vectors from three to two. The first two natural frequencies and their corresponding feature distribution in two-dimensional space are depicted in Fig. 4. The marked observations were extracted under ambient temperature below 0 °C.

Note that the last 37 observations correspond to the damage progressive testing period, which is highlighted, especially in the second frequency, by a clear drop in the magnitude. Observations 1–198 are related to baseline condition, even though under operational and environmental variability. The observed jumps in the natural frequencies are related to the asphalt layer in cold periods, which contributes significantly to the stiffness of the bridge. The heterogeneity among observations in a two-dimensional space is evidenced in Fig. 4b, which suggests the existence of groups that can be found through cluster-based methods. In conclusion, the corresponding training matrix **X** (1–198 observations) is defined with approximately 83% of all observations, while the test matrix **Z** (1–235 observations) is assigned with the entire data set.

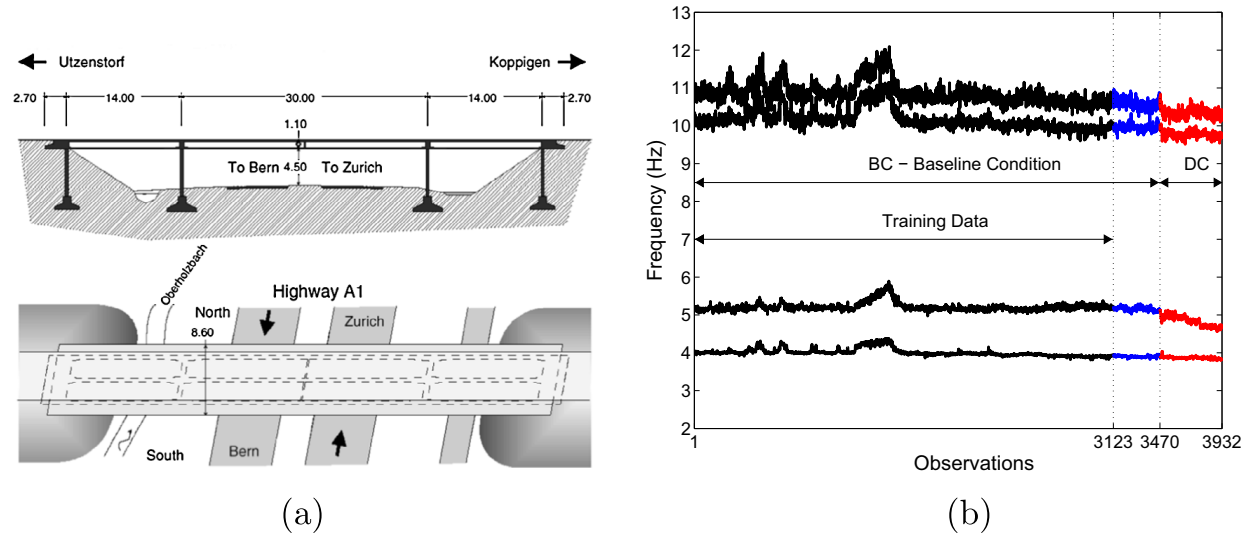

Fig. 3. Longitudinal section (upper) and top view (bottom) of the Z-24 Bridge (a). First four natural frequencies of Z-24 Bridge (b). The observations in the interval 1–3470 are the baseline/undamaged condition (BC) and observations 3471–3932 are related to the damaged condition (DC) [19].

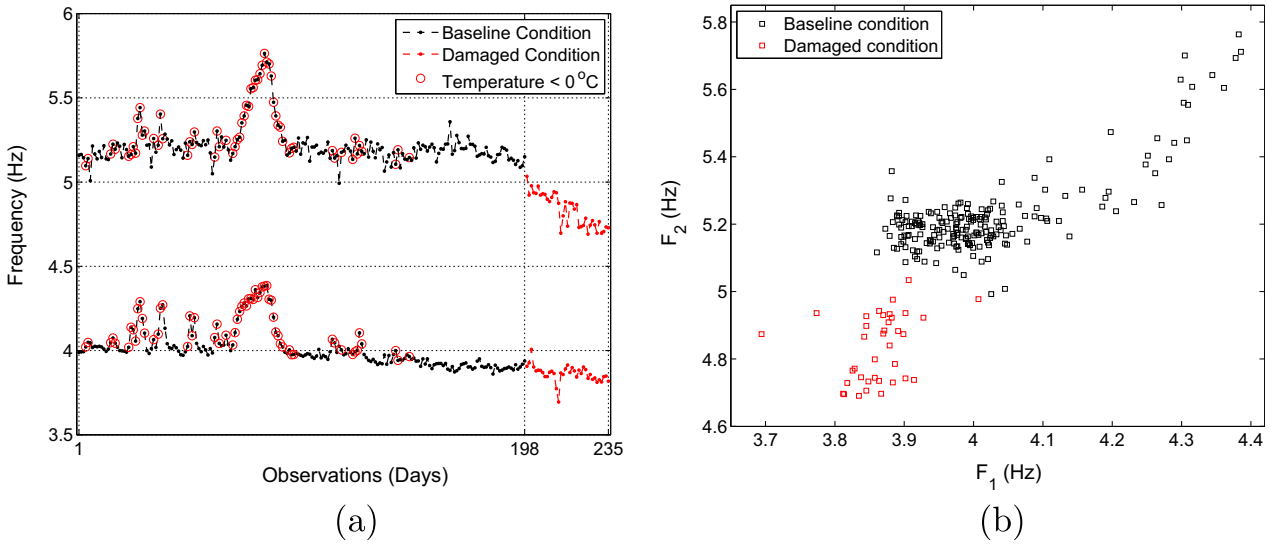

Fig. 4. The first two natural frequencies extracted daily at 5 a.m. from 11th of November 1997 to 10th of September 1998 (a); feature distribution of the two most relevant natural frequencies in bi-dimensional feature space (b).

5. Results and discussion

In this section, the performances of the ACH-, MSD-, and GMM-based approaches are compared on the basis of Type I and Type II errors as well as on their capabilities to filter nonlinear changes, when dealing with operational and environmental effects. Additionally, to determine which initialization procedure is more suitable to be employed with the ACH algorithm, a comparative study is carried out. Although the ACH- and MSD-based approaches do not require any input parameter, the GMM works through some predefined configurations and input values. The MSD- and GMM-based approaches were set as described in [19].

5.1. Comparative study of the initialization procedures

In order to perform a comparative study, the ACH was independently executed for the aforementioned three initialization procedures. Table 1 summarizes the Type I and Type II errors for all types of initializations. The random initialization makes the ACH more sensitive to detect abnormal conditions as expressed by the low number of Type II errors (4); however, it is penalized with a high number of Type I errors (220), demonstrating a loss of generalization capability. An alternative behavior is reached when deterministic initialization procedures are applied (uniform and divisive). Basically, the uniform initialization demonstrates a high degree of generalization and robustness to fit the normal condition at the cost of losing

Table 1
Number of clusters (K) as well as number and percentage of Type I and Type II errors for each ACH initialization procedure using the hourly data set from the Z-24 Bridge.

Initialization	K	Type I	Type II	Total
Random	5	220 (6.34%)	4 (0.86%)	224 (5.69%)
Uniform	6	159 (4.58%)	19 (4.11%)	178 (4.52%)
Divisive	3	188 (5.41%)	6 (1.29%)	194 (4.93%)

sensitivity to detect anomalies, as given by a relatively high number of Type II errors (19). On the other hand, the divisive initialization establishes a trade-off between generalization and sensitivity, reaching a low number of Type II errors (6) and maintaining an acceptable number of Type I errors (188), which indicates effectiveness to model the normal condition and to overcome the nonlinear effects. Furthermore, one can figure out that, for levels of significance around 5%, both random and divisive initializations are indicated, especially when the minimization of Type II errors is a critical issue.

The DIs for the entire test data are highlighted in Fig. 5, regarding each initialization procedure, along with a threshold defined over the training data. Excepting when the ACH is initialized with the uniform procedure, it outputs a monotonic relationship between the amplitude of DIs and the level of degradation accumulated on the bridge over the time. In Fig. 5b the freezing effects are highlighted by clear peaks in the DIs related to the data used in the training phase, indicating that the uniform initialization does not allow an appropriate filtering of nonlinear effects. Note that a nonlinear effect is not necessarily related to a damaged condition; it may arise from a normal variation of physical parameters on the structure not taken into account during the training phase. On the other hand, when damage is presented in the form of an orthogonal

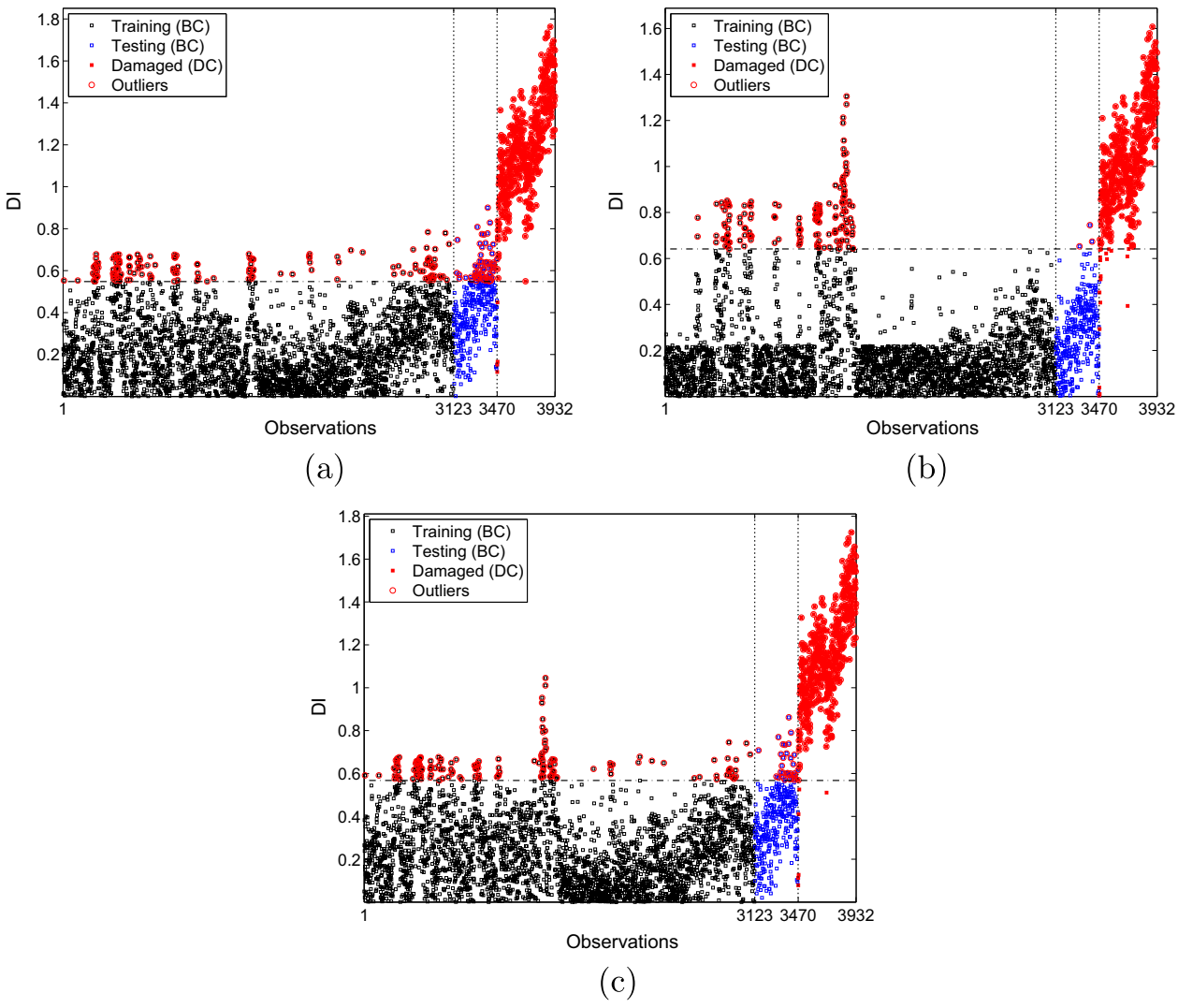

Fig. 5. DIs estimated via the ACH for different initialization procedures along with a threshold defined over the training data: (a) random-, (b) uniform-, and (c) divisive-based initialization procedures.

component that diverges from the normal condition under common operational and environmental factors, it is detected as a non-observed effect, i.e. an anomaly condition.

In relation to the number of data clusters, the ACH was able to find six, five, and three clusters when coupled with uniform, random and divisive initializations, respectively, as summarized in Table 1. Furthermore, the random and divisive initializations demonstrate to be more appropriate due to their potential to benefit the clustering step, providing a proper learning of the normal condition, even when operational and environmental variability is present. However, considering the best model as the one that establishes a trade-off between minimization of the number of errors using less clusters as possible, the divisive initialization is the most suitable procedure, as it accomplishes reliable results using a small number of clusters, being more indicated when one wants to reach a balance of sensitivity and specificity rates.

5.2. Damage detection with hourly data set from the Z-24 Bridge

For comparison purposes with algorithms from the literature, the ACH coupled with divisive initialization is chosen to accomplish a study along with MSD- and GMM-based approaches. Therefore, to quantify the classification performance, the Type I and Type II errors for the test matrix are presented in Table 2. Basically, for a level of significance around 5%, the ACH presents the best results in terms of total number of misclassifications, with less than 5% of the entire test data. On the other hand, the MSD provides the worst result, misclassifying, roughly, 9% of the entire test data. In turn, the GMM shows an intermediate performance, attaining 5.59% of misclassified observations. Nevertheless, the MSD has the smaller number of Type I errors when compared to the alternative ones. However, it demonstrates an inappropriate level of sensitivity to damage, which for high capital expenditure engineering structures is unacceptable due to the catastrophic consequences it may cause (e.g. undetected failures may cause human losses). Concerning the ACH and GMM, one can verify that both provide a high sensitivity to damage, although the ACH presents the smaller amount of misclassifications. In terms of generalization, the ACH attains the best results when compared to the GMM, as one can infer by the minimization of Type I errors.

To evaluate the performance of the ACH to model the normal condition, and to establish comparisons, the DIs are shown in Fig. 6. As mentioned before, the ACH outputs a monotonic relationship between the amplitude of DIs and the damage level accumulation, whereas the GMM fails to establish this relationship. In the case of the MSD-based approach, patterns in the DIs caused by the freezing effects can be pointed out, which indicates this approach is not able to properly attenuate the effects of environmental variations; thus, it demonstrates to be not effective to model the normal condition.

Furthermore, in relation to the ACH- and GMM-based approaches, only the first one maintains the aforesaid monotonic relationship, even when operational and environmental variability is present, as highlighted in Fig. 7. Nonetheless, the GMM misclassified undamaged observations throughout the track of observations not used in the training phase, indicating an inadequate learning of the normal condition. On the other hand, all misclassified undamaged observations accomplished by the ACH are grouped in a well known fuzzy region that may exist in the boundary frontiers of the quasi-circular clusters. This is explained by the nature of the ACH-based approach. Although the ACH aims to find out radially symmetric clusters, some clusters describe quasi-circular groups of similar observations that present, in their decision boundaries, sparse regions which represent a gradual change of some structural state.

In terms of the number of clusters, the GMM finds seven clusters ($K = 7$). However, the ACH accomplishes the best results with only three clusters ($K = 3$), indicating that the GMM has generalization problems, which can be explained by a tendency of overfitting caused by a high number of clusters. When evaluating cluster-based approaches, a trade-off between good fitting and low number of clusters is required, as the high number of clusters may lead to an overfitting; conversely, low number of clusters may conduct to an underfitting.

5.3. Damage detection with daily data set from the Z-24 Bridge

To establish further comparisons between the ACH and GMM, an additional study taking into account a limited amount of training data is carried out in the two-dimensional feature space. For all 235 observations from the daily data set, three centroids corresponding to the same number of clusters ($K = 3$) are plotted in Fig. 8a, as suggested by the ACH algorithm using the divisive initialization procedure. As indicated in Table 3, the first cluster is centered at (3.96, 5.18), attracting around 73% of all assigned data. This cluster is possibly related to the baseline condition obtained under small environmental and operational influences. The second cluster is centered at (4.21, 5.39) and it is assigned with 12% of the observations and may be related to changes in the structural response derived from stiffness changes in the asphalt layer caused by freezing

Table 2
Number of clusters (K) as well as number and percentage of Type I and Type II errors for each approach using the hourly data set from the Z-24 Bridge.

Approach	K	Type I	Type II	Total
ACH	3	188 (5.41%)	6 (1.29%)	194 (4.93%)
MSD	1	162 (4.66%)	191 (41.34%)	353 (8.97%)
GMM	7	210 (6.05%)	10 (2.16%)	220 (5.59%)

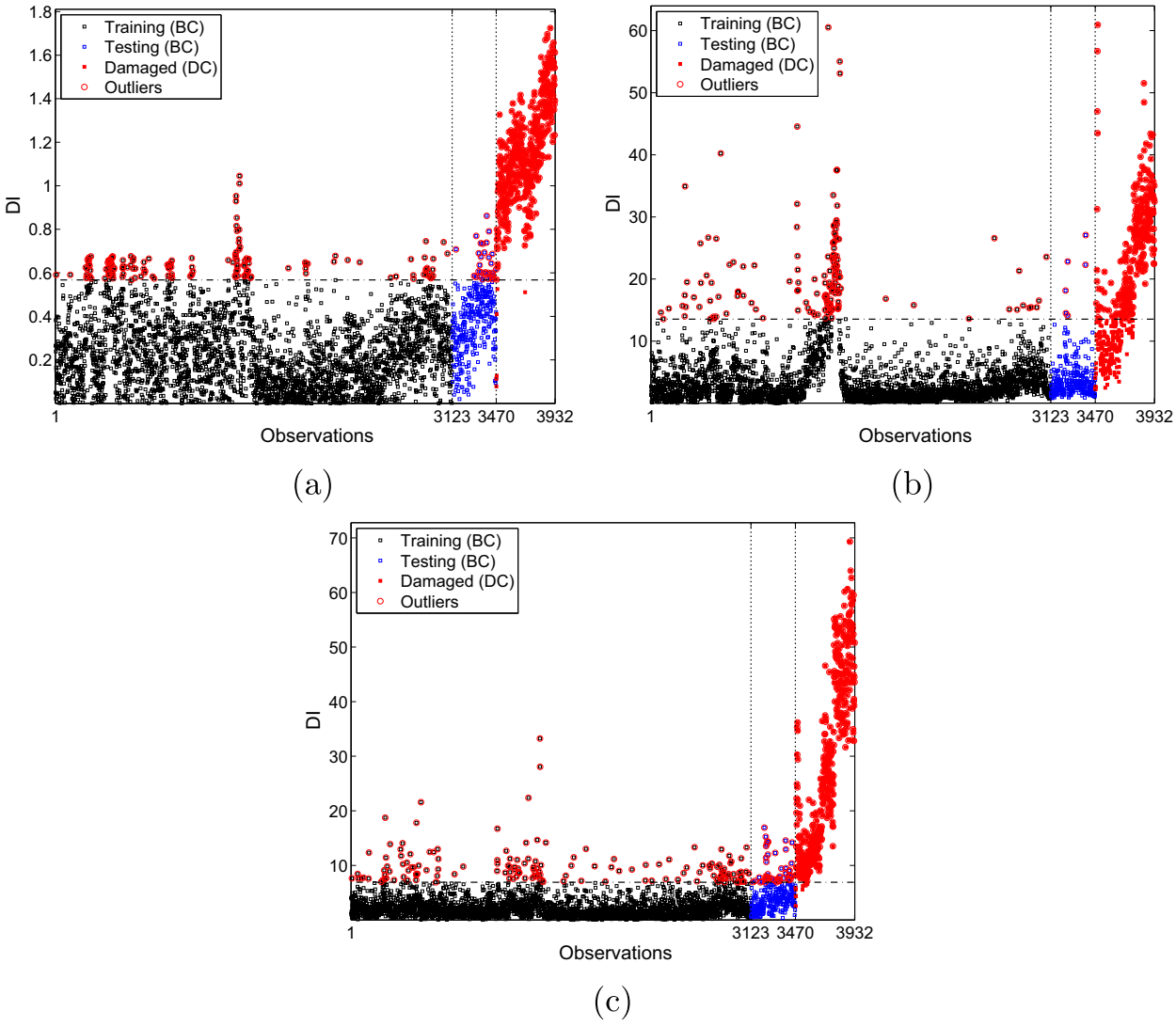

Fig. 6. DIs along with a threshold defined over the training data: (a) ACH-, (b) MSD-, and (c) GMM-based approaches.

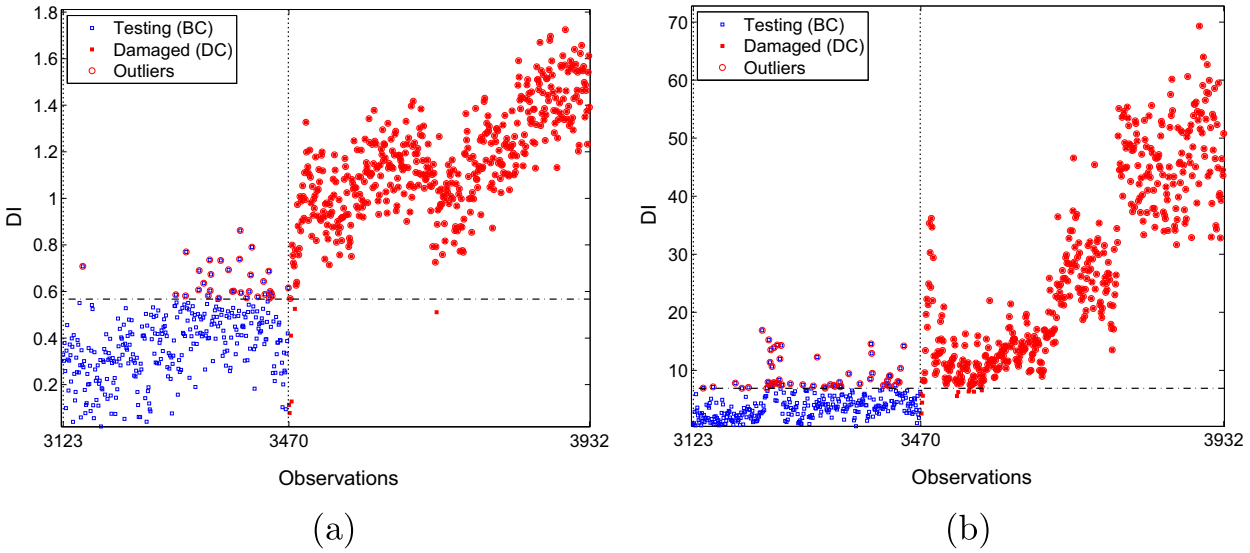

Fig. 7. Emphasis on monotonic relationship between the level of damage and the amplitude of DIs for the ACH- (a) and GMM-based (b) approaches.

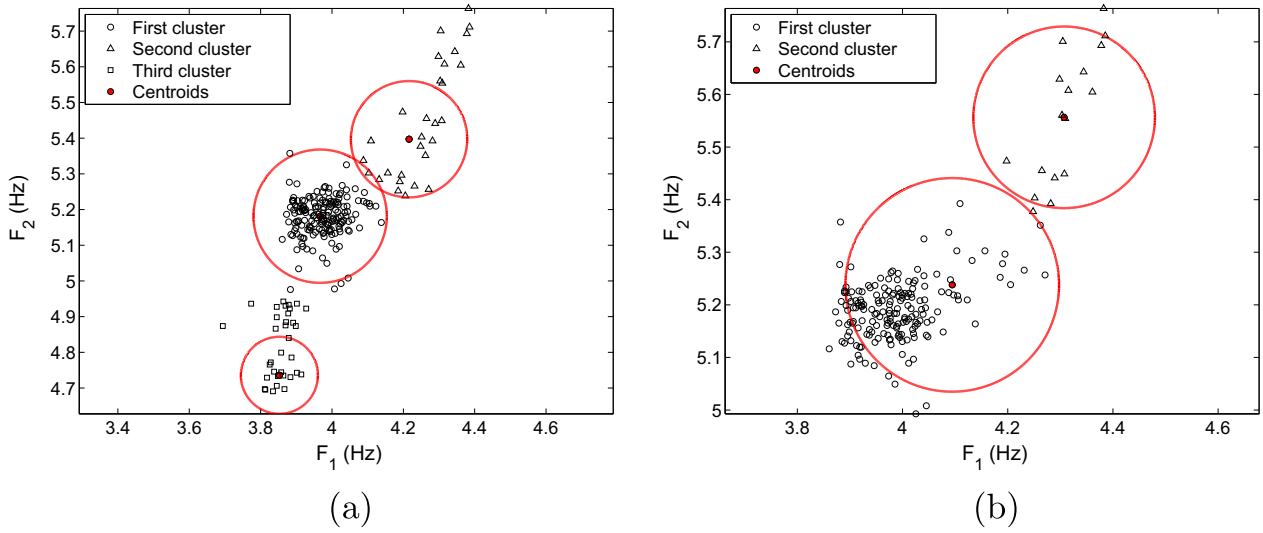

Fig. 8. Centroids estimated via the AHC along with daily observations from the Z-24 Bridge: (a) all 235 observations; (b) 1–198 observations corresponding to the baseline condition.

Table 3
Comparison of the parameter estimation using the ACH and EM algorithms on the entire daily data set (1–235) from the Z-24 Bridge (standard errors smaller than $10e-003$).

Approach	Description	Cluster 1	Cluster 2	Cluster 3
ACH	Weight (%)	73	12	15
	Mean (Hz)	(3.96, 5.18)	(4.21, 5.39)	(3.85, 4.73)
EM	Weight (%)	69	16	15
	Mean (Hz)	(3.97, 5.19)	(4.20, 5.37)	(3.86, 4.83)

temperature. Below 0 °C, the Young's modulus of asphalt rapidly increases and slightly changes the elastic properties of the structure [44]. The third cluster is positioned in the lower region of the feature space centered at (3.85, 4.73). It embeds around 15% of the entire observations and it is related to the space region assigned to the damaged condition. As demonstrated in [19], these results suggest the possibility to correlate physical states of the structure with a finite and well defined number of main data clusters. Figueiredo et al. [19] showed the existence of this phenomenon which is explained by the natural grouping of similar observations in certain regions of the feature space.

Comparing the results from the ACH- and the GMM-based approaches, one may verify the similarity of the results in Table 3, with exception for a little difference of the third cluster related to damaged condition. In all cases, the hyperspheres stop their inflation close to the regions of less observation concentration from each cluster, highlighting that the boundary regions are located close to the border of each hypersphere.

The challenges to simulate damage in real-world infrastructures are well-known, namely due to: the one-of-a-kind structural type, the cost associated with the simulation of damage in those infrastructures, and the infeasibility to cover all damage scenarios [19,58]. Therefore, the application of unsupervised approaches is often required as long as the existence of data from the undamaged condition is known a priori. Thus, and for real-world practical applications, the centroids defined by the ACH-based approach are shown in Fig. 8b, taking into account only feature vectors from the baseline condition (1–198 observations). In this case, Table 4 indicates two clusters positioned close to each other. The hyperspheres inflate until the low observation density is reached, suggesting two main data clusters. Comparing the results obtained from the ACH- and GMM-based approaches [19], one can verify differences between clusters location by a relative shift in their positions.

Table 4
Comparison of the parameter estimation using the ACH and EM algorithms on the baseline condition of daily data (1–198) from the Z-24 Bridge (standard errors smaller than $10e-003$).

Approach	Description	Cluster 1	Cluster 2
ACH	Weight (%)	95	5
	Mean (Hz)	(4.17, 5.23)	(4.30, 5.55)
EM	Weight (%)	82	18
	Mean (Hz)	(3.97, 5.18)	(4.22, 5.39)

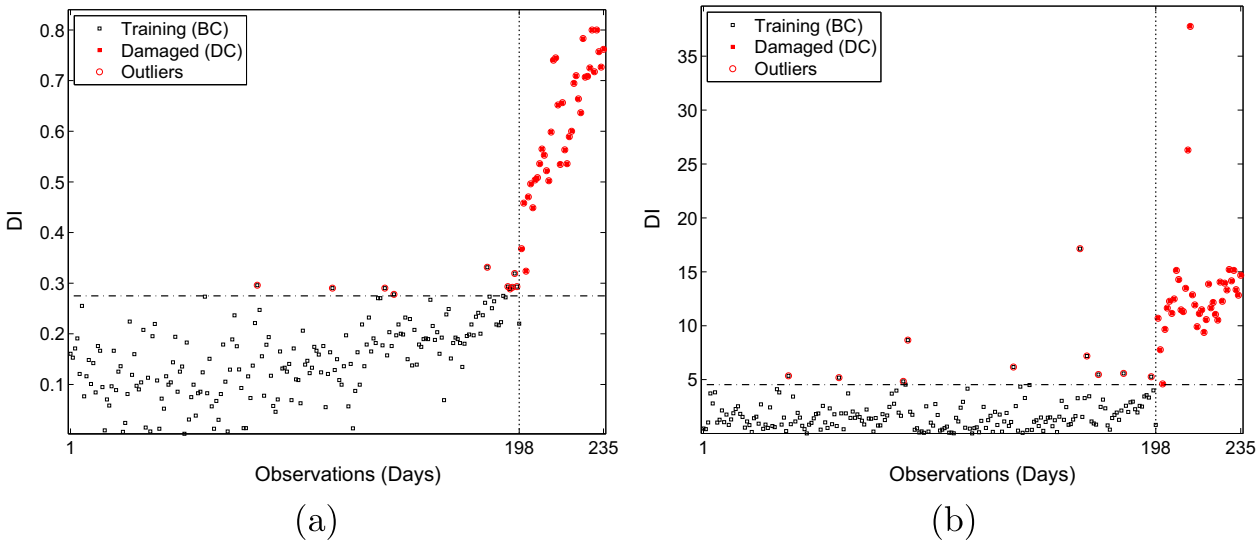

Fig. 9. DIs for daily observations from the Z-24 Bridge along with a threshold defined over the training data: (a) ACH- and (b) GMM-based approaches.

Table 5
Number and percentage of Type I and Type II errors for ACH- and GMM-based approaches using the daily data set from the Z-24 Bridge.

Approach	Type I	Type II	Total
ACH	10 (5.07%)	0 (0.0%)	10 (4.25%)
GMM	10 (5.07%)	0 (0.0%)	10 (4.25%)

The DIs obtained from test matrix **Z** (1–235 observations) are highlighted in Fig. 9. It shows, once again, that the ACH-based approach outputs a monotonic relationship between the amplitude of DIs and the damage level accumulation. On the other hand, the GMM has a poor performance when attempting to establish the aforementioned relationship. To quantify the classification performance, Table 5 summarizes the Type I and Type II errors for the test matrix. Basically, for a level of significance around 5%, the ACH- and GMM-based approaches have the same classification performance, reaching a total amount of errors equal to 4.25%. These results are quite similar due to the adopted function to evaluate the observation density within the inflated hypersphere.

6. Conclusions

This paper proposed a novel unsupervised and nonparametric cluster-based algorithm (ACH) for structural damage detection in engineering structures under varying and unknown conditions. In particular, the ACH was compared to two alternative parametric cluster-based approaches extensively studied in the literature (MSD and GMM), through their application on standard data sets from the Z-24 Bridge. This structure was under known environmental and operational influences, which caused changes in its structural dynamics.

In terms of general analysis, the ACH-based approach demonstrated to be as effective and robust as the GMM-based one to detect the existence of damage, and potentially more effective to model the baseline condition and to attenuate the effects of the operational and environmental variability, as suggested by the monotonic relationship between the amplitude of DIs and the gradual increasing of damage level.

In terms of theory formulation, the proposed approach is output-only, which implies that it is not required any information about variability sources, only the damage-sensitive features need to be extracted from the measured response data. Moreover, the ACH assumes no particular underlying distribution and it is conceptually simpler to be deployed in real-world applications, when it is not possible to make any assumption about the distribution of monitoring data. On the other hand, the GMM assumes the existence of Gaussian distributions and the EM converges toward a local optimum; while the MSD imposes the data to follow a unique multivariate normal distribution. Additionally, the ACH does not require any input parameter, it automatically finds the number of clusters and can be implemented as a totally deterministic approach, depending on the initialization procedure employed (divisive and uniformly). However, as each iteration of the ACH accomplishes a local optimization, the initialization may affect the clustering results.

This approach stands up as a relevant contribution to cluster-based models, even when dealing with a limited amount of training data, because of the completely automatic and nonparametric nature, allowing its application in scenarios where there is no prior knowledge about the structural condition.

Acknowledgements

The authors acknowledge the financial support received from CNPq (Grants 142236/2014-4 and 454483/2014-7) and CAPES. We also would like to acknowledge Professor Guido De Roeck, from the Katholieke Universiteit Leuven, for giving us the entire data as well as documentation from the Z-24 Bridge tests.

Appendix A. Theoretical properties

To demonstrate a reliable proof of convergence for the ACH algorithm, it is necessary to provide some intuition about data distribution in the worst case and the corresponding behavior of the ACH. Since $\mathbf{X} \in \mathbb{R}^{n \times m}$ is composed of the training examples and $\mathbf{C}$ is composed of K centroids disposed in the feature space, it is possible to infer two propositions inherent to the model with higher computational cost. The first proposition concerns to the maximum number of necessary iterations to the most external loop (lines 2 to 19 in Algorithm 1) before convergence.

Proposition 1. *Assuming that* $\mathbf{C}$ *is composed of non empty clusters* $C_1, C_2, \ldots, C_K \in \mathbb{R}^m$*, admitting the same operations such as* $C_i \subseteq \mathbf{C}$ *and* $\mathbf{X}$ *has only one real data cluster to be defined, then among the* $K!$ *possible permutations of centroids there is at least one which makes necessarily* $\frac{K^2+K-2}{2}$ *iterations before the algorithm converges.*

Proof. Since $\mathbf{C}$ admits anyone of the $K!$ combinations of its elements, there is unless one to keep the centroids distributed on the feature space in a such manner that the algorithm needs $K + (K-1) + (K-2) + \cdots + 2 = \frac{K^2+K-2}{2}$ loops to determine only one cluster describing the actual data shape. This occurs due to the algorithm merges only two clusters per iteration, in the worst case, forcing the algorithm to check all the clusters previously verified. □

The second proposition derives from the first and establishes a limit of iterations to the most internal loop (lines 7 to 14 in Algorithm 1), defining the number of hyperspheres in the same cluster.

Proposition 2. *Being the increment value of the hypersphere radius defined by Eq. (1) (Section 3.1) and* C_i *close to the geometric center of the cluster, then the maximum number of hyperspheres* H_y*, before the algorithm converges, is given by*

$$H_y \leqslant \left\lceil \frac{\max(\|C_i - x\|)}{R_0} \right\rceil, \quad \forall x \in \mathbf{X}. \tag{A.1}$$

Proof. When a centroid is positioned on the center of a real cluster (or in its neighborhood), the hypersphere radius increases as an AP with a common difference equal to R_0. Thus, one can naturally conclude that the hypersphere radius is never greater than the cluster radius. When the hypersphere reaches the border of the cluster, more sparser are the observations, which reduces the observation density compared to the last iteration performed by the ACH, leading to the convergence of the algorithm. □

Appendix B. Complexity proof

Based on previous propositions, this section provides the asymptotic complexity proof of Algorithm 1. However, before starting the analysis, some required cost information is introduced. To estimate a superior limit it is necessary to associate a maximum cost value to the execution of each instruction line. For each simple line (e.g. arithmetic operations and logic comparisons) it is assumed a constant value equal to one. On the other hand, for lines with function calls, the cost is calculated based on some analytical considerations.

Initially, one should analyze the lines with constant cost. The line 1 classifies each observation as belonging to a cluster, giving a cost equal to $K \times n$. In similar manner, to dislocate K centroids it is imperative to evaluate n observations in an m-dimensional space. Thus, the line 3 assumes a cost equal to the product between the feature space dimension m and the number of training data points n added to the number of centroids K. The line 4 is responsible for selecting the current pivot centroid. If none merges occurred in the last iteration, the next centroid in the set C is selected, otherwise the first centroid is chosen. For this line a constant cost is also assumed.

To compute a cluster radius, in the worst case, it is necessary evaluate $n-1$ observations. In this case, the line 5 has a complexity of $n-1$. The line 9 indicates which points are inside the hypersphere, being necessary analyze all n points in the training matrix $\mathbf{X}$, yielding a cost equal to n. In a similar manner, to compute the observation density of a hypersphere, the line 11 needs a maximum of $n \times m$ iterations before convergence.

The function in the line 15 analyzes all centroids in each iteration to define which ones can be merged. This process results in a cost equal to $|\mathbf{C}|$. In the line 17, a new function call to *calcIndexes* is made. As the number of centroids may be reduced over the iterations, this line cost depends on the cardinality of the set $\mathbf{C}$. However, asymptotically, one can apply the same cost assumed to the line 1.

To understand the maximum complexity estimated in the line 9, the Proposition 2 discussed previously is required. It is assumed that, when there is only one cluster defined on the data and $K > 1$, the maximum number of built hyperspheres depends on the cluster radius. Therefore, the number of iterations in the line 9, in the worst case, is equal to $\left\lceil \frac{\max(\|C_i - x\|)}{R_0} \right\rceil$. In a solution with K centroids it is possible to infer successive mergings performed two by two until one centroid remains. In this case, after each merge, all clusters are revalidated. Thereby, the cost is equivalent to an AP with common difference and initial term equal to two and one, respectively.

Adding the cost of all terms and multiplying those inside loops by the maximum number of iterations in Proposition 1, one can compute

$$\mathcal{F}(K,n,m) = \left(\frac{K^2+K-2}{2}\right)\left((n-1)+7+H_y(mn+n+4)+\frac{(n+1)(K^2+K-2)}{2}\right)+nK+nm+K,$$

ordering and excluding terms of less asymptotic order,

$$\begin{aligned}
\mathcal{F}(K,n,m) &= \left(\frac{nK^2-K^2+7K^2+nmK^2H_y+4K^2H_y+2nK+2nm+2K}{2}\right) \\
&\quad + \left(\frac{nK^4+K^4+2nK^3+2K^3+K^2+4}{4}\right) \\
&\quad - \left(\frac{3nK^2+4nK+4K+4n}{4}\right), \\
&< nmK^2H_y+nK^4+2nK^3+nK^2+K^4+4K^2H_y+2K^3 \\
&\quad + 6K^2+2nm+2nK+K^2+2K+4-3nK^2-4nK-4n-4K, \\
&< nmK^2H_y+nK^4+2nK^3+nK^2+K^4+4K^2H_y+2K^3+2nm \\
&\quad + 2nK+6K^2+K^2+2K.
\end{aligned}$$

Initially, one may suppose the term nK^4 as the one with highest complexity order. However, the asymptotic curve of the term nmK^2H_y is higher due to $K \ll m$. Substituting H_y and R_0

$$\begin{aligned}
\mathcal{F}(K,n,m) &= nmK^2H_y, \\
&= nmK^2\left\lceil \frac{\max(\|C_i - x\|)}{R_0} \right\rceil, \\
&= nmK^2\left\lceil \frac{\max(\|C_i - x\|)}{\log_{10}(\|C_i - x_{max}\|+1)} \right\rceil, \\
&\simeq nmK^2 \frac{\max(\|C_i - x\|)}{\log_{10}(\|C_i - x_{max}\|+1)}.
\end{aligned}$$

In the worst case, due to only one distribution fits the entire data (i.e. $K = 1$) it is assumed $D = \max(\|C_i - x\|) = \|C_i - x_{max}\|$, then

$$\begin{aligned}
\mathcal{F}(K,n,m) &= nmK^2 \frac{D}{\log_{10}(D+1)}, \\
&= nmK^2 \log_{10}(D+1)^{-D}.
\end{aligned}$$

Finally, one can conclude the algorithm computational complexity as

$$\mathcal{O}\left(nmK^2\right).$$

When $K \approx n$, the asymptotic complexity becomes a third order function. This is a little worse than most of the traditional cluster-based algorithms in literature, such as k-means and fuzzy c-means [59]. However, the agglomerative characteristic of the ACH allows to model, at the same time, the data shapes and discover the optimal number of clusters. This can be pointed out as an advance over other clustering approaches that require offline mechanisms to infer the number of clusters.

References

[1] E. Figueiredo, I. Moldovan, M.B. Marques, Condition Assessment of Bridges: Past, Present, and Future – A Complementary Approach, Universidade Católica Editora, Portugal, 2013.
[2] J. Lee, K. Sanmugarasa, M. Blumenstein, Y.-C. Loo, Improving the reliability of a bridge management system (BMS) using an ANN-based backward prediction model (BPM), Autom. Construct. 17 (6) (2008) 758–772, http://dx.doi.org/10.1016/j.autcon.2008.02.008.
[3] H. Wenzel, Health Monitoring of Bridges, John Wiley & Sons, Inc., United States, 2009.

[4] C.R. Farrar, K. Worden, An introduction to structural health monitoring, Philos. Trans. Roy. Soc.: Math. Phys. Eng. Sci. 365 (1851) (2007) 303–315, http://dx.doi.org/10.1098/rsta.2006.1928.
[5] A. Miyamoto, K. Kawamura, H. Nakamura, Development of a bridge management system for existing bridges, Adv. Eng. Softw. 32 (10–11) (2001) 821–833, http://dx.doi.org/10.1016/S0965-9978(01)00034-5.
[6] A. Estes, D. Frangopol, Updating bridge reliability based on bridge management systems visual inspection results, J. Bridge Eng. 8 (6) (2003) 374–382, http://dx.doi.org/10.1061/(ASCE)1084-0702(2003)8:6(374).
[7] V. Gattulli, L. Chiaramonte, Condition assessment by visual inspection for a bridge management system, Comput.-Aid. Civil Infrastruct. Eng. 20 (2) (2005) 95–107, http://dx.doi.org/10.1111/j.1467-8667.2005.00379.x.
[8] K. Worden, C.R. Farrar, G. Manson, G. Park, The fundamental axioms of structural health monitoring, Philos. Trans. Roy. Soc.: Math. Phys. Eng. Sci. 463 (2082) (2007) 1639–1664, http://dx.doi.org/10.1098/rspa.2007.1834.
[9] E. Figueiredo, E. Cross, Linear approaches to modeling nonlinearities in long-term monitoring of bridges, J. Civil Struct. Health Monit. 3 (3) (2013) 187–194, http://dx.doi.org/10.1007/s13349-013-0038-3.
[10] C.R. Farrar, S.W. Doebling, D.A. Nix, Vibration-based structural damage identification, Philos. Trans. Roy. Soc.: Math. Phys. Eng. Sci. 359 (1778) (2001) 131–149, http://dx.doi.org/10.1098/rsta.2000.0717.
[11] F.N. Catbas, M. Gul, J.L. Burkett, Conceptual damage-sensitive features for structural health monitoring: laboratory and field demonstrations, Mech. Syst. Signal Process. 22 (7) (2008) 1650–1669, http://dx.doi.org/10.1016/j.ymssp.2008.03.005.
[12] A. Cury, C. Cremona, J. Dumoulin, Long-term monitoring of a psc box girder bridge: operational modal analysis, data normalization and structural modification assessment, Mech. Syst. Signal Process. 33 (2012) 13–37, http://dx.doi.org/10.1016/j.ymssp.2012.07.005.
[13] J. Kullaa, Distinguishing between sensor fault, structural damage, and environmental or operational effects in structural health monitoring, Mech. Syst. Signal Process. 25 (8) (2011) 2976–2989, http://dx.doi.org/10.1016/j.ymssp.2011.05.017.
[14] H. Sohn, Effects of environmental and operational variability on structural health monitoring, Philos. Trans. Roy. Soc.: Math. Phys. Eng. Sci. 365 (1851) (2007) 539–560, http://dx.doi.org/10.1098/rsta.2006.1935.
[15] Y. Xia, B. Chen, S. Weng, Y.-Q. Ni, Y.-L. Xu, Temperature effect on vibration properties of civil structures: a literature review and case studies, J. Civil Struct. Health Monit. 2 (1) (2012) 29–46, http://dx.doi.org/10.1007/s13349-011-0015-7.
[16] N. Dervilis, K. Worden, E. Cross, On robust regression analysis as a means of exploring environmental and operational conditions for shm data, J. Sound Vib. 347 (2015) 279–296, http://dx.doi.org/10.1016/j.jsv.2015.02.039.
[17] M. Spiridonakos, E. Chatzi, B. Sudret, Polynomial chaos expansion models for the monitoring of structures under operational variability, ASCE-ASME J. Risk Uncert. Eng. Syst. Part A: Civil Eng. 2 (3). doi:http://dx.doi.org/10.1061/AJRUA6.0000872.
[18] K. Worden, G. Manson, The application of machine learning to structural health monitoring, Philos. Trans. Roy. Soc.: Math. Phys. Eng. Sci. 365 (1851) (2007) 515–537, http://dx.doi.org/10.1098/rsta.2006.1938.
[19] E. Figueiredo, L. Radu, K. Worden, C.R. Farrar, A Bayesian approach based on a Markov-chain Monte Carlo method for damage detection under unknown sources of variability, Eng. Struct. 80 (0) (2014) 1–10, http://dx.doi.org/10.1016/j.engstruct.2014.08.042.
[20] C.R. Farrar, K. Worden, Structural Health Monitoring: A Machine Learning Perspective, John Wiley & Sons, Inc, Hoboken NJ, United States, 2013.
[21] A. Diez, N.L.D. Khoa, M. Makki Alamdari, Y. Wang, F. Chen, P. Runcie, A clustering approach for structural health monitoring on bridges, J. Civil Struct. Health Monit. (2016) 1–17, http://dx.doi.org/10.1007/s13349-016-0160-0.
[22] S. da Silva, M.D. Júnior, V.L. Junior, M.J. Brennan, Structural damage detection by fuzzy clustering, Mech. Syst. Signal Process. 22 (7) (2008) 1636–1649, http://dx.doi.org/10.1016/j.ymssp.2008.01.004.
[23] A. Santos, E. Figueiredo, J. Costa, Clustering studies for damage detection in bridges: a comparison study, in: Proceeding of 10th International Workshop on Structural Health Monitoring, 2015, pp. 1165–1172, http://dx.doi.org/10.1109/ISDEA.2012.21.
[24] H. Sohn, K. Worden, C.R. Farrar, Statistical damage classification under changing environmental and operational conditions, J. Intell. Mater. Syst. Struct. 13 (9) (2002) 561–574, http://dx.doi.org/10.1106/104538902030904.
[25] T.-Y. Hsu, C.-H. Loh, Damage detection accommodating nonlinear environmental effects by nonlinear principal component analysis, Struct. Control Health Monit. 17 (3) (2010) 338–354, http://dx.doi.org/10.1002/stc.320.
[26] S. Hakim, H.A. Razak, Modal parameters based structural damage detection using artificial neural networks – a review, Smart Struct. Syst. 14 (2) (2014) 159–189, http://dx.doi.org/10.12989/sss.2014.14.2.159.
[27] E. Figueiredo, G. Park, C.R. Farrar, K. Worden, J. Figueiras, Machine learning algorithms for damage detection under operational and environmental variability, Struct. Health Monit. 10 (6) (2011) 559–572, http://dx.doi.org/10.1177/1475921710388971.
[28] K. Worden, Structural fault detection using a novelty measure, J. Sound Vib. 201 (1) (1997) 85–101, http://dx.doi.org/10.1006/jsvi.1996.0747.
[29] I. Laory, T.N. Trinh, I.F. Smith, Evaluating two model-free data interpretation methods for measurements that are influenced by temperature, Adv. Eng. Inform. 25 (3) (2011) 495–506, http://dx.doi.org/10.1016/j.aei.2011.01.001, Special Section: Engineering informatics in port operations and logistics.
[30] K. Worden, J.M. Dulieu-Barton, An overview of intelligent fault detection in systems and structures, Struct. Health Monit. 3 (1) (2004) 85–98, http://dx.doi.org/10.1177/147592170404186.
[31] F.N. Catbas, H.B. Gokce, M. Gul, Nonparametric analysis of structural health monitoring data for identification and localization of changes: concept, lab, and real-life studies, Struct. Health Monit. 11 (5) (2012) 613–626, http://dx.doi.org/10.1177/1475921712451955.
[32] A.-M. Yan, G. Kerschen, P.D. Boe, J.-C. Golinval, Structural damage diagnosis under varying environmental conditions – part i: A linear analysis, Mech. Syst. Signal Process. 19 (4) (2005) 847–864, http://dx.doi.org/10.1016/j.ymssp.2004.12.002.
[33] A.-M. Yan, G. Kerschen, P.D. Boe, J.-C. Golinval, Structural damage diagnosis under varying environmental conditions – part ii: Local pca for non-linear cases, Mech. Syst. Signal Process. 19 (4) (2005) 865–880, http://dx.doi.org/10.1016/j.ymssp.2004.12.003.
[34] J. Shlens, A tutorial on principal component analysis, Tech. rep., Cornell University, USA, 2002.
[35] A. Deraemaeker, E. Reynders, G.D. Roeck, J. Kullaa, Vibration-based structural health monitoring using output-only measurements under changing environment, Mech. Syst. Signal Process. 22 (1) (2008) 34–56, http://dx.doi.org/10.1016/j.ymssp.2007.07.004.
[36] M.A. Kramer, Nonlinear principal component analysis using autoassociative neural networks, AIChE J. 37 (2) (1991) 233–243, http://dx.doi.org/10.1002/aic.690370209.
[37] H. Zhou, Y. Ni, J. Ko, Structural damage alarming using auto-associative neural network technique: exploration of environment-tolerant capacity and setup of alarming threshold, Mech. Syst. Signal Process. 25 (5) (2011) 1508–1526, http://dx.doi.org/10.1016/j.ymssp.2011.01.005.
[38] A. Mita, H. Hagiwara, Quantitative damage diagnosis of shear structures using support vector machine, KSCE J. Civil Eng. 7 (6) (2003) 683–689, http://dx.doi.org/10.1007/BF02829138.
[39] N.L. Khoa, B. Zhang, Y. Wang, F. Chen, S. Mustapha, Robust dimensionality reduction and damage detection approaches in structural health monitoring, Struct. Health Monit. doi:http://dx.doi.org/10.1177/1475921714532989.
[40] A. Santos, E. Figueiredo, M. Silva, C. Sales, J. Costa, Machine learning algorithms for damage detection: kernel-based approaches, J. Sound Vib. 363 (2016) 584–599, http://dx.doi.org/10.1016/j.jsv.2015.11.008.
[41] L. Cheng, J. Yang, D. Zheng, B. Li, J. Ren, The health monitoring method of concrete dams based on ambient vibration testing and kernel principle analysis, J. Shock Vib. (2015), http://dx.doi.org/10.1155/2015/342358.
[42] C.K. Oh, H. Sohn, I.-H. Bae, Statistical novelty detection within the yeongjong suspension bridge under environmental and operational variations, Smart Mater. Struct. 18 (12) (2009) 125022.
[43] Z. Yuqing, S. Bingtao, L. Fengping, S. Wenlei, Nc machine tools fault diagnosis based on kernel pca and -nearest neighbor using vibration signals, J. Shock Vib. (2015), http://dx.doi.org/10.1155/2015/139217.
[44] E. Reynders, G. Wursten, G. De Roeck, Output-only structural health monitoring in changing environmental conditions by means of nonlinear system identification, Struct. Health Monit. doi:http://dx.doi.org/10.1177/1475921713502836.

[45] T. Nguyen, T.H. Chan, D.P. Thambiratnam, Controlled Monte Carlo data generation for statistical damage identification employing Mahalanobis squared distance, Struct. Health Monit. 13 (4) (2014) 461–472, http://dx.doi.org/10.1177/1475921714521270.
[46] Y.-L. Zhou, E. Figueiredo, N. Maia, R. Sampaio, R. Perera, Damage detection in structures using a transmissibility-based mahalanobis distance, Struct. Control Health Monit. 22 (10) (2015) 1209–1222, http://dx.doi.org/10.1002/stc.1743.
[47] A. Santos, E. Figueiredo, M. Silva, R. Santos, C. Sales, J.C.W.A. Costa, Genetic-based em algorithm to improve the robustness of gaussian mixture models for damage detection in bridges, Struct. Control Health Monit. (2016), http://dx.doi.org/10.1002/stc.1886, 00–00.
[48] A. Santos, M. Silva, R. Santos, E. Figueiredo, C. Sales, J. ao C.W.A. Costa, A global expectation-maximization based on memetic swarm optimization for structural damage detection, Struct. Health Monit. 15 (5) (2016) 610–625, http://dx.doi.org/10.1177/1475921716654433.
[49] S.C. Johnson, Hierarchical clustering schemes, Psychometrika 32 (3) 241–254. doi:http://dx.doi.org/10.1007/BF02289588.
[50] O. Maimon, L. Rokach, Data Mining and Knowledge Discovery Handbook, second ed., Texts and Monographs in Physics, Springer, US, 2010, http://dx.doi.org/10.1007/978-0-387-09823-4.
[51] P.J.R. Leonard Kaufman, Finding Groups in Data: An Introduction to Cluster Analysis, ninth ed., Wiley-Interscience, 1990, http://dx.doi.org/10.1002/9780470316801.
[52] M.J. Berry, G. Linoff, Data Mining Techniques: For Marketing, Sales, and Customer Support, John Wiley & Sons, Inc., New York, NY, USA, 1997.
[53] C.D. Manning, P. Raghavan, H. Schütze, Introduction to Information Retrieval, Cambridge University Press, New York, NY, USA, 2008, http://dx.doi.org/10.1017/CBO9780511809071.
[54] J.B. MacQueen, Some methods for classification and analysis of multivariate observations, in: L.M.L. Cam, J. Neyman (Eds.), Proc. of the fifth Berkeley Symposium on Mathematical Statistics and Probability, vol. 1, University of California Press, 1967, pp. 281–297.
[55] G. Hamerly, C. Elkan, Learning the k in k-means, in: Neural Information Processing Systems, MIT Press, 2003, p. 2003.
[56] B. Peeters, G. De Roeck, One-year monitoring of the z24-bridge: environmental effects versus damage events, Earthq. Eng. Struct. Dynam. 30 (2) (2001) 149–171, http://dx.doi.org/10.1002/1096-9845(200102)30:2<149::AID-EQE1>3.0.CO;2-Z.
[57] B. Peeters, G.D. Roeck, Reference-based stochastic subspace identification for output-only modal analysis, Mech. Syst. Signal Process. 13 (6) (1999) 855–878, http://dx.doi.org/10.1006/mssp.1999.1249.
[58] K.Y.K.R.J. Westgate, J.M.W. Brownjohn, Environmental Effects on a Suspension Bridge's Dynamic Response, Leuven, Belgium, 2011.
[59] S.K.D. Soumi Ghosh, Comparative analysis of k-means and fuzzy c-means algorithms, Int. J. Adv. Comput. Sci. Appl. 4 (4) (2013).